



The
University
Of
Sheffield.

Low shear stress promotes atherosclerosis through activation of EndMT

By:

Marwa Mahmoud

A thesis submitted in partial fulfilment of the requirements for the degree of
Doctor of Philosophy

The University of Sheffield
Faculty of Medicine, Dentistry and Health
Department of Infection, Immunity and Cardiovascular Disease

Submission Date
18-11-15

“Learn from yesterday, live for today, hope for tomorrow. The important thing is not to stop questioning. Curiosity has its own reason for existing.”

Albert Einstein

Acknowledgements

I have really enjoyed my time during my PhD and I owe it to all of the individuals that have contributed to making it such a positive experience. Firstly, I am very grateful to my supervisor Professor Paul Evans for being a great mentor, for all the guidance, constant support provided over the past years and for encouraging me to always aim higher. I would like to thank all members of the Evans' group (Dr. Shuang Feng, Dr. Matthew Bryan, Dr. Hayley Duckles, Dr. Ismael Gauci, Dr. Rosemary Kim, Ms. Britta Moers, Mr. Neil Bowden and Mr. Giannis Xanthis) for their support with my project. A special thanks to Dr. Sarah Hsiao and Dr. Jovana Serbanovic-Canic; not only that I am very grateful for your support, I am thankful for your friendship, for making the tough times much easier to deal with and, of course, for being great company and making my time very enjoyable! I couldn't have wished for better colleagues! I would also like to thank everyone on O-Floor and members of the IICD department for their help and support over the years. In particular, Professor Sheila Francis for her help and contribution to my project. I also wish to acknowledge Dr. Mark Ariaans (University of Sheffield) and Ms. Ruoyu Xing and Dr. Kim Van der Heiden (Erasmus MC) for their help and valuable contribution with the cuff-insertion experiments.

I am thankful to my friends for the laughs and the good times! Finally, I dedicate all of the hard work that I have put into my PhD to my amazing parents, without your never-ending love and support I would not be where I am today. I am grateful to my sisters and brother for being the best siblings I could have ever asked for! And for always motivating and supporting me, thank you!

Abstract

Introduction

Atherosclerosis is influenced by local blood flow patterns that exert wall shear stress (WSS) on endothelial cells (EC). Low, oscillatory WSS promotes atherosclerosis by influencing EC dysfunction (inflammation, permeability and proliferation), while high WSS is athero-protective. A recent microarray study by our laboratory of EC at athero-prone or athero-protective WSS regions of the porcine aorta revealed differential expression of GATA4 and TWIST1. These transcriptional activators can promote endothelial-mesenchymal transition (EndMT). We hypothesised that GATA4 and TWIST1 may control EC dysfunction and atherogenesis at sites of low WSS by inducing EndMT.

Methods & Results: Quantitative RT-PCR and *en face* staining confirmed enhanced GATA4, Twist1 and EndMT marker gene (Snail, Slug and N cadherin) expression at the inner curvature (lower-WSS) compared to the outer curvature (higher-WSS) of porcine and murine aortae. To establish a causal link, WSS was modified in murine carotid arteries using a constrictive cuff, this elevated TWIST1, GATA4 and SNAIL expression at the low WSS site. EC-specific deletion of Twist1 reduced SNAIL and N-cadherin expression and proliferation at the inner curvature of the murine aorta. Consistent with this, TWIST1 expression and EC proliferation at the inner curvature of the murine aorta was reduced by EC deletion of GATA4. Similarly, Gata4, Twist1 and EndMT effector genes were induced in PAEC or HUVEC exposed to low, oscillatory WSS using *in vitro* flow systems. Gene silencing demonstrated that GATA4 and TWIST1 are required for SNAIL induction in EC exposed to low, oscillatory WSS, and chromatin immunoprecipitation revealed GATA4 interaction with Twist1 and Snail. Low, oscillatory WSS promoted EndMT-characteristic changes including N-cadherin induction, VE-cadherin disorganization and enhanced proliferation and migration. Silencing of GATA4, Twist1 and Snail significantly reduced these processes alongside EC permeability. These results reveal that low WSS changes EC function via GATA4-TWIST1 activation.

Conclusion: Low WSS induces EndMT and subsequent EC proliferation and permeability through GATA4 and TWIST1. Our observations illuminate for the first time, the role of EndMT in arterial biomechanics and dysfunction. Future studies should define the role of EndMT in focal atherosclerosis.

Contents

Chapter 1: Introduction	10
1.1 The vascular endothelium	11
1.2 Atherosclerosis and EC dysfunction	13
1.2.1 Atherosclerosis pathophysiology.....	13
1.2.2 EC dysfunction in atherogenesis.....	15
1.3 Wall shear stress (WSS).....	17
1.3.1 EC mechanosensing of WSS.....	19
1.3.2 WSS and EC function.....	20
1.4 Focal atherosclerosis and shear stress	22
1.4.1 Low WSS promotes EC dysfunction	26
1.5 Twist1.....	29
1.5.1 The role of TWIST1 in development.....	31
1.5.2. The role of TWIST1 in adult disease.....	32
1.5.3 The regulation of TWIST1 in development and disease.....	35
1.6 GATA4	38
1.6.1 The role of GATA4 in development.....	40
1.6.2 The role of GATA4 in adult disease	41
1.6.3 Regulation of GATA4 in development and disease.....	43
1.7 Endothelial-mesenchymal-transition.....	46
1.7.1 Overview of molecular mechanisms controlling EndMT.....	46
1.7.2 EndMT in development	50
1.7.3 Role of EndMT in disease.....	52
1.8 Hypothesis.....	56
1.9 Aims:.....	56
Chapter 2: Materials and Methods	57
2.1 Materials.....	58
2.2 Methods.....	58
2.2.1 Isolation and culture of Human umbilical vein endothelial cells (HUVEC).....	58
2.2.2 Isolation and culture of porcine aortic endothelial cells (PAEC)	64
2.2.3 Isolation of RNA from EC in the porcine aorta	64
2.2.3 Exposure of EC to flow using in vitro flow systems.....	66
2.2.4 RNA extraction from EC exposed to flow.....	70
2.2.5 Gene expression analysis by qRT-PCR.....	71
2.2.6 Analysis of qRT-PCR data.....	72
2.2.7 RNA interference; HUVEC transfection with siRNA.....	74
2.2.8 Immunocytochemistry staining of cultured EC.....	74
2.2.9 In vitro tube formation assay on pre-sheared cells.....	78
2.2.10 In vitro cell migration; scratch assay on pre-sheared cells.....	78
2.2.11 EC permeability assay.....	80
2.2.12 Chromatin immunoprecipitation (ChIP).....	82
2.2.13 Immunohistochemistry staining on human coronary sections	83
2.2.14 Mouse breeding strategies and transgenic animals.....	84
2.2.16 Breeding and genotyping of SCL-Cre-ERT; GATA4 ^{KO} mice.....	87
2.2.17 Breeding and genotyping of Tie2-Twist1 ^{KO} mice.....	90
2.2.18 En face immunostaining of the mouse aortic arch	90

2.2.19 Insertion of flow altering cuff into murine carotid artery.....	93
2.2.20 Statistics.....	94
Chapter 3: Low shear stress promotes TWIST1 expression via GATA4.....	95
3.1 Introduction.....	96
3.2 Hypothesis.....	97
3.3 Aims.....	97
3.3 TWIST1 and GATA4 expression was elevated at sites of low WSS in the porcine aorta ...	98
3.4 Low WSS promoted TWIST1 expression via GATA4.....	100
3.5 Conclusions.....	105
3.6 Discussion.....	105
3.6.1 TWIST1 and GATA4 expression is driven by WSS magnitude.....	105
3.6.2 How does WSS modulate GATA4-TWIST1 expression?.....	107
3.7 Future experiments.....	113
Chapter 4: TWIST1 and GATA4 control proliferation and permeability in cells exposed to low WSS in vitro.....	114
4.1 Introduction.....	115
4.2 Hypothesis.....	116
4.3 Aims.....	116
4.3 TWIST1 and GATA4 regulate proliferation, migration and permeability in cells exposed to low WSS.....	117
4.4 TWIST1 regulates EC physiology under low WSS via a mechanism-involving Snail.....	125
4.5 Conclusions.....	135
4.6 Discussion.....	136
4.6.1 GATA4 and TWIST1 control EC proliferation, migration and permeability via the induction of EndMT in cells exposed to low WSS.....	136
4.6.2 Potential mechanisms for cell proliferation.....	140
4.5.3 Potential mechanism for the regulation of migration.....	142
4.5.4 Potential mechanism for the regulation of permeability.....	142
4.6 Future work.....	144
Chapter 5: GATA4-TWIST1 signalling controls focal EC dysfunction at sites exposed to low WSS flow in vivo.....	145
5.1 Introduction.....	146
5.2 Hypothesis.....	147
5.3 Aims.....	148
5.4 TWIST1, GATA4 and SNAIL expression is enhanced by atheroprone flow in the murine aorta.....	149
5.5 TWIST1 was expressed in adult EC exposed to low WSS in the murine aorta.....	152
5.6 Low WSS promoted partial EndMT <i>in vivo</i>	155
5.7 GATA4-TWIST1 mechanotransduction regulated EC proliferation and partial EndMT at low WSS sites in the murine aorta.....	158
5.8 TWIST1 expression in endothelial cells is increased with atherosclerosis severity in human and murine vessels.....	166
5.9 Conclusions.....	170
5.10 Discussion.....	171
5.10.1 The expression of TWIST1, GATA4 and SNAIL is driven by atherogenic, low WSS in vivo.....	171
5.10.2 TWIST1 expression is detected in adult EC.....	174
5.10.3 Potential mechanisms for the activation of TWIST1 and GATA4 by low WSS in vivo.....	175
5.10.4 Low WSS promoted partial EndMT.....	176

5.10.5 Potential mechanism for the induction of partial EndMT in EC exposed to low WSS.....	177	
5.10.6 Partial EndMT vs. Full EndMT	179	
5.10.7 Regulation of EC proliferation by GATA4 and TWIST1, is it detrimental or protective?	181	
5.10.8 Mechanism for the role of TWIST1 and GATA4 in EC proliferation at sites of low WSS.....	182	
5.10.9 Do TWIST1 and GATA4 regulate atherogenesis?	183	
5.10.10 Potential therapeutic strategies to inhibit TWIST1 and GATA4 induction of EC dysfunction.	185	
5.12 Future work.....	187	Marwa Ma Deleted: :
Chapter 6: General discussion	188	Marwa Ma Deleted: :
6.1 Mechanical TWIST1 activation has divergent effects during development and disease.....	189	Marwa Ma Deleted: :
6.1.1 Does GATA4-TWIST1 re-activation in adult EC promote repair in response to low WSS-mediated injury?	194	Marwa Ma Deleted: :
6.2 TWIST1 and GATA4 may regulate EC mechanosensing in response to low WSS	196	Marwa Ma Deleted: :
Chapter 7: Appendix	198	Marwa Ma Deleted: :
Chapter 8: Abbreviations	201	Marwa Ma Deleted: :
9. References	205	Marwa Ma Deleted: : Marwa Ma Deleted: : Marwa Ma Deleted: :

List of figures:

Figure 1. Atherosclerosis lesion formation.....	13
Figure 2. EC dysfunction.....	15
Figure 3. Focal atherosclerosis development.....	23
Figure 4. WSS patterns in the porcine aorta.....	24
Figure 5. Summary of WSS-mediated regulation of focal EC dysfunction	28
Figure 6. TWIST1 protein domain structure.....	30
Figure 7. Summary of molecular regulation of TWIST1.....	36
Figure 8. GATA4 protein domain structure.....	39
Figure 9. Summary of molecular regulation of GATA4.....	44
Figure 10. Molecular and functional changes during EndMT.....	47
Figure 11. Role of EndMT in development and disease.....	55
Figure 12. Schematic of RNA isolation from the porcine aortic arch.....	65
Figure 14. Schematic for the Ibidi™ parallel plate system.....	69
Figure 15. Schematic of scratch assay.....	79
Figure 16. Schematic for EC permeability assay.....	81
Figure 17. SCL-Cre-ER ^T ; R26R Td-tomato mice breeding and genotyping.....	86
Figure 18. SCL-Cre-ER ^T ; Gata4 ^{f/f} mouse breeding and genotyping.....	89
Figure 19. Tie2Twist1 ^{KO} breeding and genotyping.....	91
Figure 20. Schematic for en face preparation on the murine aortic arch.....	92
Figure 21. Low WSS was associated with elevated Twist1 and Gata4 expression in the porcine aorta.....	99
Figure 22. Low WSS induced TWIST1 and GATA4 expression in cultured EC in vitro	101
Figure 23. Validation of Twist1 and Gata4 silencing in cells exposed to low WSS.....	103
Figure 24. Low WSS induced TWIST1 expression via a GATA4 transcriptional mechanism.....	104
Figure 25. Potential mechanisms for GATA4 activation in cells exposed to low WSS.....	109
Figure 26. TWIST1 and GATA4 regulate tube formation in cells exposed to low WSS.....	119
Figure 27. Cells exposed to low WSS displayed enhanced migration compared to cells exposed to high WSS.....	120
Figure 28. TWIST1 and GATA4 promoted cell migration in cells exposed to low WSS.....	121
Figure 29. TWIST1 and GATA4 promoted proliferation in cells exposed to low WSS	122
Figure 30. TWIST1 and GATA4 promoted cell permeability in cells exposed to low WSS.....	124
Figure 31. Low WSS promoted partial EndMT.....	126
Figure 32. TWIST1 and GATA4 regulated partial EndMT in cells exposed to low WSS.....	127
Figure 33. TWIST1 and GATA4 regulated SNAIL protein in cells exposed to low WSS.....	128
Figure 34. GATA4 transcriptionally regulates Snail expression in cells exposed to low WSS.....	130
Figure 35. Validation of Snail silencing.....	131

Figure 36. SNAIL promotes EndMT marker expression in cells exposed to low WSS.	132
Figure 37. SNAIL promoted cell migration, proliferation and permeability in cells exposed to low WSS.....	133
Figure 38. Model for the role of TWIST1 and GATA4 in regulating EC physiology in cells exposed to low WSS in vitro.....	134
Figure 39. Potential mechanisms by which TWIST1 and GATA4 drive EC proliferation, migration and permeability under low WSS.....	141
Figure 40. Low WSS correlated with Twist1, GATA4 and Snail expression in the murine aortic arch	150
Figure 41. Low WSS promoted Twist1, GATA4 and Snail expression in cuff-inserted carotid murine arteries.....	151
Figure 42. Expression of Twist1, GATA4 and Snail in non cuff-inserted, sham control arteries	153
Figure 43. Validation of an EC tracking system in mice.....	
Figure 44. Low WSS promotes Twist1 expression in adult EC.....	156
Figure 45. Low WSS promoted the EndMT cadherin switch in the murine aorta	157
Figure 46. Intimal endothelial cells exposed to low WSS do not migrate into media	159
Figure 47. Low WSS promoted EC proliferation in the murine aorta.....	160
Figure 48. Validation of endothelial gene deletion of TWIST1 and GATA4.....	162
Figure 49. TWIST1 and GATA4 promoted EC proliferation at low WSS sites in the murine aorta.....	163
Figure 50. GATA4 regulated Twist1 expression at low WSS sites in the murine aorta	164
Figure 51. Twist1 promoted Snail and N-cadherin expression at low WSS sites in the murine aorta.....	165
Figure 52. Twist1 expression was increased with atheroseverity in human coronary arteries	167
Figure 53. Twist1 expression was increased at low WSS sites in response to hypercholesterolemia	168
Figure 54. Model for the function of TWIST1 and GATA4 in EC at low WSS sites.....	169
Figure 55. Schematic of Twist1 and GATA4 mechanical activation in embryo and adult systems.....	190
Figure 56. twist expression was downregulated by flow in zebrafish embryonic vasculature.....	191
Figure 57. Model for activation of GATA4-Twist1 by WSS in developmental angiogenesis and EC dysfunction in the adult	193

Marwa Ma
Deleted: :

Marwa Ma
Deleted: :

List of Tables:

Table 1. Summary of EC functions that are differentially regulated by exposure to WSS in vitro.....	21
Table 2. Materials used for primary cell culture/cell transfection.....	59
Table 3. Materials used for immunostaining/chIP.....	61
Table 4. Materials used for RNA isolation/ qRT-PCR/ standard PCR	62
Table 5. Materials used for in vivo techniques	63
Table 6. Primer sequences	73
Table 7. siRNA oligonucleotide information	75
Table 8. Primary antibodies.....	76
Table 9. Secondary antibodies.....	77
Table 10. Summary of WSS modulation of TWIST1 and GATA4 using in vitro and in vivo systems.....	173
Table 11. Summary of Twist1 and GATA4 inhibitory drugs.....	186

Marwa Ma
Deleted: :

List of Appendices:

Appendix 1. Growth media constituents	199
Appendix 2. PCR genotyping information.....	196

Marwa Ma
Deleted: :

Chapter 1: Introduction

1.1 The vascular endothelium

The journey to the discovery of the endothelium began in the 4th century, where the greek polymath, Aristotle provided early observations for the existence of the vascular architecture and its role in providing a “frame” for the support of the organism (Aristotle, Platt 1910). Until the 1600s, it was believed that blood is delivered to essential organs by food consumption and that the sole function of the heart was to provide heat (Reviewed in Ribatti 2009). This understanding was changed in 1628, when William Harvey provided an explanation for the cardiovascular system function. He observed that “blood in the animal body moves around in a circle continuously” and that this continuous motion is mediated by a pumping action by the heart (Ribatti 2009; Harvey 1928). It was later discovered in 1685 by Marcello Malpighi that blood travels in capillary, vessel structures (Malpighi 1685). In the 1800s, it was observed that the vessels are lined with cells and the term “endothelium” was first introduced by Wilhelm His (His 1865). Further morphological and functional analyses in the 20th century established the understanding that the endothelium lining vascular beds consists of a monolayer of endothelial cells (EC), attached to one another by cell-cell junctional proteins and that EC serve essential functions in the embryo and in the adult.

During embryonic development, EC are formed during vasculogenesis (De Val & Black 2009). In this process mesodermal progenitors in the yolk sac and the embryo differentiate to form the primitive embryonic and extraembryonic vasculature (Flamme et al. 1997; Patan 2004). The early embryonic vasculature is then remodelled via angiogenesis involving the essential contribution of EC, which undergo sprouting to form new vessels, which subsequently mature into arteries and veins (Flamme et al., 1997, Patan, 2004).

The specification of arteries and veins occurs genetically via the expression of the ligand Ephrin-B2 (Efnb2), Notch and the receptor EPH Receptor B4 (Ephb4) and COUP-transcription factor 2 (COUP-TFII) respectively (De Val 2011; Corada et al. 2014). Vasculogenesis involves transcriptional regulation through T-Cell acute lymphocytic leukemia 1/ stem cell leukemia (Tal1/SCL), GATA binding protein (GATA) 2 transcription factors and Tie2 receptors (Reviewed in De val and Black, 2009).

In the adult, EC are essential for maintaining vascular homeostasis. EC monolayers form a selective barrier for the control of the transport of substances into the vessel wall (Reviewed in Michiels, 2003). The control of the permeability to such substances is critical to the maintenance of a quiescent, healthy vasculature. EC also regulate vascular tone via establishing a balance between the secretion of vasodilative factors such as nitric oxide (NO) and vasoconstrictive factors such as endothelin 1 and angiotensin 2 (Reviewed in Michiels 2003). EC control of vascular tone directly affects oxygen supply to tissue and is dynamically altered to meet metabolic demands. Furthermore, EC regulate blood coagulation and platelet functions during quiescence and during vessel damage and inflammation (Reviewed in Michiels 2003).

In summary EC regulate the balance between vasodilative, and non-vasodilative, inflammatory and non-inflammatory signalling pathways depending on the environment to mediate vascular homeostasis. A failure of EC to establish such balance triggers EC dysfunction, which is central to the development of atherosclerosis (Reviewed in Libby 2002).

1.2 Atherosclerosis and EC dysfunction

1.2.1 Atherosclerosis pathophysiology

Atherosclerosis a disease that underlies cardiovascular diseases and stroke, is characterised by chronic inflammatory activation of EC. Alongside genetic predisposition, atherosclerosis is promoted by the presence of systemic risk factors such as the presence of low-density lipoproteins (LDL) in the circulating blood.

The initial step in atherogenesis is the transport of circulating LDL into the intimal layer of the arterial wall (Libby, 2002; Wentzel *et al*, 2012) (Figure. 1) . After moving into the sub- endothelial cell space, LDL becomes oxidised by reactive oxygen species (ROS) (Mabile *et al*, 1997). Oxidised LDL (ox-LDL) initiate inflammatory activation of endothelial cells (EC) (Libby, 2002; Witztum, 1994). This promotes the production pro-inflammatory cytokines (such as interleukin (IL-1), tumour necrosis factor (TNF)- α and monocyte chemoattractant protein (MCP)-1) and the expression of adhesion molecules on the EC surface such as vascular cell adhesion protein (VCAM)-1, intercellular adhesion molecule (ICAM)-1, P and E-selectins which together initiate the leukocyte adhesion cascade (Witztum, 1994; Libby, 2002). Once monocytes transmigrate and infiltrate into the vessel wall they differentiate into macrophages and begin to take up ox-LDL particles. This results in the differentiation into foam cells, resulting in the formation of fatty streaks. The secretion of foam cells of matrix metalloproteinases (MMPs) and ROS further sustains the inflammatory response and promotes the development of an atherosclerotic plaque (Stoneman & Bennett 2004).

Advanced atherosclerotic lesions consist of a necrotic core of cells, macrophages, leukocytes, ox-LDLs and cellular debris, which all continue to augment the inflammatory response (Rader and Daugherty; 2008; Wentzel *et al*, 2012; Schaar *et al*, 2004).

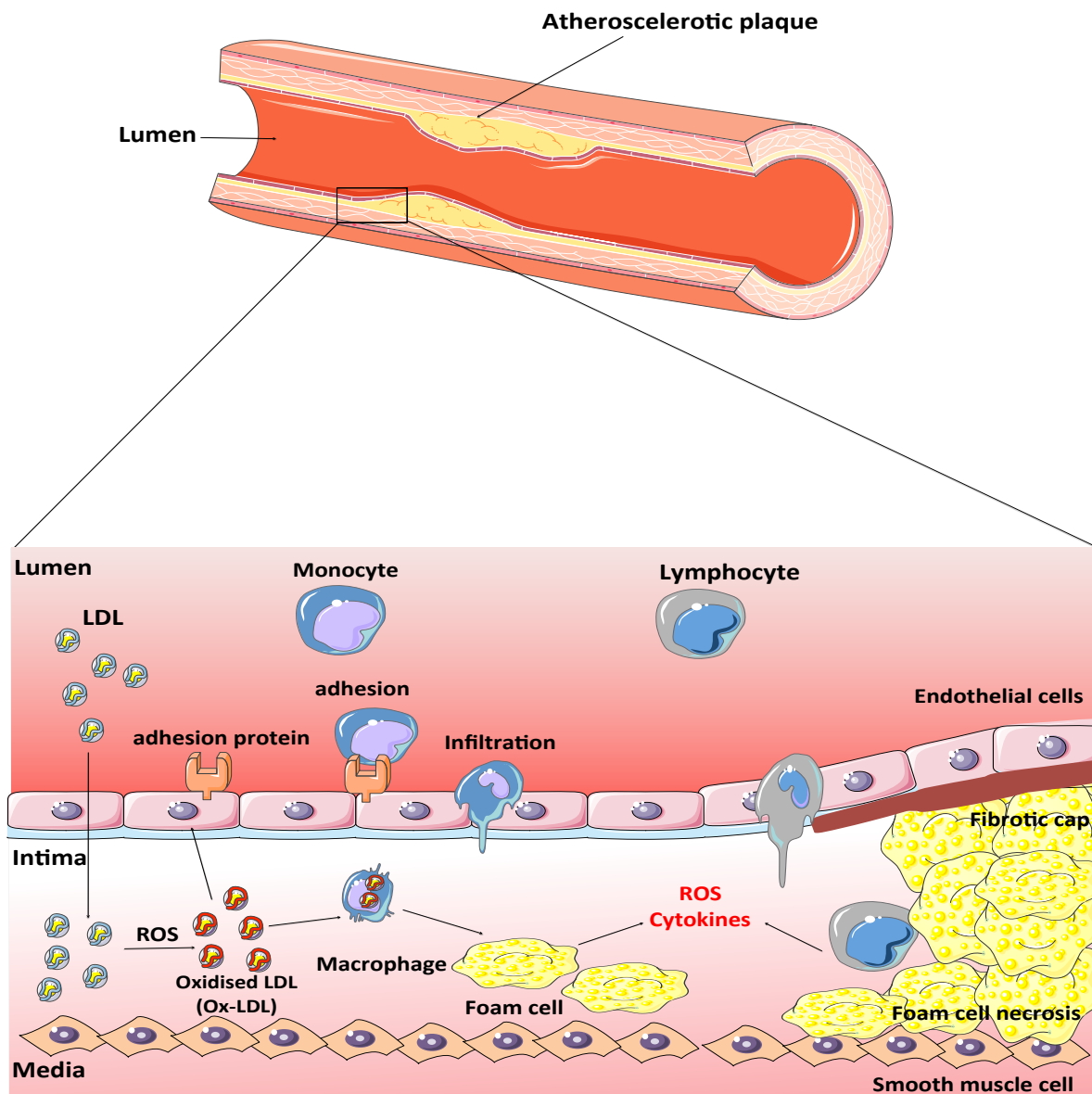


Figure 1. Atherosclerosis lesion formation. LDL that have transported into the sub endothelial space in the vascular intima, become oxidised by ROS, giving rise to ox-LDL. This triggers EC inflammatory activation, followed by the release of cytokines and the expression of adhesion proteins (VCAM-1, ICAM-1 and E-selectin) on the EC surface , which mediate monocyte infiltration. Monocytes differentiate into macrophages and take up ox-LDL. This transforms macrophages into foam cells, which exacerbate the inflammatory response by releasing ROS and cytokines. This creates a positive feedback on EC inflammatory activation, promoting the recruitment of lymphocytes. Macrophage necrosis and further inflammatory signalling gives rise to an atherosclerotic plaque, which consists of a necrotic core that is surrounded by a fibrotic cap.

The plaque may obstruct blood flow and this consequently limits oxygen supply to major organs, resulting in ischemic damage (Wentzel *et al*, 2012). Alternatively, the plaque may undergo outward remodelling which preserves the dimensions of the lumen that it exists within (Glagov *et al.* 1992). This remodelling along with the force induced by the flowing blood can render the plaque susceptible to rupture and subsequent thrombus formation (Libby, 2002).

1.2.2 EC dysfunction in atherogenesis

EC dysfunction in response to oxidative agents such as ox-LDL and disruption of the EC barrier function is a critical step in the formation of atherosclerosis (Reviewed in Libby *et al.*, 2002, Michiels, 2003). Numerous studies have linked EC dysfunction with atherosclerosis and have identified EC dysfunction as a predictor for atheroseverity (Choi *et al.* 2014; Schächinger *et al.* 1994; Halcox *et al.* 2002) Therefore, therapies that are known to treat atherosclerosis are targeted towards correcting EC dysfunction by promoting anti-oxidative and anti-inflammatory signalling (Davignon & Ganz 2004). Such successful therapies include statins which lower cholesterol content from the blood, thus inhibiting inflammation (Gould *et al.* 1994; Kinlay & Ganz 2000; Laufs *et al.* 1998) and antioxidant mediators such as sulforaphane (Zakkar *et al.* 2008; Evans 2011) and resveratrol (Berbée *et al.* 2013).

EC dysfunction involves changes in cell function, including increased inflammation, proliferation and permeability, which influence one another (Figure 2). EC inflammation is mediated by NF- κ B, p38 and JNK MAPK signalling (Reviewed in (Kempe *et al.* 2005; Kyriakis & Avruch 2001). The direct effect of NF- κ B signalling in atherosclerosis has been demonstrated by studies showing a marked reduction in atherosclerosis development as a result of genetic inhibition of NF- κ B signalling in murine atherosclerotic murine models (Gareus *et al.* 2008; Wolfrum *et al.* 2007). NF- κ B, p38 and JNK MAPK signalling inflammatory pathways sustain EC activation and initiate the leukocyte adhesion cascade in EC, which results in an increase in EC permeability via vascular endothelial (VE)-cadherin proteolysis, to facilitate leukocyte infiltration (Miyazaki *et al.* 2011; Zoja *et al.* 2002). This results in a further increase in the uptake of LDL molecules and subsequently increased inflammation.

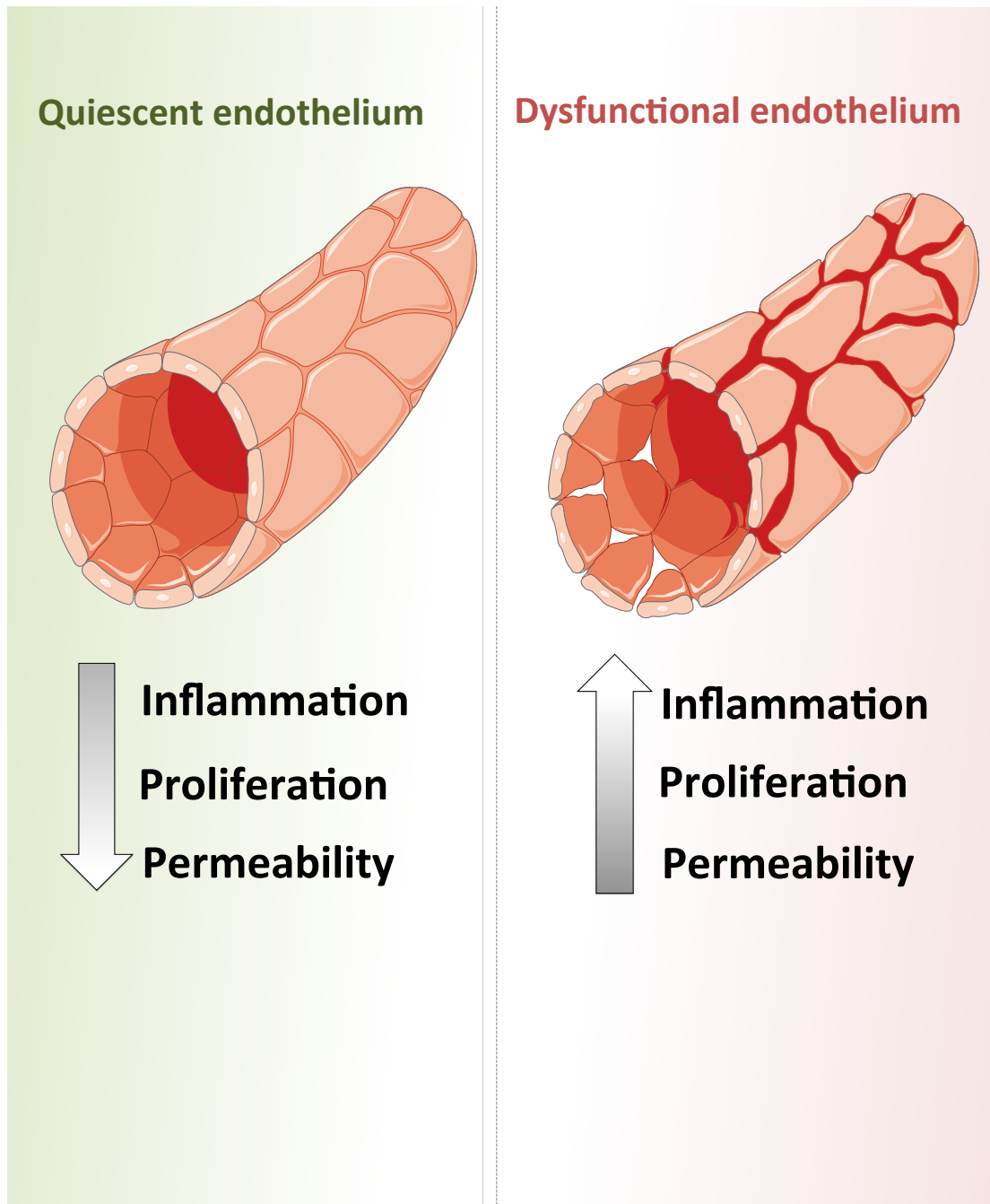


Figure 2. EC dysfunction. Quiescent EC control a balance between pro and anti inflammatory pathways which cause a low rate of inflammation, proliferation and permeability that maintains tissue homeostasis. EC loss of this balance between pro and anti inflammatory, proliferative pathways results in an increase in inflammation, proliferation and permeability, which mediates atherosclerosis.

Proatherogenic agents (such as, TNF- α and ox-LDL) also trigger EC apoptosis and proliferation, leading to elevated cell turnover (Chaudhury et al. 2010; Foteinos et al. 2008; Hansson et al. 1985; Davies et al. 1986). This is partly mediated by JNK inflammatory signalling, which has a direct effect on EC turnover (Chaudhury et al. 2010; Chen et al. 2011; Han, Y, Moon, J You, R, Kim, S. Z., Kim, S. H., Park 2009). Cell turnover, in turn, results in a transient loss of EC-EC contacts (Cancel & Tarbell 2011; Cancel & Tarbell 2010; Birukova et al. 2004; Forteinos et al. 2008) this further exacerbates permeability and inflammation. Moreover, increased EC proliferation promotes oxidative stress, which contributes to furthering inflammatory activation (Schaefer et al. 2006; Dong et al. 2005). Guevera *et al.* demonstrated that genetic deletion of the cell cycle regulator p53 resulted in an increase in EC proliferation and increased atheroseverity (Guevara et al. 1999), thus suggesting that EC proliferation plays a dominant role in atherogenesis. Consistent with this, genetic deletion of JNK lowered EC proliferation and inhibited atherosclerosis development (Amini et al. 2014), which further demonstrates the importance of EC proliferation in EC dysfunction and atherosclerosis.

Taken together, EC inflammation, proliferation and permeability in dysfunctional EC, positively feedback onto one another and contribute to the progression of atherosclerotic lesion formation and influence atherosclerosis development.

1.3 Wall shear stress (WSS)

EC lining the vessel wall are exposed to mechanical stresses that are mediated via the presence of pulsatile blood flow; these include circumferential stress, axial stress, and wall shear stress (WSS) (Hoefer et al. 2013). WSS, measured in dyne/cm² or in pascals (Pa=N/m²; 1 dyne/cm²= 0.1 Pa) is defined as the tangential drag force that is produced by the movement of blood flow on the surface of the endothelium (Cheng et al. 2006). WSS magnitude is directly proportional to blood viscosity and is

highly dependent on the vessel radius, the bigger the radius, the lower the WSS and *vice versa* (Davies 2009). WSS measurements can be derived using Poiseuille's law. The Hagen- Poiseuille equation is used to model blood flow characteristics of steady, laminar blood flow through a straight, circular tube;

$$\tau=4\mu Q/\pi R^3$$

The Hagen- Poiseuille equation shows that shear stress (τ) is directly proportional to the velocity of the fluid, the flow rate (Q) and fluid viscosity (μ). Flow velocity is directly determined by the flow rate (defined as volume of blood/ time) which in turn is dependent on the arterial radius. Shear stress is inversely proportional to the arterial radius (R) (Davies, 2009). WSS values in large arteries such as the aorta, descending thoracic aorta and carotid arteries range between 5-20 dyne/cm² in human and porcine systems (Cheng et al., 2006). Whereas in the murine system, due to smaller vasculature diameters these values range between 20-250 dyne/cm² (Suo et al. 2007).

The Poiseuille equation measures blood flow characteristics through a straight vessel (non-disturbed flow), however at areas of complex geometry such as at branches and bends, blood flow directionality becomes altered (disturbed flow). Reynolds number (Re) is used to define changes in flow directionality. Reynolds number is a dimensionless ratio of blood flow inertial and viscous forces;

$$\text{Re} = \text{inertial forces} / \text{viscous forces} = \rho V D / \mu$$

In the Reynolds equation, ρ is the density of blood, V is the velocity, D is the vessel diameter and μ is blood viscosity. High Reynolds numbers (≥ 4000) are reflective of a dominance of inertial forces over viscous forces, and are used to describe turbulent

flow. Whereas a low Re number is reflective of a dominance of viscous forces and thus laminar flow (Davies et al., 2009).

1.3.1 EC mechanosensing of WSS

EC translate external mechanical signals generated by WSS into biomolecular events through mechanosensing. Several mechanisms have been postulated to mediate EC mechanosensing. Tzima *et al.* identified a mechanosensory protein complex consisting of cluster of differentiation 31 (CD31), VE-cadherin and vascular endothelial cell growth factor receptor (VEGFR) 2 on the cell surface that mediates downstream signalling in response to WSS (Tzima et al. 2005; Conway et al. 2013). Furthermore, cell surface proteins such as glycocalyx glycoproteins and the primary cilium were shown to control calcium signalling and NO production in response to WSS, which further regulate other signalling pathways in EC (Yao et al. 2007; Florian et al. 2003; Nauli et al. 2008). Integrins are heterodimeric α/β chains that mediate cell–extracellular matrix interaction. Integrins transduce signalling downstream of mechanosensors, depending on the cellular context, thus acting as mechanical switches (Shyy & Chien 2002; Ingber 1991; Ingber 1998). However it is unlikely that the EC mechanotransduction is controlled by the activation of a single mechanosensor. The EC cytoskeleton is physically linked via protein interactions to all of the mechanosensors mentioned above, thus WSS-mediated deformations is likely to alter the activation of numerous mechanosensors at the same time, resulting in a wide mechano-response in EC. In summary, EC sense WSS through a number of mechanosensors and it is unknown whether there is a preferential activation of a combination of specific mechanosensors in response to certain magnitudes of WSS, or whether the same mechanosensors are activated by WSS which then regulate downstream signalling events depending on the WSS magnitude.

1.3.2 WSS and EC function

EC mechanotransduction in response to WSS results in the activation of signalling events that promote transcriptional and epigenetic changes, which in turn change EC function (Brooks et al. 2012; Passerini et al. 2004; Dunn et al. 2014; Jiang et al. 2015). *In vitro* experiments have enabled testing the direct effects of the exposure of WSS on EC function as a result of global transcriptional changes (summarised in table 1). Cytoskeletal reorganisations in response to WSS almost occur instantaneously, which subsequently cause changes in cell morphology (following ≥ 24 h of exposure to WSS). EC exposed to low WSS display a round, cobble-stone morphology, whereas cells exposed to high WSS display an elongated, aligned morphology (Brooks et al. 2012; Davies et al. 1986; Coon et al. 2015; Hahn et al. 2011).

Proinflammatory signalling pathways such as p38 MAPK, NF- κ B become activated in cells exposed to low WSS, whilst being suppressed in cells exposed to high WSS (Brooks et al. 2012; Passerini et al. 2004; Orr et al. 2005; SenBanerjee et al. 2004). This promotes the expression of inflammatory molecules such as VCAM-1, E-selectin and MCP1 (Brooks et al., 2004, Davies et al., 1986, Orr et al., 2005). Consistent with this, antioxidant molecules involved in anti-inflammatory signalling such as kruppel-like factor (KLF) 2, KLF 4, nuclear factor (erythroid-derived) (Nrf) 2 and endothelial nitric oxide synthase (eNOS) show increased expression in cells exposed to high WSS, whilst being suppressed in cells exposed to low WSS (Brooks et al. 2012; Fang et al. 2010; Chien 2008; Jiang et al. 2015; Fledderus et al. 2007). Thus, cells exposed to low WSS *in vitro* display increased inflammatory activation compared to cells exposed to high WSS that are anti-inflammatory. Moreover, cells exposed to low WSS display an increase in pathways that promote cell cycle progression, including Transforming growth factor β (TGF- β) signaling via Smad1/5 and p38 signalling, leading to increased turnover compared to cells exposed to high WSS (Davies et al. 1986; Zhou et al. 2012). In addition, following the exposure to low WSS, EC display higher EC permeability (Miao et al. 2005; Sill et al. 1995; Orsenigo et al. 2012).

Table 1. Summary of EC functions that are differentially regulated by exposure to WSS *in vitro*

EC function	Exposure to high WSS	Exposure to low WSS	Reference
Inflammation	Low	High	(Chaudhury et al., 2010, Passerini et al., 2004, Davies et al., 2001, Brooks et al., 2004)
Proliferation	Low	High	(Davies et al., 1986, Brooks et al., 2004)
Permeability	Low	High	(Warboys et al., 2010, Ding et al., 2012, Orsenigo et al., 2013)
Migration	Low	High	Tressel et al., 2007, Syzimanski et al., 2008)
Apoptosis	Low	High	(Davies et al., 1986, Passerini et al., 2004, Brooks et al., 2004)
Oxidative stress	Low	High	(Fang et al., 2009, Jiang et al., 2014, Zakkar et al., 2008, Chien et al., 2008)

Several mechanisms have been implicated, one of these mechanisms proposed by the Dejana group involves VE-cadherin phosphorylation by Src kinases that promote VE-cadherin degradation and a subsequent increase in EC junctional permeability to macromolecules (Orsenigo et al. 2012). A second mechanism is proposed by the Weinberg group this involves a pathway involving phosphatidylinositol-4,5-bisphosphate 3-kinase(PI3K) and NO signalling, which in turn could contribute in explaining the anti-inflammatory effects of NO on EC, by linking EC permeability and inflammatory protection in cells exposed to high WSS (Warboys et al. 2010). Therefore cells exposed to low WSS have higher junctional permeability compared to cells exposed to high WSS.

In summary, *in vitro* studies on EC exposed to WSS, have demonstrated that EC inflammation, proliferation and permeability, processes that underlie EC dysfunction are enhanced in cells exposed to low WSS. Whereas, cells exposed to high WSS display a quiescent phenotype. This suggests that blood-flow generated WSS plays a direct role in altering EC phenotype *in vivo* and subsequent vascular disease susceptibility.

1.4 Focal atherosclerosis and shear stress

Despite the presence of systemic and genetic risk factors, atherosclerosis shows a non-random distribution in the vasculature, with atherosclerotic plaques preferentially developing at branches and bends (Figure. 3). At these sites blood flow exerts low WSS (time-averaged mean value approximately 5 dyne/cm²), whereas atheroprotected areas are subjected to relatively high WSS (time-averaged mean value approximately 15 dyne/cm²) (Figure 4). The establishment of the effect of WSS on atherogenesis was derived based on the cumulative contribution of early studies; More than five centuries ago, the great scholar Leonardo Da Vinci was the first to observe that atherosclerosis formation in large arteries was focal and postulated the involvement of mechanical forces in disease pathology (Keele & KD. 1952).

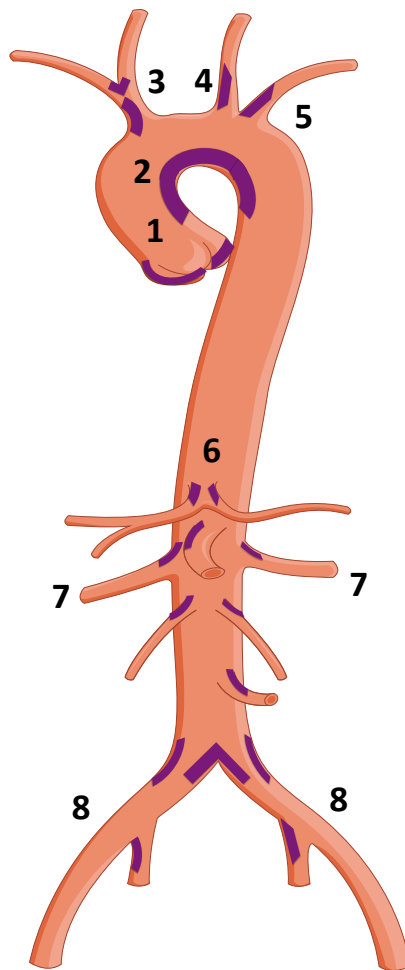


Figure 3. Focal atherosclerosis development. Atherosclerosis (plaques depicted as purple) shows a non-random distribution in the vasculature, where plaques tend to occur at regions that contain bends and branches; 1) Aortic sinus, 2) Inner aortic curvature, 3) Right carotid artery, 4) Left carotid artery, 5) Subclavian artery, 6) Thoracic descending aorta, 7) Renal artery, 8) Iliac artery.

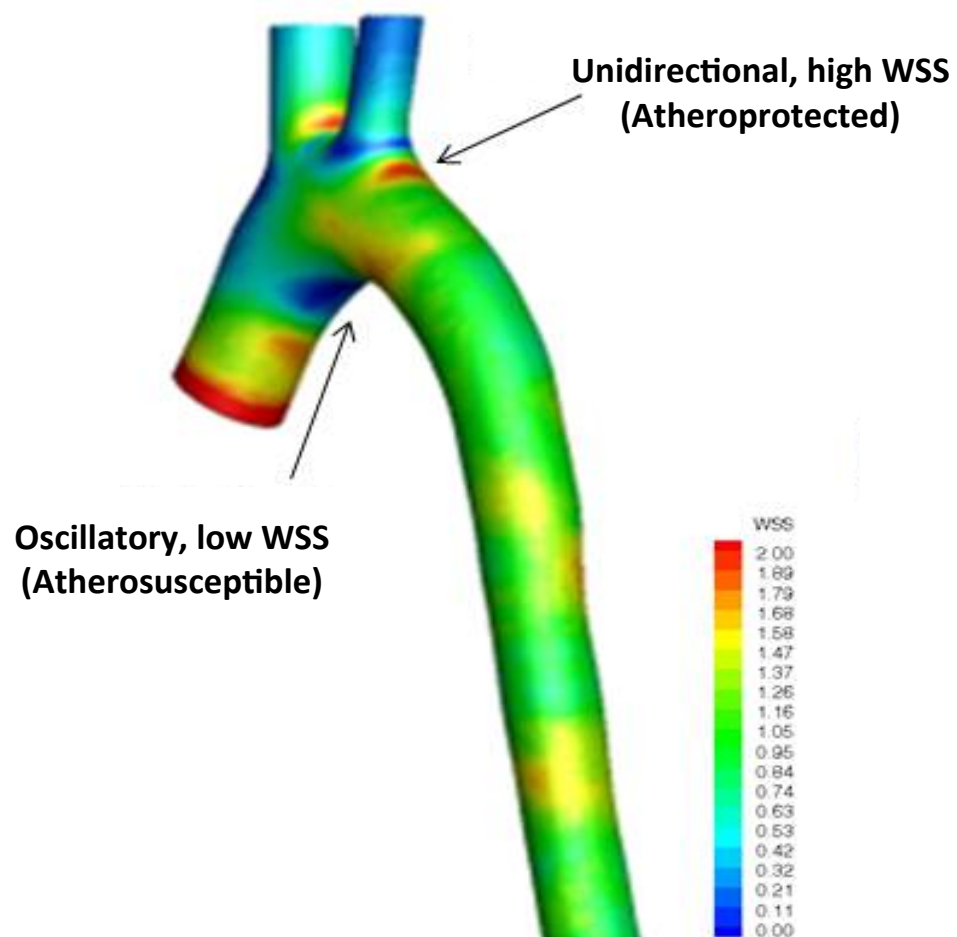


Figure 4. WSS patterns in the porcine aorta. WSS (Pa; N/m²) magnitudes are indicated in the WSS scale on the right. At the inner curvature of the porcine aortic arch, blood flow exerts oscillatory, low WSS. These regions are atherosusceptible. Whereas, at the outer curvature, flow exerts unidirectional, high WSS, which is atheroprotective. Image courtesy of Serbanovic-Canic, et al. Manuscript submitted.

In the 19th century, pathologists Rokitansky and Virchow concluded that differences in blood flow in the arterial tree differentially promoted lipid deposition and intimal thickening (Rokitansky 1855; Virchow 1971). In 1966, Caro *et al.* defined the flow characteristics that correlated with atherosclerosis based on simplified modelling of blood flow in the circulation, Caro *et al.*, measured the dispersion of a water and dye mixture through curved tubes. The observation correlated geometrical influences with varied flow pattern characteristics, and it was proposed that regions of the arterial tree containing bends and branches are exposed to flow disturbances as opposed to non-disturbed flow which occurs at straight and unbranched regions of the arterial tree (Caro 1966). Further experimental work by Caro *et al* on autopsy derived aortic casts showed that the regions of arterial vessels at bends and bifurcations were subjected to a low, oscillatory WSS (disturbed flow), while straight and un-branched regions were subjected to unidirectional, high WSS (non-disturbed flow) (Caro *et al*, 1971). Moreover, Caro *et al* noted that the distribution of atherosclerotic lesion in the arterial tree correlated with low, oscillatory WSS (Caro *et al*, 1971).

In vivo investigations in animal model systems further established the link between low, oscillatory WSS and the spatial distribution of atherosclerotic plaques (Gambillara *et al*, 2006a; Buchanan *et al*, 1999; Cornhill and Roach, 1976). *In vivo* experimentation involving computational fluid dynamics, coronary angiography along with magnetic resonance imaging provided a quantitative measure of WSS characteristics and the correlation with atherosclerotic plaque distribution (Wentzel *et al*, 2005; Stone *et al*, 2003; Steinman, 2002; Suo *et al*, 2007). Cheng *et al* designed a system in which the causal relationship between haemodynamic forces and atherogenesis was established, the experimental procedure involved the insertion of a constrictive cuff into the carotid arteries of atherosusceptible (high fat diet fed, apolipoprotein E (ApoE)^{-/-}) mice. The cuff altered flow, giving rise to high WSS within the constriction, low unidirectional WSS upstream and low, oscillatory WSS downstream of the constriction. Following 6 weeks of cuff insertion, atherosclerotic plaques occurred at regions subjected to low WSS (upstream and downstream of

cuff constriction), thus revealing that low WSS directly promoted atherosclerosis (Cheng *et al*, 2006).

1.4.1 Low WSS promotes EC dysfunction

1.4.1.1 Inflammatory activation

In vivo studies have reported that atheroprone, low WSS promotes EC dysfunction (EC inflammation, proliferation and permeability) and that high WSS promotes EC quiescence. Studies by our group and others on the murine aorta aortic arch have demonstrated that pro-inflammatory NF- κ B, p38 and JNK MAPK signalling preferentially occurred at sites of low WSS (inner curvature) compared to regions of high WSS (outer curvature) (Cuhlmann *et al.* 2011; Chaudhury *et al.* 2010). The activation of these pathways increased EC inflammation and proliferation, thus suggesting that low WSS promoted EC dysfunction via enhanced inflammatory signalling. Consistent with this, anti-inflammatory, anti-oxidant signalling mediated by Nrf2, KLF2 and KLF4 was inhibited in EC at sites of low WSS and activated in EC at sites of high WSS (Fledderus *et al.* 2007; Fang *et al.* 2010; Jiang *et al.* 2015; Zakkar *et al.* 2009; Chien 2008). Causal evidence for the activation of EC inflammation by low WSS provided by Cuhlmann *et al*, following the insertion of a flow constrictive cuff it was evident that RelA (a member of the NF- κ B family proteins) and VCAM-1 expression was markedly increased at sites exposed to low WSS compared to high WSS (Cuhlmann *et al*, 2011). Thus, demonstrating that low WSS triggers EC inflammatory activation and athero-susceptibility, whereas high WSS is protective (Cuhlmann *et al*, 2011, Jiang *et al*, 2015, Fang *et al*, 2010).

1.4.1.2 Proliferation

It was reported by Wright in 1972, that EC mitosis was enhanced at sites of low WSS, suggesting that low WSS promoted EC proliferation (Wright, 1972). It was later proposed that the preferential increase in EC proliferation at low WSS is mediated via Smad1/5 signalling (Zhou *et al*, 2012), JNK MAPK signalling (Chaudhury *et al.*, 2008) and by p21-mediated mechanisms (Obikane *et al.* 2007). These studies have demonstrated that EC proliferation is preferentially enhanced at low WSS sites. Inhibition of JNK signalling, reduced EC proliferation and apoptosis at sites of low

WSS and gave rise to a marked reduction in atherosclerosis development (Amini et al. 2014). Moreover, EC proliferation at low WSS sites *in vivo* correlates with ROS generation, DNA-damage and senescence, all of which have been linked with inflammatory activation (Reviewed in Andreassi 2008; Warboys et al. 2014). This reflects the relationship between low WSS-mediated EC inflammation and proliferation during EC dysfunction.

1.4.1.3 Permeability

Studies by the Weinberg group have shown that EC uptake of macromolecules was enhanced at bends and branches (areas of low, oscillatory WSS) in the arterial tree of rabbit and murine models (Staughton et al. 2001; Clarke et al. 2012; Mohri & Weinberg 2012). Moreover, the Weinberg group has shown that the enhancement of EC permeability is a direct response to low WSS. Mohri et al., measured EC permeability in constrictive-cuff inserted mouse carotid arteries. It was demonstrated that EC permeability as measured by tracer fluorescence was markedly increased at regions upstream and downstream of cuff constriction and that these sites correlated with plaque formation in ApoE^{-/-} mice sites, thus indicating that low WSS directly caused an increase in EC permeability and subsequently atherogenesis (Mohri & Weinberg 2012). Observations in the porcine aorta by Conklin et al., also showed that EC permeability was enhanced at low WSS sites in the arterial tree (Conklin et al. 2002). These studies therefore show that low WSS promotes EC permeability *in vivo*. As proposed by Miyazaki et al., the mechanism controlling EC permeability involves VE-cadherin proteolysis via calpain. This in turn gives rise to VE-cadherin junctional disorganisation and a loss of the EC-barrier function and subsequent inflammation (Miyazaki et al. 2011). Another mechanism for enhanced cell permeability at sites of low WSS is due to a consequence of increased cell turnover, which consequently gives rise to a transient loss of EC contacts (Cancel & Tarbell 2010; Cancel & Tarbell 2011; Birukova et al. 2004).

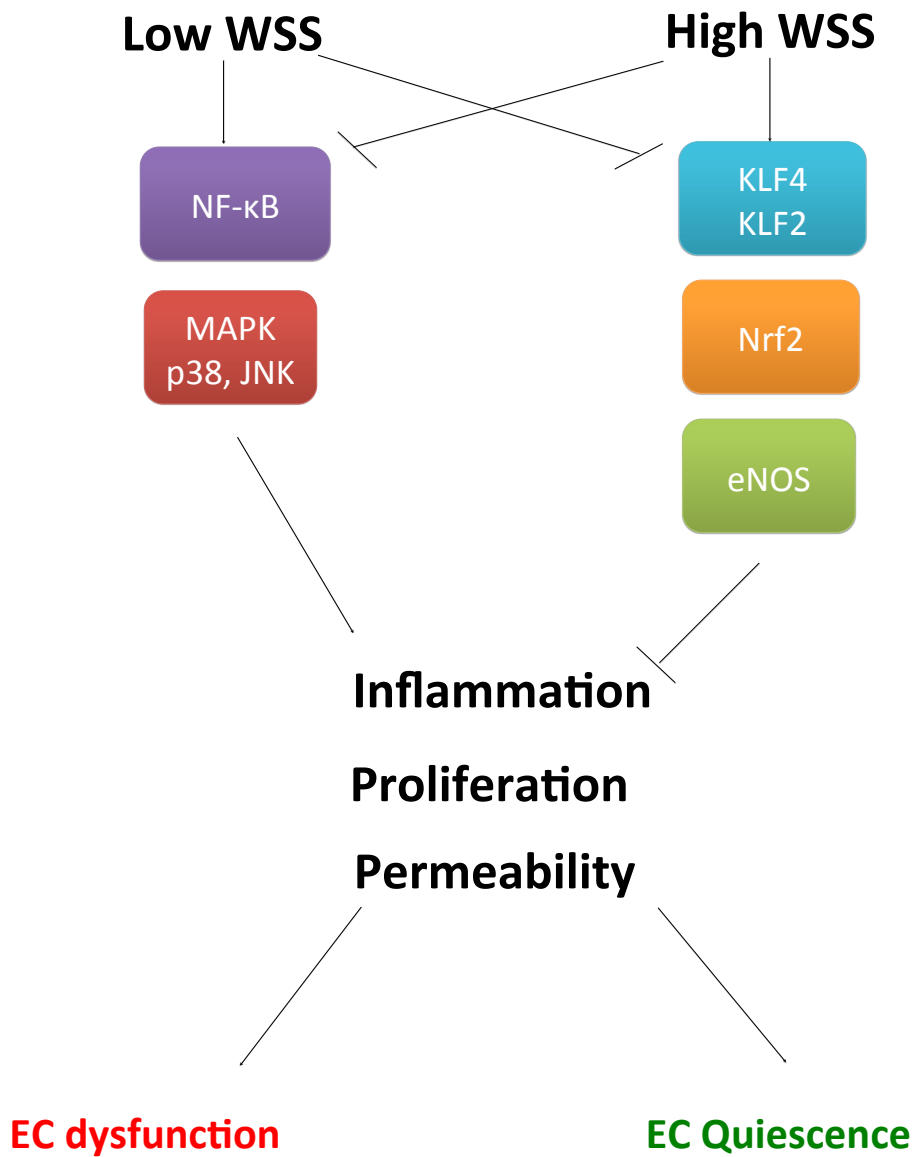


Figure 5. Summary of WSS-mediated regulation of focal EC dysfunction

In conclusion, low WSS plays a central role in governing the spatial distribution of atherosclerosis in the vasculature by promoting EC dysfunction (Figure. 5). Establishing the link between the low-WSS mediated regulation of NF- κ B, MAPK and antioxidant signalling has significantly contributed to the understanding of the molecular basis of focal EC dysfunction in atherogenesis. However there are ample avenues to be explored to fully understand the complexity of the molecular networks that govern focal EC dysfunction.

1.5 TWIST1

TWIST1 is a transcription factor that belongs to the beta-Helix-Loop-Helix (bHLH) family (Thisse et al. 1988). bHLH transcription factors are classified into three families; Class A, B and C. TWIST1 belongs to the class B family, alongside HAND2 and TWIST2. These transcription factors are characterised by having tissue-specific expression and forming heterodimers with class A bHLH transcription factors such as E47 and Id1 (Castanon & Baylies 2002). The Human Twist1 gene located at 7q21.2, contains one coding exon which encodes a 21 KDa protein (Wang et al. 1997) (Figure. 6). The N-terminus of the protein contains binding sites for histone acetyltransferases (HATs) proteins; cAMP-response element binding protein (CREB)-binding protein and p300/CBP-associated factor (PCAF). This interaction enables Twist1 to inhibit the HAT activities of these proteins and the suppression of target gene expression (Hamamori et al. 1999). The N-terminus also contains nuclear localisation signals to mediate Twist1 localisation to the nucleus where it can bind to conserved DNA E-box sequences (5' NCANNTGN-3') located in the regulatory regions of many genes to promote gene transcription (Murre et al. 1989).

TWIST1 was originally discovered in *Drosophila*, as one of the genes essential for mesoderm specification (Thisse et al, 1987). *Drosophila* embryos lacking the Twist1 gene died at embryogenesis with a “twisted” appearance, hence the name of the gene (Thisse et al, 1987). The Twist1 gene is highly conserved, where the Human TWIST1 bHLH domain shares 96% homology to the *Drosophila* TWIST1 and 100% homology to the mouse TWIST1 bHLH domains (Howard et al. 1997).

TWIST1

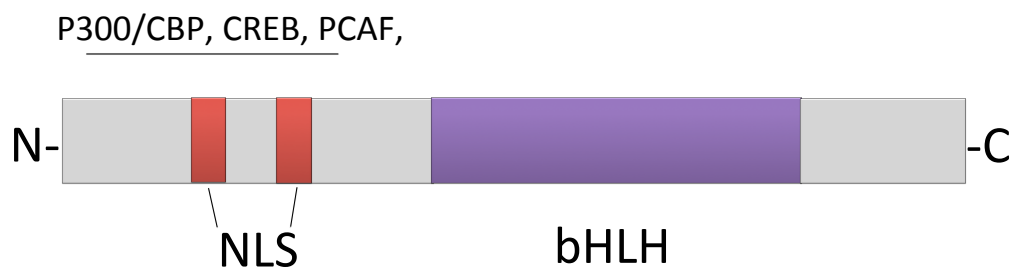


Figure 6. TWIST1 protein domain structure. The human TWIST1 protein (21 kDa) contains two nuclear localisation signals (NLS) at the N-terminal. At this region, chromatin remodelling proteins (P300/CBP, CREB and PCAF) bind and modulate Twist1 function. A beta-Helix-Loop-Helix (bHLH) domain is required for Twist1 binding to target DNA sequences.

In humans, *Twist1* genetic mutations give rise to Saethre-Chotzen, a rare autosomal dominant disease with a population incidence of 1 in 2,000, which is characterised by craniocytosis (premature closure of the clavial (skull) structure), (Bourgeois et al. 1998). Heterozygous *Twist1*^{+/-} mice demonstrate craniofacial defects, thus resembling those from Saethre-Chotzen patients and developmental abnormalities in the limb. Whereas *Twist1* null mice are embryonically lethal (Chen & Behringer 1995).

1.5.1 The role of TWIST1 in development

TWIST1 plays an indispensable role during multiple stages of embryonic development, from controlling mesodermal differentiation during gastrulation estimated at embryonic day (E) 6 in murine embryonic development, up to controlling valve formation at E 16 (Reviewed in Qin et al. 2012).

During early embryonic development, gastrulation gives rise to three germ cell layers; the ectoderm, mesoderm and endoderm. This process is highly intricate and is tightly controlled by multiple transcriptional regulators including TWIST1, which is central to mesoderm formation and specification and the differentiation into different tissue types (cardiac, skeletal and epithelial tissue) (Nusslein-Volhard et al. 1987; Thisse et al. 1988). TWIST1 is also essential at controlling body patterning in the developing embryo, specifically at controlling the dorsal-ventral axis, which is established via the formation of a TWIST1 expression gradient (Simpson 1983).

In later stages in embryogenesis, TWIST1 acts as a master regulator of the osteoblast differentiation program by controlling the activity of downstream pathways that are central to osteoblast differentiation and development, including fibroblast growth factor (FGF) and bone morphogenic protein (BMP) signalling by controlling FGFR2, FGF8, FGF10, and BMP4 transcription (Bialek et al. 2004; Connerney et al. 2008; Loebel et al. 2002; Rice et al. 2010). TWIST1 also controls the expression of RUNX2, a critical osteoblast-differentiation transcriptional regulator that is essential for bone formation (Bialek et al, 2004). TWIST1 controls limb formation and muscle cell

differentiation, via controlling FGF, BMP and sonic hedgehog (SHH) signalling pathways (O'Rourke et al. 2002). The formation of the heart valve involves the differentiation of progenitor cells of the endocardial cushions to mature valve interstitial cells (VIC) that are underlined by extracellular matrix proteins (ECM), (Reviewed in Wirrig & Yutzey 2014). TWIST1 controls endocardial cushion cell proliferation and migration via controlling the transcriptional activation of T-box protein (*Tbx*) 20, *Mmp13* and *cadherin-11* (Chakraborty et al. 2010). This promotes the migration of endocardial cushion cells into the intervening ECM known as cardiac jelly where the endocardial remodels into mature valve leaflets. Finally, TWIST1 drives hematopoietic lineage differentiation by driving myeloid (macrophages) and lymphoid (T and B-lymphocyte) cell development (Reviewed in Merindol et al. 2014).

TWIST1 shares 66% sequence homology with TWIST2, however both proteins play non-redundant, distinctive roles during development (Reviewed in Franco et al., 2011). Moreover *Twist2 null* mice display normal embryogenesis, but die 3 days after birth of cachexia (Šošić et al. 2003), thus suggesting that TWIST1 plays a more dominant role in early embryogenesis.

1.5.2. The role of TWIST1 in adult disease

In the adult, under normal conditions TWIST1 is expressed in adult stem cells of the bone marrow and its expression in other adult cells is rarely reported (Zhao & Hoffman 2004; reviewed in Figeac et al. 2007). However in the disease context, TWIST1 is a prominent oncogene that drives the progression of many types of cancer including breast, gastric, pancreatic, bladder and oesophageal cancer (Reviewed in Qin et al. 2012). The discovery of the role of *Twist1* in cancer was by Yang *et al.* To investigate the molecular mechanism underlying tumour survival and metastasis Yang et al., injected four types of mammary tumour cell lines into mice to induce tumour formation *in vivo* and carried out microarray analysis on isolated tumours from the mice. The study revealed that *Twist1* was one of the most highly expressed genes and that its expression correlated positively with the metastatic potential of the isolated tumours. Consistent with this, the expression of TWIST1 was detected in

human tumour cells, more prominently in more invasive and metastatic tumour types. Moreover, Yang *et al.*, further demonstrated that Twist1 controls tumour metastasis by treating tumour cell lines with Twist1-specific oligonucleotides following injection into mice. It was revealed that Twist1-siRNA treated tumours showed a marked reduction in tumour severity and metastasis compared to control-siRNA treated tumours (Yang *et al.* 2004). Therefore, the study by Yang *et al.*, clearly established a prominent role of TWIST1 in driving cancer cell metastasis. The mechanism by which TWIST1 drives metastasis and invasion is via N-cadherin, Platelet derived growth factor receptor α (PDGFR α), AKT2 and MMPs (Niu *et al.* 2007; Eckert *et al.* 2011; Feng *et al.* 2009).

Alongside its prominent role in metastasis TWIST1 promotes cancer by driving proliferation. Microarray analyses on cancer cells either overexpressing Twist1 or treated with Twist1 siRNA revealed that TWIST1 positively regulated the expression of genes known to be involved in cell proliferation, these included cyclin D1, sushi-repeat containing protein, X-linked (SrpX), epidermal growth factor receptor tyrosine kinase (ErbB)3 and myeloblastosis transcription factor (Myb) in cancer cells (Feng *et al.* 2009). Consistent with the role of TWIST1 in cancer cell survival, TWIST1 suppressed apoptosis by inhibiting tumour suppressor genes p53 and retinoblastoma (Rb) (Maestro *et al.* 1999). By doing so TWIST1 promotes cancer cell survival and resistance to chemotherapeutic drugs (Wang *et al.* 2003). Therefore, since the inhibition of tumour metastasis is an aim of anti-cancer drug targets, TWIST1 makes a prominent therapeutic target and currently TWIST1-specific therapeutics are being developed.

TWIST1 is involved in the pathogenesis of several fibrotic disorders these include renal fibrosis where TWIST1 promotes fibrotic development via driving epithelial cell proliferation and inflammation in hypoxia-induced and in injury-induced renal fibrosis (Sun *et al.* 2009; Lovisa *et al.* 2015). Interestingly, Lovisa *et al.*, have recently shown that Twist1 gene suppression was sufficient to significantly reverse renal fibrosis (Lovisa *et al.* 2015) thus reflecting the dominant role of TWIST1 in this process. In addition, recently Ranchoux *et al.* demonstrated that TWIST1 expression

was increased in pulmonary arterial hypertension (PAH) patients compared to healthy controls, suggesting that there is a correlation between TWIST1 expression and disease pathogenesis (Ranchoux et al. 2015).

Heart valve disease commonly known as aortic valve stenosis is characterised by enhanced proliferation of EC lining the aortic valves and the formation of fibrotic calcified caps. Within the fibrotic core angiogenesis and neovascularisation take place, which further exacerbate fibrotic growth. The fibrotic cap creates a stenosis in the valve leaflets, which impedes blood flow (Reviewed in Leopold 2012; Wirrig & Yutzey 2014). TWIST1 plays a central role in mediating aortic valve stenosis as evidenced by its enhanced expression along with its target genes Runx1 and Bmp4 and Bmp2 in human aortic valve disease patients compared to healthy controls (Chakraborty et al. 2010; Wirrig & Yutzey 2014). Chakraborty *et al.*, overexpressed Twist1 in mouse models this resulted in valve fibrosis and calcification, thus providing a direct evidence for the involvement of TWIST1 in mediating aortic valve disease (Chakraborty et al. 2010).

Interestingly, cancer metastasis is described as a “disrupted developmental phenotype” (Ishii & Saito 2008) and the “return of a fetal gene program” (Leopold, 2012) has been described for the pathogenesis of aortic valve stenosis. A common factor in the induction of these adult disease processes is the activation of TWIST1 expression. This suggests that TWIST1 plays a dual role in organismal biology where it mediates beneficial processes required for organismal development during embryogenesis, whereas in the adult TWIST1 controls processes that encompass a detrimental impact.

1.5.3 The regulation of TWIST1 in development and disease

The regulation of TWIST1 occurs via transcriptional and post-transcriptional mechanisms during development and in disease (Summarised in Figure. 7). During embryonic development the gene expression of Twist1 in the mesoderm is controlled by the combination of SHH and FGF signalling, interestingly SHH or FGF signalling in separation do not induce Twist1 expression (Hornik et al. 2004) suggesting that only when both signalling pathways are present Twist1 expression is mediated. Moreover TWIST1 controls the expression of FGF and SHH later on during embryonic development, during mesoderm cell specification into osteoblast, suggesting that there is a positive feedback loop, where SHH and FGF promote TWIST1 expression then TWIST1 feeds back to activate these pathways (Hornick et al. 2004). In the developing valves TWIST1 expression is controlled by BMP2-Smad signalling, which then subsequently mediates TWIST1-mediated endocardial cushion cell differentiation (Ma et al. 2005). Consistent with the positive feedback between FGF and SHH signalling with TWIST1, this positive feedback loop exists between BMP signalling as TWIST1 promotes Bmp2 and 4 expression during limb formation (Bialek et al. 2004; O'Rourke et al. 2002).

In cancer cells Twist1 gene expression is regulated by STAT3 (a transcription activator belonging to the Janus kinase/ signal transducer and activator of transcription (JAK/STAT) family of proteins)). The regulation of TWIST1 by STAT3 was essential for the induction of metastasis (Cheng et al. 2008) suggesting that STAT3 is one of the upstream molecular mechanisms that promotes TWIST1 expression during metastasis. NF- κ B signalling via p65/RelA has been linked with the transcriptional activation of TWIST1 and metastasis of non-small lung cell carcinoma (nSLCC) and in breast cancer (Liu et al. 2015; Yang et al. 2004; Yang et al. 2008). This suggests that NF- κ B signalling could be acting as a switch alongside STAT3 signalling in promoting TWIST1-mediated cancer cell metastasis. TWIST1 is reported to be a direct target of hypoxia inducible factor- α (HIF1 α) in hypoxia-mediated renal fibrosis, reflecting that Twist1 is activated by hypoxic conditions (Sun et al. 2009).

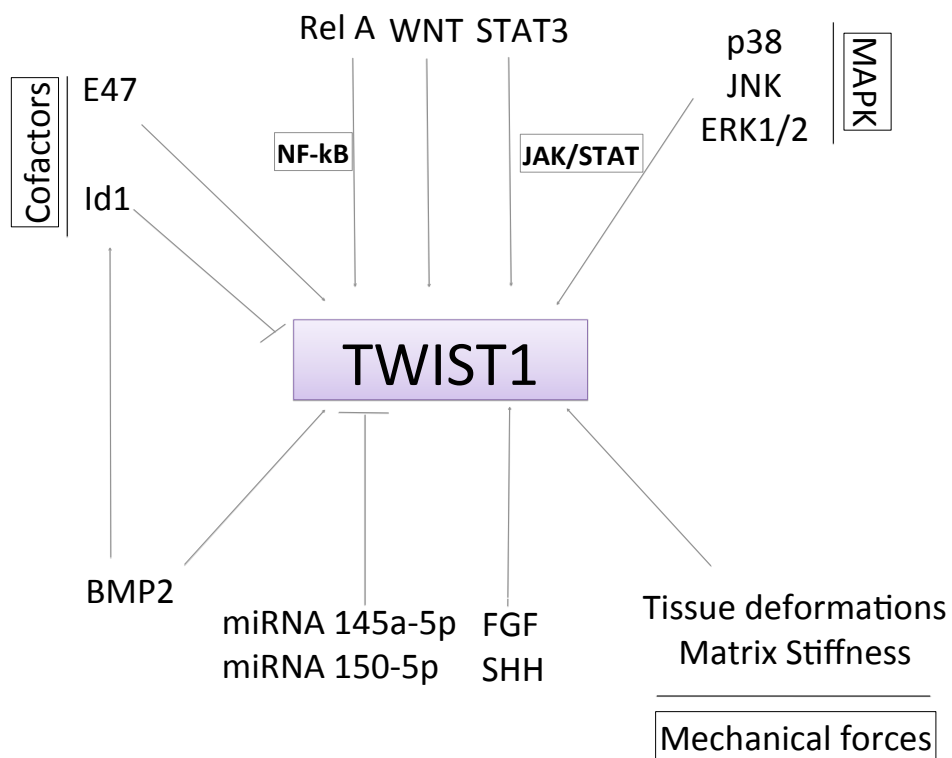


Figure 7. Summary of molecular regulation of TWIST1

Micro RNA molecules (miRNAs) are also proposed to control TWIST1 expression. Nairismägi *et al* showed that miR145a-5p and miR151-5p repressed Twist1 expression and inhibited cancer cell survival, proliferation, invasion and metastasis in a number of human cancer cell lines, suggesting that the regulation of Twist1 in cancer metastasis also occurs via regulatory RNA (Nairismägi et al. 2013).

Post translationally TWIST1 protein stabilisation occurs via phosphorylation mechanisms. MAPK signalling through p38, JNK and extracellular-signal-regulated kinases (ERK)1/2 promotes phosphorylation of TWIST1 at serine-68 (Hong et al. 2011). This modification protects Twist1 from degradation through ubiquitination. In addition, MAPK-mediated phosphorylation of TWIST1 is regulated by TGF- β signalling in cancer cells. Furthermore, TWIST1 stability is controlled by its formation of specific heterodimers from the class A of bHLH proteins. For example, TWIST1 interaction with E47 promotes TWIST1 protein stability, whereas interaction with Inhibitor of DNA 1 (ID1) promotes TWIST1 destabilisation and ubiquitous degradation (Ghouzzi et al. 1997). Interestingly ID1 expression is driven by BMP signalling during early stages of embryonic development, which is important for the spatio-temporal regulation of TWIST1 in the embryo that is required for body patterning (Das & Crump 2012).

TWIST1 expression is controlled by mechanical forces in development and in cancer. In the *Drosophila* embryo TWIST1 is responsive to mechanical cues such as tissue deformations. The mechanical activation of Twist1 in the study by Desprat *et al* was reported to be mediated by β -catenin WNT signalling (Desprat et al. 2008). Whereas in cancer cells Twist1 expression was enhanced by an increase in matrix stiffness in tumour cells (Wei et al. 2015). Interestingly, TWIST1 can directly alter the mechanical properties of cells, Gajula et al. show that Twist1 overexpression in cancer cells increased matrix stiffness and cell traction forces (defined as the tangential tension exerted on the ECM) at the migratory front of metastatic cells, thus enabling enhanced cell metastasis (Gajula et al., 2013). Therefore in addition to mechanical forces regulating Twist1 expression, it can also directly alter the

mechanical properties of cells, which could act as a positive feedback loop to maintain Twist1 expression and could activate other mechanoresponsive genes.

1.6 GATA4

GATA4 is a zinc finger transcription factor that belongs to the GATA family of transcription factors, containing GATA1-GATA6 proteins. GATA proteins play non-redundant roles and display tissue-specific expression; GATA1-3 are more closely related in sequence and are predominantly expressed in the hematopoietic system, whereas GATA4-6 are more closely related and are expressed in the cardiovascular system and the gonads (Zhou et al. 2012). The human *Gata4* gene (located at 8p23.1) encodes a 44.6 kDa protein (Figure. 8), which contains two Zinc finger domains, located at the N and C- terminals of the protein, along with a NLS domain at the C-terminal. The zinc finger domains are highly conserved between GATA1-6, with a 75% sequence homology and across species (Zhou et al. 2012). The zinc finger domain is conserved. This zinc finger domain enables GATA4 to bind to its target GATA box sequence (A/TGATAA(G)) that is located in the regulatory region of target genes (Zhou et al. 2012). The first GATA protein to be discovered was GATA1, Tsai et al. identified GATA1 as part of the study that investigated transcription factor regulation of erythrocyte immunoglobulin genes (Tsai et al. 1989). Based on sequence homology GATA 2-6 were then later identified.

Gata4 null mutations in mice are embryonically lethal due severe defects in heart development. Heterozygous *Gata4*^{+/-} mice are viable but they suffer from cardiac hyperplasia, heart valve defects along with sexual development disorders (Jay et al. 2007; Rajagopal et al. 2007; Lourenço et al. 2011). In humans, mutations in *Gata4* are linked in sporadic and familial cases of congenital heart disease and have been reported to cause gonad development abnormalities (Wang et al. 2013; Rajagopal et al. 2007).

GATA4

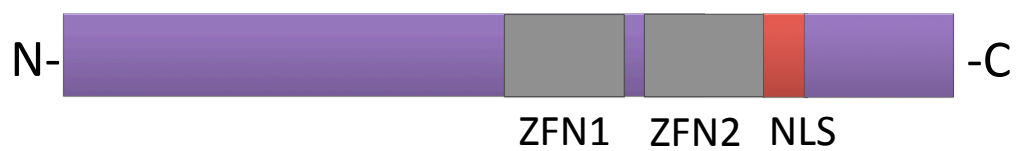


Figure 8. GATA4 protein domain structure. The human GATA4 protein (41.5kDa) contains two zinc finger (ZFN1) binding domains, which facilitate GATA4 binding to DNA target sequences. A nuclear localisation signal is located at the C-terminal to allow nuclear expression and transcriptional activity.

1.6.1 The role of GATA4 in development

The process of mammalian heart development begins with looping of the early heart tube (consisting of cardiomyocytes and endothelial cells), which then becomes divided into four chambers that are separated by heart valves, this process is controlled by a tightly regulated cardiac transcriptional network. GATA4 is regarded as a master cardiac transcription factor as it sits upstream of the transcriptional gene network controlling heart development, including myocyte enhancer factor (Mef)2c, NK2 homeobox 5 (Nkx2.5), serum response factor (Srf) and Hand2 (Schlesinger et al. 2011; McFadden et al. 2000; Zeisberg et al. 2007). Grepin *et al.* established the dominant role of GATA4 in cardiac development by revealing that Gata4 overexpression in pluripotent P19 embryonal carcinoma cells committed the cells to undergo differentiation to the cardiac lineage and gave rise to beating cardiomyocytes (Grépin et al. 1995). Genetic inhibition of Gata4 restricted beating cardiomyocyte differentiation (Grépin et al. 1995) thus indicating that Gata4 expression is required to drive cardiomyocyte differentiation. A study by Takeuchi and Bruneau demonstrated that ectopic expression of Gata4 alone triggered cardiomyocyte differentiation of uncommitted mesodermal cells (Takeuchi & Bruneau 2009). Strikingly, the ectopic expression of Gata4 in combination with cardiac transcription factors Mef2c and Tbx5 reprogrammed fibroblasts into cardiomyocytes (Ieda et al. 2010). These studies have demonstrated that GATA4 is an essential driver of cardiomyocyte differentiation. Studies carried out on Gata4 deficient embryos (which died during embryonic development) demonstrated the requirement of Gata4 in the formation of the early heart tube and subsequent looping and compartmentalisation. GATA4 is essential for the regulation of several compartments of the developing heart, including the epicardium, myocardium and endocardium. Consistent with this, GATA4 deficiency promotes valve defects as it is required to promote in endocardial cushion cell differentiation and maturation (Rivera-Feliciano et al. 2006).

GATA4 also plays important roles in non-cardiac development where it is required for the regulation of sex determination and differentiation in mammals (Tevosian et al. 2002; Hu et al. 2013). GATA4 expression was detected in the early genital ridge (an early precursor of the testis or ovary) and was required to promote genital ridge differentiation by controlling the expression of downstream transcriptional regulators Sry, Lhx9 and Sf1 (Hu et al. 2013).

1.6.2 The role of GATA4 in adult disease

Under non-disease conditions in the adult GATA4 promotes tissue homeostasis by regulating endothelial and cardiomyocyte proliferation and apoptosis. Oka *et al.* demonstrated that cardiomyocyte-specific deletion of Gata4 in mice reduced hypertrophic responses following pressure overload of the ventricles (Oka et al. 2006). Therefore in the adult GATA4 controls cardiac homeostasis by controlling hypertrophy, which is required for normal heart function. This function of GATA4 is proposed to be controlled by p38 MAPK signalling (Oka et al. 2006). GATA4 also promotes cardiac repair following injury, Heineke et al. demonstrated that GATA4 promotes a pro-proliferative phenotype and promoted the expression of an angiogenic gene profile (containing VEGF and Angptl2) in adult cardiomyocytes and endothelial cells of the heart following ischemic cardiac injury (Heineke et al. 2007). GATA4, along with MEF2C and TBX5 regulate cardiac repair and cardiomyocyte generation following myocardial infarction in murine hearts (Inagawa et al. 2012).

Under disease conditions GATA4 expression is linked with a range of cancers in the gastrointestinal tract, the lungs, ovaries and the brain (Reviewed in Zheng & Blobel 2010). GATA4 is proposed to be a potent prognostic predictor in the development of breast carcinoma- Takagi et al. reported that GATA4 expression was detected in early human breast carcinoma tissue and its expression increased in late-stage metastatic breast carcinoma tissue, indicating that GATA4 promotes tumour survival and metastasis (Takagi et al. 2014). The mechanism by which GATA4 promotes cancer survival involves the activation of pro-proliferative target genes. Recently, Chia et al. revealed that GATA4 forms a complex with GATA6 and KLF5 and this

complex promotes the expression of hepatocyte nuclear factor- alpha (HNF- α) expression, which in turn was required to promote gastric cancer proliferation (Chia et al. 2015). In Granulosa cell tumours GATA4 was shown to protect ovarian granulosa cells from apoptosis via promoting the expression of anti-apoptotic Bcl-2 gene (Kyrönlahti et al. 2008). Moreover, GATA4-mediated inhibition of granulosa cell apoptosis was responsible for resistance to TRAIL-induced apoptosis (Kyrönlahti et al. 2010). This suggests that alongside the role of GATA4 in promoting cancer cell proliferation it promotes cancer cell survival by inhibition of apoptosis. GATA4 expression by MYC-induced epigenetic activation was shown to be important for the induction of metastasis in lung adenocarcinoma cancer cells (Castro et al., 2013). The potential mechanism by which GATA4 drives cancer cell metastasis includes the activation of N-cadherin expression (Reviewed in Zheng & Blobel 2010). In summary, these studies demonstrate that Gata4 acts as an oncogene via promoting cancer cell survival, proliferation and metastasis. However, a study by Agnihotri *et al.*, suggested GATA4 can act as a tumour-suppressor in glioblastoma. Agnihotri *et al.* revealed that mutations in Gata4 that resulted in reduced expression correlated with a reduction in astrocyte proliferation, suggesting that GATA4 inhibited astrocyte proliferation and cancer survival (Agnihotri et al. 2011). Consistent with this, GATA4 was recently shown to positively regulate cellular senescence in fibroblasts in response to DNA damage (Kang et al. 2015). Since p53-mediated cellular senescence is a known tumour suppressor mechanism this study provided further evidence for the role of GATA4 as a tumour suppressor gene. Therefore, the role of GATA4 in cancer is context dependent, which reveals the complex nature of GATA4-mediated changes in cell function in disease and in development.

1.6.3 Regulation of GATA4 in development and disease.

Regulatory control of GATA4 occurs at transcriptional and post-transcriptional levels (Summarised in figure. 9). GATA4 is regulated at the transcriptional level in cardiac cells by both canonical WNT signalling through β -catenin and by non-canonical WNT signalling through nuclear factor of activated T-cells (NFAT) (Lin & Xu 2008; Sussman et al. 1998; Morad & Suzuki 2000). During cardiac hypertrophy and fibrosis following injury, GATA4 expression is mediated by C-Rel-mediated NF- κ B signalling (Gaspar-Pereira et al. 2012). Another pathway that controls GATA4 expression is the BMP pathway, Rojas *et al* demonstrated that BMP4 directly promotes GATA4 expression through Smad proteins in the lateral mesoderm during early embryonic development (Rojas et al. 2005). Additionally, GATA4 expression is regulated by cardiac-specific miRs. Studies by Callis *et al.*, and Ikeda *et al.*, revealed that miR208 and miR1 deficient mice showed a marked reduction in Gata4 expression, thus revealing that miRs 208 and 1 positively regulate Gata4 expression (Ikeda et al. 2009; Callis et al. 2009).

GATA4 DNA binding to target sequences is stabilised by interactions with cofactors and transcription factors. One of these co-factors is friend of GATA (FOG)-2. Whilst FOG 2 alone does not control gene expression, it physically interacts with GATA4 and stabilises GATA4 target gene activation. Ablation of FOG 2-GATA4 interaction in murine embryos, gave rise to embryonic lethality due to defects in heart morphogenesis and valve development (Rivera-Feliciano et al. 2006; Zhou et al. 2009). In addition, Chip-seq analyses in cardiomyocytes showed that FOG 2 binding coincided with all GATA4 binding sites (Zhou et al. 2009). These observations provide strong evidence for the regulation of GATA4 DNA binding by interaction with the cofactor FOG 2. Consistent with this, GATA4 interaction with transcription factors GATA6, TBX5 and MEF2C further stabilises GATA4 transcriptional activation during development and in cancer cells (Chia et al. 2015; Charron et al. 1999; Garg et al. 2003; Lee et al. 1998). Thus, demonstrating the importance of GATA4 interactions with transcription factors and cofactors in promoting downstream gene activation.

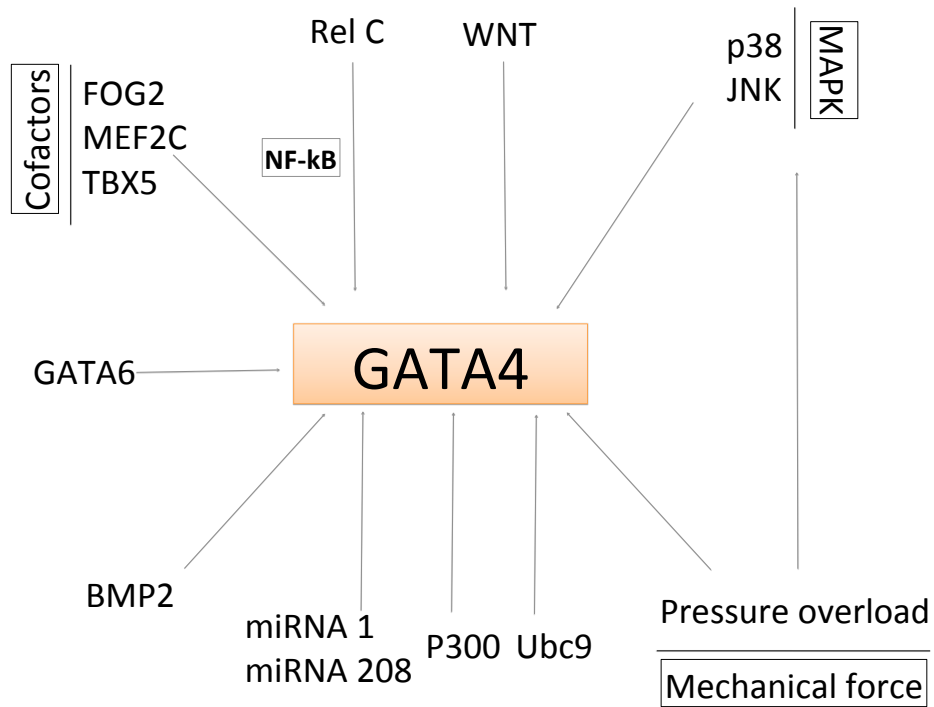


Figure 9. Summary of molecular regulation of GATA4.

At the protein level, GATA4 is stabilised by post-translational modifications-phosphorylation, sumoylation and acetylation. Following pressure overload in the ventricles, p38 MAPK promotes phosphorylation at serine-105. This phosphorylation was required for mediating GATA4 transcriptional activation of target genes involved in hypertrophy (Tenhunen et al. 2004). The direct effects of MAPK-mediated GATA4 phosphorylation was tested by genetic substitution of serine-105 residue into alanine, which inhibited GATA4-mediated hypertrophy (van Berlo et al. 2011). Therefore GATA4 phosphorylation by p38 is required during hypertrophy. Furthermore, GATA4 sumoylation at lysine-366 by SUMO-conjugating enzyme Ubc9 increased GATA4 transcriptional activity. Similarly, GATA4 acetylation by P300 had a stabilising effect on GATA4 DNA binding activity. These studies revealed that GATA4 DNA binding activity and transcription of target genes is enhanced by post-translational modifications. Recently, GATA4 activity was shown to be controlled by p62 mediated autophagy and subsequent degradation. GATA4 autophagy was inhibited following the activation of DNA damage sensors ATM/ ATR, which subsequently released GATA4 from p62 interaction, to allow GATA4 to induce cellular senescence (Kang et al. 2015). Thus GATA4 autophagy was proposed to act as a “control switch” of cellular senescence in this study (Kang et al. 2015). Interestingly, Tenhunen *et al* proposed that mechanical forces could regulate GATA4 activity. This was directly revealed by GATA4 enhanced expression following balloon-inflation in isolated rat ventricles (Tenhunen et al. 2004).

1.7 Endothelial-mesenchymal-transition

Endothelial-mesenchymal transition (EndMT) is a form of cellular transformation of mature endothelial cells into a mesenchymal, plastic phenotype (Figure. 10). EndMT was discovered by Markwald et al., where it was observed that cells of the endocardium transformed into a mesenchymal state during valve formation (Markwald et al. 1975). EndMT is closely related to a parallel process that occurs in epithelial cells; known as epithelial mesenchymal-transition, which was identified in 1894 by Platt in *Drosophila* gastrulation (Platt 1894). Thus EndMT is a specialised form of EMT. During EndMT (Figure. 10) cells express mesenchymal gene markers such as Twist1, Snail, Slug, N-cadherin and α -SMA. These mesenchymal genes drive phenotypic changes that involve the loss of EC markers VE-cadherin and CD31 and subsequent loss of tight cell-cell contacts. These changes are followed by changes in cell function including enhanced cell proliferation and migration. Ultimately EndMT-undergoing cells separate from the monolayer and penetrate the underlying ECM (a process referred to as delamination) and become highly migratory and invasive (Lim & Thiery 2012a). Therefore enhancements in cell proliferation, migration and invasion are all functional outputs of cells undergoing EndMT.

1.7.1 Overview of molecular mechanisms controlling EndMT

There are close parallels between the molecular mechanisms that control EMT and EndMT, which further supports the close relation between the two processes. Since this thesis is more focused on EndMT, the molecular mechanisms that control EndMT will be discussed.

Members of the TGF- β cytokine family, including BMPs and TGF- β subfamilies are examples of well-studied molecular switches of EndMT. TGF- β and BMP binding to TGF- β receptors types 1 (TGF- β receptor 2, ALK1 and 5) and type 2 (BMP R2) promotes the phosphorylation of Smad (Smad 1-5 and 8) transcriptional regulators, which move into the nucleus and activate downstream target genes (Reviewed in (Lim & Thiery 2012)).

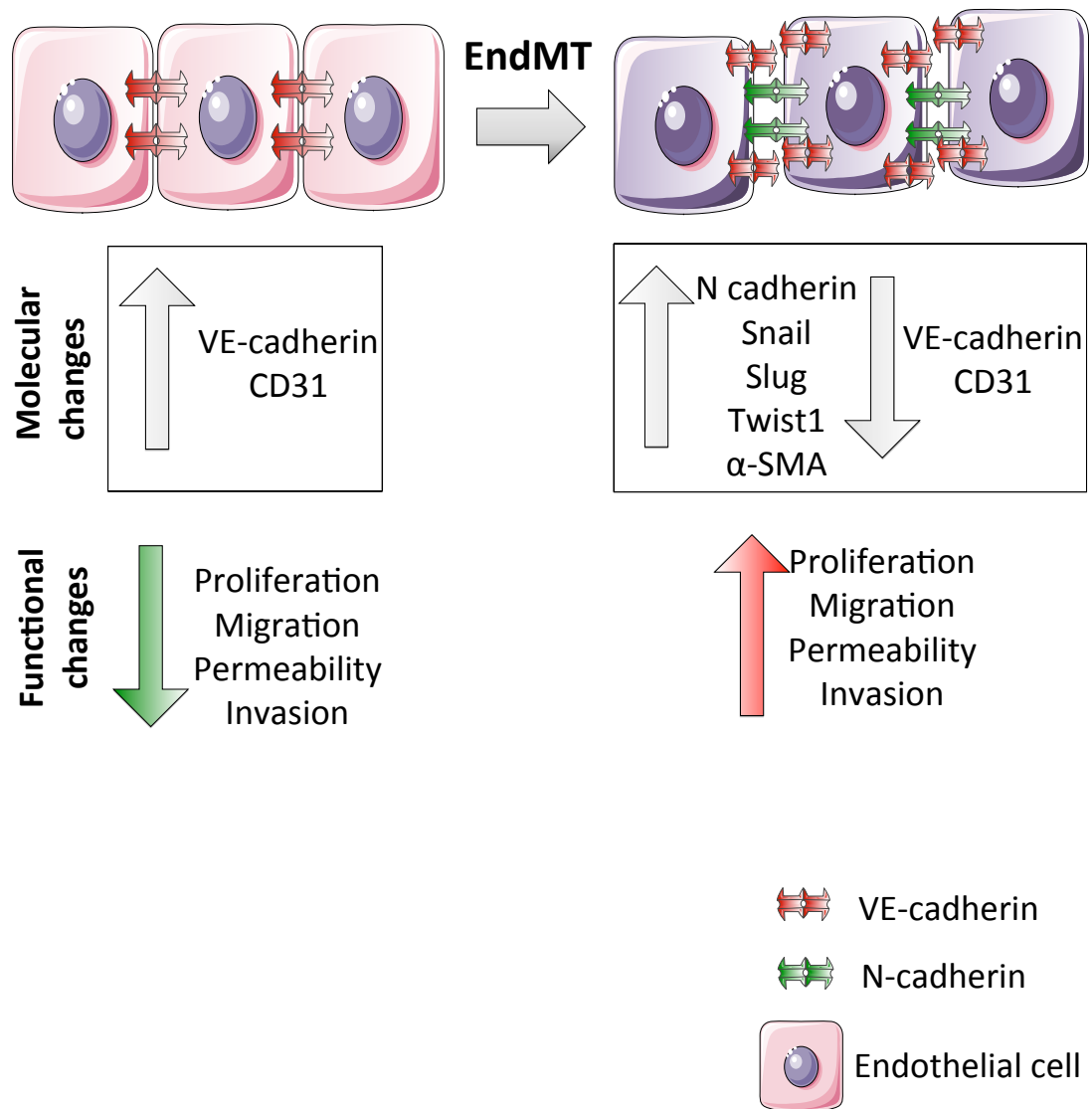


Figure 10. Molecular and functional changes during EndMT. EC undergoing EndMT undergo molecular changes, including an increased expression of mesenchymal genes (N-cadherin, Snail, Slug, Twist1 and α -SMA) and a reduction in EC marker genes (VE-cadherin and CD31). These molecular changes give rise to changes in EC function; an increase in proliferation, migration, permeability and invasion .

TGF- β activation promotes the activation of the EndMT gene programme, including the expression of EndMT-controlling transcription factors Snail, Slug, Twist1 (Reviewed in Lamouille et al. 2014). *In vitro* and *in vivo* functional studies have shown that inhibition of TGF- β signalling, specifically TGF- β 2, BMP2 and 4 blocked the induction of EndMT, thus revealing that these specific TGF- β signalling mediators play a dominant role in the induction of EndMT (Medici et al. 2010; van Meeteren & ten Dijke 2012; Azhar et al. 2009; Deissler et al. 2006; Medici et al. 2011; McCulley et al. 2008; Kokudo et al. 2008; Ma et al. 2005). Whereas, BMP7 binding to ALK2 receptors acts to inhibit EndMT induction, which suggests that within the TGF- β family, there are balance-keeping mechanisms such as BMP7, which together regulate EndMT (Zeisberg et al. 2007). TGF- β signalling also activates smad-independent molecules such as p38 MAPK, MAPK/ERK kinase (MEK)/ERK and PI3K, which promote transcriptional activation of EndMT transcription factors including SNAIL, TWIST1 and GATA4 and stabilises TGF- β 2 signalling (Medici et al. 2011; Rysä et al. 2010; Tenhunen et al. 2004; Hong et al. 2011a; Echeverría et al. 2014). Notch signalling through Notch ligand-receptor interactions and WNT signalling (canonical via β -catenin and non canonical via NFAT) are also positive regulators of EndMT as shown by *in vitro* and *in vivo* studies. Specifically, Notch and WNT signalling have a direct role in inducing EndMT by transcriptional induction of the EndMT programme or indirectly through the activation of EndMT-promoting pathways such as TGF- β (Liebner et al. 2004; Chang et al. 2011; Maddaluno et al. 2013). Interestingly, it has been reported that Notch and WNT signalling play a synergistic role with TGF- β signalling in the activation of EndMT regulators such as Snail and Slug (Kokudo et al. 2008; Lim & Thiery 2012). All of these pathways lead to EndMT, which causes changes in EC function including proliferation, migration and invasion.

Although TWIST1 and GATA4 regulate various separate pathways in disease and development, they are both potent activators of EndMT (Rivera-Feliciano et al. 2006; Hirasawa et al. 2011; Chakraborty et al. 2010). TWIST1 and GATA4 are downstream targets (through direct transcriptional activation or through post

translational modifications) of EndMT promoting pathways; TGF- β , BMP, Notch and WNT signalling (Lamouille et al. 2014; Daoud et al. 2014; Lin & Xu 2008; Reinhold et al. 2006; George et al. 2015). Interestingly, TWIST1 and GATA4 can also act as positive regulators of these EndMT promoting pathways (Chen et al. 2014; O'Rourke et al. 2002; Moskowitz et al. 2011). *In vivo* studies have shown that endothelial-specific deletion of Twist1 or Gata4 blocks the EndMT programme, suggesting that they play an important role in regulating EndMT. Specifically, the EndMT-promoting mechanism of TWIST1 and GATA4 involves the transcriptional activation of mesenchymal genes Snail, Slug, α -sma (smooth muscle cell actin) and N-cadherin (Rivera-Feliciano et al. 2006; Lamouille et al. 2014; Hong et al. 2011; Chakraborty et al. 2010). TWIST1 directly inhibits VE-cadherin transcription through binding to E-box sequences in the VE-cadherin promoter and blocking transcription through chromatin remodelling (Reviewed in Lamouille et al. 2014; Lopez et al. 2009). This subsequently promotes loss of EC-EC contacts and cell migration. *In vitro* and *in vivo* studies have shown that TWIST1 and GATA4 promote EC proliferation, migration and invasion (Lee & Yutzey 2011; Zeisberg et al. 2005; Rivera-Feliciano et al. 2006; Vrljicak et al. 2012). TWIST1 and GATA4 can control the expression of one another through indirect mechanisms during EndMT. One of these mechanisms includes the activation of TWIST1 through GATA4-dependent Smad4 activation. Moreover, GATA4 and TWIST1 both interact with BHLH transcription factor HAND2 to promote target gene activation (Dai et al. 2002; Firulli et al. 2005). Thus TWIST1 and GATA4 are key regulators of EndMT and present in in-direct crosstalk during the induction of EndMT.

1.7.2 EndMT in development

EMT is essential during gastrulation. Platt was the first to identify this role of EMT. Specifically, it was reported that cells from the ectoderm transformed into a mesenchymal form and contributed to forming mesodermal tissue (Platt 1894). Genetic studies in *Drosophila*, *Xenopus* and chick embryos revealed that the process of EMT is essential in gastrulation and is evolutionary conserved (Reviewed in Thiery et al. 2009). Four “waves” of EMT occur at multiple stages during embryonic development, starting from gastrulation in early stages of development leading up to organogenesis in later stages of development. During gastrulation, EMT is required to mediate cellular movement and proliferation, which are central to promoting morphogenesis. For example, neural crest cells (cells of the primitive neural tube) undergo EMT in order to delaminate and migrate into their target sites, where they differentiate into their specified fate (Minoux & Rijli 2010; Theveneau & Mayor 2011). Similarly, during heart morphogenesis, cardiac-specified cells undergo EMT to first form the heart tube, this is followed by a second EMT “wave” and the reverse process; mesenchymal-epithelial transition to form the epicardium and the myocardium linings of the heart, followed by the formation of the endocardial cushions (Chua et al., 2011). The molecular mechanisms controlling EMT during development include transcriptional activation by TWIST1, SNAIL and GATA4, where they act as master regulators during this process (Jiang et al. 1999; Kuo et al. 1997). TWIST1, regulates the balance between growth factor signalling pathways such as BMP, TGF- β and FGF, which play opposing roles in mediating EMT during gastrulation (Connerney et al. 2006). BMP-WNT and TGF- β signalling forms a gradient in the mesoderm that promotes EMT and delamination, whereas a gradient of FGF signalling inhibits this process (Reviewed in Lin et al. 2012; Lim & Thiery 2012).

During heart valve formation, endocardial cushion cells lining the heart undergo EndMT in order to migrate and invade the cardiac jelly and form a mesenchymal cell layer in the out flow tract and atrioventricular (AV) canal that will later form the heart valve, giving rise to the mature heart valves (von Gise & Pu 2012). This

involvement of EndMT in heart valve formation was first identified by Markwald in 1975. In the 1980s Markwald further established the role of EndMT in heart valve formation by studying the behaviour of chick endocardial cushion explants in 3D collagen culture. It was observed that the endocardial cushion cells migrated and invaded into the collagen gel and later formed mesenchymal cells on the surface of the gel, thus recapitulating endocardial cushion formation that occurs *in vivo* (Bernanke & Markwald 1982; Runyan & Markwald 1983).

GATA4 controls one of the most prominent pathways that regulates endocardial cushion EndMT (Zeisberg et al., 2005, Rivera-Feliciano et al., 2006). EC-specific Gata4 deletion caused endocardial cells to fail to undergo EndMT and gave rise to cardiac cushion defects (Rivera-Feliciano et al. 2006). The mechanism involves the activation of Erb-B2 Receptor Tyrosine Kinase 3 (ERBB3), a cell surface receptor belonging to the epidermal growth factor receptor (EGFR) tyrosine kinase family (Rivera-Feliciano et al. 2006). Erbb3, another essential endocardial EndMT signalling component, mediates ERK activation, which gives rise to the induction EndMT gene programme (Rivera-Feliciano et al., 2006). GATA4 also regulates TGF- β signalling through feeding into Smad 4 activation, which then activates EndM via TWIST1 (Moskowitz, et al. 2011). Smad 4 activation promotes β -catenin- mediated EndMT (Lim & Thiery 2012b; Medici et al. 2011).

Notch signalling is another essential molecular activator of endocardial EndMT. Studies have shown that Notch receptor mutants fail to undergo EndMT and displayed cardiac cushion defects (Timmerman et al., 2004). These mutants also displayed a reduction in TGF- β 2, indicating that Notch signalling is required for TGF- β 2 signalling in endocardial EndMT (Timmerman et al. 2004). Notch signalling promotes the activation of HEY2, which together with BMP2 triggers EndMT (Luna-Zurita et al. 2010). Of note, TWIST1 and SNAIL interact with HEY2 and BMP2 in promoting EndMT and inhibition of this interaction gave rise to valve malformations (Luna-Zurita et al. 2010). Several studies have revealed that TWIST1 promotes essential genes that control EC migration, proliferation and invasion during valve

formation, such as neuronal (N)-cadherin, osteoblast (OB)-cadherin, Tbx20 and Mmp2 (Lee & Yutzey 2011; Chakraborty et al. 2010; Shelton & Yutzey 2008). In addition, TWIST1-mediated Tbx20 activation is required for the induction of canonical WNT signalling (Cai et al. 2013) which is required for valve formation as revealed in functional studies (Liebner et al. 2004). Moreover, EndMT plays an important role in mediating sprouting angiogenesis in the retina development (Coultas et al. 2005). Cells at the tips of the angiogenic sprouts were shown to be undergoing EndMT. The proposed mechanism was via VEGF and TWIST1 signalling (Li et al. 2014; Coultas et al. 2005).

1.7.3 Role of EndMT in disease

1.7.3.1 EndMT in cancer

The tumour microenvironment supports cancer cell survival by promoting angiogenesis, vasculogenesis and tumour metastasis. Carcinoma-associated fibroblasts (CAFs) contribute to the supportive role of the tumour microenvironment by promoting metastasis (Reviewed in Medici & Kalluri 2012). Zeisberg et al., identified the role of EndMT in the formation of CAFs using a combination of *in vivo* cancer models, *in vitro* cell cultures and cell lineage tracing. Zeisberg et al. showed that 40% of tumour CAFs originated from EC in the tumour microenvironment that underwent EndMT via TGF- β signalling. Subsequently EC transform into a myofibroblasts to form CAFs, which positively feedback into the EndMT pathway by secreting TGF- β 1, triggering tumour metastasis via EMT and angiogenesis via EndMT (Zeisberg et al. 2007). Of note EMT is the primary mechanism by which tumours metastasise and is mainly driven by Twist1 and Snail transcriptional activation of target genes and suppression of E-cadherin (Reviewed in Heerboth et al. 2015). Other studies have highlighted the importance of EndMT in cancer survival by demonstrating that tumour hypoxia triggers angiogenesis through HIF1- α mediated activation of Twist1 and subsequent EndMT. EndMT transcription factors TWIST1, SNAIL and GATA4 promote cancer cell survival by activating cell proliferation and migratory genes, whilst inhibiting pro-apoptotic and for TWIST1 inhibition of senescence pathways (Chakraborty et al. 2010; Kyrönlahti et al. 2008).

1.6.3.2 EndMT in fibrotic diseases

Heart failure following cardiac stress such as pressure overload and acute ischaemic injury is associated with cardiac fibrosis. This process of cardiac fibrosis involves the proliferation of cardiac fibroblasts. The Kalluri lab provided an insight into the involvement of EndMT in fibrotic diseases. In a study by Zeisberg *et al* it was revealed in murine models of pressure overload and chronic allograft rejection EC underwent TGF- β 1-dependent EndMT to form fibroblasts which in turn contributed to cardiac fibrosis (Zeisberg et al. 2007). This study thus provided a novel insight into the mechanisms that are involved in cardiac fibrosis. BMP7 treatment prevented EndMT-mediated conversion of EC into fibroblasts, thus suggesting that BMP7 administration is a relevant therapeutic strategy to reverse cardiac fibrosis (Zeisberg et al. 2007). Interestingly, cell tracking experiments by Ubil et al. showed that fibroblasts could undergo a reverse process of EndMT, known as mesenchymal-endothelial transition (MEndT) (Ubil et al. 2014). During this process fibroblasts convert into EC which directly contribute to cardiac repair by promoting neovascularisation following cardiac injury (Ubil et al. 2014). The mechanism underlying MEndT is dependent on p53 activation by DNA damage sensor YH2AX. Ubil *et al.*, show that inhibition of p53 blocks MEndT and diminishes cardiac repair and function (Ubil et al. 2014). Since TWIST1 inhibits p53 and drives EndMT (Maestro et al. 1999; Wang et al. 2003) it could be that TWIST1 is potential molecular switch between EndMT and MEndT. Thus inhibition of TWIST1 may be a potential therapeutic strategy to activate MEndT following cardiac injury.

The Dejana lab identified the involvement of EndMT in the pathogenesis of cerebral cavernous malformations (CCM) a disease that is characterised by the formation of fibrotic lesions and vascular malformations in the brain. The mechanism by which EndMT supported CCM lesion formation was by TGF- β signalling through BMP6, which gave rise to an increase in EC proliferation and invasion (Maddaluno et al. 2013). The Kalluri lab revealed the involvement of EndMT in renal fibrosis as evidenced by the co-expression of EC marker (CD31) with mesenchymal gene α -Sma

following renal injury in three different murine models of kidney fibrosis (Zeisberg et al. 2008). Additionally, a recent study by Ranchoux *et al.*, showed that EndMT is a key driver of fibrosis in pulmonary arterial hypertension (PAH) (Ranchoux et al. 2015). The mechanism proposed of EndMT in PAH was via TWIST1 and TGF- β -induction of EndMT (Ranchoux et al. 2015).

Since EndMT changes influences cell proliferation, migration and permeability, it is plausible that EndMT could be involved in promoting atherosclerosis. Evidence for involvement of EndMT in atherosclerosis was recently provided by Sánchez-Duffhues *et al.* and Moonen *et al.*, where both of these studies showed the expression of mesenchymal proteins SLUG and α -SMA in the luminal EC layer of atherosclerotic plaques (Sánchez-Duffhues et al. 2015; Moonen et al. 2015). In addition, these studies showed that EndMT is activated *in vitro* and *in vivo* by pro-atherogenic low WSS through TGF- β signalling (Sánchez-Duffhues et al. 2015; Moonen et al. 2015). However, very recently the Simons group showed direct evidence for the role of EndMT in atherosclerosis. Chen et al., showed that low WSS inhibited FGF signalling and increased TGF β signalling, which then triggered EndMT. EC-specific blocking of FGF signalling enhanced atherosclerosis, suggesting that FGF signalling blocks EndMT and is atheroprotective (Chen et al. 2015). Interestingly FGF signalling has been shown to promote EndMT in corneal fibrosis (Lee & Kay 2006), thus revealing that FGF-mediated regulation of EndMT is context dependent and may rely on the control of an upstream molecular switch. The involvement of EndMT in atherosclerosis is novel and given the involvement of various EndMT regulators in other fibrotic diseases, there are other possible EndMT regulators that could be playing a role in promoting EndMT in atherosclerosis.

In summary, EndMT is an essential process during development. However in the adult, the re-activation of EndMT acts a potent driver of cancer and fibrotic diseases (Figure 11). The underlying pathology of these conditions is dependent upon EndMT-mediated cellular proliferation, migration and invasion, which are controlled by several pathways and transcriptional regulators including TWIST1 and GATA4.

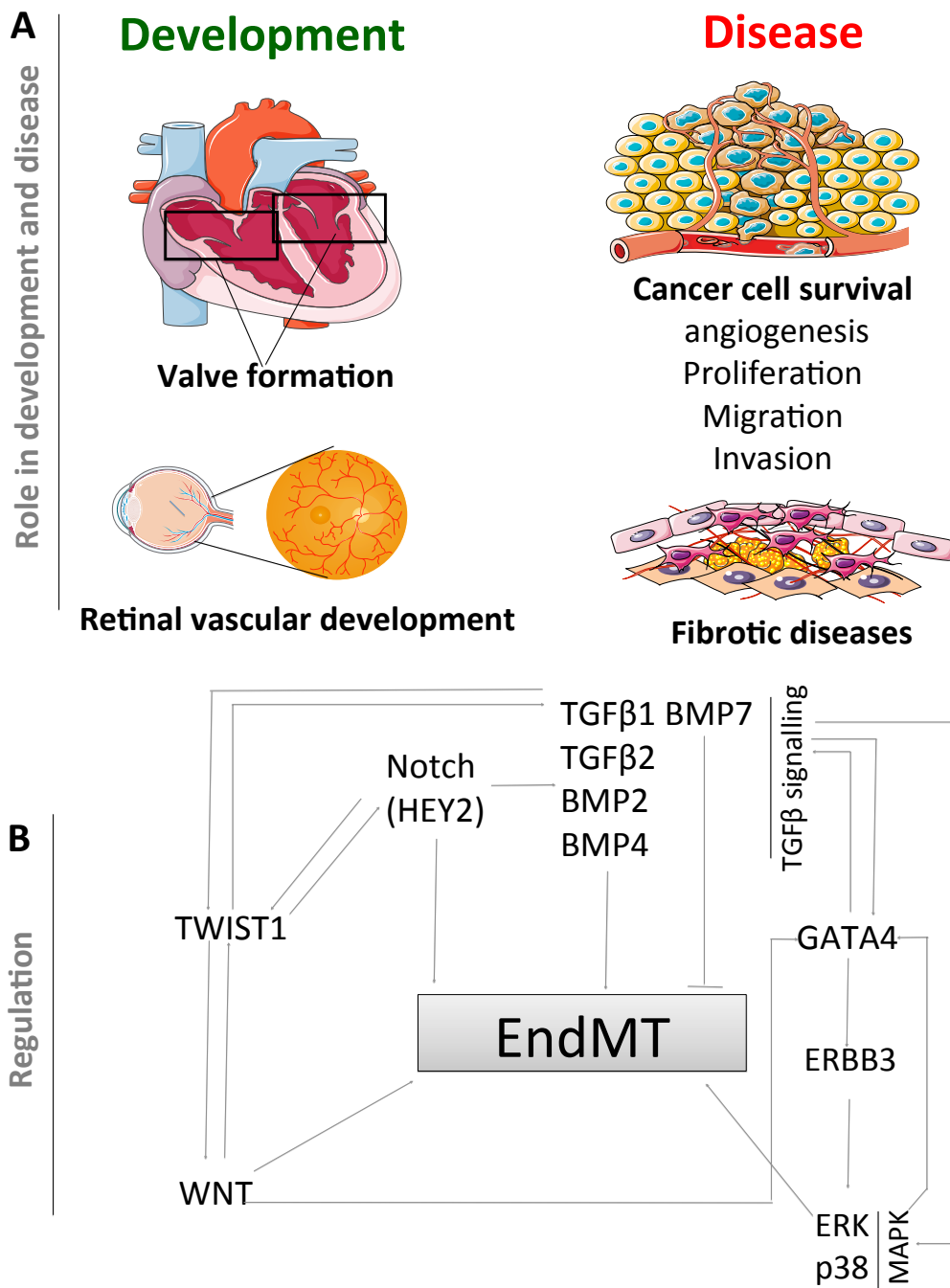


Figure 11. Role of EndMT in development and in disease. A) Summary for the role of EndMT in development and disease. The left panel depicts a schematic for the role of EndMT in valve formation and in retinal vascular development. The panel on the right depicts a schematic for the role of EndMT in cancer cell survival and in fibrotic diseases.

1.8 Hypothesis

Low WSS promotes EC dysfunction and atherosclerosis through TWIST1 and GATA4-mediated induction of EndMT.

1.9 Aims:

1. To study the effects of WSS on TWIST1 and GATA4 gene expression in cultured cells using *in vitro* flow systems.
2. To study the effects of WSS on TWIST1 and GATA4 gene expression *in vivo*, in the porcine and murine aortic arch and in experimental cuffed carotid arteries.
3. To study the functional output of TWIST1 and GATA4 on EC function, by assessment of EndMT, EC proliferation, permeability and migration *in vitro* and *in vivo*.

Chapter 2: Materials and Methods

2.1 Materials

Materials and reagents used are listed in the following;

- 1) Primary cell culture/ cell transfection (table 2)
- 2) Immunostaining/ Chromatin Immunoprecipitation (ChIP) (table 3)
- 3) RNA isolation/qRT-PCR/standard PCR (table 4)
- 4) *In vivo* techniques (table 5)

2.2 Methods

2.2.1 Isolation and culture of Human umbilical vein endothelial cells (HUVEC)

HUVEC were isolated from umbilical cords, collected anonymously, without patient identifiers with ethical consent (Sheffield REC 10/H1308/25). The cords were cleaned from excess blood using Azowipe™ tissue. A 14 gauge, 2x45 mm cannula was inserted into the umbilical vein and clipped in place using crocodile clips. 10 ml of serum-free M199 was flushed through the vein to remove blood clots. The distal end of the cord was sealed with a crocodile clip and 10 ml of pre-warmed serum free media containing 1 mg/ml collagenase (from *Clostridium histolyticum*; sterile filtered using a 0.2 µm Filtropur filter) was injected into the vein. The cord was incubated with the collagenase for 10-15 min at room temperature. Following incubation the clip at the distal end was removed and the flow-through containing the extracted HUVEC in collagenase was flushed into a tube and was centrifuged at 1200 rpm (210 G) for 5 min to collect the cells. The cell pellet was resuspended in 12 ml of complete M199 growth medium (all media constituents are in appendix 1) and were seeded onto 1% gelatin coated T75 cell culture flasks. The cells were maintained in a 37°C incubator with 5 % CO₂ and the following day the cells were washed using phosphate buffer saline (PBS) and the growth media was changed. The media was then changed every 2-3 days. Once the cells reached approximately 90 % confluence they were passaged using trypsin (Table 2). The cells were used at a passage of 3-5 for all experiments.

Table 2. Materials used for primary cell culture/cell transfection

Material name	Product number; Company
Primary cell culture/ cell transfection	
14 gauge, 2x45mm cannula, Vetiflon™	47776, BD Biosciences
34 mm diameter 6-well plates, Cellstar®,	657160, grenierbio-one
Amphotericin B	BP264550, Thermo-sceitnfc
Azowipe™ tissue	Synergy health
Collagenase from Clostridium histolyticum	C8051; Sigma-Aldrich
Endothelial growth factor (EGF) supplement	02-101, Millipore
Filtropur™ filter (0.2µm)	40645103,SARDT EDT
Gelatin from bovine skin	G9391, Sigma-Aldrich
Gentamicin	15710-080, Invitrogen
Heparin	H3149, Sigma-Aldrich
L-Glutamine	25030-081; Thermo-scientific
M199 media, Gibco®	21180-021, Sigma-Aldrich
Three-way tap	39511; BD biosciences
Trypsin-EDTA X1 (in PBS)	B10613, GmbH
96-well flat bottom plate, Cellstar®	655180, Grenierbio-one
T75cm ² tissue culture flask, Nunc®	598287; Thermo-scientific
T25 cm ² tissue culture flask, Nunc®	136196; Thermo-scientific
Transwell inserts, Corning® (24mm, 0.4µm polyester membrane)	CC401; Appleton woods

Collagen solution (from bovine skin)	C4243; Sigma-Aldrich
Recombinant murine VEGF	450-32; Peprtech
Pen/Strep	15140122; Thermo-scientific
Phosphate buffered saline (PBS)	P4417; Sigma-Aldrich
Fetal Bovine serum	Sigma-Aldrich
Fibronectin	F0895; Sigma-Aldrich
Lipofectamine RNAiMAX™	56532; Invitrogen
M199 Gibco® cell culture medium	11150-059; Thermo-Scientific
DMEM cell culture medium (With 1g/l glucose)	12614-Q; Lonza

Table 3. Materials used for immunostaining/ChIP

Material name	Product number; Company
Immunostaining/ chromatin immunoprecipitation (ChIP)	
SIGMAFAST™ DAB with Metal Enhancer tablet.	D0426; Sigma-Aldrich
Avidin-biotin complex (ABC) kit, Vectastain®	PK4000; Vector laboratories
TOPRO	T3605; Thermo-scientific
DPX mountant	06522; Sigma-Aldrich
Triton™X-100	T8787, Sigma-Aldrich
Menzel-Gläser, Superfrost® microscope slide	AA00000112E; Thermo-scientific
Absolute goat serum	G9023; Sigma-Aldrich
4% Formaldehyde	9713.5000, VWR Chemicals
4',6-diamidino-2-phenylindole (DAPI)	D9452, Sigma-Aldrich
34mm round Menzel-Gläser glass cover slips	1283, Thermo-scientific
Carazzi's haematoxylin	75290; Raymona A. Lamb; Company
Trypsin	215240; DIFCO
SimpleChip chromatin plus enzymatic IP kit	9005; Cell signalling
Prolong® gold antifade mountant	P1044; Thermo-scientific
PKH26 membrane label	PKH26GL; Sigma-Aldrich

Table 4. Materials used for RNA isolation/ qRT-PCR/ standard PCR

Material name	Product number; Company
RNA isolation/qRT-PCR/ standard PCR	
Hotstart Taq mastermix kit	203443; Qiagen
RNeasy minikit	74106; Qiagen
β -mercaptoethanol	M6250; Sigma-Aldrich
Scalpel blade	66XX; Swann-Morton
Plastipak™ syringes (1ml)	30013, BD biosciences
RNase zap®	AM9780 ; Life technologies
iScript™ cDNA synthesis kit	170-8891, BIORAD
Ethanol	E7023, Sigma-Aldrich
Clear adhesive film for 384-well plate	95016806, Anachem
384 well plate	HSP3805, BIORAD
21 gauge needle, MicroLance™	;BD Biosciences
Q5® High fidelity Taq DNA polymerase kit	M0491L; NEB
Agarose	A9539; Sigma-Aldrich
DNA gel loading dye	R0611; Life technologies
100bp DNA ladder	N3231; NEB
Tris-HCl	T5941; Sigma-Aldrich

EDTA	ED; Sigma-Aldrich
Tween-20	P1379; Sigma-Aldrich
Proteinase K	P10144; Life technologies

Table 5. Materials used for *in vivo* techniques

Material name	Product number; Company
<i>In vivo</i> techniques	
25 gauge needle, MicroLance™	BD Biosciences
Corn oil	15256; Sigma-Aldrich
Tamoxifen	T5648; Sigma-Aldrich
Ethanol	E7023, Sigma-Aldrich

2.2.2 Isolation and culture of porcine aortic endothelial cells (PAEC)

PAEC were isolated from descending aortae of approximately 60 kg, 6 month old female pigs collected from a local abattoir. The aortae were cleaned from connective tissue and the inter-costal arteries were sealed using a cotton thread and/or crocodile clips. A three-way tap was inserted into the aorta and 10 ml of serum free DMEM media was flushed through the vessel. The distal end of the vessel was sealed using cable ties and 10-15 ml of serum-free DMEM media containing 0.2 mg/ml of collagenase (sterile filtered) was injected into the vessel. This was covered with Azowipes™ and was placed in a 37°C incubator for 10 min, in order to enhance the enzymatic activity of the collagenase. Following incubation, the flow-through containing the PAEC was collected into a tube and was then centrifuged at 1200 rpm (210 G) for 5 min to collect the cells. The cell pellet was resuspended in 7 ml of complete DMEM growth medium and cells were seeded into a T25 tissue culture flask. The cells were maintained in a 37 °C incubator with 5 % CO₂. The following day, the cells were washed with PBS and given fresh complete DMEM growth medium 1. Once the cells reach confluence, they were passaged accordingly and the media was changed every 2-3 days. Once the cell passage was beyond P1 complete DMEM growth media 2 was given. The cells were used at passage 3-5 for experiments.

2.2.3 Isolation of RNA from EC in the porcine aorta

Porcine hearts with the intact aortic arch and descending aorta (from approximately 60 kg, 6 month old female pigs) were collected from a local abattoir. The tissue was stored in ice- cold transport media. The aortic arch was cleaned from excess connective tissue and blood. A 1x1 cm square region was dissected from the inner curvature (low WSS region) and the outer curvature (high WSS region) (Figure 12; as identified by reference to a shear stress map, de Luca, Serbanovic-canic and Evans et al. Manuscript Submitted).

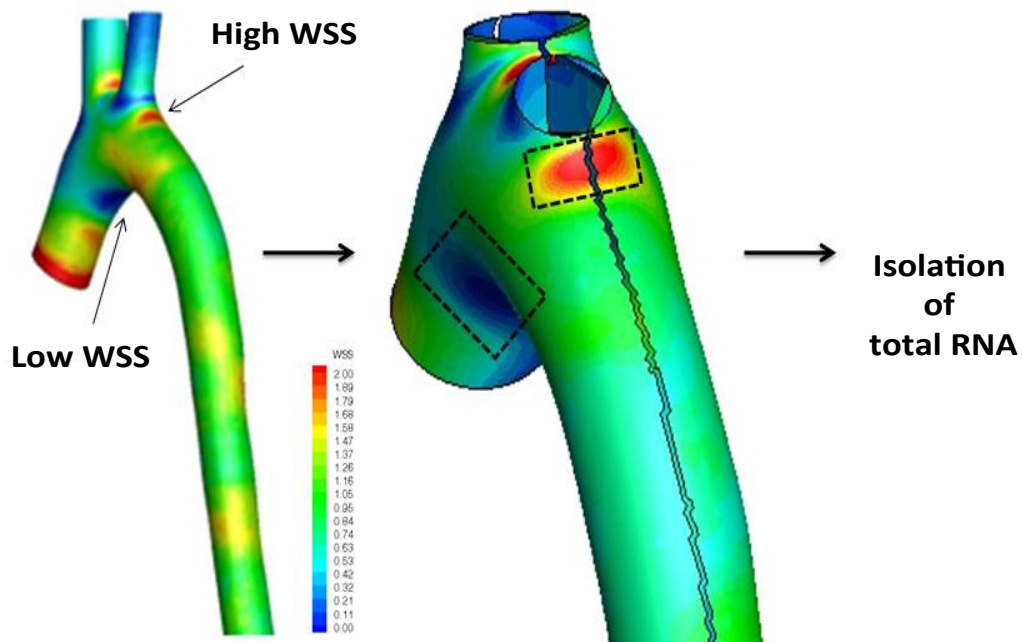


Figure 12. Schematic of RNA isolation from the porcine aortic arch. To study the expression of genes of interest from the distinct flow areas in the porcine aorta, a 1x1cm region was dissected from the inner (low WSS) and the outer (high WSS) region of the porcine aorta. Endothelial RNA was extracted using collagenase treatment followed by RNA purification. The shear stress map was generated by measurement of vascular geometry (via MRI) followed by computational fluid dynamics (CFD) by Dr. Amalia de Luca (unpublished).

The tissue sections were placed lumen-side down onto a 1 ml drop of collagenase solution (1 mg/ml collagenase added to serum free DMEM; placed on RNase zap[®] cleaned parafilm) and incubated at room temperature for 10 minutes. The collagenase solution was collected into a 1.5 ml microfuge tube and the tissue sections were gently scraped using a scalpel blade in order to isolate the endothelial cell layer of the lumen intima. The cells were centrifuged at 3000 rpm (564 G) for 3 min. The pellet of EC from each tissue section was resuspended into 350 μ l lysis buffer solution, prepared by adding 0.01% of β -mercaptoethanol to a final volume of 350 μ l per aortic tissue section of lysis buffer (RLT buffer; Qiagen RNeasy kit[™]). The cell lysate was homogenised by passing it through a 21 gauge needle 5-6 times. 350 μ l of 70 % Ethanol was added and total RNA was extracted using the RNeasy[™] mini kit, following the manufacturer's protocol. RNA concentration and purity were assessed spectrophotometrically with a Nano Drop ND-1000 (Life technologies). Analysis of RNA quality involved measurement of optical density to determine 260-280 nm and 260-230 nm ratios, using the ND-1000 v 3.7.0 software.

2.2.3 Exposure of EC to flow using *in vitro* flow systems

To study the direct effects of flow-induced WSS on EC physiology, two complimentary *in vitro* flow systems were used for this purpose, and the method used to set up both systems will be presented.

2.2.3.1 The 6-well orbiting plate system

HUVEC and PAEC were seeded onto 1 % gelatin coated 6-well (34 mm diameter) culture plates at a density of approximately 300,000 cells /well, the cells were cultured overnight and became confluent the following day. The media was then removed and 3 ml of complete M199 growth media was added to each well and the cells were placed on an orbital shaking platform (PSU-10i; Grant instruments) housed inside a cell culture incubator (37 °C, 5 % CO₂) rotating at 210 rpm with an orbiting radius of 10 mm, for the duration of 72 h (Figure 13).

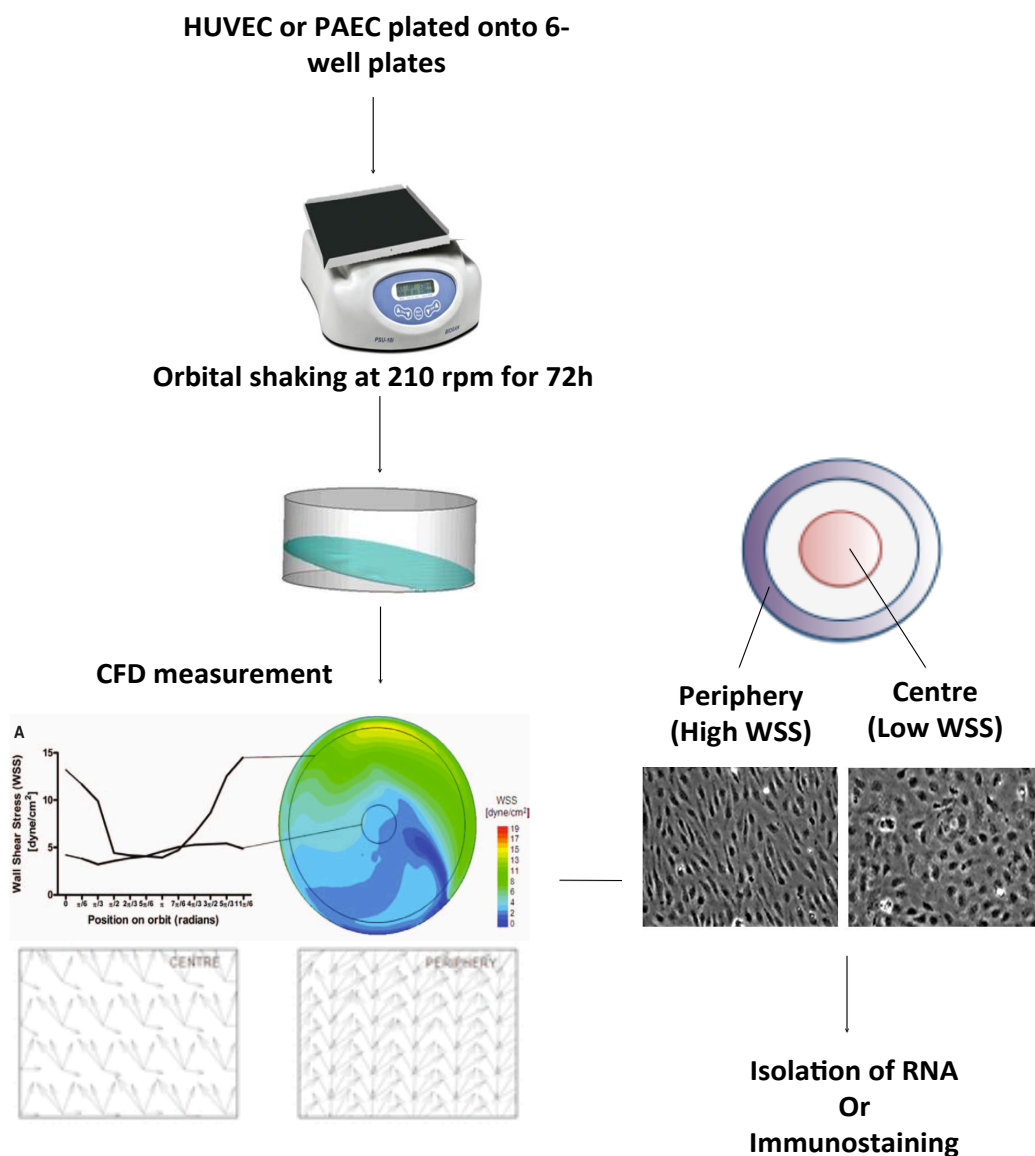


Figure 13. Schematic for orbital shaking system. A) The effects of flow on EC was studied using the orbital plate system. HUVEC and PAEC cultured onto 6-well plates were placed onto an orbital shaking platform, rotating at 210 rpm with an orbiting radius of 10 mm, for the duration of 72h. The orbital shaking creates a swirling motion of media in the well and computational fluid dynamics and particle imaging velocimetry analyses show that at the centre of the well, cells are exposed to a constant low mean WSS magnitude (4.8 dyne/cm²) but rapid in variations in directions (biaxial/ disturbed flow), whilst in the periphery of the well the WSS magnitude is relatively high WSS (13 dyne/cm²) and with pulsatile relatively uniform flow direction (uniaxial/ non disturbed flow). Following orbital shaking, cells from the low and high WSS were either isolated for total RNA extraction or were directly used for immunostaining. CFD measurements of WSS were generated in Warboys et al., 2014.

The orbital shaking creates a swirling motion of media in the well and measurements of computational fluid dynamics and particle imaging velocimetry analyses have revealed that at the centre of the well, cells are exposed to a constant low mean WSS magnitude (4.8 dyne/cm²) but rapid in variations in directions (biaxial/ disturbed flow), whilst in the periphery of the well the WSS magnitude is relatively high WSS (13 dyne/cm²) and with pulsatile relatively uniform flow direction (uniaxial/ non disturbed flow) (Warboys et al. 2010; Warboys et al. 2014; Dardik et al. 2005). Following orbital shaking, cells from the low and high WSS were either isolated for total RNA extraction or were fixed and used for immunostaining.

2.2.3.2 The Ibidi™ pump parallel plate system

HUVEC were seeded onto 1 % coated Ibidi™ µ 0.4 Luer slides at a seeding density of 250,000 cells/slide in a total of 120 µl complete M199 growth medium. Following 1-2 h from seeding, the cells were checked for attachment and for the presence of a confluent monolayer. The slide was then connected to the Ibidi™ fluidic units following the Ibidi™ pump set up manual. Flow parameters were set on the Ibidi™ pump control software, (v 1.5.3) and the cells were exposed to flowing media by the pressure driven by the Ibidi™ pumps feeding into the reservoirs of the fluidic units (Figure 14). The flow parameters studied were high, unidirectional WSS at 13 dyne/cm², low, unidirectional WSS at 4 dyne/cm² and low, oscillatory WSS at 4 dynes/cm², with 0.2Hz oscillations. Cells were exposed to flow for 72 h then the cells were isolated for total RNA extraction.

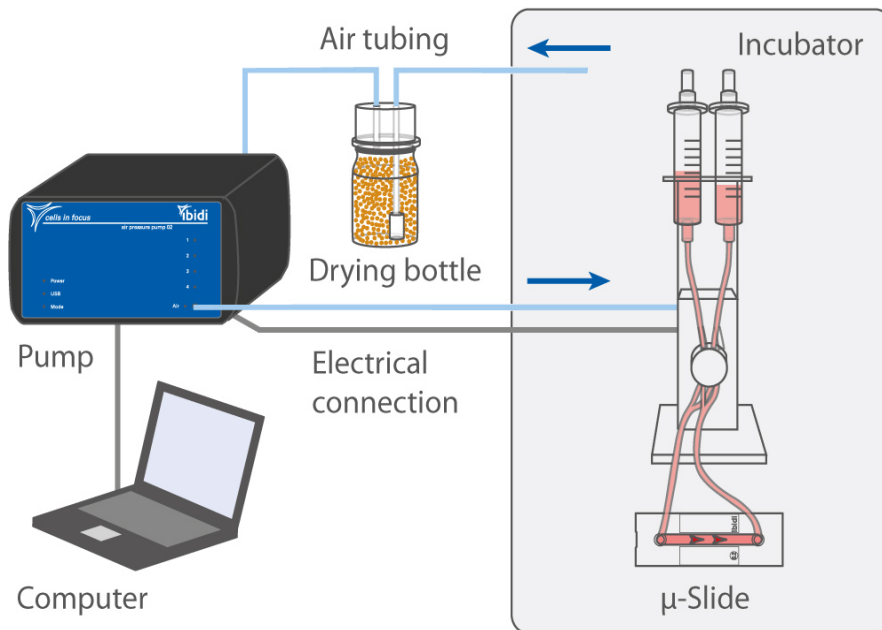


Figure 14. Schematic for the Ibidi™ parallel plate system. Specific flow parameters (flow magnitude; WSS in dyne/cm^2 and flow direction) were set on the Ibidi™ pump control software on a computer. The parameters set onto the software are relayed to the Ibidi™ pump, which then controls the air pressure to create the specific flow characteristics by controlling the flow of media from the fluidic units onto the cells plated onto the Ibidi™ μ slide, housed inside of an incubator. Schematic image courtesy of Ibidi™ (GmbH).

2.2.4 RNA extraction from EC exposed to flow

Following the exposure of cells to flow using the orbital plate system, the 6-well plate was kept on ice, media was removed and 2 ml/ well of ice-cold PBS x2 was used to wash the cells. 1 ml of ice-cold PBS was added per well and the plate was placed on a map (Figure 13), which outlines the specific low (centre) and high (periphery) WSS areas on the plate. Using the plunger of a 1 ml syringe cells were first scraped from the periphery of each well on the plate and collected in a tube kept on ice. Excess, uncollected cells were removed by washing twice with 2ml of PBS and the process was repeated for cells in the centre of the well. To isolate the cells collected from the centre and the periphery, the tubes were centrifuged at 1200 rpm (210 G) for 5 min. Lysis buffer was prepared by adding 0.01% of β -mercaptoethanol into the RLT lysis buffer. The cell pellets were resuspended in 350 μ l of lysis buffer, and the cell lysate was homogenised by passing the suspension through a 21 gauge needle using a 1ml syringe five-six times. A volume of 350 μ l of 70 % ethanol was added to the cell lysate to precipitate the nucleic acid content and total RNA was extracted using the Rneasy kit, following the manufacturer's protocol. RNA concentration and purity was assessed as described previously. For cells exposed to the Ibidi flow system, the cells were also kept on ice and 120 μ l x3 of lysis buffer was flushed through the inlet of the Ibidi® μ I 0.4 Luer slide and was collected in a 1.5 ml microfuge tube. The cells were pelleted by centrifugation at 3000 rpm for 5 min (564 G). The cell lysate was homogenised and total RNA extracted as described previously.

2.2.5 Gene expression analysis by q-PCR

2.2.5.1 cDNA synthesis

The expression of the genes of interest was assessed by quantitative real time PCR (qRT-PCR). Total RNA at a concentration of 200 ng/ μ l was used for reverse transcription/ cDNA synthesis using the iScript™cDNA synthesis kit (Table 4). The reaction constituents added were; 5 μ l of 5x iScript reaction mix, 1 μ l of iScript reverse transcriptase, RNA template (200 ng) x μ l and nuclease-free water at x μ l to give a total reaction volume of 25 μ l. A thermal cycler (Veriti 96 well; Applied biosystems) was used for the synthesis. The thermal profile of the reaction used was; step 1 at 25°C for 5 min, step 2 at 42°C for 30 min, step 3 at 85°C for 5 min and step 4 at 4°C for 10 min.

2.2.5.2 qRT-PCR

A 384 well plate set-up was adopted. A total of 10 μ l reaction volume was used, this consisted of; 4.4 μ l of cDNA (1.46 ng/ μ l) and 5.6 μ l of qRT-PCR SsoAdvanced universal SYBR® Green master mix (0.3 μ l forward primer, 0.3 μ l reverse primer and 5 μ l SsoAdvanced universal SYBR® Green supermix was added per well). For each gene of interest, the reaction was carried out in triplicate. The 384 well plate (Table 4) was then sealed with clear adhesive film and was centrifuged at 1000 rpm (123 G) for 1 minute. qRT-PCR was conducted using the CFX384™ Real-time instrument (BIORAD). The thermal profile used was; Step1 at 95 °C for 3 min, step 2 at 95 °C for 5 seconds, step 3 at 60 °C for 30 seconds x 40 repeat, a final dissociation step at 60°C then at 95 °C for 5 with gradual temperature increase by 0.5 °C increments. The primer melting curve was analysed to assess amplification of product and rule out primer-dimer contributions. The human and porcine primers used are listed in table 6.

2.2.6 Analysis of qRT-PCR data.

During the PCR reaction, the SYBR dye is incorporated into double stranded DNA sequences belonging to the gene of interest that is being amplified ; this results in an increase in the fluorescent signal emitted by the dye which is proportional to the amount of amplified DNA present in the sample. A threshold cycle (Ct) value is given; this is the number of cycles required for the PCR product to exceed the threshold/baseline level of fluorescence. Therefore this value is inversely correlated with the amount of DNA sequence present in the sample, the more abundant the sequence is the lower the number of cycles required to exceed the threshold level (Ct value). Analysis of the qRT-PCR data was carried out via the BIO-RAD CFX manager 3.0 software that determined the Ct value for each gene of interest being investigated. The data was analysed using the comparative Ct ($2^{-\Delta\Delta CT}$) method (Schmittgen & Livak 2008). The Ct of each sample was normalised to the Ct value of a non-flow responsive housekeeping gene (Hypoxanthine phospho ribosyl transferase (HPRT)), to give the ΔCT value. The $\Delta\Delta CT$ was calculated by subtracting the average ΔCT value of sample 1 (eg. Low WSS sample) from sample 2 (High WSS sample; experimental control), and then subtracting the average ΔCT value of sample 2 (High WSS; experimental control) from itself. Relative mRNA fold change between sample 1 and sample 2 was calculated using the $2^{-\Delta\Delta CT}$ calculation. An mRNA relative fold change of greater than 1 was indicative of an increase in gene expression compared to the experimental control, whereas a value lower than 1 was indicative of a decrease in expression.

Table 6. Primer sequences**A) Human primers**

Gene	Forward primer	Reverse primer
Gata4	TCCCAGACGTTCTCAGTCAG	GGAGCTGGTCTGTGGAGACT
Twist1	CGGACAAGCTGAGCAAGAT	CTGGAGGACCTGGTAGAGGA
Klf4	GAACCCACACAGGTGAGAAA	CCCGTGTGTTTACGGTAGTG
Slug	CTGGCCAAACACAAGCAG	ACCCAGGCTCACATATTCT
N-cadherin	GCACAGATGTGGACAGGATT	CAGCACAAGGATAAGCAGGA
α -sma	TTTCAGCTTCCCTGAACACCA	GGGCAACACGAAGCTCATTG
Cd31	GGTGTGGTGGGAAGGACTG	GGGACAGAACAGTTGACCCCT
Hprt	TTGGTCAGGCAGTATAATCC	GGGCATATCCTACAACAAC
Klf2	ACCAGTCACAGTTTGGGAG	GCACGCACACAGGYGAGAAG
Mcp-1	GCAGAAAGTGGGTTCCAGGATT	TGGGTTGTGGAGTGAGTGTT
VE-cadherin	GCCAGTTCTTCCGAGTCACA	TTTCCTGTGGGGTTCCAGT
Twist1 promoter	AGCAATCCCAAATCGGCC	TGGCAACAGCTTCTACACAGT
Snail promoter	GCGGAGGTGACAAAGGGG	AACCACTCGCTAGGCCGT

B) Porcine primers

Gene	Forward primer	Reverse primer
Gata4	GGAAGGCAGAGAGTGTGTCA	GCTGATGCCATTCATCTTGT
Twist1	GGGAGTCCGCAGTCCTAC	TGGATCTTGCTCAGCTTGTC
B2m	GGTTCAGGTTACTCACGCCAC	CTTAACACTTGGGCTTATCG
cJun	GAAAAGGAAGCTGGAGAGGAT	CTGCTGCGTTAGCATGAGTT
Mcp-1	TCACCTGCTGCTATACACTTAC	ATCACTGCTTCTTTAGGACACTTG
Cd31	TCAATGCTCCGTGAAAGAAG	CCTGGGTGTCATTCAAAGTG
VE-cadherin	GAGTTCACCTTGTCGAGGA	GAGGGAGATCACTGCGATGG
α -sma	CCAGAGCAATCAGGGACC	CAATGGACGGGAAAACAGCC
Slug	CCTGGTCAAGAAGCATTTC	CTCCGGTTGTGGTATGACAG
N-cadherin	CCACAGACACCTCAAACCTG	GACCCAGAGAAGCAGGGATA
Klf4	CTAAGCAGCAGGGACTGTCA	GGCATGAGCTCTTGGTAATGG
Snail	GCGAGCTACACGACTCTTCT	GCCAGGAGAGAGTCCCAGAT

2.2.7 RNA interference; HUVEC transfection with siRNA

To assess gene function, genes of interest were silenced using gene specific siRNA oligonucleotides (Table 7). HUVEC were plated into 1 % gelatin coated 6-well plates at 250,000 cells/ well. Gene specific siRNA or scrambled non targeting control oligonucleotides (final concentration of 25 nM) were introduced into the cells via transfection using the Lipofectamine RNAiMAX transfection system following the manufacturer's protocol. Briefly, the transfection mix, consisting of the Lipofectamine reagent (7.5 µl Lipofectamine in 142.5 OPTIMEM media/ well) and gene specific siRNA oligonucleotides (1.25 µl in 148.75 µl OPTIMEM/well) were added to cells cultured in 700 µl M199 transfection medium. The cells were then incubated with the transfection mix for 5 hours (37°C, 5 % CO₂). The transfection media was then removed and this was replaced with 3ml of complete M199 growth media for 2 h following the 5 h incubation period, the media was changed to allow the cells to recover and the cells were exposed to flow using the orbital plate system, in order to assess gene function under the effect of WSS.

2.2.8 Immunocytochemistry staining of cultured EC

The expression of proteins of interest was assessed by immunostaining using specific antibodies (Tables 8 and 9) followed by widefield fluorescence microscopy (LeicaDMI4000B). HUVEC exposed to flow were either stained directly on the 6-well plate or on 34 mm glass slides (cells seeded onto glass slide prior to exposure to flow). Following orbital shaking, media from cultured HUVEC was removed and 500 µl/well of 4 % formaldehyde (10 min; room temperature) was added to fix the cells. The cells were then permeabilised by adding 700 µl of 0.1 % triton (10 min; room temperature). To block non-specific interactions with the secondary antibody (Table 9), 500 µl/well 20 % goat serum was added (30 mins; room temperature). This was followed by adding 500 µl/well of specific antibodies diluted at the final concentration in 5% goat serum. Alternatively, non-specific isotype controls (matching the species of the primary antibody) were added as a control for background / non-specific fluorescence. The primary antibodies were incubated overnight at 4 °C. The primary antibody was then removed and the cells were washed x3 with 1 ml/well PBS (for 5 min at room temperature, with shaking) and

Table 7. siRNA oligonucleotide information

Gene	SiRNA product number; company purchased from
Gata4	Silencer® select s5603; Thermo-scientific
Twist1	Silencer® select s14523; Thermo-scientific
Snail	OnTargetPlus smartpool L-010847-01; Dharmacon
Scrambled	OnTargetPlus Non targeting siRNA 1 D-001810-01-50; Dharmacon

Table 8. Primary antibodies

		Application and final dilution used					
Antibody name	Host species	Company/Product number	Immunocytochemistry	Immunohistochemistry	Chromatin IP (ChIP)	En face immunostaining	
N-cadherin	Rabbit	ab12221; Abcam	(1:250; 4 µg/ml)	-	-	-	
N-cadherin	Rabbit	ab18203; Abcam	-	-	-	(1:384; 1.25 µg/ml)	
Ki67	Rabbit	Ab 15580; Abcam	(1:225; 4 µg/ml)	-	-	(1:180; 5 µg/ml)	
Alexa Fluor® 488 anti-mouse CD31 conjugate	Rat	102514; Biolegend	-	-	-	(1:100; 5 µg/ml)	
Mouse IgG	Mouse	I5381; Sigma	Matched to primary	Matched to primary	-	Matched to primary	
Rabbit IgG	Rabbit	I5006; Sigma	Matched to primary	Matched to primary	-	Matched to primary	
Goat IgG	Goat	I5256 ; Sigma			Matched to primary		

Table 9. Secondary antibodies

Antibody name	Product no./company purchased from	Host	Target species	Dilution/final concentration
AlexaFlour®568	A-11011; ThermoScientific	Goat	Rabbit	(1:500; 4µg/ml)
AlexaFlour®568	A11004; ThermoScientific	Goat	Mouse	(1:500; 4µg/ml)
AlexaFlour®568	A11077; ThermoScientific	Goat	Rat	(1:500; 4µg/ml)
Alexa Fluor® 488	A-11088; ThermoScientific	Goat	Rabbit	(1:500; 4µg/ml)
Biotinylated	BA1000; Vector-laboratories	Goat	Rabbit	1:200

500 µl/well of secondary antibodies were incubated for 2 h at room temperature, with shaking. The cells were washed with PBS as described previously and the nuclei were stained using a DNA-binding dye; DAPI added at 500 µl/well, in PBS (Incubated for 10 mins, at room temperature). At least 5 images were captured from every WSS region (i.e. At least 5 images from the centre and 5 from the periphery of the well). The images were captured using the same exposure and gain for all conditions, and were normalized to the background signal of an isotype control stained sample. The expression of the proteins of interest was quantified by either assessing the fluorescent intensity of blindly selected multiple cells (at least 50 per site) using Image J (version 1.49p) or by determining the % positive cells. Different experimental numbers (N) correspond to independent experiments using HUVEC from different human donors.

2.2.9 *In vitro* tube formation assay on pre-sheared cells

Tube formation was assessed as described (Zhao et al. 2007). 50,000 cells/ well were seeded onto 1mg/ml collagen (bovine skin collagen, made up in DMEM media), which was added at 50 µl/well in a 96 well- flat bottom tissue culture plate. The collagen was added overnight and maintained at 37 °C, 5 % CO₂ prior to cell seeding. The cells were cultured with 110 µl of 2 % serum complete M199, containing 50 ng/ml VEGF. Following 48 h, the cells were fixed with 4 % formaldehyde. To visualise the formed tube structures, the cells stained with membrane labelling dye PKH26 and nuclei were labelled using DAPI, followed by widefield fluorescence microscopy (LeicaDMI4000B). The tube structures were quantified by assessing cumulative tube length and by counting the branch points per frame of view, using Image J version (1.49p). A scientist blinded to the experimental conditions recorded the measurements.

2.2.10 *In vitro* cell migration; scratch assay on pre-sheared cells

Cell migration was assessed as described (Warboys 2014; Liang et al., 2007). Following orbital shaking, a scratch using a P200 pipette tip was created vertically along each well of the 6-well plate, to create a “wound” in the monolayer at both the periphery (high WSS) and the centre (low WSS) region of the well (Figure 15). The media was replaced with 2ml of complete M199 growth media.

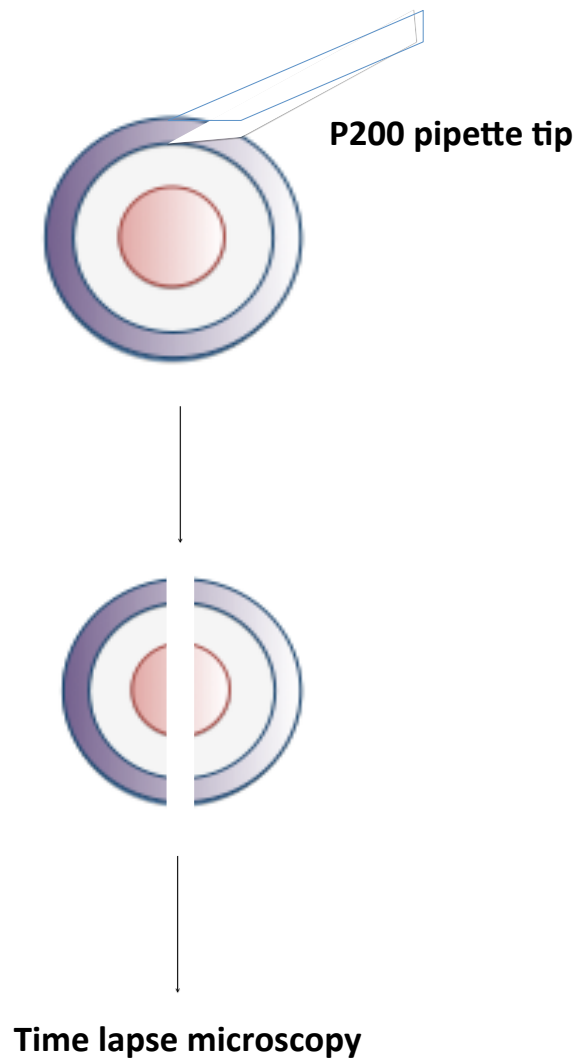


Figure 15. Schematic of scratch assay. Following 72h of orbital shaking, a scratch across the well of the 6-well plate was made using a P200 pipette tip, this created a wound in the monolayer at the region of high WSS (periphery; purple) and the region of low WSS (centre; red). Cell migration into the wounded area was monitored by time lapse microscopy.

Cell migration into the wounded area following the formation of the scratch (Time 0 time point) was visualized using time-lapse microscopy (Leica AF6000 Timelapse microscope). Images were captured from every well at 3 min intervals for up to 20h after scratch formation. The distance migrated was determined by measuring the position of the monolayer edge in relation to the starting point (at 3 points per field of view) using the LAS_AF Lite software (v 2.3.0). The average velocity was calculated by dividing the average distance migrated over time.

2.2.11 EC permeability assay

To assess the effect of gene function on EC permeability under flow, a method published by the Weinberg group (Warboys et al. 2010) was followed. Briefly, HUVEC were seeded at 200,000cells/ well onto fibronectin (50 µg/ml) coated transwell inserts (24 mm diameter, 0.4 µm pore, polyester membrane; Table 2) placed in a 6-well plate and were then cultured overnight. 2.6 ml of complete M199 growth media was added to the bottom compartment and 1.5 ml to the top compartment (Figure 16), the cells were then placed on an orbital shaking platform at 150 rpm for 72h. At 24h before taking the permeability measure (at 48 hours of orbital shaking) the media was changed from 20 % complete M199 growth media into 10 %. And, 1 hour before taking the permeability measure, media in the top compartment was changed into 10 % serum M199 media, containing 1 % BSA. A Rhodamine-albumin tracer (Warboys et al., 2010) at a concentration of 1 mg/ml was used to assess EC permeability. Following 72h of orbital shaking (alternatively cells were cultured under static conditions for 72h) media in the top compartment was changed into media containing the tracer (10 % M199 growth medium; rd-albumin tracer 1 mg/ml; 1 % BSA). Following 1 hour of incubation of cells in the top compartment (under static conditions) of the transwell with the tracer the transwell inserts were removed from the plate, and media from the bottom compartment was collected, to assess EC permeability by measuring the concentration of tracer that had passed from the top compartment through the EC monolayer. The concentration of Rd-Albumin (mg/ml) was assessed using a fluorimeter (Varioskan, Thermoscientific) with excitation at 570 nm and emission at 600 nm.

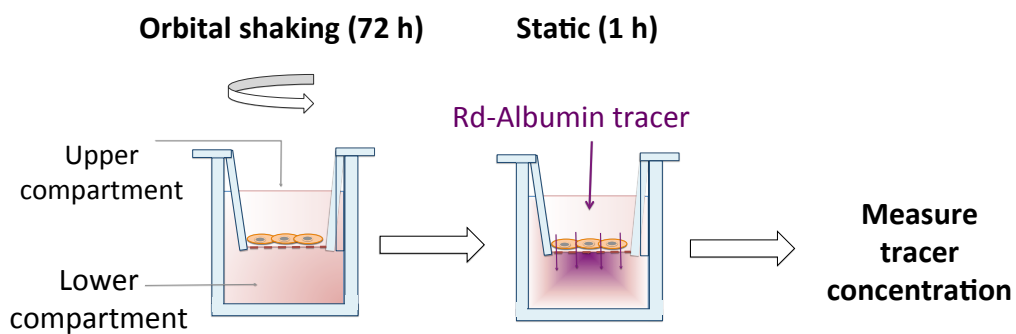


Figure 16. Schematic for EC permeability assay. HUVEC were cultured onto transwell inserts. Following 72h of orbital shaking, under static conditions a rhodamine-albumin tracer was added to the top compartment of the transwell plate for 1 hour. The concentration of tracer in media collected from the bottom compartment was used as a measure of permeability.

2.2.12 Chromatin immunoprecipitation (ChIP)

ChIP was used to assess whether GATA4 interacts with the Twist1 or Snail promoters. Genomic (Twist1 or Snail) sequences were interrogated for putative GATA4 binding sites (A/TGATAA (G) using the Eukaryotic promoter database (EPD; <http://epd.vital-it.ch/>). ChIP Primers (Table 6) were then designed based on the identified GATA4 binding site DNA sequences in the promoter regions of Twist1 and Snail using Primer3 (primer3.ut.ee/) Following 72 h of orbital shaking, HUVEC were fixed with formaldehyde (1 % for 10 min, room temperature). The following steps of the ChIP experiment were carried out using the simpleChIP®Plus Enzymatic Chromatin IP Kit (9005; Cell signalling) following the manufacturer's protocol. For one immunoprecipitation a cell density of 4.5×10^6 (three 6-well plates, with 250,000 cells/well) was used. ChIP-grade GATA4 antibodies (C-20 sc-1237, Santa Cruz) or isotype-matched control (Goat IgG) were used in 5% goat serum. Following the purification of precipitated genomic DNA sequences using the DNA purification columns present in the simpleChIP®Plus Enzymatic Chromatin IP Kit. The assessment of the specific Twist1 or Snail promoter DNA sequences co-precipitated with the GATA4 antibody or non specifically bound with the isotype control was carried out by qRT-PCR. The thermal profile used was; Step 1 at 95°C for 3 min, step 2 at 95°C for 15 seconds and step 3 at 60°C for 1 min x 45 repeats. The qRT-PCR results were assessed using the ΔC_t method (following normalisation to a housekeeping gene). Values of the DNA sequences co-precipitated by the GATA4 antibody were normalised to those of the isotype control.

2.2.13 Immunohistochemistry staining on human coronary sections

Immunohistochemistry was used to assess the expression of specific proteins in coronary sections isolated from human patients of heart transplants, either with ischemic heart disease (severe atherogenesis) or from patients of idiopathic cardiomyopathy (mild atherogenesis), obtained with ethical consent from the donors (National Research Ethics number, 12/NW/0036). 5µm sections were made from paraffin-wax embedded human coronary tissue (fixed with 4% formaldehyde) using a microtome (LeicaRM2135; Leica). The sections were de-waxed and re-hydrated by incubating through graded alcohol solutions to water (Xylene; 10 min minimum, 100% Ethanol (EtOH), 90% EtOH, 70% EtOH, 50% EtOH, water (all for 10 seconds). Endogenous peroxidase activity was blocked by incubation in 3% hydrogen peroxide for 10 min, followed by rinsing in water. For staining using anti-TWIST1, anti-SNAIL and anti-GATA4 antibodies the antigen retrieval method adopted involved incubation of sections in citrate buffer at pH6 for 20 min at 95°C, followed by cooling for 20 min, at room temperature and rinsing in PBS. Alternatively, for anti-vWF staining (to label EC) the sections were incubated in 0.1% trypsin/TBS for 10 min at 37°C, followed by rinsing in water.

Incubating the sections with 1% milk in PBS for 30 min, at room temperature, blocked non-specific antibody binding. The sections were then incubated with primary antibodies either overnight at 4°C (for TWIST1, GATA4 and SNAIL) or for 1 hour at room temperature (for vWF). A PBS washing step, x3 washing at 5 min intervals at room temperature was carried out. This was followed by incubation with biotinylated secondary antibodies for 30 min, at room temperature. The sections were then washed (PBS x3, 5 min, at room temperature) then incubated with Avidin-Biotin complex (ABC) complex (for 30 min at room temperature. The sections were washed (PBS x3, 5 min intervals at room temperature) then 3,3'-Diaminobenzidine (DAB) substrate was added to the slides, for approximately 5 min (until the reaction resulted in a change in colour of the tissue sections). The sections were then rinsed in water to end the DAB reaction and counterstained by incubation in Carazzi's haematoxylin for 30 seconds (room temperature). This was then followed by rinsing in water and dehydration through graded alcohol solutions, to xylene and mounting

onto microscope slides using DPX mountant. The sections were imaged using a light microscope coupled to the NIS elements software (v3.22.15). Assessment of protein expression was calculated as a percentage out of cells positive for vWF to give a measure of % positive endothelial cells. Different experimental numbers (N) correspond to different tissue sections collected individually from different human patients.

2.2.14 Mouse breeding strategies and transgenic animals

All animal work was carried out in accordance with the UK Animal (Scientific procedures) Act, 1986 and the NIH Guide for the care and use of laboratory animals.

2.2.14.1 Genotyping

To assess the genotype of mice, DNA was isolated from earclips by adding 150ul of earclip lysis buffer (1M Tris-HCl (pH 8.5), 0.5M EDTA (pH 8.0), 10% Tween-20; with 30 µl/ 1000 µl Proteinase K; Table 4) to each ear clip, which was then incubated at 55°C overnight. The earclip lysate was vortexed briefly and the proteinase-K was inactivated by incubation at 100°C for 12 min. A volume of 600 µl of sterile nuclease-free water was added and the earclip DNA was stored on ice at 4°C. A standard PCR reaction was set up to a final volume of 25 µl consisting of 10 µl earclip DNA + 15 µl PCR master mix (PCR primer sequences are in 2). The PCR master mix contained 1.25 µl of specific forward and reverse primers (used at 20µM) to detect specific transgenic alleles, 0.5 µl dNTPs, 5µl Reaction buffer, 0.25 µl DNA polymerase (all from Q5 high fidelity DNA polymerase kit) and 6.75 µl of water to give a final volume of 15 µl. The thermal profile of the PCR reaction consisted of; 95°C for 1min, 95°C for 30 seconds (annealing temperature depending on specified different primer sets) x40 repeats, 72°C for 1 minute and final step at 4°C for storage of the sample. The PCR products were separated using gel electrophoresis. The samples were loaded onto a 1.5% agarose gel with DNA gel loading dye (used at 1X). The gel was imaged using a bioimaging system (Chemi-genius; GeneFlow) and using the GeneSnap software (v 7.04.05).

2.2.15 The *SCL-Cre-ER^T*; *R26R-Td tomato transgenic model*

For EC lineage tracing, the cells were genetically marked using a transgenic model developed by Göthert *et al.* (Göthert et al. 2004). A basic helix-loop-helix (bHLH) Stem cell enhancer locus/ T-cell acute lymphocytic leukemia 1 (SCL/Tal) is essential for haematopoiesis and endothelial cell differentiation. The SCL locus contains two distinct elements, an SCL 5' endothelial enhancer which directs expression to the adult endothelium and embryonic hematopoietic progenitors whereas an SCL 3' enhancer is responsible for SCL expression in early hematopoietic progenitors and embryonic endothelium (Göthert et al. 2004). To achieve an endothelial specific expression of a tamoxifen-inducible recombinase Cre-ER^T, mice expressing a 5' SCL /TAL driven Cre ER^T (tal-tg Cre ER^T) were used (mice used are heterozygous; carried one copy of Cre-ER^T to avoid non-specific Cre-mediated genomic recombination). To label the EC, the endothelial-SCL-Cre-ER^T expressing mice were bred with mice expressing a Td-tomato reporter allele to create *SCL-Cre-ER^T*; *R26R-Td tomato* mice. The Td-tomato allele was flanked by LoxP sites, with a stop cassette inserted downstream of the ROSA26 promoter. Cre-ER^T activation by tamoxifen results in the recombination-mediated excision of the Lox P sites, mediating the transcription of the Tomato td allele by the ROSA 26 promoter (Figure 17 A). To activate the Cre-ER^T, mice were given an intraperitoneal (I.P) injection of 20 mg/ml tamoxifen for 5 consecutive days. The fluorescent R26R Td-tomato protein expressed in the cytoplasm and the nucleus of EC indicates positive adult endothelium.

SCL-Cre-ER^T male mice (heterozygous for Cre) were bred with R26R Td-tomato (homozygous) expressing female mice from approximately 6 weeks old animals. Following DNA isolation from ear clips, PCR reactions followed by gel electrophoresis were performed. Genotyping results revealed the proportion of R26R heterozygote mice carrying the Cre-ER^T allele, which was approximately 50% Cre-ER^T positive and 50% Cre-ER^T negative (Figure 17 B). Double transgenic mice *SCL-Cre-ER^T*; *R26R Td-tomato* (heterozygous for both alleles) were used as experimental mice and R26R Td-tomato heterozygote mice were used as experimental controls.

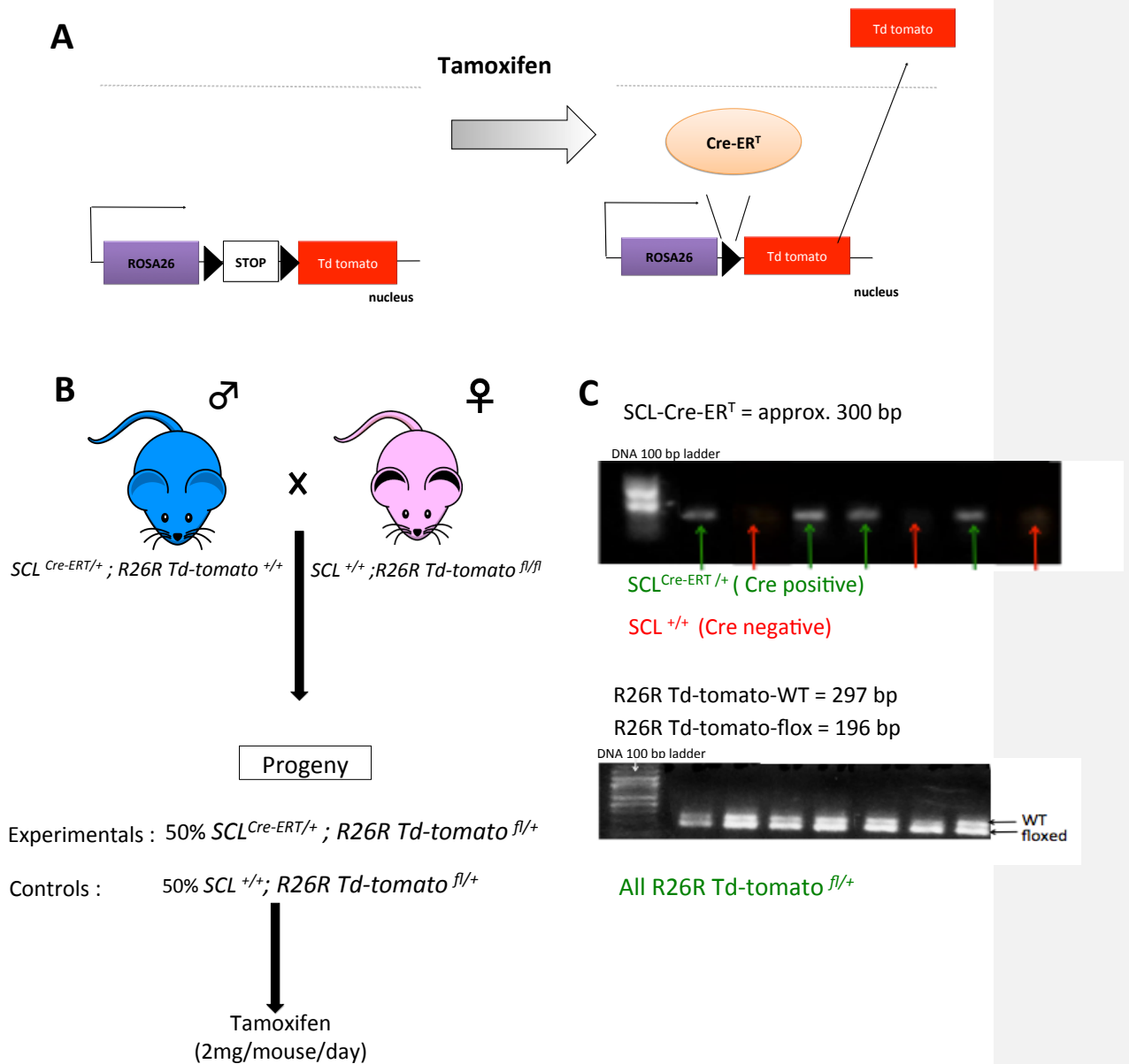


Figure 17. *SCL-Cre-ER^T; R26R Td-tomato* mice breeding and genotyping. A) *SCL*-driven Cre activity is switched on following tamoxifen treatment. Activated Cre-recombinase mediates excision of a loxp-flanked LoxP –flanked stop codon upstream of a Td-tomato coding gene that is under the activity of the Rosa26 promoter, giving rise to the expression of Td-tomato in endothelial cells. B) *SCL-Cre-ER^T* male mice were crossed with *R26R Td-tomato^{fl/fl}* females, the genotypes of expected progeny are indicated. C) PCR followed by gel electrophoresis was carried out. *SCL-Cre-ER^T* (approx. 300bp band) was detected in approximately 50% of the litter. All the progeny were Td-Tomato heterozygote; they expressed both the *R26R-Td tomato* floxed allele (297 bp band) and the WT allele (196 bp band).

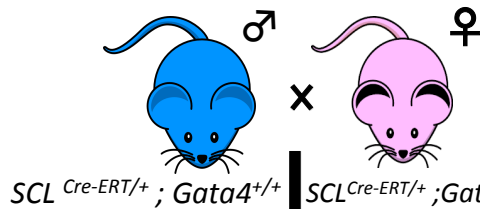
2.2.16 Breeding and genotyping of *SCL-Cre-ER^T*; *Gata4*^{KO} mice

Since the absence of GATA4 is embryonically lethal (Kuo et al. 1997), conditional, EC-specific knock out (KO) animals were generated. Multiple breeding steps were carried out to achieve this. Firstly, *Gata4* floxed (LoxP sites flanking *Gata4* coding exons) homozygous female mice (Carrasco et al. 2012) were bred with heterozygous *SCL-Cre-ER^T* male mice. Genotyping carried out as described previously (Figure 18 A) revealed that 50% of the progeny was heterozygous for the *Gata4* floxed allele and for the *SCL-Cre-ER^T* allele, these *SCL-Cre-ER^T*^{+/-}; *Gata4*^{fl/+} animals were then used for the next breeding step.

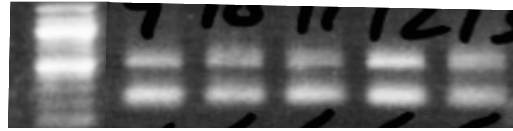
Secondly, to ensure that both of the *Gata4* alleles in the transgenic mice are floxed (for complete loss of function in EC) *SCL*^{Cre-ERT/+}; *Gata4*^{fl/+} animals were backcrossed with *SCL*^{+/+}; *Gata4*^{fl/fl} mice (Figure 18 B). Since the experimental mice are required to be *SCL*^{Cre-ERT/+}; *Gata4*^{fl/fl} mice, whilst experimental controls to be *SCL*^{+/+}; *Gata4*^{fl/fl} mice it was important to introduce a third breeding step in order to eliminate the possibility of having progeny which are heterozygous for the *Gata4* floxed allele. Therefore, *SCL*^{Cre-ERT/+}; *Gata4*^{fl/+} mice were backcrossed with *SCL*^{+/+}; *Gata4*^{fl/fl} mice. The resultant progeny were 50% experimental and 50% experimental controls (Figure 18 C).

Finally, *SCL*^{Cre-ERT/+}; *Gata4*^{fl/fl} mice and experimental controls *SCL*^{+/+}; *Gata4*^{fl/fl} were injected with tamoxifen as described previously to activate the *Cre-ER^T* mediated gene deletion (Figure 9 D). The inserted LoxP sites flank the coding exons 3-5 of the *Gata4* gene, this exon codes for the zinc finger binding domain and the nuclear localization signal that is essential for GATA4 function. Cre-mediated deletion therefore gives rise to a *Gata4* deletion in the endothelium (*SCL-Cre-ER^T*; *Gata4*^{KO}).

A *SCL-Cre-ERT^T; Gata4 flox* mice breeding step 1

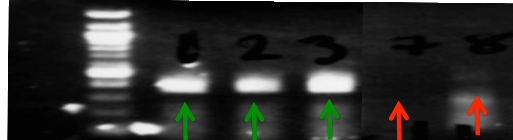


$Gata4^{fl/fl} = 455$ bp
 $Gata4^{+/+} = 355$ bp



All $Gata4^{fl/+}$

$SCL-Cre-ERT^T = \text{approx. } 300$ bp



$SCL-Cre-ERT^T$ positive

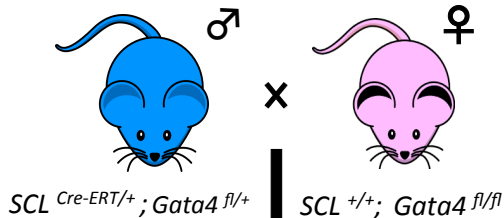
$SCL-Cre-ERT^T$ negative

50% $SCL^{Cre-ERT/+}; Gata4^{fl/+}$

50% $SCL^{+/+}; Gata4^{fl/+}$

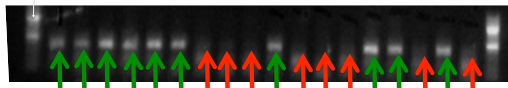
Progeny

B *SCL-Cre-ERT^T; Gata4 flox* mice breeding step 2



$SCL-Cre-ERT^T = \text{approx. } 300$ bp

DNA 100 bp ladder



$SCL^{Cre-ERT/+}$ (Cre positive)

$SCL^{+/+}$ (Cre negative)

25% $SCL^{Cre-ERT/+}; Gata4^{fl/fl}$

25% $SCL^{Cre-ERT/+}; Gata4^{fl/+}$

25% $SCL^{+/+}; Gata4^{fl/+}$

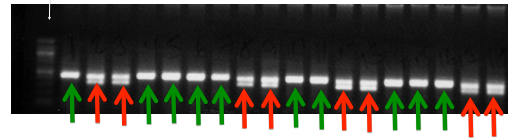
25% $SCL^{+/+}; Gata4^{fl/fl}$

Progeny

$Gata4^{fl/fl} = 455$ bp

$Gata4^{+/+} = 355$ bp

DNA 100 bp ladder



$Gata4^{fl/fl}$

$Gata4^{fl/+}$

D *SCL-Cre-ER^T; Gata4* flox mice breeding step 3

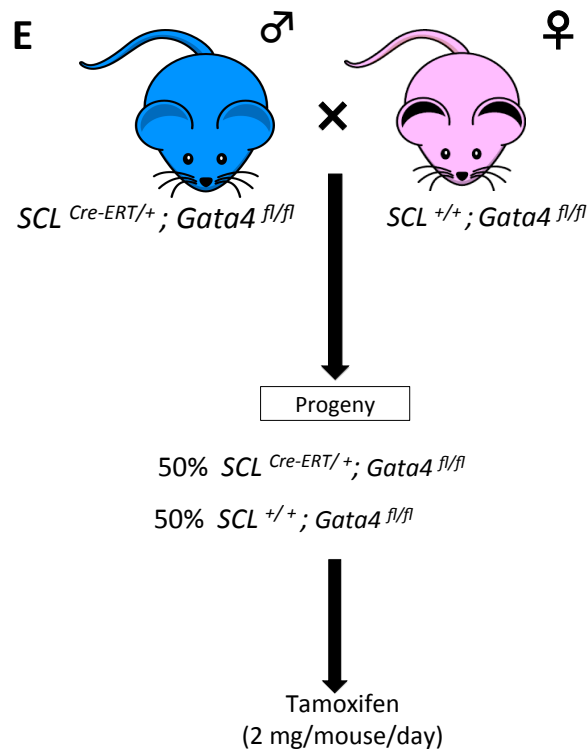
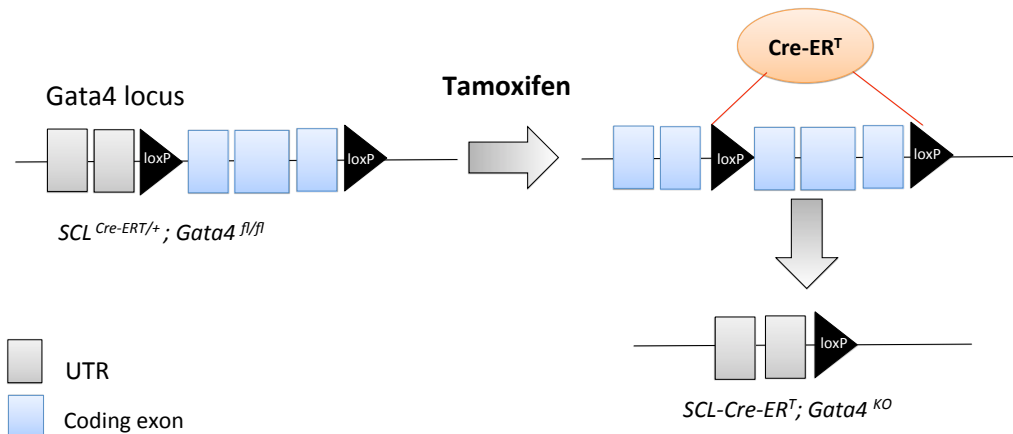


Figure 18. *SCL-Cre-ER^T; Gata4^{fl/fl}* mouse breeding and genotyping. A) *SCL^{Cre-ERT/+}; Gata4^{+/+}* males were crossed with *SCL^{+/+} Gata4^{fl/fl}* females, the expected progeny genotypes are indicated. PCR followed by gel electrophoresis was carried out. All the litter were heterozygote for the *Gata4* floxed allele, they expressed both the *GATA4* floxed allele (455 bp band) and the WT allele (355 band). *SCL-Cre-ER^T* (approx. 300bp band) was detected in approximately 50% of the litter. B) In the second breeding step, males expressing Cre (*SCL^{Cre-ERT/+}; Gata4^{+/+}*) were back crossed with *SCL^{+/+} Gata4^{fl/fl}* females, the expected progeny and their ratios are shown. C) *SCL*-driven Cre activity is switched on following tamoxifen treatment. Activated Cre recombinase mediates excision of a lox P flanked *Gata4* coding exons, giving rise to the *Gata4* deletion in EC. D) *SCL-Cre-ER^T; Gata4^{fl/fl}* mouse breeding and genotyping, breeding step 3 involved the crossing between *SCL-Cre-ER^T* males with *Gata4^{fl/fl}* females, the expected progeny were 50% Cre-positive (*SCL-Cre-ER^T*) and 50% Cre negative (*Gata4^{fl/fl}*). Experimental and control mice were injected with tamoxifen (2 mg/mouse/day) for 5 consecutive days to result in the *SCL-Cre ER^T* mediated loss of *Gata4* function in EC.

2.2.17 Breeding and genotyping of *Tie2-Twist1*^{KO} mice

Deletion of *Twist1* is embryonically lethal (Chen et al. 1995), therefore conditional *Twist1* deletion strategy in EC was adopted. The *Tie2* gene encodes for an angiopoietin receptor that is expressed in EC throughout embryonic development and in adult cells (Davis et al. 1996; Kisanuki et al. 2001). Therefore, *Tie2*-driven Cre expressing mice were crossed with *Twist1* floxed mice (lox P sites flanking coding exon 1) to create *Tie2-Twist1*^{KO} animals (Chen et al., 2007; Li et al., 2014) (Figure 19 A). The *Tie2-Twist1*^{KO} (*Tie2*^{cre/+} ; *Twist1*^{fl/fl}) animals were then backcrossed with *Twist1*^{fl/fl} animals (*Tie2*^{+/+} ; *Twist1*^{fl/fl}) (Figure 19 B) to give rise to a progeny containing approximately 50% experimental mice *Tie2-Twist1*^{KO} and 50% *Twist1*^{fl/fl} experimental controls (Figure 19 C).

2.2.18 *En face* immunostaining of the mouse aortic arch

To assess the expression of the proteins of interest *in vivo* at areas exposed to atherosusceptible chronic low (inner curvature) or atheroprotective high WSS (outer curvature), *en-face* immunostaining was carried out on the murine aortic arch as described (Hajra et al. 2000; Warboys et al. 2014; Cuhlmann et al. 2011). Briefly, the mice were culled by I.P injection of pentobarbital or by isofluorane overdose. The mouse ribcage area was exposed to reveal the heart, following the severing of the right atrium; 10 ml of PBS was injected into the left ventricle to flush blood from the vasculature. To perfuse fix the tissue, 10 ml of 4% formaldehyde was injected. The heart/ribcage was isolated and incubated in 2% formaldehyde for 1 hour at room temperature before storage. The aortic arch, with the connecting descending aorta was dissected from the ribcage. A cut was made through the aortic arch to reveal the inner and outer curvature regions (Figure 20), which were then processed for immunostaining in a 96 well, flat bottom plate. The tissue was permeabilised and blocked by incubating with 20% goat serum in 0.5% Triton-X overnight at 4°C. To be able to assess expression in endothelial cells lining the intimal layer of the tissue. Conjugated 488-alexafuor-anti mouse CD31 antibodies (in 5% BSA in 0.1% PBST) were incubated with aortic preparations for 4 days at 4°C.

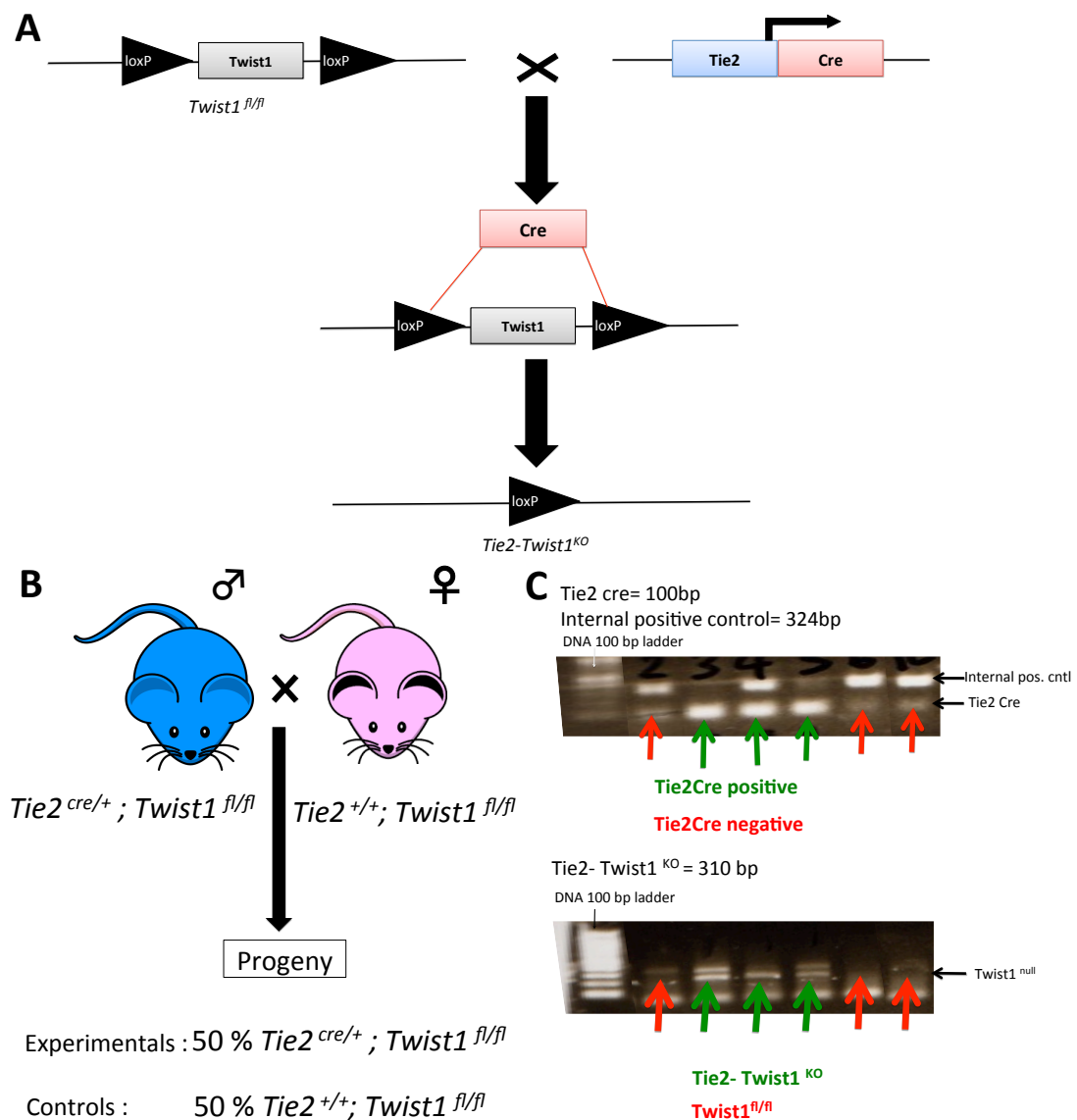


Figure 19. *Tie2Twist1^{KO}* breeding and genotyping. A) The expression of Cre driven by the *Tie2* promoter results in cre-mediated recombination of the loxP flanked *Twist1* coding exon and subsequently a loss of *Twist1* expression in endothelial cells. B) *Tie2-Twist1^{KO}* (*Tie2^{cre/+}; Twist1^{fl/fl}*) male mice were crossed with *Twist1^{fl/fl}* (*Tie2^{+/+}; Twist1^{fl/fl}*) females. The expectant progeny were 50% positive for Cre expression and 50% were Cre negative. C) Standard PCR followed by gel electrophoresis was carried out. *Tie2-Cre* (100bp band) was detected in approximately 50% of the litter. An internal positive control (324 bp band) was used in the reaction to further validate a lack of Cre expression. Following Cre mediated recombination the *Tie2-Twist1^{KO}* allele (310bp band) was detected in mice expressing *Tie2-Cre*, further confirming the genotype of the *Tie2-Twist1^{KO}* mice.

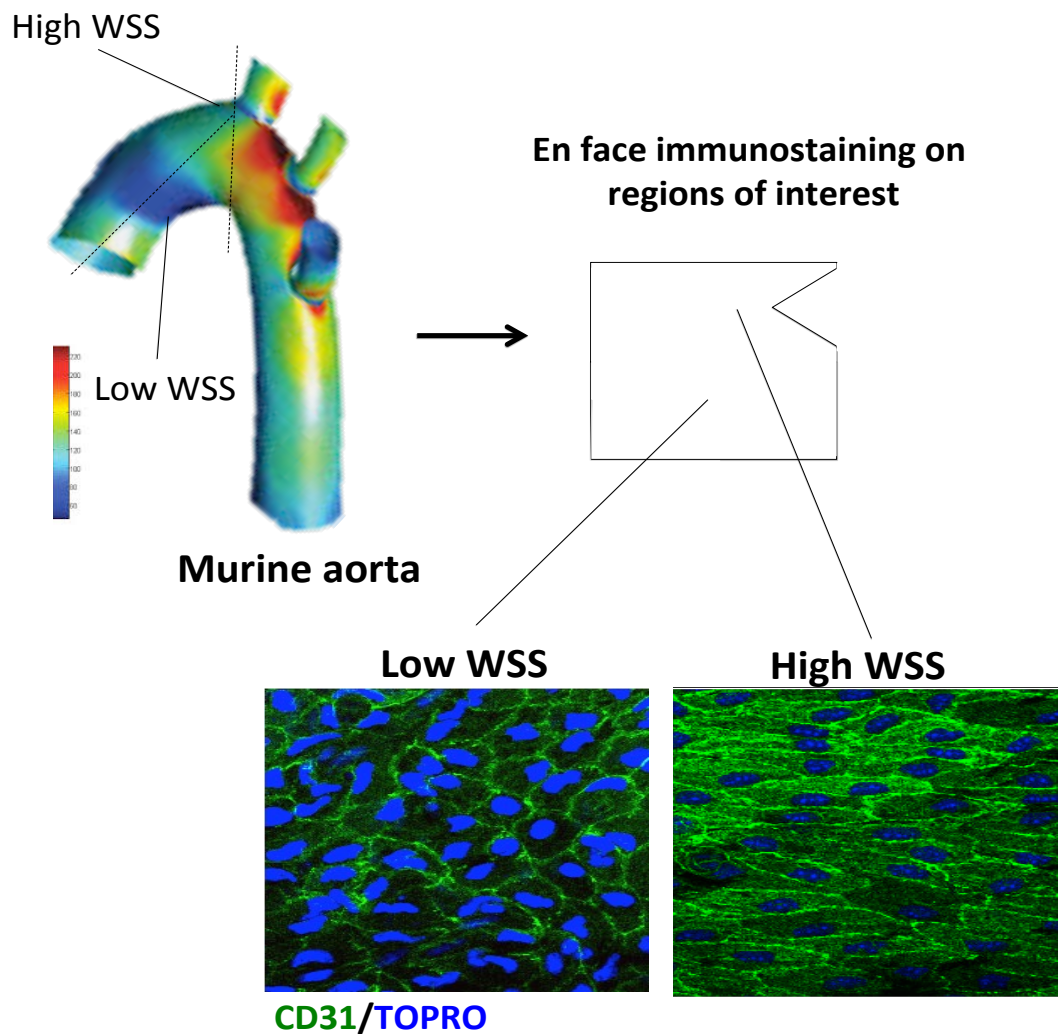


Figure 20. Schematic of *en face* preparation on the murine aortic arch. To study the protein expression of proteins of interest at specific flow sites in the murine aorta, regions of the inner curvature (low wSS) and the outer curvature (high WSS) were cut open out (dotted lines) of the dissected aortic arch and opened *en face*. Immunostaining revealed the distinct EC alignment in cells at the distinct flow regions, CD31 (green) labelled the endothelium and the nuclei were stained using TOPRO DNA binding dye. The WSS map of the murine aortic arch was taken from Suo et al., 2007.

The tissue segments were then washed with PBS x3 for 5 min at room temperature. This was followed by incubating the tissue with primary rabbit antibodies against the mouse proteins of interest or an isotype control overnight at 4°C. Following washing of the segments (with PBS x3 for 5 min, at room temperature) they were incubated with goat anti-rabbit alexafluor568 labeled secondary antibodies (in 5% BSA in 0.1% PBST) for 5 hours, at room temperature. This was followed by washing steps (PBS x3, 5 min, room temperature). To label the nuclei, a DNA-binding dye Topro-3 was used. The segments were then opened *en face* and mounted facedown on glass coverslips using Prolong gold anti-fade mountant which were then placed on microscope slides. The tissue segments were imaged using confocal laser scanning microscopy (Zeiss LSM510 NLO inverted microscope). The isotype control stained tissue segments were used as a control for non-specific staining. The same exposure settings on the microscope were used for all samples. At least 5 images were captured from every WSS region (i.e. 5 images from the outer and 5 from the inner curvature). The expression of the proteins of interest was quantified by either assessing the fluorescent intensity of blindly selected multiple cells (at least 50 per site) using Image J (version 1.49p) or by determining the % positive cells. Different experimental numbers (N) correspond to different animals.

2.2.19 Insertion of flow altering cuff into murine carotid artery

To gain a causal relationship between flow and protein expression *in vivo*, a flow-altering cuff method was used to directly create distinct regions of flow in the inserted vessel. Cuff insertion alters flow, giving rise to low WSS upstream of the cuff, high WSS in the cuff region and low, oscillating WSS in the region downstream of the cuff (Cheng et al. 2006; Cuhlmann et al. 2011). Constrictive cuffs with an internal diameter of 400 µm diameter tapering to 200 µm over 1.5 mm were used (manufactured by PTFE). The cuffs were inserted into the right carotid artery of isofluorane-anaesthetised mice (8 weeks old, C57BL/6 or SCL-Cre-ER^T; R26R-Td tomato animals) following published methods (Cheng et al., 2006; Cuhlmann et al.,

2011). The left carotid artery did not have a cuff inserted and was therefore used as a sham control.

2.2.20 Statistics

Quantitative analyses were carried out on at least three independent experimental repeats. Every experimental repeat corresponds to an experiment carried out independently using either different animals or independently isolated HUVEC or PAEC. All the quantitative analyses shown are presented as the mean value \pm SEM. For the assessment of significant differences, paired, unpaired students t-tests, one or two way ANOVA (Bonferroni's multiple comparison test) statistical tests were carried out. Data was accepted as being statistically significant when the P value was $p < 0.05$.

Chapter 3: Low shear stress promotes TWIST1 expression via GATA4

3.1 Introduction

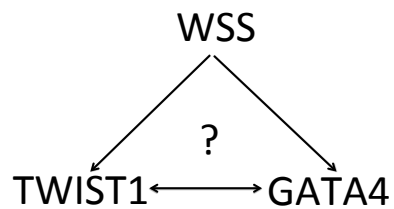
TWIST1 and GATA4 transcription factors play indispensable roles during embryonic development. TWIST1 is important for regulating gastrulation and mesoderm migration (Simpson 1983; Thisse et al. 1988). GATA4 is an upstream master regulator of the gene network controlling cardiac development and specification (Kuo et al. 1997; Zeisberg et al. 2005). Although TWIST1 and GATA4 regulate distinct processes during embryonic development, they both play important roles in controlling valve formation in the developing atrioventricular canal. Both TWIST1 and GATA4 function in a common developmental pathway that drives EndMT in valve formation. It has been shown that GATA4 regulates twist-family transcription factors during this process (Zeisberg et al. 2005; Mcfadden et al. 2002; Vrljicak et al. 2012).

EC lining the vasculature are known to alter physiology according to the mechanical environment they are exposed to. EC in the atherosusceptible sites (low WSS) are “primed” for atherogenesis where they display a higher rate of cell proliferation, permeability and activation compared to quiescent EC in the atheroprotected regions (high WSS) (Lin et al. 2000; Passerini et al. 2004; Davies 2009; Davies et al. 2013).

Although the mechanical activation of TWIST1 and GATA4 has been shown in non-endothelial cell types (Desprat et al. 2008; Wei et al. 2015; Tenhunen et al. 2004), it is unknown whether TWIST1 and GATA4 are modulated by WSS in EC and more specifically if the GATA4- TWIST1 network is involved in EC mechanotransduction.

3.2 Hypothesis

I hypothesised that WSS differentially regulates the expression of TWIST1 and GATA4 in EC exposed to flow using *in vitro* flow systems.



3.3 Aims

To address the hypothesis the following aims were assessed;

1. To confirm that TWIST1 and GATA4 are differentially expressed at low and high WSS sites in the porcine aorta
2. To directly assess the effect of WSS on TWIST1 and GATA4 induction in cultured EC, using *in vitro* flow systems.
3. To assess if TWIST1 and GATA4 cross-regulate one another in EC exposed to WSS.

3.3 TWIST1 and GATA4 expression was elevated at sites of low WSS in the porcine aorta

The microarray study carried out by our group suggested that TWIST1 and GATA4 were more highly expressed at low WSS sites of the porcine aorta compared to high WSS sites (Figure 21 A). To validate the microarray results, EC were isolated from distinct flow sites (low WSS vs. high WSS) of the aorta in a separate cohort of pigs and gene expression was assessed by qRT-PCR. Several quality control measures were put in place to; 1) ensure that the RNA samples were from pure EC and not from the underlying smooth muscle cells. This was accomplished by assessing the relative expression of Cd31 (EC marker) with α -Sma (smooth muscle cell marker). 2) To confirm that the RNA samples were from the distinct flow sites, the expression of several known flow-induced genes was assessed. Mcp-1 is a gene that is known to be more highly expressed in EC exposed to low WSS (Hwang et al., 2003), whereas our group has previously shown that c-Jun expression is preferentially expressed EC exposed to high WSS (De Luca, Serbanovic-Canic and Evans, manuscript submitted). In all samples used, Cd31 levels were at least three fold higher in expression compared to α -Sma levels and Mcp-1 expression was enhanced at the low WSS sites and c-Jun at the high WSS sites (Figure 21 B, 21 C). Samples that did not meet the quality control criteria were excluded from further analysis. Twist1 and Gata4 expression was enriched in EC exposed to low WSS compared to high WSS sites (Figure 21 D) therefore validating the results from the microarray experiment.

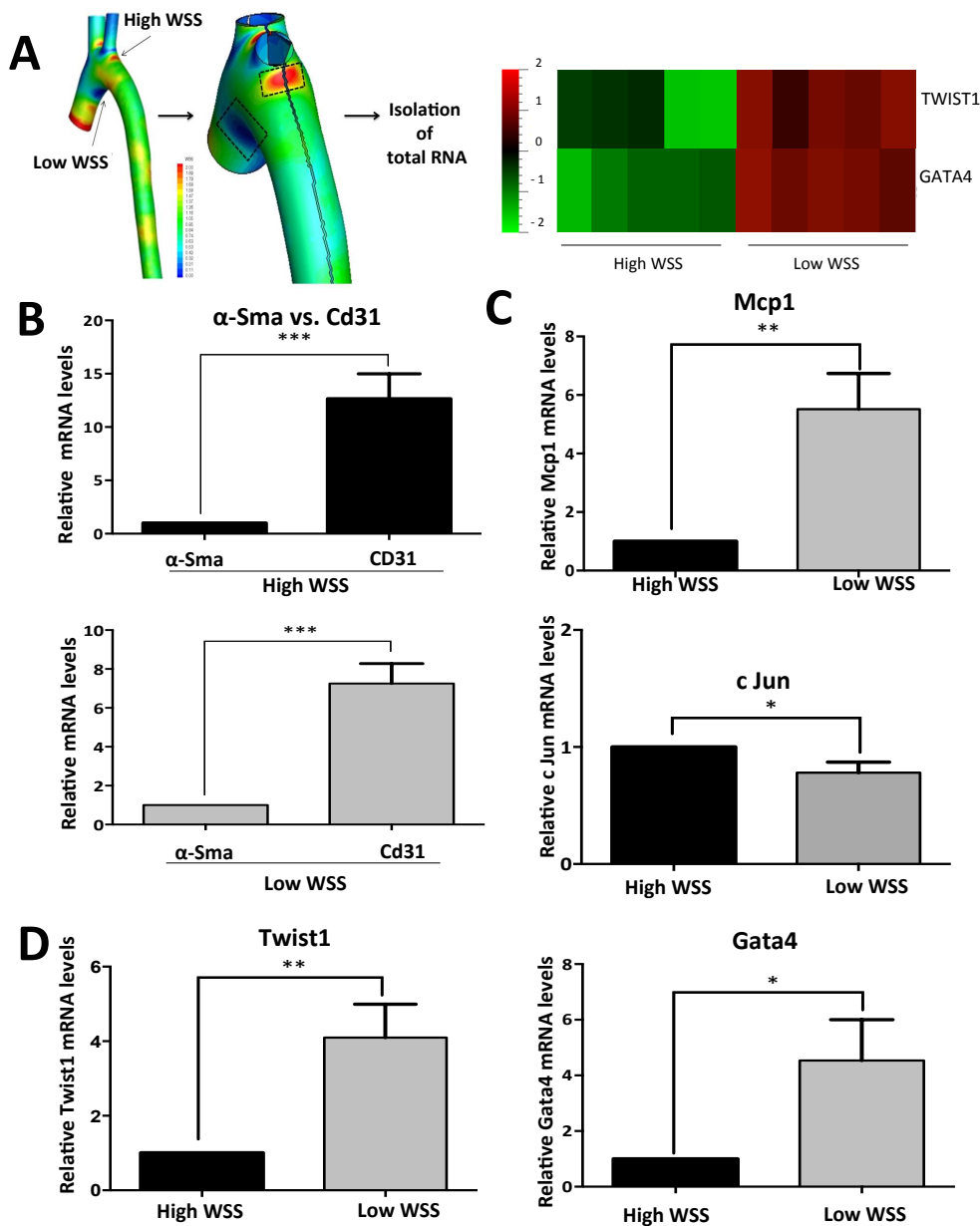


Figure 21. Low WSS was associated with elevated Twist1 and Gata4 expression in the porcine aorta.

A) The transcriptome of EC was studied at low WSS (inner curvature) and high WSS (outer curvature) regions of the porcine aorta. Differentially expressed genes were identified using microarray analysis (N=5 pigs) and the expression patterns of Twist1 and Gata4 are presented as a heat map with red indicating an increase in gene expression. To validate the microarray results, RNA was isolated from EC at low and high WSS of the porcine aorta using collagenase. Quality control checks were carried out to ensure that the samples were from the endothelium; B) Cd31 expression relative to smooth muscle cell marker α -Sma was assessed in samples from the low and high WSS regions (N=6). C) The expression of flow-responsive genes Mcp-1 and eNos was assessed in samples from the low vs. high WSS regions (N=6) D) In quality controlled samples, Twist1 and Gata4 expression levels were assessed in high quality samples from low and high WSS regions (N=6). Mean levels \pm SEM are shown. * $p < 0.05$, ** $p < 0.01$, *** $p < 0.001$.

3.4 Low WSS promoted TWIST1 expression via GATA4

The enhanced expression of Twist1 and Gata4 at low WSS sites in the porcine aorta could be attributed to factors other than WSS such as the effect of altered mass transport and inflammation. Therefore, to establish whether a direct link exists between the expression of Twist1 and Gata4 and WSS, the expression of these genes was studied under flow using *in vitro* model systems. Two complementary systems were used, an orbital plate system and a parallel plate apparatus. Our group and others have previously used computational fluid dynamics to define WSS in an orbiting 6-well plate system, which generates relatively constant low WSS (4.8 dyne/cm²), with rapid variations in direction in the centre of the well and generates a high mean, pulsatile WSS (13 dyne/cm²) in a relatively uniform direction in the periphery of the well (Warboys et al. 2010; Dardik et al. 2005). HUVEC and PAEC were exposed to flow using the orbital plate system and following 72h of orbital shaking, cells in the periphery of the well displayed the characteristic aligned morphology (observed at high WSS sites *in vivo*) whereas cells in the centre of the well exhibited a characteristic polygonal, cobble-stone-like morphology. RNA was isolated from cells at the low and the high WSS sites. The expression of known flow-responsive genes was assessed as a quality control check to ensure that the response of EC to WSS recapitulated those observed previously (Hwang et al. 2003; Fang et al. 2010; SenBanerjee et al. 2004; Jiang et al. 2015; Lee et al. 2006). Mcp-1 (pro-inflammatory gene) expression was higher in cells exposed to low WSS in HUVEC (Figure 22 A) and PAEC (Figure 22 B). Whereas the expression of Klf4 (anti-oxidative gene) was enhanced in cells exposed to high WSS (Figure 22 A for HUVEC; Figure 22 B for PAEC) thus validating the system. Subsequently, the expression of Twist1 and Gata4 was enhanced by low WSS at the mRNA level in PAEC (Figure 22 C) and in HUVEC both at the mRNA (Figure 22 D) and protein level (Figure 22 E). Twist1 and GATA4 protein localisation was almost exclusively nuclear, indicating that these transcription factors were active in EC exposed to low WSS.

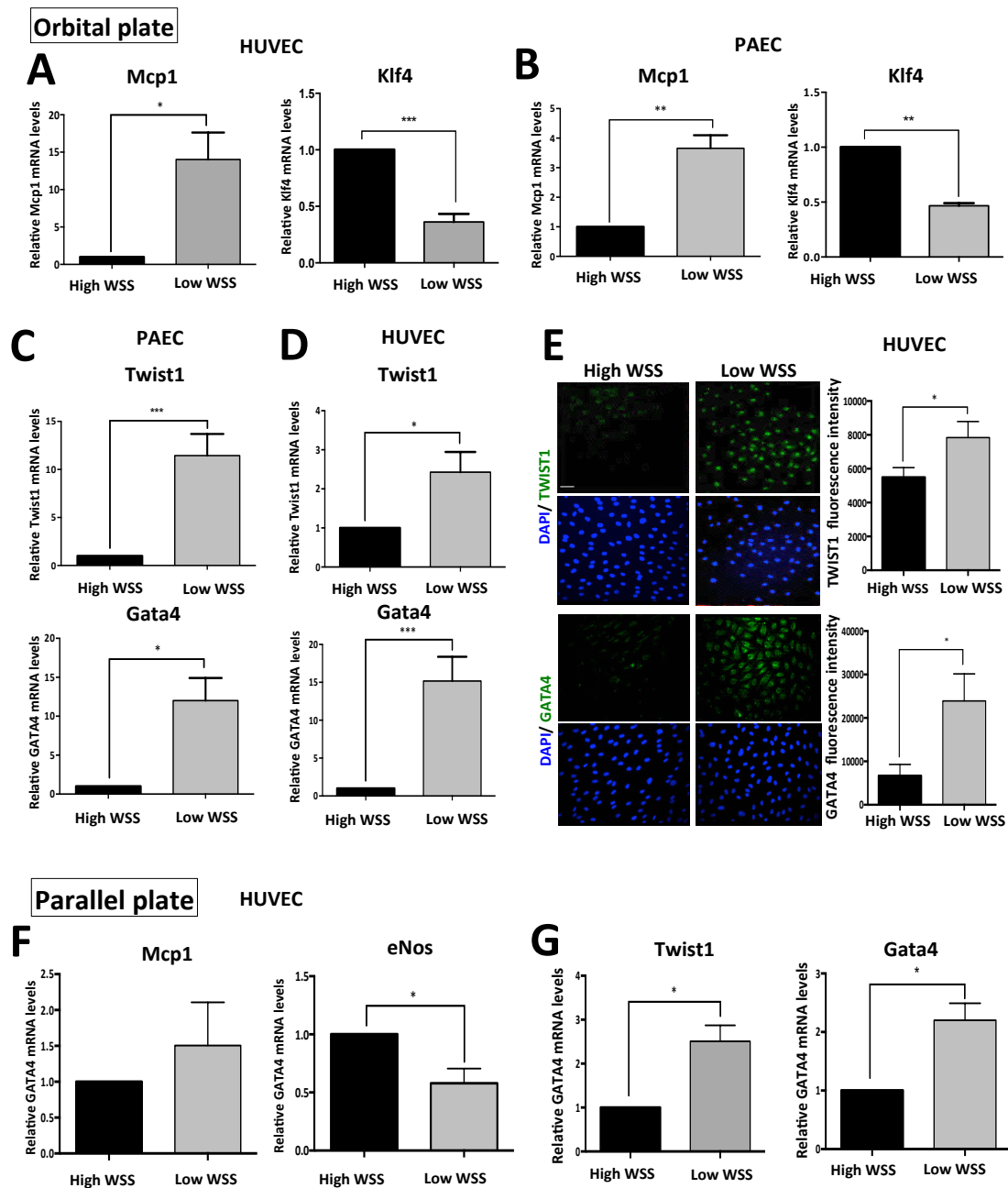


Figure 22. Low WSS induced Twist1 and Gata4 expression in cultured EC *in vitro*. EC were exposed to flow using the orbital plate system for 72h. RNA was isolated from cells exposed to low and high WSS conditions. Quality control checks were carried out, by assessing the expression of known flow-responsive genes MCP1 and KLF4 in A) HUVEC (N=7) and in B) PAEC (N=7). The expression of Twist1 and Gata4 was assessed by qRT-PCR in EC exposed to low and high WSS conditions in C) PAEC and D) HUVEC mRNA (N=7) and E) Expression of Twist1 and Gata4 proteins in HUVEC exposed to low or high WSS was determined by immunofluorescent staining using Twist1 or Gata4 antibodies (green) and the nuclei were stained with DAPI (blue), N=4. Scale bar, 50 μ m. Protein expression levels were quantified by assessing fluorescent intensity levels of signals detected in the nucleus, shown are average values F) EC were exposed to flow using the ibidi™ parallel plate system for 72h. RNA was isolated from cells exposed to high, low and low/oscillatory WSS conditions. F) Quality control checks were carried out, by assessing the expression of known flow-responsive genes Mcp1 and Klf2. G) The expression of Twist1 and Gata4 was assessed by qRT-PCR in cells exposed to high, low and low/oscillatory WSS conditions Mean levels \pm SEM are shown. * $p < 0.05$, ** $p < 0.01$, *** $p < 0.001$.

Similarly, exposure of HUVEC to flow using the Ibidi™ parallel plate system revealed that the expression of quality control genes, MCP1 was enhanced under low WSS (4 dyne/cm²) compared to high WSS (13 dyne/cm²) and low, oscillatory WSS (4 dyne/cm², with 0.2 Hz oscillations), whereas KLF2 (anti-oxidative gene) was induced by high WSS, (Figure 22 F). Using this system, the expression of Twist1 and Gata4 was elevated under low compared to high WSS (Figure 22 G). These results provide direct evidence that low WSS promotes the expression of TWIST1 and GATA4 in EC.

It was next determined whether TWIST1 and GATA4 cross-regulated one another in EC exposed to low WSS. This was assessed using siRNA-mediated gene silencing, Twist1 and Gata4 gene silencing was carried out using specific siRNA molecules transfected into HUVEC prior to the exposure to flow via orbital shaking. Gene silencing was validated by showing a reduction in expression at the mRNA (Figure 23 A) and the protein level (Figure 23 B). The expression of GATA4 was assessed in Twist1-silenced cells, which showed that Gata4 mRNA expression was not affected by the reduction of Twist1 expression (Figure 24 A). However, Gata4 silencing resulted in a marked reduction in Twist1 expression (Figure 24 A), indicating that GATA4 is required for the expression of TWIST1 in EC exposed to low WSS. I hypothesised that GATA4 directly regulates TWIST1 transcription in EC exposed to low WSS. A search for putative consensus GATA4 sequence (A/TGATAA (G)) in the Twist1 promoter (-500 to +100bp relative to transcriptional start site) was carried out using a transcription factor binding site database (TF SEARCH). The results revealed the presence of multiple GATA4 binding sites in the Twist1 promoter sequence (bp 51 to 150; Figure 24 B). To test directly if GATA4 binds to the Twist1 promoter ChIP coupled to qRT-PCR revealed Twist1 promoter sequences co-precipitated with anti-GATA4 antibodies but not with non-specific isotype IgG (Figure 24 C). Collectively, these observations demonstrate that low WSS promotes TWIST1 expression via a GATA4-mediated transcriptional mechanism, whereas this network is inhibited in cells exposed to high WSS.

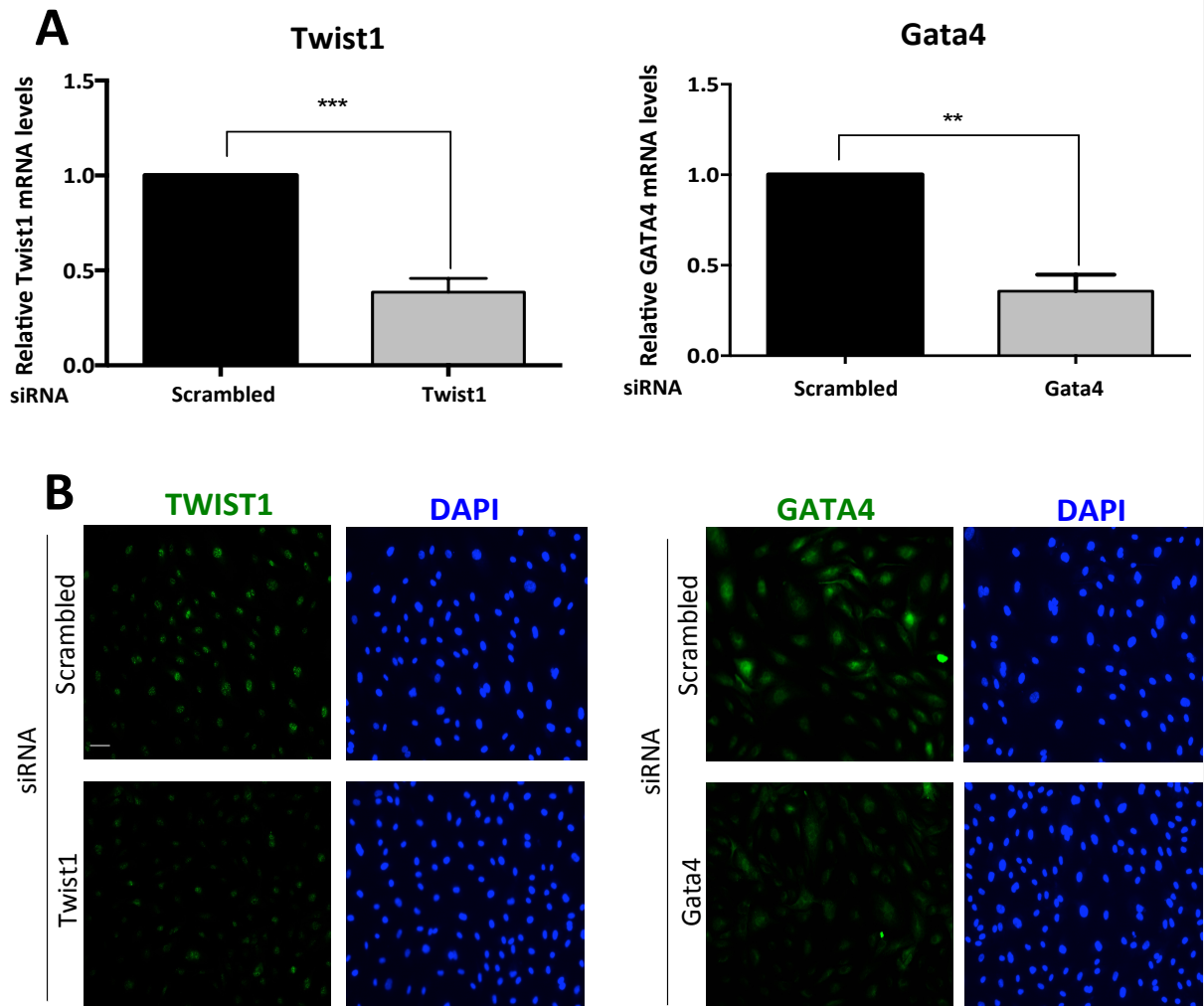


Figure 23. Validation of Twist1 and Gata4 silencing in cells exposed to low WSS. HUVEC were transfected with Twist1, Gata4 or scrambled, non-targeting siRNA oligonucleotides, prior to the exposure of flow using the orbital plate system for 72h. To assess the effect of gene silencing, transcript levels were assessed by A) qRT-PCR (N=3) and protein levels by B) immunocytochemistry, cells were stained with TWIST1 or GATA4 antibodies (green). Nuclei were stained using DAPI (blue). Scale bar, 50 μ m. Mean levels \pm SEM are shown. ** $p < 0.01$, *** $p < 0.01$.

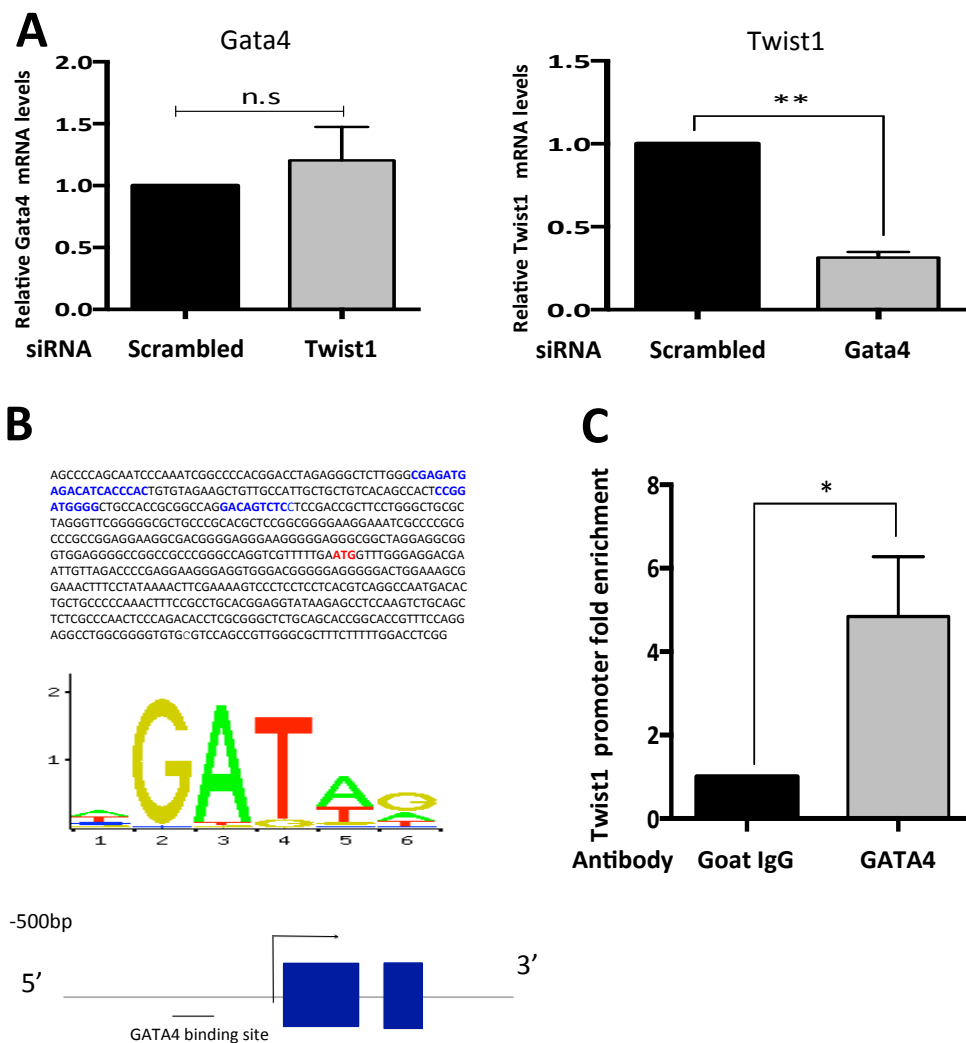


Figure 24. Low WSS induced TWIST1 expression via a GATA4 transcriptional mechanism.

A) HUVEC were treated with Twist1 or Gata4 or scrambled siRNA oligonucleotides prior to the exposure of flow using the orbital plate system for 72h. Transcript levels of Twist1 and Gata4 were quantified by qRT-PCR in cells exposed to low WSS (N=3). B) Twist1 promoter sequence was interrogated for putative GATA4 binding sites (A/TGATAA (G)). Multiple predicted GATA4 binding sites were detected (blue) and their position in relation to the transcriptional start site (red) is shown. Lower panel shows position weight matrix for the GATA binding motif (provided from JASPAR). C) HUVEC were exposed to orbital shaking for 72h prior to ChIP using anti-GATA4 or irrelevant isotype-control antibodies. The levels of Twist1 promoter DNA were assessed by qRTPCR and fold enrichment in anti-GATA4 compared to control precipitates was calculated (N=4). Mean levels \pm SEM are shown. * $p < 0.05$, ** $p < 0.01$.

3.5 Conclusions

1. Low WSS promotes TWIST1 and GATA4 expression in the porcine aorta and in cultured cells (HUVEC and PAEC).
2. GATA4 transcriptionally promotes Twist1 expression in cells exposed to low WSS.

3.6 Discussion

3.6.1 TWIST1 and GATA4 expression is driven by WSS magnitude

In this chapter I have shown that Twist1 and GATA4, genes that orchestrate essential processes during embryonic development were enriched at atheroprone sites in the porcine aorta. It was hypothesised that disturbed flow at these sites enhances TWIST1 and GATA4 expression by generating low WSS on EC. However, the enrichment of Twist1 and GATA4 at these sites may be attributed to other factors such as the presence of circulating inflammatory mediators that are readily transported into EC at atherosusceptible sites due to an increase in mass transport (Tarbell 2003; Bailey et al. 2015). Another factor could be the embryonic origin of the specific areas of the aorta (Trigueros-Motos et al. 2013; Cheung et al. 2014). Therefore, to address if the enhanced expression of Twist1 and Gata4 at the atheroprone sites was directly affected by WSS, the expression of these genes was tested using two simplistic, complementary *in vitro* flow systems, the orbital shaking plate and the Ibidi™ parallel plate systems. The expression of Twist1 and Gata4 was enhanced in the centre of the orbital plate, where flow is disturbed and complex, differing in magnitude and direction (low and oscillatory WSS).

Although flow in the centre of the well recapitulates flow at regions of branches and bends in the vasculature where flow also exerts low and oscillatory WSS, the co-existence of high WSS in the periphery of the well with low, oscillatory WSS conditions in the centre of the well results in a number of caveats in assessing the

expression of Twist1 and Gata4 and in concluding that WSS is directly affecting the expression of these genes; 1) It is known that WSS can modulate the release of cytokines and endothelial microvesicles (Dolan et al. 2012; Vion et al. 2013), thus the physiology of cells in the periphery of the well could be affected by the release of factors from the centre of the well and *vice versa*, 2) Cell turnover is also influenced by WSS where a transient loss of EC-EC contacts in the monolayer as a result of cell turnover could result in the migration of cells from the different regions in the orbiting well. Therefore, such factors could have affected the expression of Twist1 and Gata4 in cells exposed to flow using the orbital plate system. To firstly dissect whether WSS magnitude or direction that is driving Twist1 and Gata4 expression in the centre of the well (where WSS is low, oscillatory), and secondly to test the expression of these genes in cells exposed to spatially distinct WSS environments, I tested the expression of Twist1 and Gata4 in the Ibidi™ parallel plate system. The results revealed that Twist1 and Gata4 were more highly induced in cells exposed to low, unidirectional WSS compared to low, oscillatory and high, unidirectional WSS conditions. Given that TWIST1 and GATA4 expression was enhanced in cells exposed to low, oscillatory WSS in the orbital plate system and in cells exposed to low, unidirectional WSS in the parallel plate system, this suggests WSS magnitude is the dominant factor in triggering the expression of TWIST1 and GATA4 in cells exposed to flow using *in vitro*.

However, it could be argued that the conclusions made on the expression of TWIST1 and GATA4 using *in vitro* flow systems are premature, as these flow systems do not fully recapitulate the flow environment cells are exposed to *in vivo*. Cells in the vasculature at distinct flow sites are exposed to flowing blood, containing inflammatory cells and secreted factors, which could have an additive effect with WSS in driving the expression of TWIST1 and GATA4. Also, although flow in the orbital plate and the parallel plate systems is pulsatile, the pulsatility differs to that in the vasculature and in different vascular beds. Moreover, the pulsatility *in vivo* results in mechanical stretching of the vessel wall, which does not occur *in vitro* due to cells being cultured on plastic, thus mechanical stretching could also have an additive effect with WSS in driving TWIST1 and GATA4 expression. EC in the orbital

plate and the parallel plate systems were attached using gelatin. This is different to extracellular matrix attachments in the vasculature. EC present at low WSS and high WSS sites bind to either collagen or fibronectin (Meng et al. 2007; Orr et al. 2005) and ECM-cell interactions can alter signalling pathways and subsequently gene expression (Orr et al. 2005).

To conclude, *in vitro* flow systems are subject to caveats of not fully recapitulating flow conditions *in vivo*, hence the use of multiple flow systems *in vitro* and the validation of *in vitro* observations *in vivo* are important in fully understanding how WSS modulates TWIST1 and GATA4 gene expression.

3.6.2 How does WSS modulate GATA4- TWIST1 expression?

The regulation of TWIST1 and GATA4 by mechanical forces has been shown previously. TWIST1 is responsive to mechanical cues, such as tissue deformation during gastrulation in the *Drosophila* embryo (Desprat et al. 2008) and in response to matrix stiffness in tumour cells (Wei et al. 2015). Also, Twist1 expression was reported to be enhanced in cells lacking primary cilia, suggesting that the expression of Twist is mechanosensitive (Sanchez-Duffhues et al. 2015). Similarly GATA3, a member of the GATA transcription factor family, regulates the function of the mechanically-sensitive vestibular inner ear sensory organ (Alvarado et al. 2011). In addition, GATA4 induces target genes involved in cardiac hypertrophy in response to pressure overload in the heart ventricle (Tenhunen et al. 2004). The activity of Twist1 and GATA4 has been linked with a number of known mechano-sensing components such as Ras homolog gene family (Rho), kinase (ROCK), (RhoA/ROCK) signalling and integrins (Yanazume et al. 2002; Liu et al. 2004; Yang et al. 2012; Liu et al. 2009; Alexander et al. 2006). In addition, TWIST1 and GATA4 regulate valve formation, a process in itself that has been shown to be regulated by blood flow in the heart (Bartman et al. 2004; Hove et al. 2003). In summary these studies either directly or indirectly link Twist1 and GATA4 activation with mechanical cues. However, here I reveal for the first time that WSS can activate TWIST1 and GATA4 expression in EC. I then showed that GATA4 transcriptionally activates Twist1 in EC

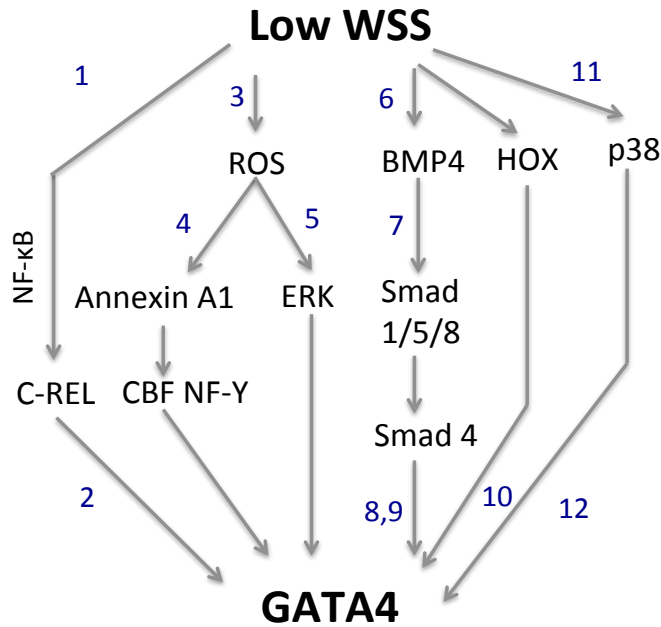
exposed to low WSS. These results are consistent with previous studies that have demonstrated a transcriptional link between GATA4 and TWIST-family transcription factors during embryonic development (Mcfadden et al., 2005). GATA4 interacts with binding partners such as FOG2, MEF2C, TBX5 and GATA6 to promote target gene activation (Chia et al. 2015; Charron et al. 1999; Garg et al. 2003; Lee et al. 1998) it would therefore be interesting to investigate whether GATA4 binding partners are modulated by WSS and whether they are required to promote GATA4-induced Twist1 transcriptional activation under low WSS. The mechanism for GATA4-driven Twist1 activation by WSS should be investigated in future work. The potential mechanisms by which low WSS could be driving GATA4- TWIST1 activation will now be discussed.

3.6.2.1 Transcriptional regulation of GATA4 by low WSS-sensitive signalling pathways

The transcriptional activation of GATA4 in cells exposed to low WSS could potentially be mediated via several WSS-sensitive signalling pathways (Figure 25). Low WSS activates pro-inflammatory p38 MAPK signalling (Chaudhury et al. 2010). It has been reported that p38 regulates GATA4 transcriptionally and post transcriptionally to enhance GATA4 binding to its target DNA sequences (Charron et al. 2001; Rysä et al. 2010). Interestingly, in response to mechanical loading in the rat heart ventricle, GATA4 is activated via p38 and ERK leading to subsequent activation of GATA4-target genes involved in cardiac hypertrophy (Tenhunen et al. 2004). Low WSS is also known to promote inflammatory NF- κ B signalling (Zakkar et al. 2008; Cuhlmann et al. 2011). One member of the NF- κ B family C-Rel promotes GATA4 transcription in cardiac cells during cardiac hypertrophy and fibrosis (Gaspar-Pereira et al. 2012). Thus it is plausible that low WSS induces GATA4 via p38 and/or NF- κ B. TGF- β signalling via BMP is activated in cells exposed to low WSS and has been shown to be involved in focal atherogenesis (Sorescu et al. 2004; Jo et al. 2006; Kim et al. 2013). BMP4-mediated TGF- β signalling and downstream homeobox binding proteins (HOX) regulate Gata4 gene expression during embryogenesis (Daoud et al. 2014; Rojas et al. 2009) these factors may also induce Gata4 at atheroprone sites.

A

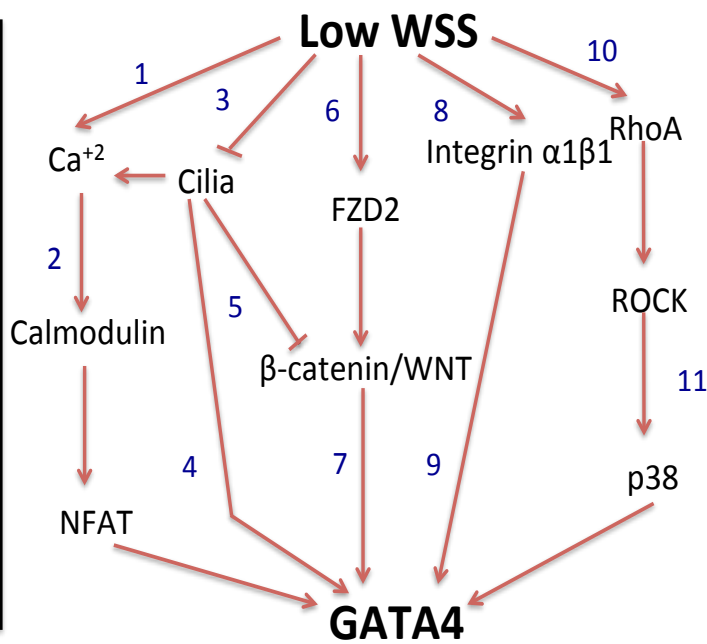
WSS-sensitive pathways



1. Zakkar *et al.*, 2008
2. Gaspar-Pereira *et al.*, 2012
3. Willet *et al.*, 2011
4. Park *et al.*, 2010
5. Liu *et al.*, 2004
6. Kim *et al.*, 2012
7. Ueki and Reh, 2012
8. Moskowitz *et al.*, 2011
9. Daoud *et al.*, 2014
10. Rojas *et al.*, 2009
11. Chaudhury *et al.*, 2010
12. Tenhunen *et al.*, 2004

B

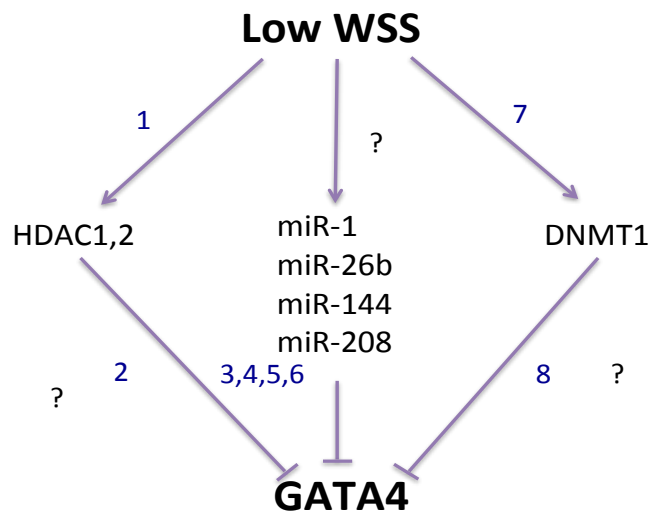
Mechanosensors



1. Ando and Yamamoto, 2013
2. Morad and Suzuki, 2000
3. Sanchez-Duffhues *et al.*, 2015
4. Clement *et al.*, 2009
5. Lancaster *et al.*, 2011
6. Rotherham and Haj, 2015
7. Lin and Xu *et al.*, 2009
8. Shyy and Chien, 2002
9. Liu *et al.*, 2009
10. Liu *et al.*, 2008
11. Tenhunen *et al.*, 2004

C

WSS-sensitive epigenetics and miRNAs



1. Lee *et al.*, 2012
2. Stefanovic *et al.*, 2013
3. Callis *et al.*, 2009
4. Hu *et al.*, 2014
5. Han *et al.*, 2012
6. Ikeda *et al.*, 2009
7. Dunn *et al.*, 2014
8. Oda *et al.*, 2013

Figure 25. Potential mechanisms for GATA4 activation in cells exposed to low WSS. A schematic for the potential regulation of GATA4 in EC exposed to low WSS via A) WSS-sensitive pathways B) Mechanosensors and C) WSS-sensitive epigenetic regulators.

Moreover low WSS promotes an increase in ROS production in EC, which promotes EC dysfunction (Willett et al. 2011). ROS may contribute to GATA4 induction by low WSS since it promotes GATA4 activation in other systems via two mechanisms. The first mechanism involves the activation of CBF/NF- κ B transcription factor which then promotes GATA4 transcription (Park et al. 2010). The second mechanism involves ROS-mediated ERK activation via RhoA/ROCK signalling. Subsequently, activated ERK promotes GATA4 transcriptional activity (Liu et al. 2004).

3.6.2.2 Transcriptional regulation of GATA4 by mechanosensors

GATA4 transcription under low WSS is likely to be controlled by upstream, cell surface mechanosensing components. Several of these are discussed in relation to GATA4 expression. Integrins are involved in mechanosensing in EC in response to WSS (Ingber 1991; Shyy & Chien 2002). In endothelial cells integrin α 1 β 1 (also expressed in adult EC) promotes GATA4 nuclear localisation, thus increasing the transcription of GATA4 target genes (Liu et al. 2009). Rho/ROCK signalling promotes cytoskeletal reorganisation in response to mechanical force (Tzima 2006; Wojciak-Stothard & Ridley 2003). This pathway activates GATA4 in cardiac cells and it is plausible that it may function in mechanically-stimulated EC (Tenhunen et al., 2004). Calcium flux in response to mechanosensors such as primary cilia, glycocalyx, caveolae and ion channels is a well studied mechanoresponse (Ando and Yamamoto et al, 2013). During cardiac muscle contraction calcium flux activates calmodulin which activates the transcription factor NFAT. Active NFAT interacts with GATA4 in the nucleus and enhances GATA4 transcription of target genes (Sussman et al. 1998; Dolmetsch et al. 1997; Jones et al. 1998). It will be interesting to assess if parallel systems exist in EC. It has recently been shown by Rotherham and El Haj that cell surface WNT receptors Frizzled proteins (FZD) are mechanosensors (Rotherham & El Haj 2015). They showed that the application of oscillatory force using anti-FZD2 coated magnetic nanoparticles promoted the activation of β -catenin-mediated WNT signalling (Rotherham & El Haj 2015). GATA4 is a direct transcriptional target of β -catenin (Lin

& Xu 2008), thus FZD2-mechanoactivation could be driving GATA4 expression in EC. Primary cilia, another mechanosensor has been linked with GATA4 activation. Clement *et al* have showed that cardiomyocytes with gene knock downs of primary cilium components *ift88* and *ift20* showed a reduction in GATA4 mRNA, indicating that GATA4 transcription is dependent on primary cilia activity (Clement et al. 2013) (Clement et al., 2009). Since at low WSS sites in the vasculature EC express cilia whereas EC at high WSS do not (Van der Heiden et al. 2007), this could be a mechanism by which GATA4 activation occurs in EC exposed to low WSS conditions. Additionally, syndecan-1 (a component of the glycocalyx) is a positive regulator of WNT signalling in cancer cells (Rehmet et al. 2007; Alexander et al. 2000). Moreover, WNT signalling is a known activator of Gata4 gene expression (Morad & Suzuki 2000; Lin & Xu 2008), therefore Gata4 expression under low WSS may be indirectly controlled by glycocalyx mechanotransduction.

3.6.2.3 Epigenetic and miRNA regulation of GATA4 expression

Another mechanism for the activation of GATA4 in cells exposed to low WSS could be through epigenetic regulation of GATA4 mRNA. Low WSS gives rise to genome wide DNA methylation changes through DNA methyltransferase 1 (DNMT1) (Dunn et al. 2014). Histone deacetylases are another example of low WSS-mediated epigenetic mediators (Lee et al. 2012). In addition, DNMT1 and HDAC inhibit Gata4 expression during stem cell differentiation (Oda et al. 2013; Stefanovic et al. 2014). Thus, potentially, HDAC and DNMT1-mediated Gata4 gene inhibition in EC exposed to low WSS could be a balance-keeping mechanism to ensure that GATA4 levels do not exceed a certain threshold.

miRNA molecules are likely to be regulating GATA4 expression in EC exposed to low WSS. MiR-1, 26b, 144 and 208a regulate Gata4 gene expression during cardiac hypertrophy and embryonic development (Callis et al. 2009; Han et al. 2012; Ikeda et al. 2009). Although low WSS differentially activates the expression of miRNA molecules (Schober et al. 2014; Son et al. 2013; Callis et al. 2009; Fang et al. 2010), it is unknown whether the miRs implicated in GATA4 regulation are modulated by WSS

in EC, but it could be a potential mechanism for GATA4 mRNA stability in EC exposed to low WSS.

To conclude, the activation of GATA4-TWIST1 in cells exposed to low WSS could potentially involve a number of post transcriptional, transcriptional and epigenetic mechanisms (Figure 16). Future work will be focused on dissecting the mechanisms upstream of GATA4 activation by low WSS in EC.

3.7 Future experiments

To further assess if GATA4 transcriptionally activates Twist1 under low WSS;

1. The induction of Twist1 by GATA4 could be assessed using a luciferase reporter gene *in vitro* assay. This would involve inhibiting or enhancing GATA4 expression, followed by the assessment of luciferase activity.
2. To assess whether GATA4 promotes Twist1 gene expression via binding to interacting partners. This could be tested by expressing a Gata4 gene that is mutated in the sites required for interacting partner binding, followed by the assessment of Twist expression.
3. Studying the relative effect of WSS on GATA4 mRNA stability vs. transcription.
4. Determining mechanosensitive-signalling pathways upstream of GATA4.

**Chapter 4: TWIST1 and GATA4 control
proliferation and permeability in cells exposed to
low WSS in *vitro***

4.1 Introduction

TWIST1 and GATA4 regulate a number of processes involved in cellular reorganisation and patterning during embryonic development; these processes include cell proliferation, migration, and invasion (Shelton & Yutzey, 2008; Lee & Yutzey 2011; Rojas et al. 2008; Vrljicak et al. 2012). TWIST1 and GATA4 have been implicated in EMT in epithelial cells and in the parallel process in endothelial cells known as EndMT.

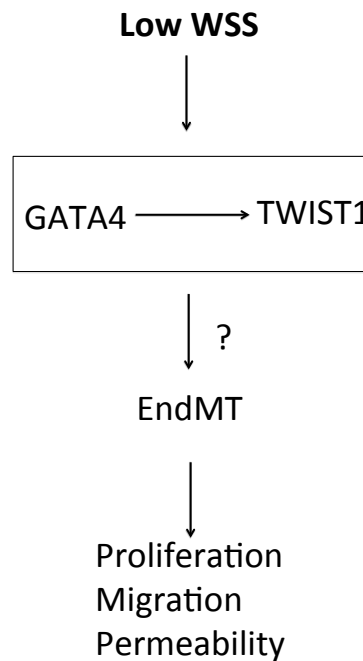
EndMT is essential during cardiac valve formation, this process is heavily dependent on the expression of TWIST1 and GATA4 (Zeisberg et al. 2005; Vrljicak et al. 2012, reviewed in Lamouille et al. 2014; Yang et al. 2004; Rivera-Feliciano et al. 2006). During EndMT cells transform into a more mesenchymal state, characterized by several physiological and morphological changes (Reviewed in Medici & Kalluri 2012). Firstly, cells express EndMT master regulators such as TWIST1, SNAIL and SLUG bHLH transcription factors, which trigger subsequent changes in gene expression involving loss of EC markers such as VE-cadherin and CD31 and the expression of mesenchymal genes such as N-cadherin and α -SMA. Secondly, as a result of the change in gene expression the cells display morphological changes where they become more spindle-like and undergo the so-called “cadherin switch”, which involves the expression of N-cadherin and disorganisation of VE-cadherin at the cellular junctions (Maddaluno et al. 2013). The cells also become more proliferative, invasive, migratory and as a consequence more “leaky” with higher cell permeability. Eventually EndMT can result in cellular delamination (reviewed in Medici & Kalluri, 2012 and Birukova et al. 2004).

In addition to its role in development, EndMT has also been linked with a number of pathological conditions including cancer, renal fibrosis and cerebral cavernous malformations (Maddaluno et al. 2013; Zeisberg et al. 2007; Zeisberg et al. 2008; Ranchoux et al. 2015). Consistent with this, TWIST1 and GATA4 are known to be prominent oncogenes that trigger metastatic cell migration via the induction of EMT (Takagi et al. 2014; Yang et al. 2004). However, it has not been explored yet whether

TWIST1 and GATA4 regulate EC function in cells exposed to low WSS and in particular if they do this via EndMT.

4.2 Hypothesis

TWIST1 and GATA4 regulate EC function under low WSS via inducing EndMT.



4.3 Aims:

- 1- To study TWIST1 and GATA4 functions in cells exposed to low WSS by assessing tube formation, proliferation, migration and permeability.
- 2- To assess if low WSS promotes EndMT and, if so, whether TWIST1 and GATA4 are drivers of this process.

4.3 TWIST1 and GATA4 regulate proliferation, migration and permeability in cells exposed to low WSS

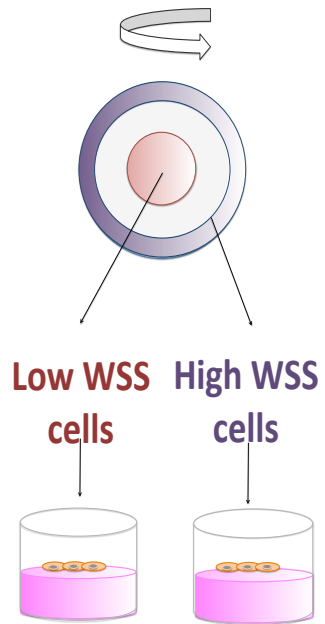
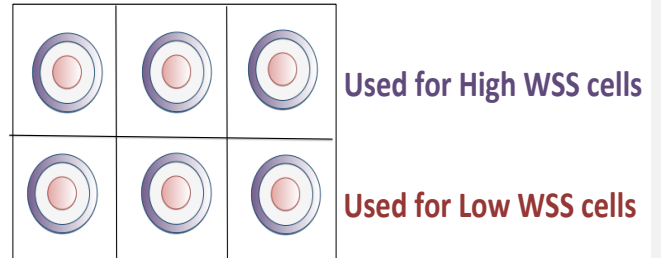
The potential role of TWIST1 and GATA4 in tube formation, a process that involves migration and proliferation was studied. EC were exposed to 72h of flow via orbital shaking and then cells from the low or high WSS regions were seeded onto collagen-coated wells for up to 48h under static conditions (Figure 26 A). Cells seeded from the low WSS region showed significantly more tube formation compared to cells seeded from the high WSS region as quantified by the cumulative length of tube structures and by quantifying the number of branch points (Figure 26 B). Twist1 and Gata4 silencing reduced tube length and complexity (branch points) in cells exposed to low WSS (Figure 26 C) suggesting that they promote tube formation in these cells.

To further dissect function the contribution of TWIST1 and GATA4 to cell migration and proliferation was studied. For cell migration a “scratch” was made across the well of pre-sheared cells to form a wound. Cell migration into the wounded area was quantified by measuring the distance and the velocity of the migrating cells. Cells exposed to low WSS showed a higher rate of cell migration as indicated by distance and velocity compared to cells exposed to high WSS (Figure 27) and the silencing of Twist1 and Gata4 resulted in a reduction in this process (Figure 28).

Next, cell proliferation by ki67 immunofluorescent staining was assessed in cells exposed to flow. Initial studies revealed that there was no significant difference in proliferation in cells exposed to low vs. high WSS using the orbital plate system (data not shown), indicating that the flow parameters were not sufficient to induce a difference in proliferation. However, since TWIST1 and GATA4 expression was significantly enhanced in cells exposed to low WSS via orbital shaking, the effect of Twist1 and Gata4 gene silencing on cell proliferation was assessed under these conditions. Twist1 and Gata4 silencing reduced cell proliferation in cells exposed to low WSS (as assessed by quantifying % positive ki67 cells/frame of view) (Figure 29).

A

HUVEC cultures
↓
Expose to WSS for 72 h
(High or Low WSS)
↓
Plate onto collagen
↓
Culture under static
conditions (48 h)
↓
Stain cells and quantify
tube formation



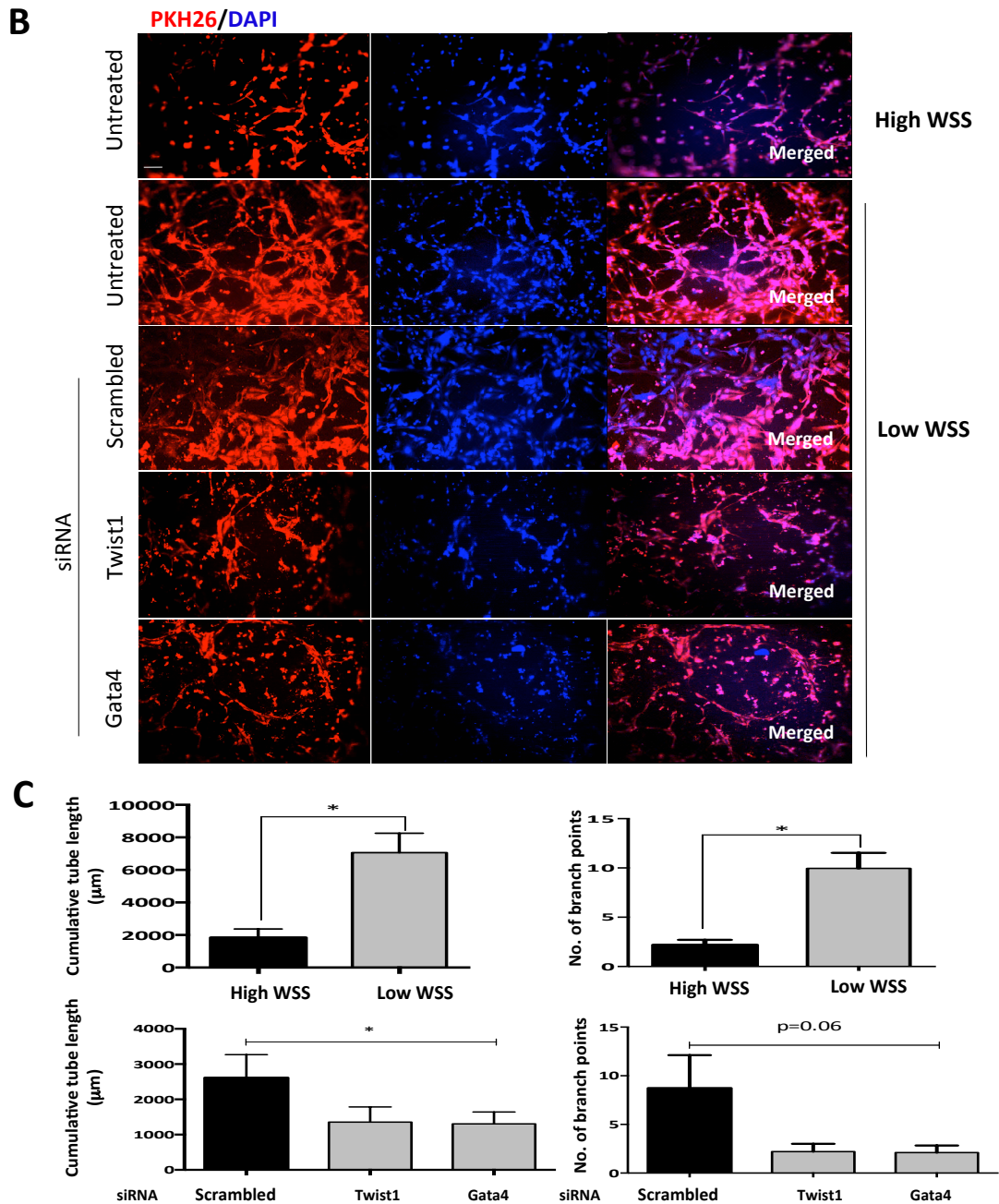


Figure 26. TWIST1 and GATA4 regulate tube formation in cells exposed to low WSS. HUVEC were treated with siRNA targeting Twist1 and Gata4, or with scrambled non-targeting siRNA (or were untreated as a control) A) Cells were exposed to flow via orbital shaking and were then plated onto collagen coated wells and cultured for up to 48h in media containing VEGF to mediate tube formation. B) The cells were fixed and stained with DAPI (blue) and PKH26 (red) to label the tube structures formed, and were then visualised by fluorescent microscopy. Representative images are shown. Scale bar, 75 µm. (B-C) The cumulative tube length and number of branch points were determined for multiple fields of view and mean values were calculated. Data were pooled from 5 independent experiments and mean values ± SEM are shown. * $n < 0.05$ using paired t-test or a one-way ANOVA.

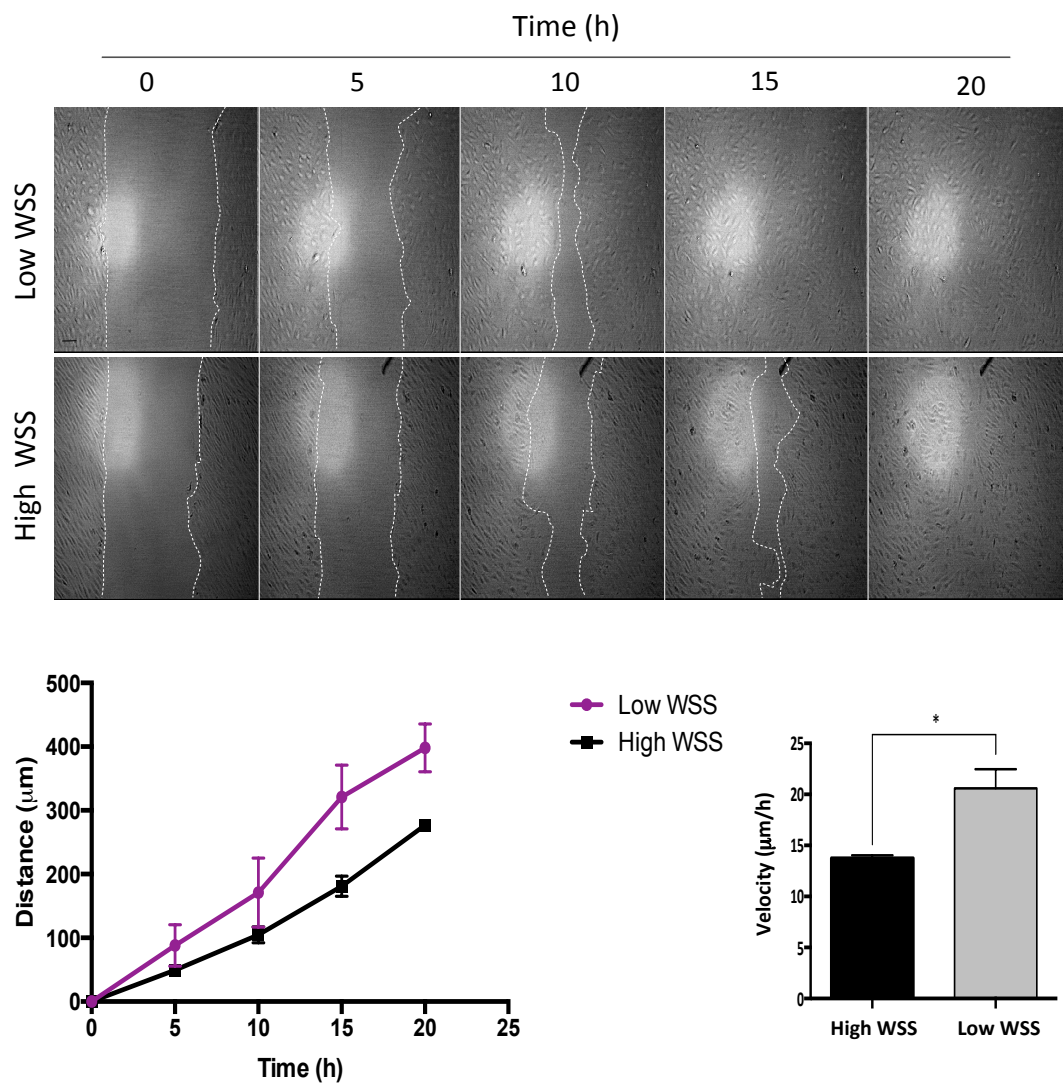


Figure 27. Cells exposed to low WSS displayed enhanced migration compared to cells exposed to high WSS. HUVEC were exposed to 72h of flow via orbital shaking. A scratch was made using a P 200 pipette tip across the well, to form a wound in areas of high and low WSS. Migration into the wounded area was visualised by time-lapse microscopy, cells were imaged every 3 minutes for 20h. Representative images captured at 5h intervals are shown. Scale bar, 100 μm . The distance migrated into the wounded area was quantified from at least three points in the monolayer. Average velocity was calculated. Data were pooled from 5 independent experiments and mean values \pm SEM are shown. * $p < 0.05$, using a paired t-test.

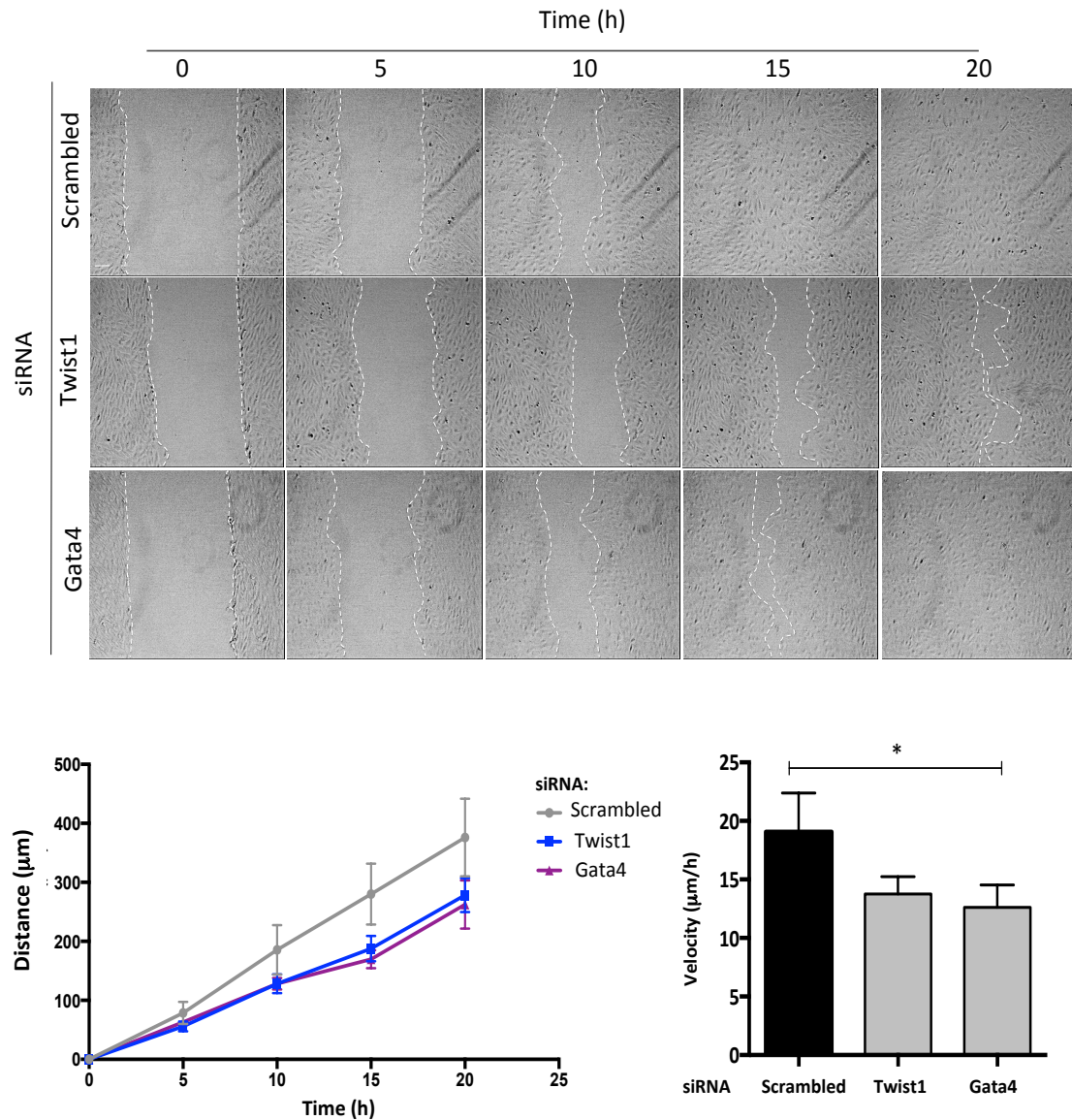


Figure 28. TWIST1 and GATA4 promoted cell migration in cells exposed to low WSS. HUVEC were treated with siRNA targeting Twist1, Gata4 or a scrambled non-targeting siRNA, followed by the exposure of flow via orbital shaking for 72h. A scratch was made using a P 200 pipette tip across the well, to form a wound in areas in the well of high and low WSS. Migration into the wounded area was visualised by time-lapse microscopy, cells were imaged every 3 minutes for 20h. Representative images captured at 5h intervals are shown. Scale bar, 100 µm. The distance migrated into the wounded area was quantified from at least three points in the monolayer. Average velocity also calculated. Data were pooled from 5 independent experiments and mean values \pm SEM are shown. * $p < 0.05$, using a One-way ANOVA.

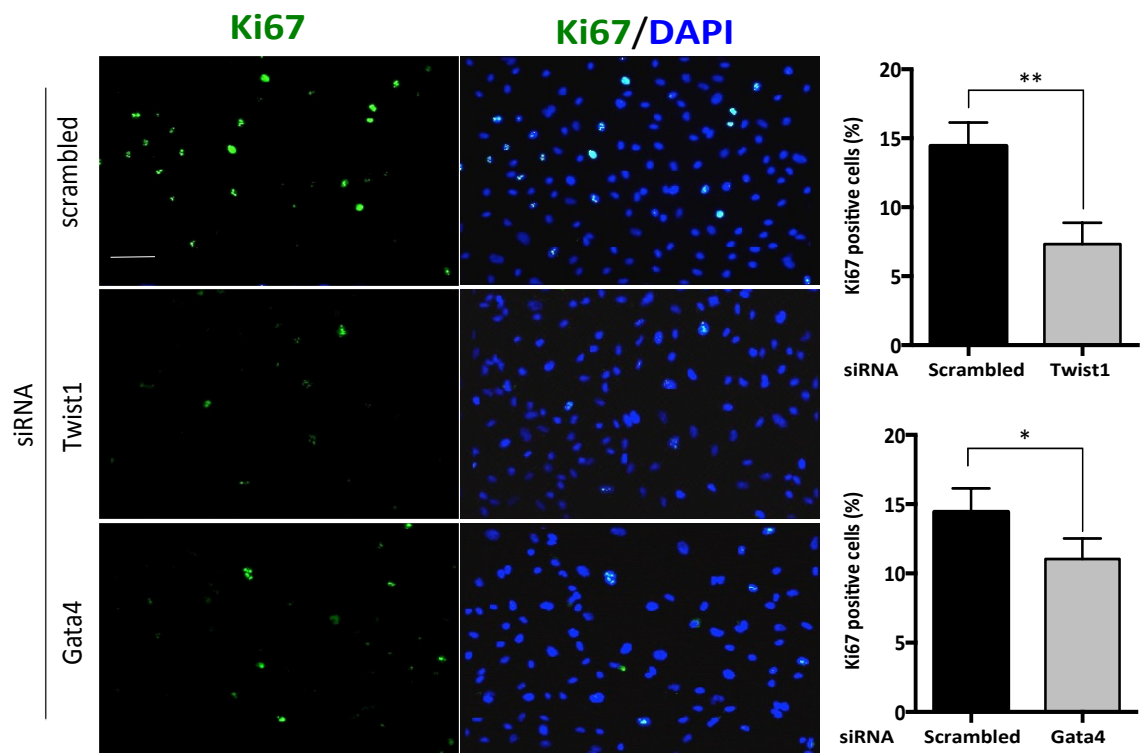


Figure 29. TWIST1 and GATA4 promoted proliferation in cells exposed to low WSS. HUVEC were treated with siRNA targeting Twist1, Gata4 or a scrambled non-targeting siRNA, followed by the exposure of flow via orbital shaking for 72h. Cells were fixed and immunostained with anti-ki-67 antibodies (green) to label proliferative cells and were co-stained with DAPI (blue). Representative images are shown. Scale bar, 50 μ m. % ki-67-positive cells was calculated. Data were pooled from 5 independent experiments and mean values \pm SEM are shown. * $p < 0.05$, ** $p < 0.01$ using a paired t-test.

The above data demonstrate that TWIST1 and GATA4 are positive regulators of cell migration and proliferation under low WSS conditions. Since these processes are known to enhance vascular permeability (Cancel et al. 2011, Cancel et al. 2010 Birukova et al. 2004) I determined whether TWIST1 and GATA4 regulate EC permeability under low WSS. A method developed by the Weinberg group was used (Warboys et al. 2010), which involved culturing cells on transwell inserts, followed by orbital shaking at 150 rpm for 72 h. CFD analysis demonstrated that cells are exposed to a relatively constant low WSS across the transwell insert (0.2 to 3.6 dyne/cm²) with a spatially and temporally average value of the entire well of 1.82 dyne/cm² (Warboys et al. 2010). Following the exposure to flow, a rhodamine-albumin tracer was added to the top compartment of the transwell and incubated for 1 h under static conditions. Media from the bottom compartment was collected to measure the concentration of tracer as a measure of cell permeability (Figure 30 A). To validate the use of the system in our laboratory, I repeated an experiment reported by the Weinberg group (Warboys et al. 2010), by comparing cell permeability in cells either exposed to prolonged flow (72h) of orbital shaking or cultured under static conditions. It was revealed that cells exposed to flow had a higher level of cell permeability compared to cells cultured under static conditions (Figure 30 B), thus replicating experimental findings from Warboys *et al.*, 2010. Following the validation of the system, Twist1 and Gata4 were silenced and cell permeability was assessed. It was revealed that silencing of either gene reduced cell permeability (Figure 30 C), indicating that they promote this process in cells exposed to low WSS. Therefore, it was concluded that the application of low WSS to EC monolayers led to GATA4-mediated induction of TWIST1, promoting cell migration, proliferation and increased permeability to macromolecules.

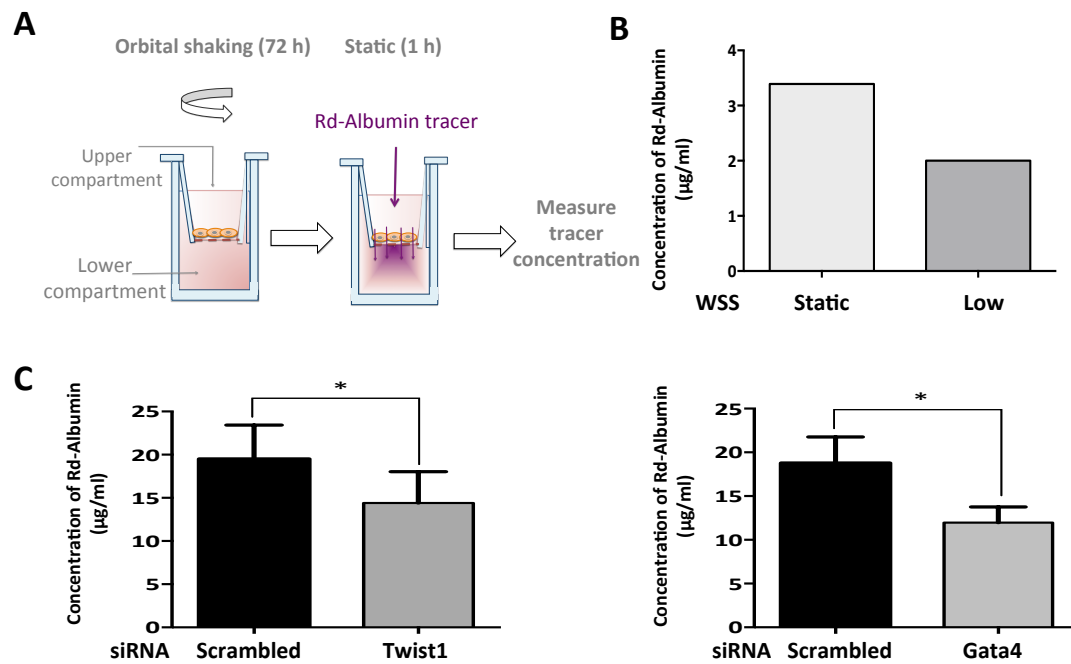


Figure 30. TWIST1 and GATA4 promoted cell permeability in cells exposed to low WSS. A) HUVEC were seeded onto transwell plates and exposed to flow via orbital shaking at 150 rpm for 72h. Following orbital shaking, a rhodamine-albumin tracer was incubated for 1 hour under static conditions. Media from the bottom compartment was collected to assess the concentration of tracer as a measure of cell permeability. B) To validate the method, we replicated results from the study which the method was adapted (Warboys et al., 2010). Cells exposed to static conditions had higher levels of cell permeability compared to cells exposed to prolonged flow (72h), N=1. C) Prior to the exposure of flow, the cells were treated with Twist1, Gata4 or scrambled non-targeting siRNA. And cell permeability was assessed. Data were pooled from 5 independent experiments and mean values \pm SEM are shown. * $p < 0.05$, using a paired t-test.

4.4 GATA4-TWIST1 regulate EC physiology under low WSS via a mechanism-involving SNAIL.

Cell proliferation and migration are processes that are also known to occur in cells undergoing EndMT and Twist1 and GATA4 promote EMT and EndMT in other cellular systems. Therefore, I next hypothesised that GATA4-Twist1 signalling promotes the induction of EndMT in cells exposed to low WSS. Consistent with this, several markers of EndMT (Snail, Slug, N-cadherin, α -SMA) were enriched at the low WSS site in the porcine aorta (Figure 31 A) and were induced by low WSS in cultured HUVEC (Figure 31 B,D) and PAEC (Figure 31 C). Furthermore, HUVEC exposed to low WSS expressed a significantly higher level of N-cadherin at the cell junctions (Figure 31 E) and displayed VE-cadherin disorganisation as assessed by measuring VE-cadherin junctional width compared to cells exposed to high WSS conditions (Figure 31 F). However, although cells exposed to low WSS displayed EndMT-like features such as expressing EndMT marker genes and the N-cadherin/ VE-cadherin switch, the retention of EC markers and the absence of a spindle-like morphology that is characteristic of EndMT suggested that the transition to a mesenchymal state was partial.

I next assessed the potential involvement of GATA4-TWIST1 signalling in regulating partial EndMT under low WSS. Gene silencing of Twist1 and Gata4 resulted in a marked reduction in the junctional expression of N-cadherin (Figure 32 A) and reduced VE-cadherin disorganisation, by reducing VE-cadherin junctional width (Figure 32 B) indicating that they are positive regulators of changes in junctional expression induced by low WSS. The expression of EndMT markers was determined to understand the molecular mechanism. Gene silencing of Twist1 and Gata4 significantly reduced the expression of the EndMT inducer Snail in cells exposed to low WSS (Figure 32 C and D). To further validate the link between GATA4-Twist1 signalling with Snail, protein expression was assessed. Cells exposed to low WSS displayed a higher SNAIL expression compared to cells exposed to high WSS and Twist1 and Gata4 gene silencing resulted in a reduction of SNAIL protein (Figure 33).

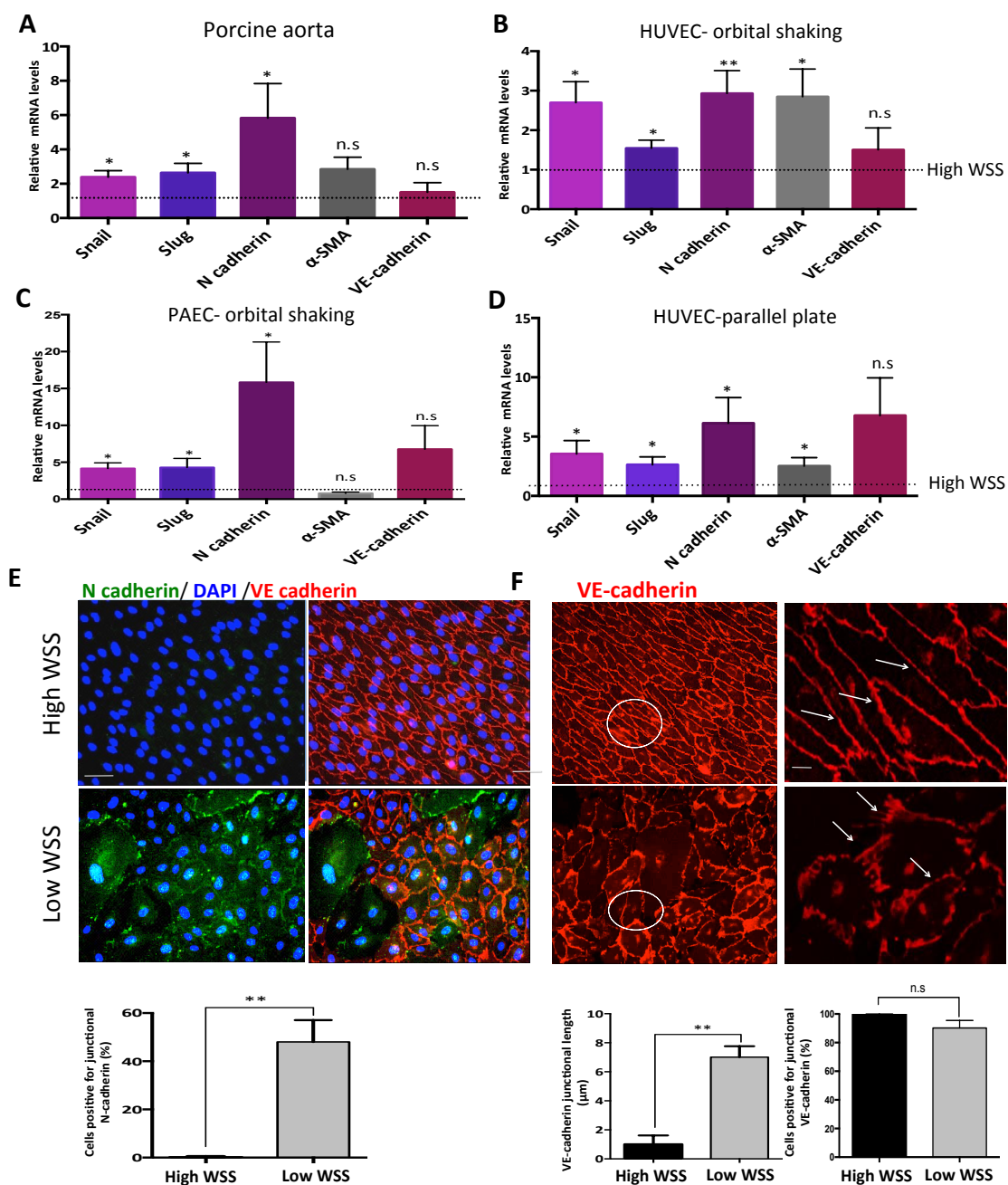


Figure 31. Low WSS promoted partial EndMT. A) EndMT marker transcripts were assessed in cells isolated from low (inner curvature and high WSS (outer curvature) of the porcine aorta, N=4. B-D) EndMT marker transcripts were assessed in cells exposed to 72h of flow via orbital shaking or via the parallel plate ibidi™ system, N=4. The dotted line indicates high WSS expression to which the low WSS expression values were normalised. E-F) Following 72h of exposure to flow via orbital shaking, cells were fixed and were immunostained with anti-N-cadherin (green) and VE-cadherin (red) antibodies, cells were counterstained with DAPI (blue). Representative images are shown. Scale bar, 50 μm E) The expression of N cadherin was calculated as % positive cells expressing junctional N-cadherin. F) VE-cadherin junctional width was measured using Image J. Left panel shows zoomed image, arrows indicate VE-cadherin junctional width. At least four measurements were taken in one field of view. % positive cells expressing VE-cadherin was calculated (right panel). Data was pooled from 5 independent experiments. Mean values ± SEM are shown. * p<0.05, **p<0.01, ***p<0.001 using a one way ANOVA or un paired t-test.

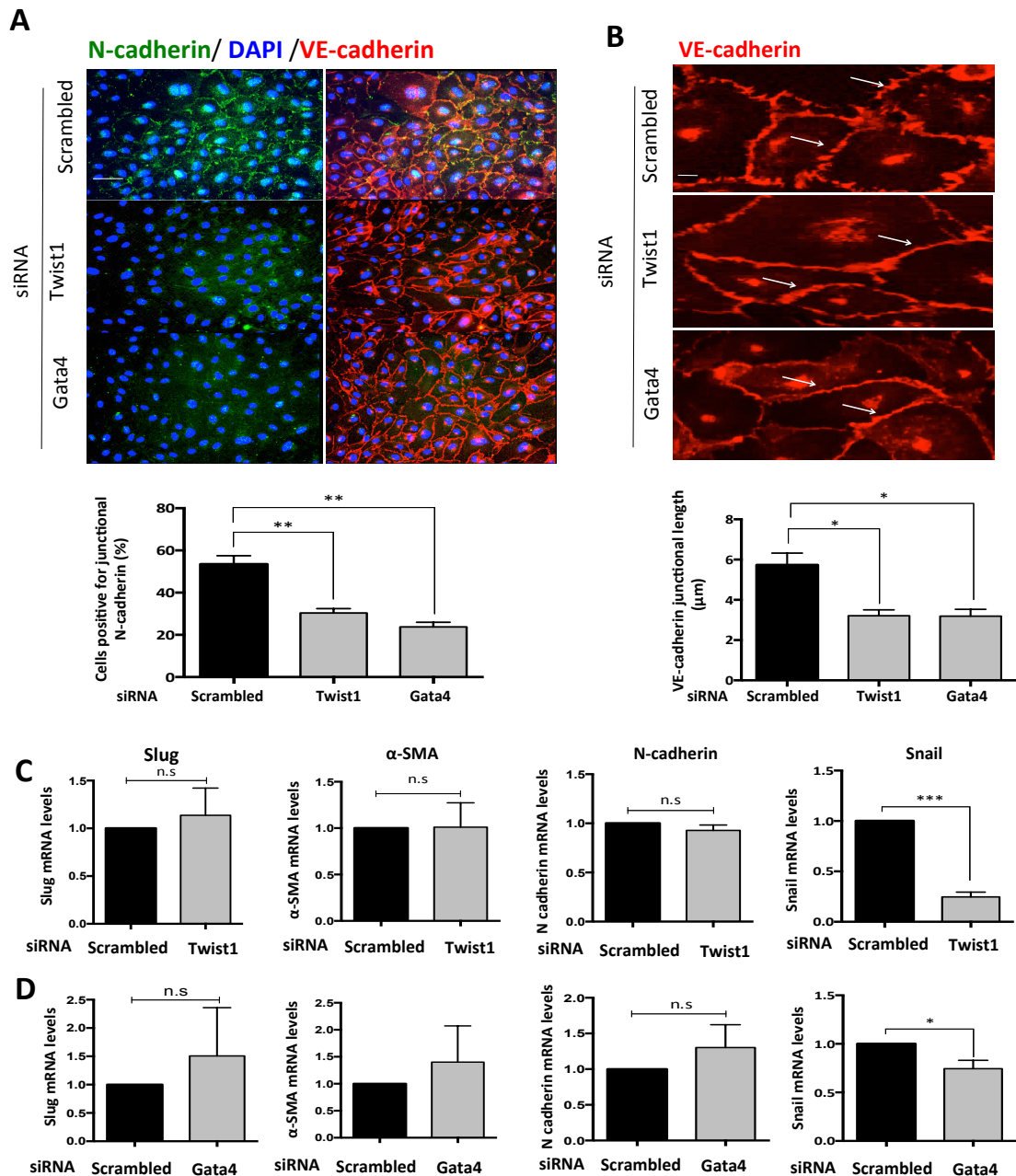


Figure 32. TWIST1 and GATA4 regulated partial EndMT in cells exposed to low WSS. HUVEC were treated with siRNA targeting Twist1, Gata4 or a scrambled non-targeting siRNA, followed by the exposure of flow via orbital shaking for 72h. A-B) Cells exposed to low WSS were fixed and were immunostained with anti-N-cadherin (green) and VE-cadherin (red) antibodies. Cells were counterstained with DAPI (blue). Representative images are shown. Scale bar, 50 μm . A) The expression of N cadherin was calculated as % positive cells expressing junctional N-cadherin, N=5. B) VE-cadherin junctional width was measured using Image J, N=5. Arrows indicate VE-cadherin junctional width. Atleast four measurements were taken in each field of view/per region. C-D) EndMT marker transcripts were assessed in cells exposed to low WSS, following the silencing of Twist1 (C) or Gata4 (D) N=3). Mean values \pm SEM are shown. * $p < 0.05$, ** $p < 0.01$ using a One-way ANOVA or an unpaired t-test.

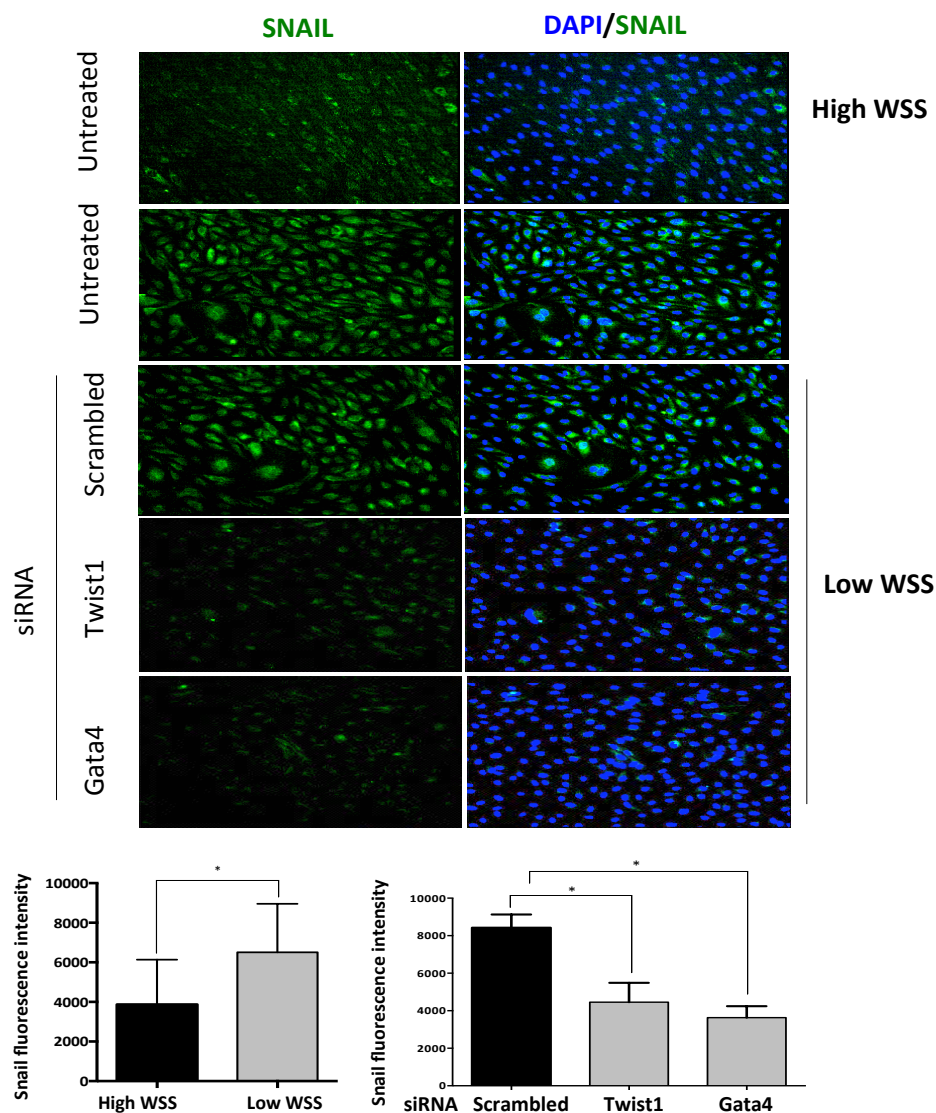


Figure 33. TWIST1 and GATA4 regulated SNAIL protein expression in cells exposed to low WSS. HUVEC were treated with siRNA targeting Twist1 and Gata4, or with scrambled non-targeting siRNA (or were untreated as a control) prior to the exposure to flow via orbital shaking for 72h. Cells were fixed and immunostained with anti-SNAIL (green) antibodies and the cells were counterstained with DAPI (blue). Representative images are shown, N=3. Scale bar, 50 μ m. Fluorescent intensity in the nuclei of multiple cells was assessed using Image J. Mean levels \pm SEM are shown * $p < 0.05$, using a One-way ANOVA or paired t-test.

These results suggest that TWIST1 and GATA4 promote SNAIL mRNA and protein expression in cells exposed to low WSS. To assess if this regulation was at the transcriptional level, ChIP analysis was carried out, which revealed that GATA4 binds to the Snail promoter region (GATA4 binding site located at bp 423-450) (Figure 34 A, B) suggesting that GATA4-Twist1 signalling induces Snail via a transcriptional mechanism.

I then assessed whether Snail promotes EndMT-related transcriptional changes. To do so, snail gene silencing was first validated in cells exposed to low WSS at the mRNA and protein level (Figure 35). EndMT marker expression was assessed, which showed that the silencing of Snail resulted in a reduction of EndMT markers Slug, α -Sma and N-cadherin, which indicated that SNAIL promotes EndMT marker expression in cells exposed to low WSS (Figure 36).

Interestingly, cell migration (Figure 37 A) proliferation (Figure 37 B) and permeability (Figure 37 C) were all reduced in cells with Snail gene silencing, suggesting that Snail regulated these processes. Therefore, these results suggest that TWIST1 and GATA4 co-operate to induce SNAIL in cell exposed to low WSS, and this transcription factor contributes to EC proliferation, migration and permeability under these conditions (Figure 38).

A

```
CAGTGATGTGCGTTTTCCCTCGTCAATGCCACGCTCTCCAGGCGCCAGCCGGGCGGAGGAA
ATTTCCGCCCCCTCCAAGCCCGAGGCGGGGGCGGGCGTCCGGAAGGTCAGGTGTCCCGGC
CGGCGCGCAGCGCCAGGGGGCGTCAAGCGCTCAGACCACCGGGCGCTGAGCCGGTGG
GCGCGCGGCGTCTGCCGGGGTCCCACCTCGCAGAGGCCTCGTTTCGCTCGACGTCCCGCC
CCGGACAGCCCCAGCACCGGGGACGACCCGCGCTGCGCCAGCGAACCCCGCCTCGGAGGA
GTCCCCGCCCCGGGCTCTACCGCCACGCGGCGCGAGCCCGCCAGCAGCCGGCGCACCTGC
TCGGGGAGTGGCCTTCGGCGGAGACGAGCCTCCGATTGGCGCGGAGGTGACAAAGGGGCG
TGGCAGATAAGGCCCCGCCCTCCCACCCCCACCACCCCCGGAGTACTTAAGGGAGTTG
GCGGCGTGCTGCATTCATTGCGCCGCGGCACGGCCTAGCGAGTGGTTCTTCTGCGCTACTG
CTGCGCGAATCGGCGACCCAGTGCCTCGACCACTATGCCGCGCTTTTCCTCGT
```

B

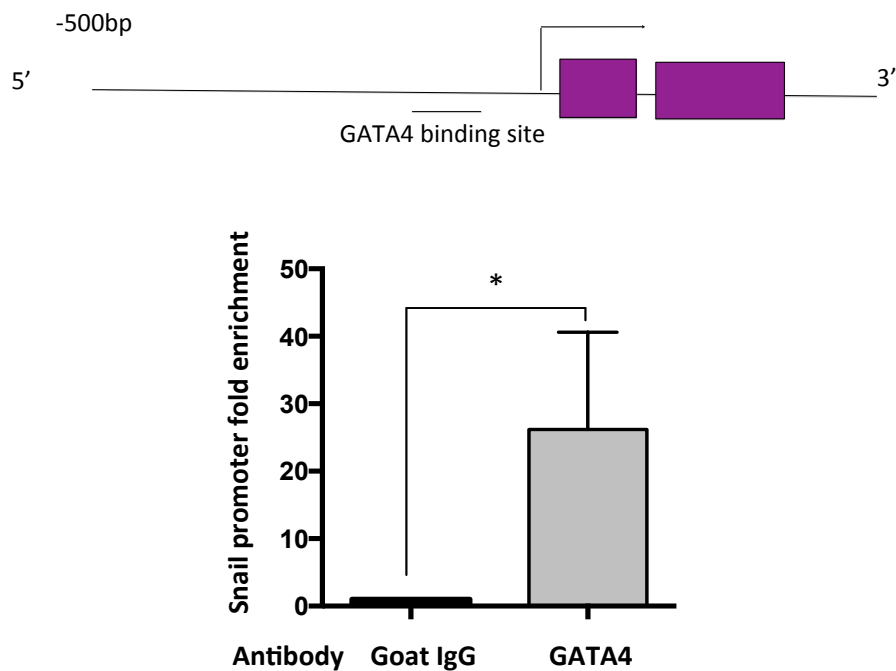


Figure 34. GATA4 transcriptionally regulated Snail expression in cells exposed to low WSS. A) The Snail promoter sequence was interrogated for putative GATA4 binding sites (A/TGATAA (G)). A predicted GATA4 binding site was detected (blue) and its position in relation to the transcriptional start site (red) is shown. B) HUVEC were exposed to orbital shaking for 72h prior to ChIP using anti-GATA4 or irrelevant isotype-control antibodies. The levels of Snail promoter DNA were assessed by q-RT-PCR and fold enrichment in anti-GATA4 compared to control precipitates was calculated (N=4). Mean levels \pm SEM are shown. * $p < 0.05$, using an unpaired t-test.

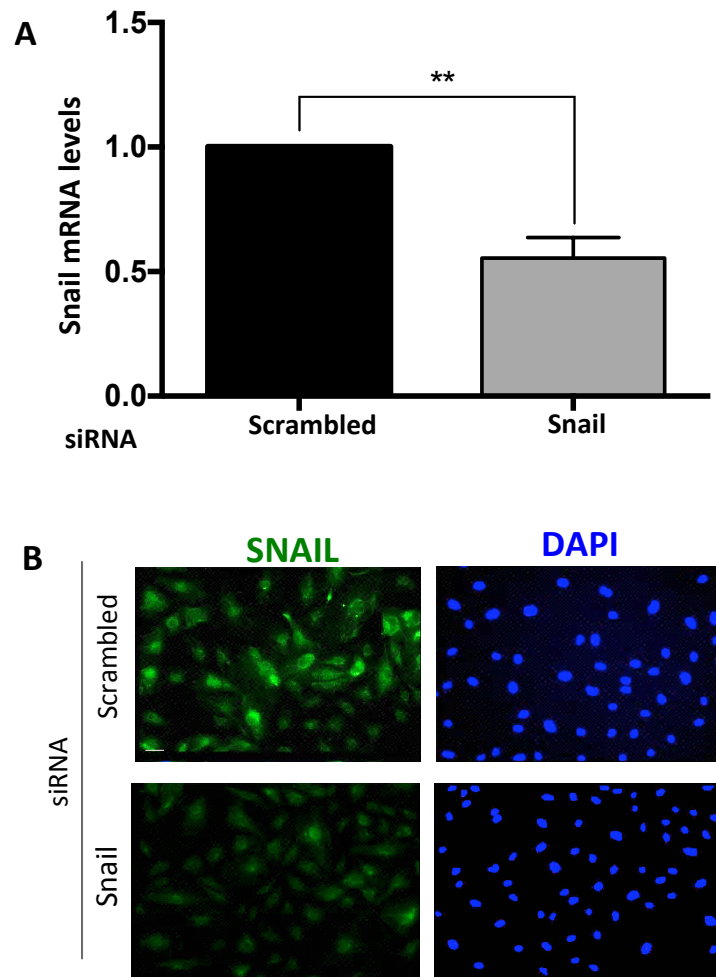


Figure 35. Validation of Snail silencing. HUVEC were transfected with siRNA targeting Snail or scrambled, non-targeting siRNA, prior to the exposure of flow using the orbital plate system for 72h. To assess the effect of gene silencing, transcript levels were assessed by A) qRT-PCR (N=3) and protein levels by B) immunocytochemistry, cells were stained anti-SNAIL antibodies (green). Nuclei were stained using DAPI (blue). Scale bar, 50 μ m. Mean levels \pm SEM are shown. ** $p < 0.01$, using an unpaired t-test.

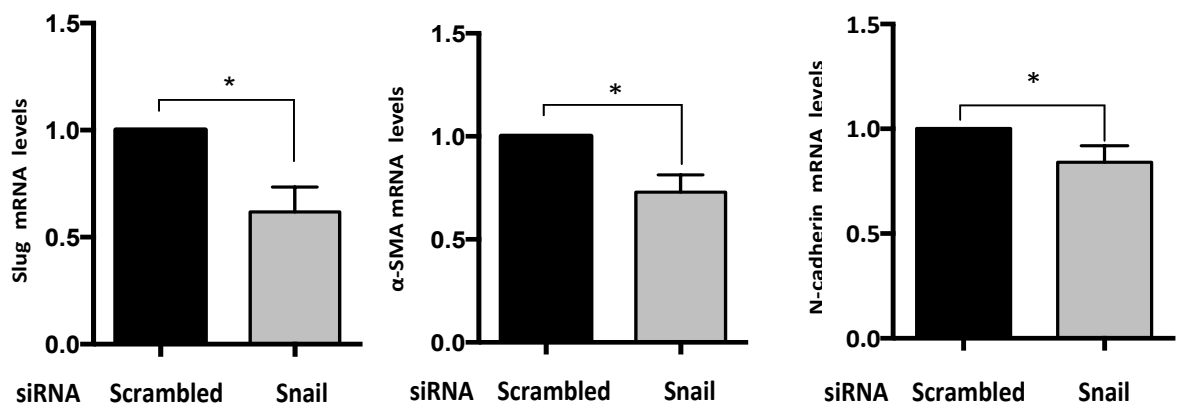


Figure 36. SNAIL promoted EndMT marker expression in cells exposed to low WSS. HUVEC were transfected with targeting Snail or scrambled, non-targeting siRNA, prior to the exposure of flow using the orbital plate system for 72h. EndMT marker transcripts were assessed in cells exposed to low WSS N=3. Mean values \pm SEM are shown. * $p < 0.05$ using an unpaired t-test.

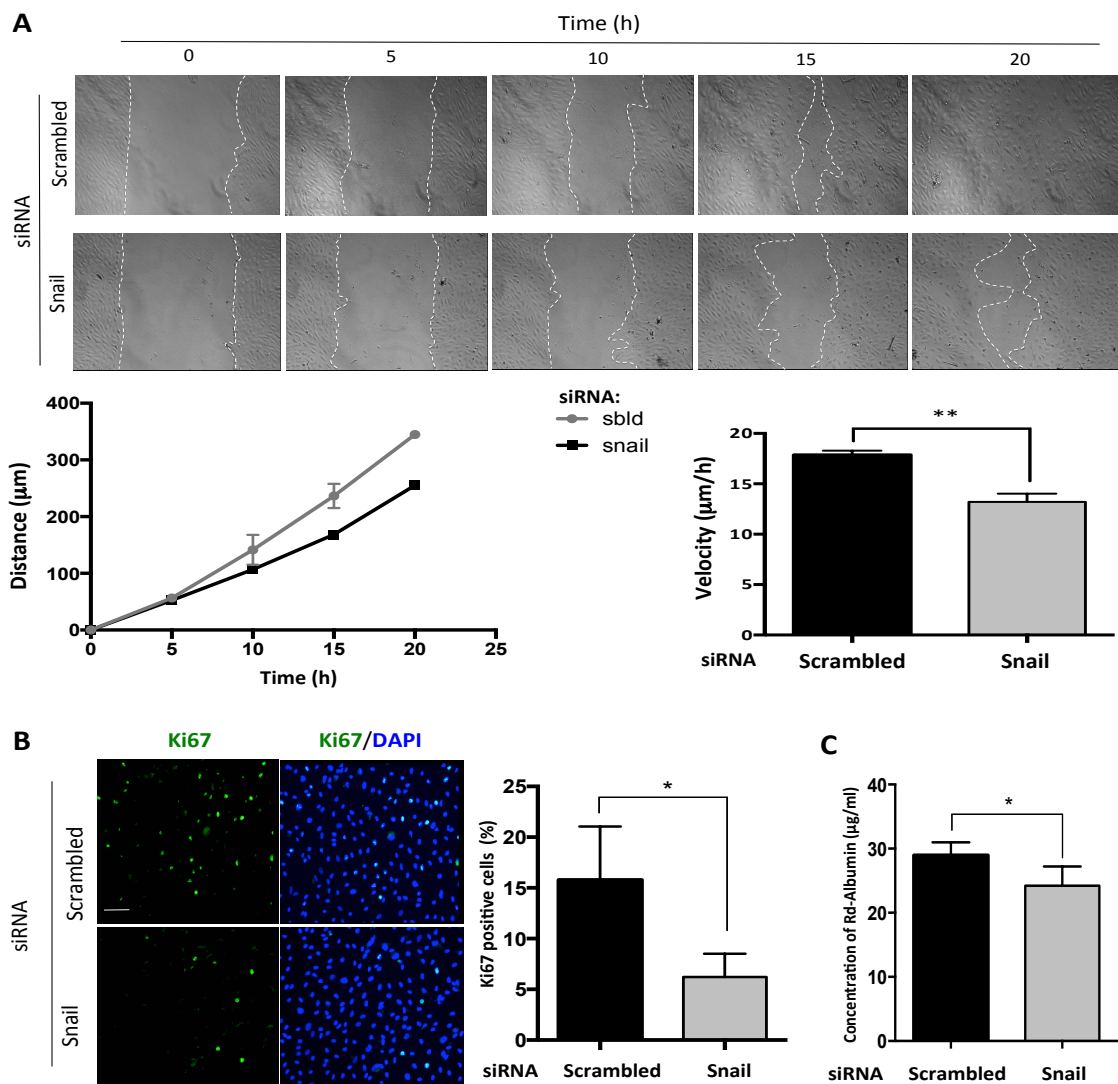


Figure 37. SNAIL promoted cell migration, proliferation and permeability in cells exposed to low WSS. HUVEC were transfected with targeting Snail or scrambled, non-targeting siRNA, prior to the exposure of flow using the orbital plate system for 72h. A) A scratch was made using a P200 pipette tip across the well, to form a wound in areas in the well of high and low WSS. Migration into the wounded area was visualised by time-lapse microscopy, cells were imaged every 3 minutes for 20h. Representative images captured at 5h intervals are shown. Scale bar, 100 μm . The distance migrated into the wounded area was quantified from at least three points in the monolayer. Average velocity also calculated by quantifying the slope, N=4. B) Cells were fixed and immunostained with an anti-ki-67 (green) antibody to label proliferative cells and were co-stained with DAPI (blue). Representative images are shown. Scale bar, 50 μm . % Ki-67-positive cells was calculated as a measure of proliferation, N=4. C) HUVEC were seeded onto transwell plates and exposed to flow via orbital shaking at 150 rpm for 72h. Following orbital shaking, a rhodamine-albumin tracer was incubated for 1 hour under static conditions. Media from the bottom compartment was collected to assess the concentration of tracer as a measure of cell permeability, N=5. * $p < 0.05$, ** $p < 0.01$ using a paired t-test.

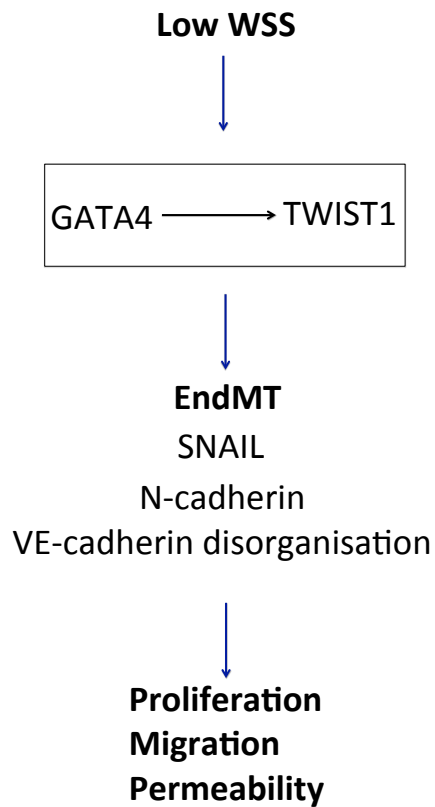


Figure 38. Model for the role of Twist1 and GATA4 in regulating EC physiology in cells exposed to low WSS *in vitro*. Low WSS promoted GATA4-Twist1 expression. Twist1 and GATA4 promote partial EndMT by inducing SNAIL and N-cadherin expression. Twist1, GATA4 and Snail promote proliferation, migration and permeability.

4.5 Conclusions

1. TWIST1 and GATA4 promote cell proliferation, migration and permeability in cells exposed to low WSS.
2. TWIST1 and GATA4 induce SNAIL and markers of EndMT in EC exposed to low WSS.
3. SNAIL promotes cell proliferation, migration and permeability in cells exposed to low WSS.

4.6 Discussion

4.6.1 GATA4 and TWIST1 control EC proliferation, migration and permeability via the induction of EndMT in cells exposed to low WSS.

In this chapter, I have demonstrated that cell migration, proliferation and tube formation are enhanced in cells exposed to low WSS compared to high WSS conditions, which is consistent with previous studies (Szymanski et al. 2008; Lin et al. 2000; Tressel et al. 2007).

Previous studies have showed that EC exposed to low WSS *in vivo* and *in vitro* showed a higher rate of cell proliferation compared to cells exposed to high WSS (Chaudhury et al. 2010; Obikane et al. 2007; Schober et al. 2014; Davies et al. 1986). However, I did not detect a difference in cells exposed to low or high WSS via orbital shaking. There are multiple reasons to explain this discrepancy; 1) it is known that cells change their responses based on particular thresholds of WSS (Dolan et al. 2012; Ostrowski et al. 2014). It may be that WSS in the orbital plate does not reach the threshold required to trigger proliferation. 2) Cells exposed to low WSS and high WSS exist within the well of the orbiting well, therefore the release of autocrine factors and the effects of cell migration from the different flow regions could have contributed to cell turnover. To overcome this, I assessed EC proliferation in cells exposed to flow using the Ibidi™ parallel plate system. The results revealed that proliferation was significantly enhanced in cells exposed to low, unidirectional WSS (data not included). Future experiments will include assessing TWIST1 and GATA4 function using the Ibidi™ parallel plate system.

Nevertheless, TWIST1 and GATA4 expression was significantly enhanced in cells exposed to low WSS using the orbital plate, therefore I tested whether the increase in expression results in a functional change in EC physiology using this system. I have shown that Twist1 and Gata4 silencing reduced tube formation, proliferation and migration indicating that the expression of these genes under low WSS controls cell function. Since cell proliferation and migration are processes that give rise to a transient loss in EC-EC contacts (Cancel et al. 2011, Cancel et al. 2010, Birukova et al.

2004; Forteiniois et al. 2008) cell permeability was assessed using a transwell plate. It was evident that Twist1 and GATA4 genes also promoted permeability in cells exposed to low WSS. However, the transwell based method which was used to study EC permeability under flow exhibited much lower WSS magnitude compared to cells that are exposed to flow in the centre of the 6-well orbital plate (1.82 vs. 4.8 dyne/cm² respectively). In addition, in the flow of media in orbiting transwell plate may exert interstitial forces on the cells. Thus, there are differences in the type of flow used to study proliferation, migration and permeability and it may be incompletely accurate to compare the effect of GATA4 and TWIST1 on migration and proliferation detected using the orbital system to their effect on permeability using the transwell system. To overcome this, a method developed by Velasco et al. of measuring cellular impedance (as a measure of permeability) of cells located in the centre of the 6-well orbital plate could be used (Velasco et al. 2015). Collectively, I have demonstrated for the first time that GATA4-TWIST1 signalling contributes to low WSS-induced changes in cell function, including cell proliferation, migration and permeability.

The observations discussed above are consistent with previous studies. TWIST1 and GATA4 are known to regulate cell proliferation and migration during embryonic development (valve formation, gastrulation, heart development) and in cancer (Zeisberg et al. 2005; Vrljicak et al. 2012; Yang et al. 2004). Moreover, other GATA family transcription factors (GATA2 and 6) regulate angiogenesis by controlling tube formation, migration and proliferation (Froese et al. 2011; Song et al. 2009). In addition, it has been shown by the Ingber lab that GATA2 regulates retinal angiogenesis *in vivo*, involving migration and proliferation in response to changes in matrix stiffness, providing a precedent for the regulation of EC physiology in response to mechanical cues via GATA family genes (Mammoto et al. 2009). TWIST1 also regulates retinal angiogenesis through promoting cell proliferation and migration (Li et al. 2014). In addition, Li *et al.* demonstrated the role of TWIST1 in the regulation of EC permeability in the lung vasculature via a Tie2-dependent mechanism (Mammoto et al. 2013), and it will be interesting to see whether a similar mechanism for cell permeability operates under low WSS conditions.

I then hypothesised that TWIST1 and GATA4 regulate cell function via EndMT due to the following reasons; 1) TWIST1 and GATA4 are inducers of EndMT during valve development (Zeisberg et al. 2005; Vrljicak et al. 2012; Chakraborty et al. 2010; Rivera-Feliciano et al. 2006), 2) Recently, studies have linked the induction of EndMT by low WSS (Chen et al. 2015; Moonen et al. 2015; Sanchez-Duffhues et al. 2015; Mahler et al. 2014), 3) TWIST1 and GATA4 regulate cell functions including cell proliferation and migration, processes that are attributed to EndMT (Zeisberg et al. 2005; Yang et al. 2004; Vrljicak et al. 2012; Chakraborty et al. 2010). In this chapter I have demonstrated that low WSS promotes a partial transition into EndMT as evidenced by cells expressing EndMT markers (α -Sma, Slug, N-cadherin) but retaining EC marker VE-cadherin. These findings are in agreement with recent studies that have shown that low WSS or no flow (cells lacking cilia) conditions promote EndMT marker expression compared to cells exposed to high WSS (Ergorova et al., 2011, Mahler et al., 2014, Moonen et al. 2015; Sanchez-Duffhues et al. 2015; Chen et al. 2015). In addition, these *in vitro* studies demonstrate that cells exposed either low WSS or no flow conditions (with TGF- β) show a reduction in VE-cadherin. However, in my studies I did not detect a reduction in VE-cadherin expression in cells exposed to low WSS. This discrepancy could be due to TGF- β (a known EndMT inducer), which was used in studies demonstrating VE-cadherin loss but not in my work, which showed VE-cadherin retention under low WSS. Alternatively, the transition into a mesenchymal state depends on the precise mechanical conditions that the cells are exposed to, which varies in different *in vitro* flow systems. Therefore, it could be that a full or partial transition into a mesenchymal state depends on the conditions that the cells are exposed to.

I showed that TWIST1 and GATA4 promoted partial EndMT in cells exposed to low WSS as they promoted the induction of N-cadherin and the EndMT regulator SNAIL. GATA4 transcriptionally activated Snail expression as revealed by ChIP analysis on the Snail promoter, indicating the GATA4 and Twist1 co-operate to induce Snail expression. Previous studies have shown that Twist1 and GATA4 can activate snail and N-cadherin expression (Vrljicak et al. 2012; Smit et al. 2009; Moskowitz et al.

2011), however I show for the first time that this activation occurs in EC exposed to low WSS. The molecular mechanism proposed by other studies for the WSS-dependent induction of EndMT involves TGF- β , FGF and antioxidant signalling via KLF4 and MAPK (ERK5) signalling (Egorova et al. 2011; Moonen et al. 2015; Sánchez-Duffhues et al. 2015; Mahler et al. 2014; Chen et al. 2015). Interestingly, both GATA4 and TWIST1 interact with these signalling pathways by either directly regulating these pathways or as downstream targets (Rivera-Feliciano et al. 2006; Xue, D. F. Restuccia, et al. 2012; Belaguli et al. 2007; Connerney et al. 2008; O'Rourke et al. 2002). It would therefore be of interest to assess if TGF- β , FGF, antioxidant signalling via KLF4 and MAPK signalling pathways promote TWIST1 and GATA4 to drive EndMT in cells exposed to low WSS or whether TWIST1 and GATA4 act upstream of these pathways to drive EndMT in cells exposed to low WSS.

Gene silencing studies revealed that SNAIL contributes to the regulation of partial EndMT and to regulating functions that are promoted by TWIST1 and GATA4. Consistent with previous studies, Snail has been well established in controlling EndMT and subsequent changes in cell proliferation and migration (Kokudo et al. 2008; Timmerman et al. 2004; Leroy & Mostov 2007). However, the molecular mechanism of Twist1 and GATA4 regulation of cell function under low WSS could potentially involve targets other than Snail (Figure 39). These potential mechanisms will now be discussed.

4.6.2 Potential mechanisms for cell proliferation

TWIST1 and GATA4 have been shown to promote the activation of target genes involved in proliferation including Tbx20, Pdgfr- α , Foxm1, cell division control protein (CDC) 42, cyclinD2, cyclinA2, cyclin-dependent kinase (Cdk)4 and growth arrest and DNA-damage-Inducible (Gadd)45 α (Lee & Yutzey 2011; Heineke, Auger-messier, et al. 2007; Chia et al. 2015; Rojas et al. 2008) Qian 2013. Moreover, Twist1 and GATA4 interact with and regulate p38 and WNT signalling (Lin & Xu et al. 2009; Tenhunen et al. 2004; Hong et al. 2011). Since p38 MAPK and WNT signalling have been linked with the regulation of low WSS-mediated cell proliferation (Chaudhury et al. 2010; Rotherham & El Haj 2015; R. Li et al. 2014; Biswas et al. 2003; Masckauchán et al. 2005) this could be a potential mechanism by which TWIST1 and GATA4 regulate this process. In addition, Twist1 promotes the expression of miR-199a and miR214 and both GATA4 and TWIST1 promote the expression of miR1, all of which regulate cell proliferation in cancer cells and in cardiomyocytes (Sun et al. 2010; Schlesinger et al. 2011; Yin et al. 2010). It is plausible that these mechanisms operate in EC exposed to low WSS.

TWIST1 and GATA4 could regulate cell proliferation through indirect mechanisms. I have shown that TWIST1 and GATA4 promoted N-cadherin protein expression at the cell junctions, this could also contribute to cell proliferation. It has been previously demonstrated that the expression of N-cadherin at cellular junctions enhanced proliferation compared to the expression of VE-cadherin (Luo & Radice 2005; Giampietro et al. 2012) via a potential mechanism involving the interaction of cytoplasmic catenin proteins and downstream signalling events (Zhang et al. 2013; Giampietro et al. 2012). TWIST1 and GATA4 indirectly regulate cell cycle progression through p53. TWIST1 inhibits p53-mediated cell cycle arrest, apoptosis and senescence in cancer cells (Piccinin et al. 2012; Burns et al. 2013). Whereas, GATA4 promotes p53 expression and senescence in fibroblasts in response to DNA damage (Kang et al. 2015).

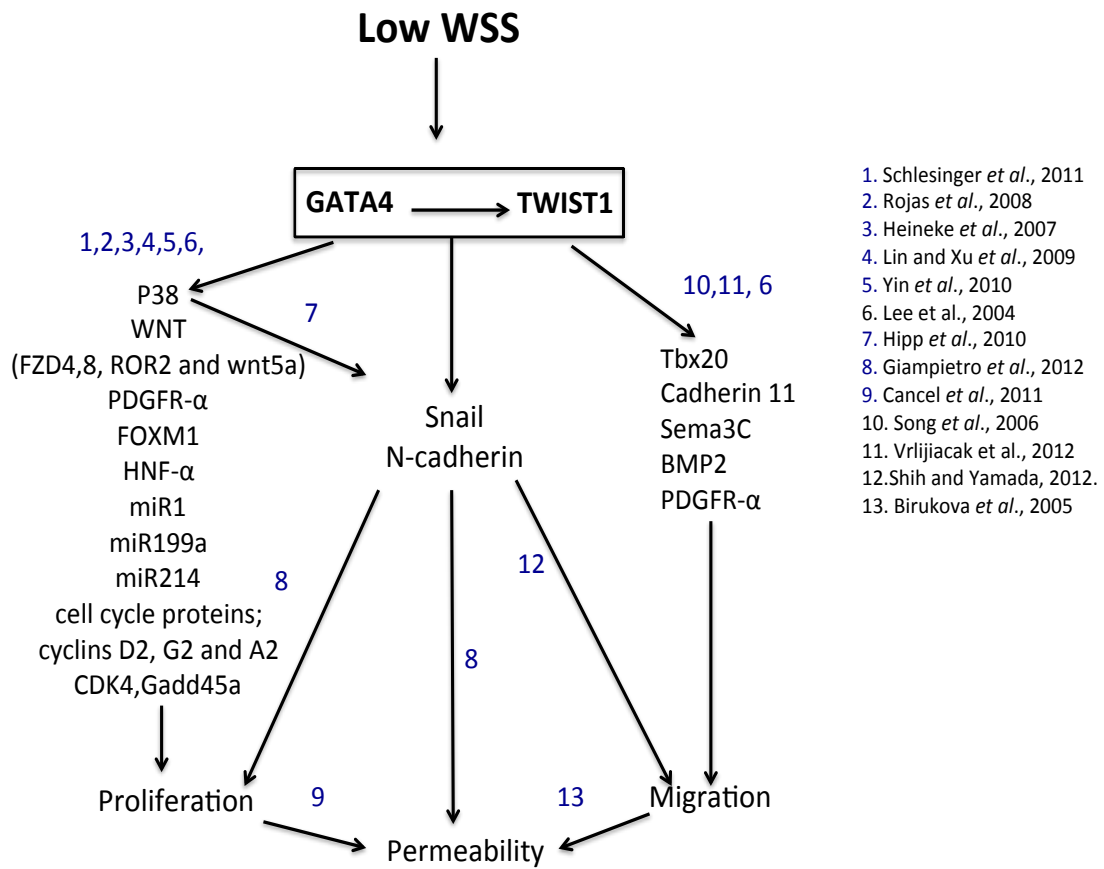


Figure 39. Potential mechanisms by which Twist1 and GATA4 drive EC proliferation, migration and permeability under low WSS.

The regulation of p53 by TWIST1 and GATA4 is indicative of their role in differentially regulating cell cycle progression and subsequently proliferation under specific contexts. Moreover, it is interesting that TWIST1 and GATA4 can play opposing roles in p53-mediated senescence, this indicates that even though TWIST1 and GATA4 cooperate to drive the same functions (proliferation, migration, permeability) in cells exposed to low WSS they can play opposing roles in other functions depending on the cellular context.

4.5.3 Potential mechanism for the regulation of migration

TWIST1 and GATA4 promote the activation of several migratory genes such as N-cadherin, cadherin 11 (OB-cadherin), claudin 5, Sema3c and Tbx20 (Lee & Yutzey 2011; Rojas et al. 2008; Chakraborty et al. 2010; Soo et al. 2002; Song et al. 2006). The induction of N-cadherin at the cell junctions by TWIST1 and GATA4 in cells exposed to low WSS could be an inducer of cell migration since N-cadherin promotes an increase in cell motility in other systems (Reviewed Shih & Yamada 2012; Giampietro et al. 2012). Moreover, in cancer cells, Twist1 has been shown to drive metastasis via PDGFR- α mediated formation of invadopodia (Eckert et al. 2011) and this could also be involved in EC exposed to low WSS.

4.5.4 Potential mechanism for the regulation of permeability.

Cell migration and proliferation is associated with an increase in cell permeability (Cancel et al. 2011; Cancel et al. 2010; Birukova et al., 2004). TWIST1 and GATA4-mediated induction of these processes could be a potential mechanism of indirectly promoting cell permeability. TWIST1 has been linked with the regulation of EC permeability in the lung vasculature via regulating the levels of Tie2 (Mammoto et al. 2013). An analogous mechanism may control permeability in sheared EC. Moreover, the regulation of TWIST1 and GATA4 of VE-cadherin junctional width may be a mechanism by which cell permeability is controlled by these genes. An increase in VE-cadherin junctional width is associated with increased monolayer permeability

(Huynh et al. 2011). The proposed molecular mechanism has been suggested to be via Src-mediated VE-cadherin phosphorylation, which promotes VE-cadherin internalisation from the cellular junctions (Orsenigo et al. 2012; Gavard & Gutkind 2006; Miao et al. 2005). Since VE-cadherin is in competition with N-cadherin for junctional expression (Navarro et al. 1998; Giampietro et al. 2012) this could promote N-cadherin expression at the junctions. Therefore, whether TWIST1 and GATA4 regulate VE-cadherin phosphorylation via interacting with signalling mediators upstream of Src, whether this process indirectly promotes the expression of N-cadherin at the cellular junctions and the contribution of these processes to permeability under low WSS conditions should be investigated.

In summary, low WSS is known to drive changes in cell physiology, including proliferation, migration and permeability to macromolecules. Here I provide a novel molecular mechanism for low WSS-induced changes in cell function. Specifically, low WSS promotes GATA4- TWIST1 signalling which then promote Snail expression, contributing to the induction of partial EndMT and changes in cell function. However, more experiments are required to fully establish whether the GATA4-TWIST1-SNAIL axis controls cell proliferation, migration and permeability via EndMT or whether these processes occur independently. Moreover, it would be interesting to test whether cells undergo partial EndMT *in vivo* at atherosusceptible sites in the murine aorta and, if so, whether the molecular mechanism involves the GATA4-TWIST1-SNAIL axis. The latter question is addressed in the next chapter.

4.6 Future work

- 1- To validate whether TWIST1 and GATA4 regulate EC proliferation, migration and permeability via SNAIL, overexpression studies should be performed to test if Snail can rescue the resulting phenotype of TWIST1 and GATA4 silencing. Moreover, to assess if Twist1 also regulates Snail transcriptionally, a TWIST1 ChIP could be carried out.

- 2- To assess if changes in cell function with TWIST1 and GATA4 are attributed to low-WSS induced EndMT, known EndMT inhibitors such as SB-431542 and LY294002 could be used to test this.

- 3- To assess the potential involvement of TGF β and MAPK signalling with low WSS-mediated regulation of EC function by Twist and GATA4; 1) Cells would be treated with TGF- β and TWIST1 and GATA4 siRNA will be used to assess Snail expression and EC function, 2) These pathways could be blocked (pharmacologically or via siRNA) prior to assessment of TWIST1 and GATA4 expression.

- 4- To gain a deeper mechanistic insight into the regulation of TWIST1 and GATA4 of cell function, target genes should now be investigated by carrying out ChIP-seq analyses.

- 5- The functional significance of the cadherin switch in cells exposed to low WSS can be assessed by the silencing of N-cadherin and/or enhanced expression of VE-cadherin prior to the assessment of cell function.

- 6- Gata4, Twist1 and Snail gene function could be validated under low WSS, by using a second *in vitro* flow system, e.g. the Ibidi™ parallel plate system.

**Chapter 5: GATA4-TWIST1 signalling controls
focal EC dysfunction at sites exposed to low WSS
flow *in vivo***

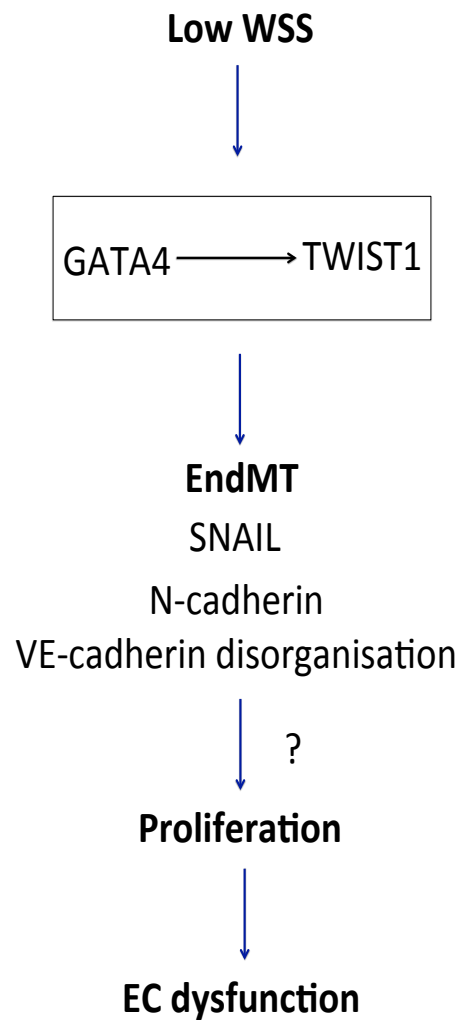
5.1 Introduction

WSS plays a prominent role in controlling the spatial distribution of atherosclerosis. Despite the presence of systemic risk factors, atherosclerosis preferentially develops at branches and bends in the vasculature, areas that are exposed to low WSS, whereas areas exposed to high WSS are protected. The physiology of EC at sites exposed to low WSS includes an enhanced rate of cell proliferation and permeability, processes that are characteristic of EC dysfunction. This in turn promotes EC activation and renders these sites “hot spots” for atherogenesis. On the other hand, EC in the vasculature that are exposed to high WSS are quiescent and these sites are therefore atheroprotected (Reviewed in Chiu & Chien 2011).

I have showed in the previous chapters that TWIST1 and GATA4 control partial EndMT in cells exposed to low WSS in cultured cells. I have also shown that the activation of the GATA4-TWIST1-SNAIL axis promotes proliferation, migration and permeability. However, these observations were made using *in vitro* flow systems, which do not fully recapitulate the mechanical and physiological environments EC are exposed to *in vivo*. Thus, it is important to validate the TWIST1 and GATA4 by low WSS and secondly the functional role of these transcription factors in cells exposed to low WSS conditions.

5.2 Hypothesis

GATA4-TWIST1 mechanotransduction promotes focal EC dysfunction and atherosusceptibility.



5.3 Aims

1. To assess if low WSS correlates with Twist1, GATA4 and Snail expression in the murine aortic arch.
2. To directly test whether WSS regulates Twist1, GATA4 and Snail *in vivo*, using a flow-altering constrictive cuff.
3. To assess if Twist1 is expressed in adult endothelial cells, under low WSS via cell tracing experiments.
4. To assess Twist1 and GATA4 function in cells exposed to low WSS in the murine aortic arch using EC-specific, conditional knock out animal models.
5. To assess the expression of Twist1 in human and murine atherosclerotic plaques.

5.4 TWIST1, GATA4 and SNAIL expression is enhanced by atheroprone flow in the murine aorta

As GATA4-mediated TWIST1 expression was enhanced by low WSS flow conditions in cultured cells, this suggested that TWIST1 and GATA4 are involved in mediating EC responses to flow. To validate this *in vivo*, it was firstly investigated whether WSS correlates with the expression of TWIST1, GATA4 and SNAIL in the murine aortic arch of C57BL/6 animals. The expression of all three proteins was assessed at regions of low WSS (inner curvature) and high WSS (outer curvature). All three transcription factors TWIST1, GATA4 and SNAIL showed a marked increase in expression at low WSS sites compared to high WSS sites (Figure 40). Moreover the proteins were expressed almost exclusively in the nucleus, indicating that they are active in these cells. These data reflected that the expression of these genes correlates with low WSS *in vivo*.

Atherosusceptible regions of arteries are associated with increased inflammation and altered uptake of substances from the arterial wall as well as low WSS. Thus these observations only provide a correlation between WSS and gene expression. Moreover, at these regions the flow patterns are disturbed, as characterised by low and oscillating WSS, thus it is important whether flow magnitude or directionality are the driving forces in TWIST1 and GATA4 activation *in vivo*. To establish a causal link between WSS and gene activation, a constrictive, flow-altering cuff was used. The insertion of the cuff into the right carotid arteries results in a constriction, which consequently alters flow, giving rise to high WSS at the stenosis, low WSS upstream and low, oscillatory WSS downstream and the left carotid artery was used as a sham control. Following 14 days of cuff insertion, both carotids and the aortic arch were isolated and prepared for *en face* immunostaining. In the cuff-inserted vessels, it was revealed that TWIST1, GATA4 and SNAIL showed enhanced expression at the upstream site compared to the stenosis (Figure 41), indicating that low WSS is an activating stimulus for all three genes.

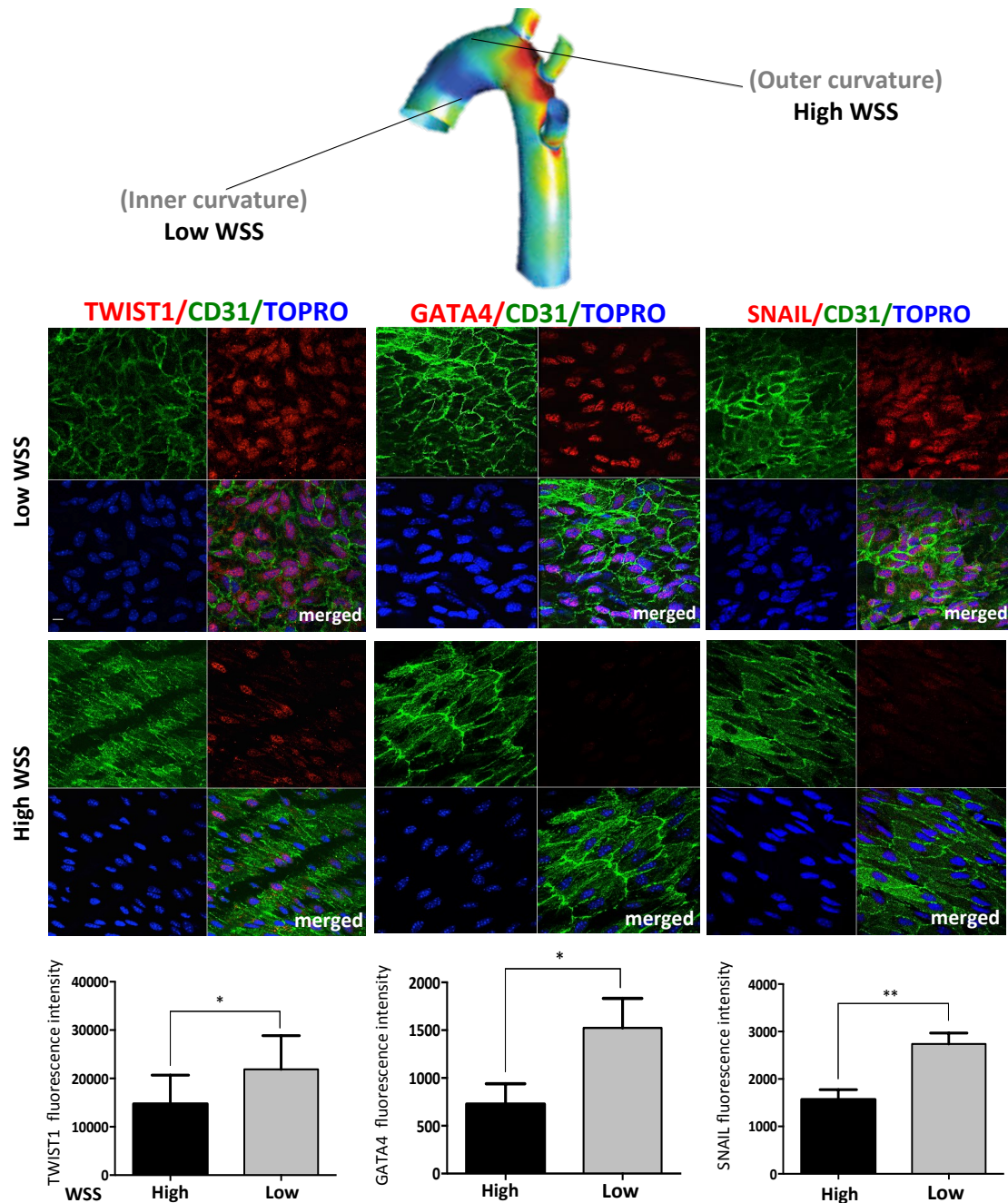


Figure 40. Low WSS correlated with TWIST1, GATA4 and SNAIL expression in the murine aortic arch. Expression levels of Twist1, GATA4 or Snail in EC were assessed by *en face* immunofluorescent staining of low WSS (susceptible) or high WSS (protected) regions of the aorta in C57BL/6 mice (red). EC were identified by co-staining with anti-CD31 antibodies conjugated to FITC (green). Cell nuclei were identified using TOPRO (blue). Representative images are shown, scale bar 20 μ m. TWIST1, GATA4 and SNAIL expression was quantified by measuring fluorescent intensity of the cells per field of view using Image J. Data were pooled from 5 independent experiments and mean values \pm SEM are shown. * p < 0.05, ** p < 0.01 using a paired t-test.

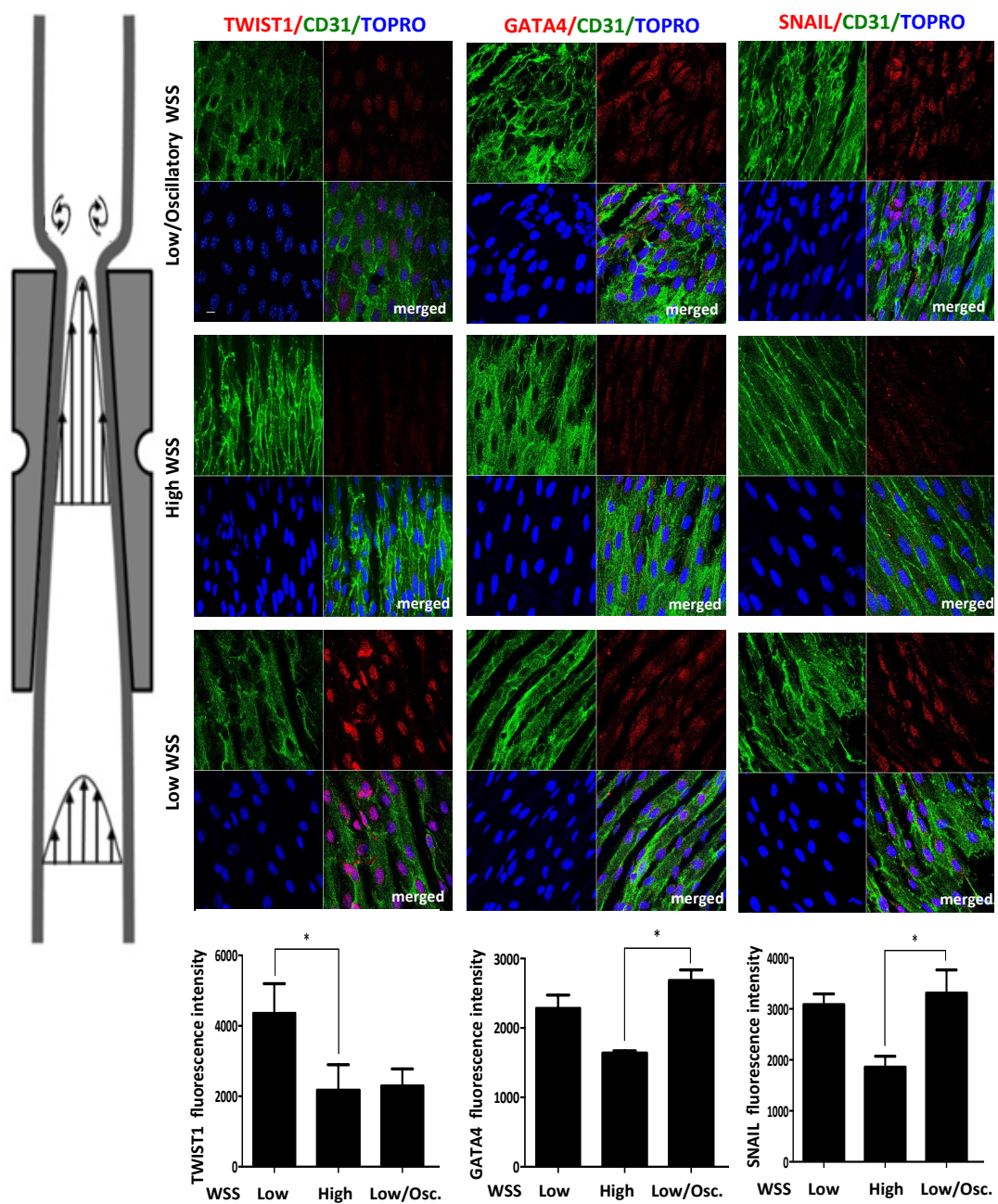


Figure 41. Low WSS promoted TWIST1, GATA4 and SNAIL expression in cuff-inserted carotid murine arteries. Flow-altering, constrictive cuffs were placed on the right carotid arteries of C57BL/6 mice. Right carotid arteries were harvested after 14 days and *en face* staining was performed using anti-TWIST1, anti-GATA4 or anti-SNAIL antibodies (red), anti-CD31 antibodies conjugated to FITC (green) and the nuclear counter stain TOPRO (blue). Representative images and quantitation of TWIST1, GATA4 or SNAIL expression (mean \pm SEM) are shown. Scale bar, 10 μ m. Data were pooled from four-six independent experiments. * $p < 0.05$, ** $p < 0.01$, using a one-way ANOVA.

Surprisingly, GATA4 and SNAIL were found to be induced at the downstream region, where TWIST1 expression was reduced. In the non-cuff inserted left carotid vessel, the expression of all three transcription factors was assessed at regions that are equivalent to the cuff-inserted vessel as a control. The data revealed that there was no significant difference in TWIST1, GATA4 and SNAIL expression at the different sites (Figure 42), which suggested that the differences in expression detected in the cuff-inserted vessels were directly due to the different flow conditions.

5.5 TWIST1 was expressed in adult EC exposed to low WSS in the murine aorta

I hypothesised that TWIST1 was expressed in adult EC in response to WSS. However, since TWIST1 is a mesenchymal gene there could be other potential mechanisms to explain the accumulation of TWIST1-positive EC at sites of low WSS. For example, there has been evidence from the Xu group to suggest that endothelial progenitor cells migrate into sites of low WSS in the murine vasculature (Foteinos et al. 2008). To distinguish between these possibilities Cre-based cell tracking was used to determine whether TWIST1 expression occurs in differentiated carotid artery EC at sites of low WSS. This was performed using transgenic mice containing a loxP-flanked STOP cassette preventing the transcription of a fluorescent Td-Tomato transgene, under the expression of the ROSA26 promoter (Rosa26-tdTomato) and an inducible Cre that is exclusively expressed in adult endothelial cells under the control of the 5'SCL promoter (*SCL-Cre-ER^T; R26R-Td tomato* transgenic mice). The SCL-Cre-ER^T protein is activated upon tamoxifen treatment, which allows the translocation of the protein into the nucleus where it promotes the excision of the STOP cassette through loxP site recombination, allowing the irreversible activation of the R26R-Td tomato gene and the labelling of EC (Figure 43 A). To validate the use of the reporter system, *SCL-Cre-ER^T; R26R-Td tomato* mice were treated with tamoxifen for five consecutive days and the expression of the R26R-Td tomato protein was assessed via *en face* immunostaining.

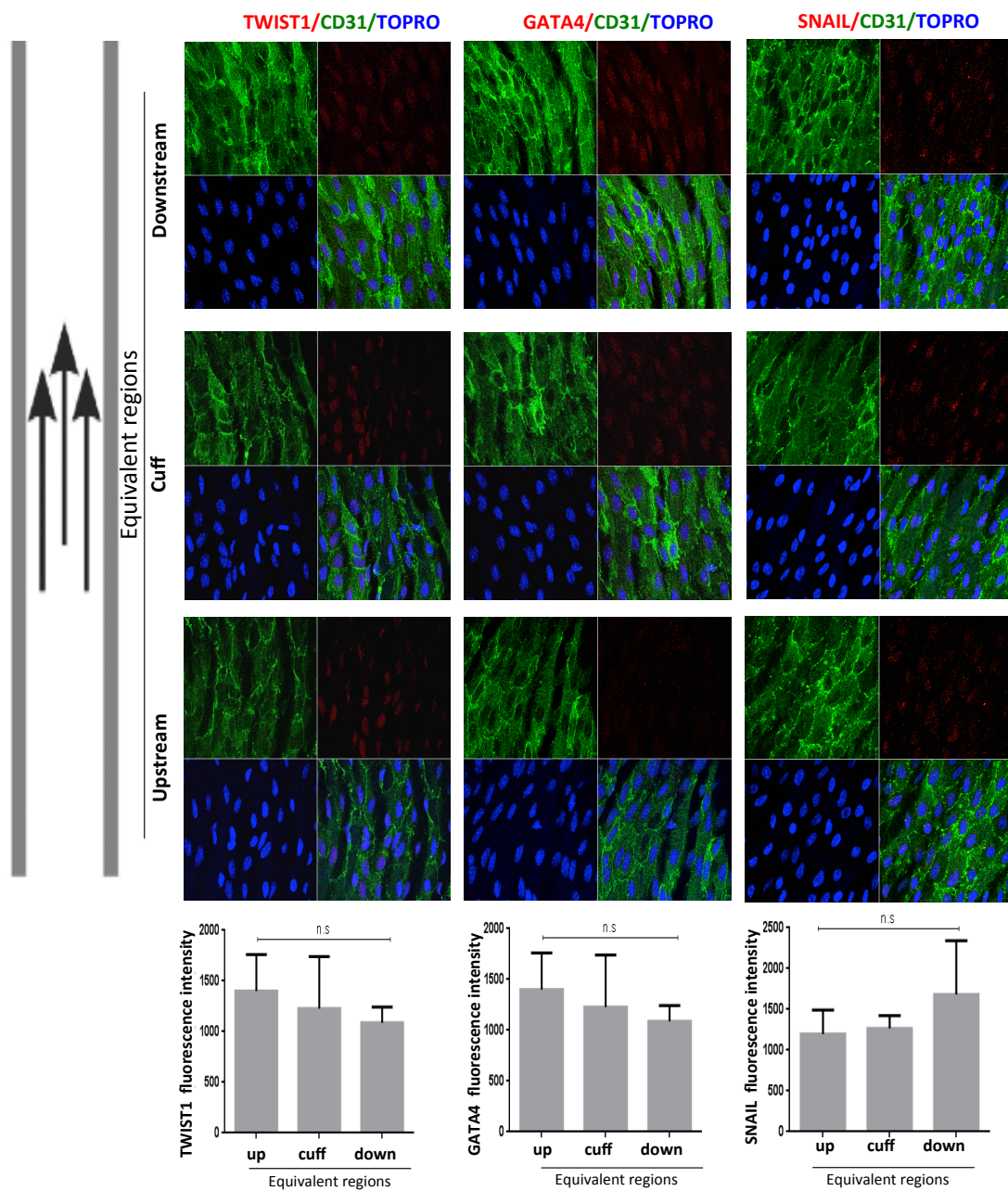


Figure 42. Expression of TWIST1, GATA4 and SNAIL in non cuff-inserted, sham carotid arteries. As a control for cuff-insertion on the right carotids, the left carotids did not have a cuff insertion and were used as sham controls. Left carotid arteries were harvested after 14 days and *en face* staining was performed using anti-TWIST1, anti-GATA4 or anti-SNAIL antibodies (red), anti-CD31 antibodies conjugated to FITC (green) and the nuclear counter stain TOPRO (blue). Representative images and quantitation of TWIST1, GATA4 or SNAIL expression (mean \pm SEM) are shown. Scale bar, 10 μ m. Data were pooled from four-six independent experiments. Statistical analysis was carried out using a one-way ANOVA.

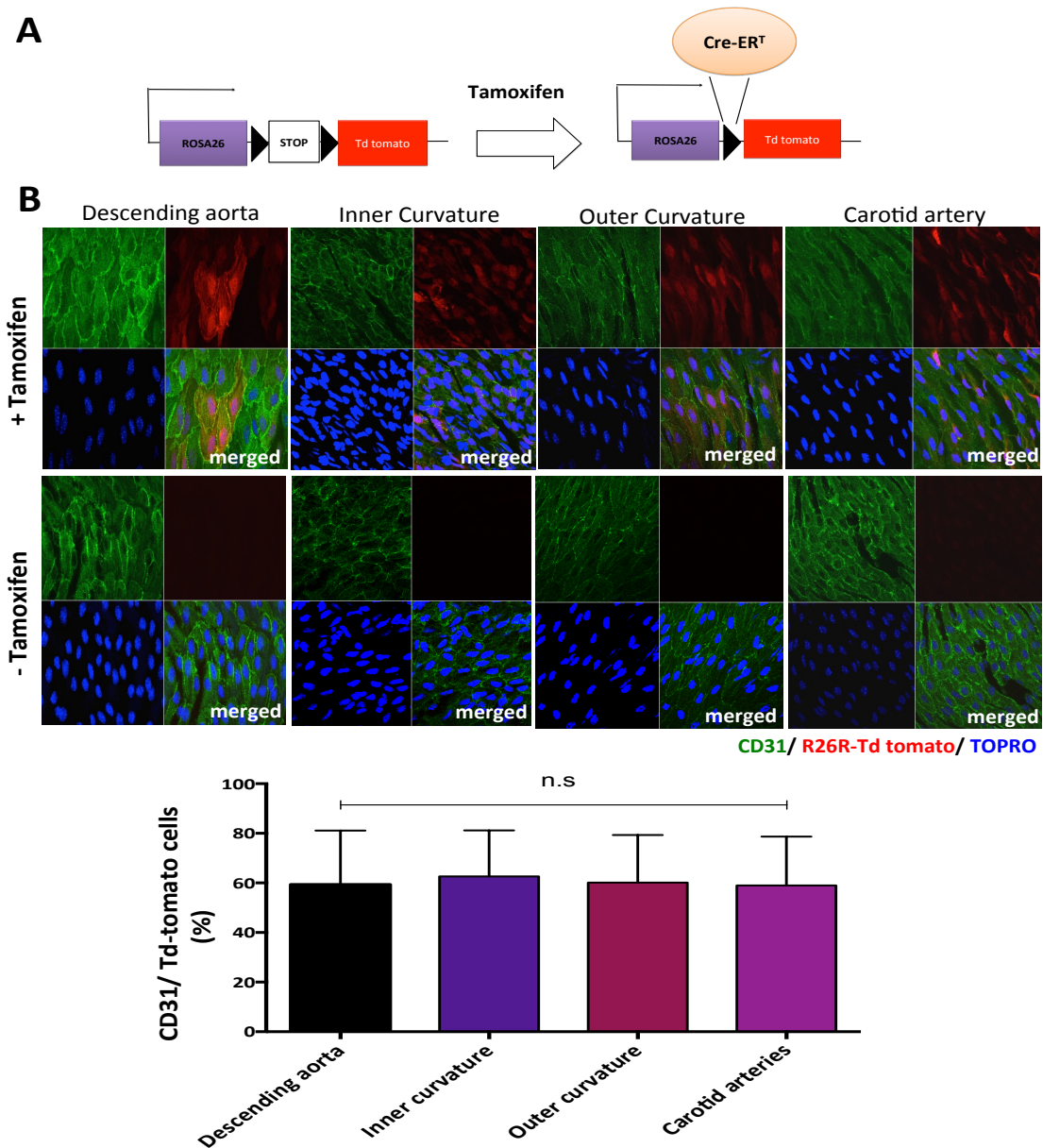


Figure 43. Validation of an EC tracking system in mice. A) Transgenic SCL-Cre-ER^T/R26RtdTomato mice were used to track endothelial cells. This strain drives endothelial cell expression of a form of Cre that can be activated by tamoxifen. The administration of tamoxifen induces nuclear localization of Cre, which subsequently excises a floxed STOP signal from the tdTomato promoter thus inducing tdTomato expression. B) To validate the system, SCL-Cre-ER^T/R26RtdTomato mice were treated with tamoxifen for 5 consecutive days (+ TAMOXIFEN). Alternatively, mice were treated with vehicle as a control (- TAMOXIFEN). After 7 days, carotid arteries were harvested and *en face* staining was performed using anti-CD31 antibodies (green), and the nuclear counter stain TOPRO (blue). Representative images are shown. TdTomato (red) was expressed in the majority of EC in mice treated with tamoxifen, but was not identified in untreated mice. Representative images are shown, scale bar 10 μ m. To quantify TdTomato labelling of EC, %Td-tomato cells that were CD31 positive was calculated. Data were pooled from 3 independent experiments and mean values \pm SEM are shown. Statistical analysis was carried out using a one way ANOVA.

Moreover, to exclude the possibility of labelling efficiency being altered by flow the expression of the Cre-reporter in CD31-positive cells was assessed in the descending aorta, aortic arch (inner and outer curvature) and the carotid artery, sites that differ in flow magnitude, directionality and pulsatility. The expression of the R26R-Td tomato protein was apparent in all studied vascular sites and there was no significant difference in the labelling efficiencies as determined by quantifying % positive R26R-Td tomato cells that are CD31 positive (Figure 43 B). Next, the expression of Twist1 was assessed in adult EC exposed to low WSS via cuff insertion in *SCL-CreER^T; R26R-Td tomato* mice. The procedure involved the treatment of the transgenic mice with tamoxifen for 5 days to label adult EC irreversibly followed by cuff insertion for two weeks to induce low WSS. TWIST1 expression was enhanced at the upstream site (low WSS) compared to the stenosis (high WSS) and Twist1-expressing cells were >90% R26R-Td tomato positive (Figure 44 A-C). These results show that TWIST1 expression at sites of low WSS occurs in adult EC, thus excluding the possibility of TWIST1-positive cells being derived from bone marrow derived EPCs.

5.6 Low WSS promoted partial EndMT *in vivo*.

I have shown that low WSS promotes partial EndMT in EC *in vitro* by promoting the expression of EndMT markers, including N-cadherin. It was next determined whether low WSS alters cadherin expression *in vivo*. Junctional N-cadherin expression and VE-cadherin disorganisation (as assessed by junctional width) were both enhanced in EC at low WSS sites (Figure 45 A,B), indicating that low WSS altered cadherin expression (increased N-cadherin and induced VE-cadherin disorganisation) in EC *in vivo*. However the expression of VE-cadherin and CD31 was not abolished in cells at the low WSS site, suggesting that the transition into EndMT was partial. To further investigate the effect of low WSS on EndMT I determined the direct effect of low WSS on EC delamination using *SCL-CreER^T; R26R-Td tomato* cell tracking coupled with cuff inserted into the carotids of these animals. It was investigated whether labelled EC were present beyond the sub-endothelial layers of the mouse aorta.

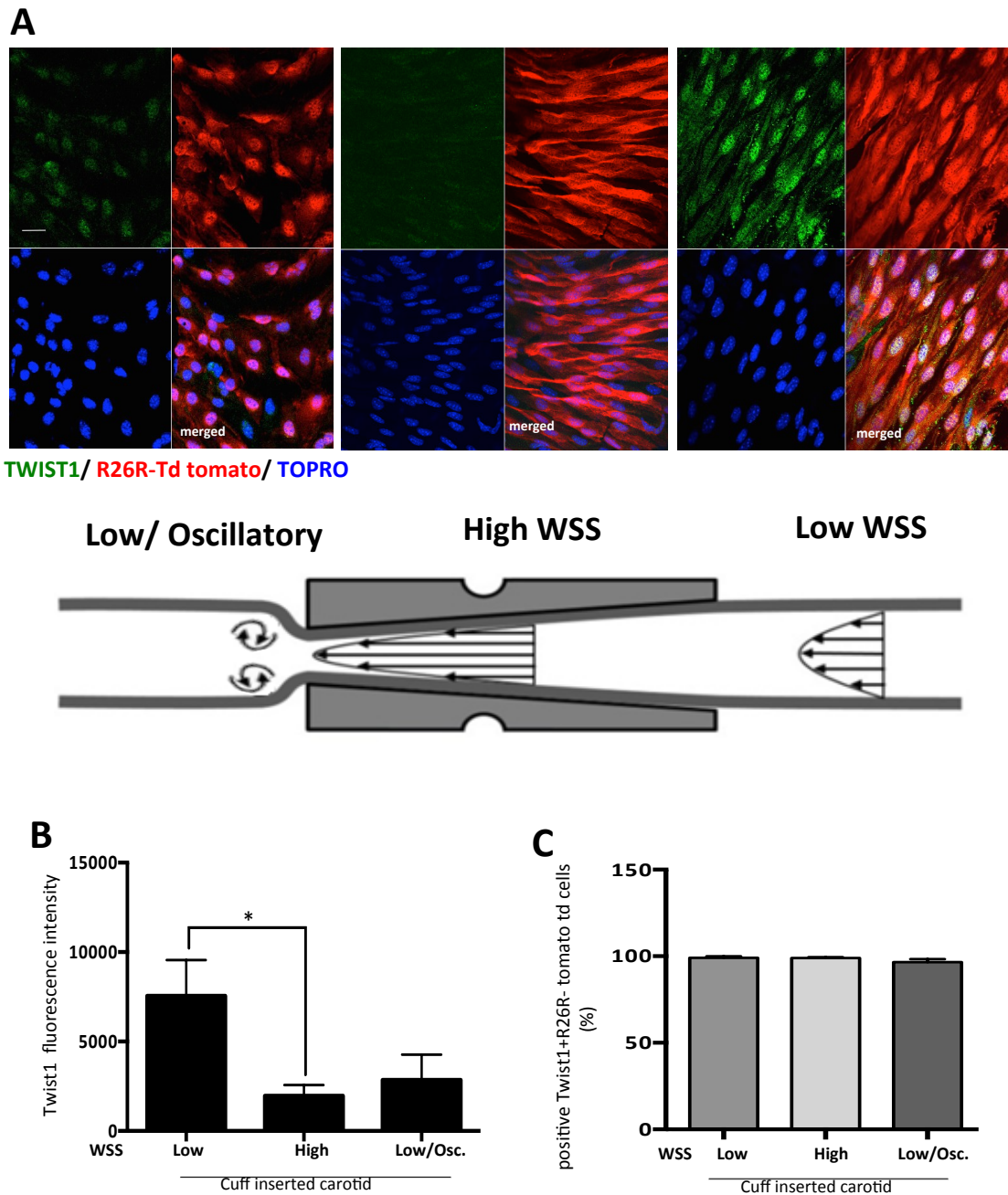


Figure 44. Low WSS promoted TWIST1 expression in adult EC. Transgenic SCL-Cre-ERT/R26RtdTomato mice were treated with tamoxifen for 5 consecutive days to activate tdTomato (red) expression in EC. One week after the final tamoxifen treatment, flow-altering constrictive cuffs were placed on the right carotid arteries. After 14 days, the aortic arch (A) and carotid arteries (B) were harvested and *en face* staining was performed using anti-Twist1 antibodies (green), and the nuclear counter stain TOPRO (blue). Representative images and quantitation of TWIST1 expression (mean \pm SEM) are shown. Scale bar, 10 μ m. * p <0.05 using a paired t-test or one-way ANOVA. C) Twist1 positive cells were quantified as a percentage of Td-tomato labelled cells in the aortic arch and carotid arteries.

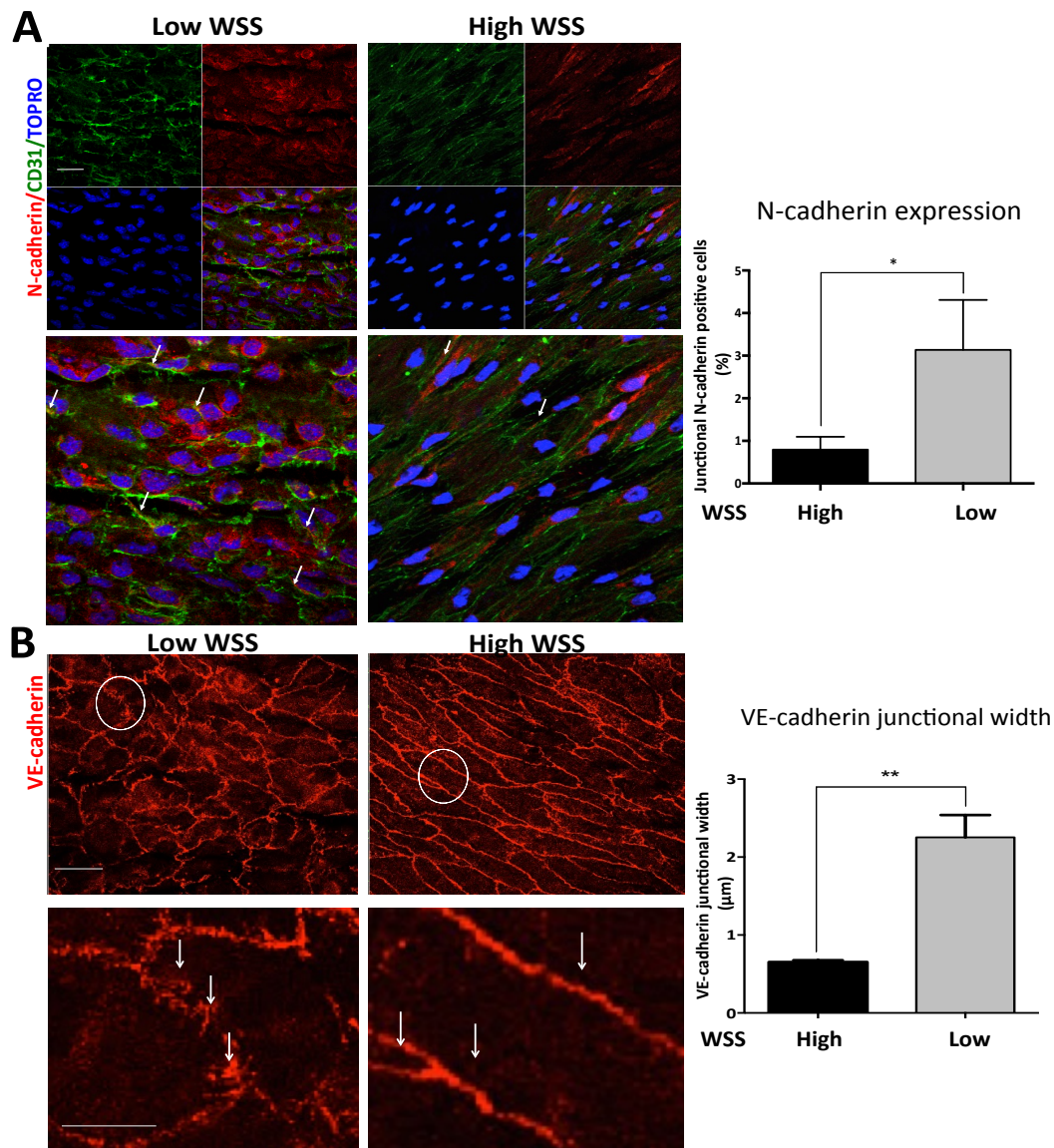


Figure 45. Low WSS promoted the EndMT cadherin switch in the murine aorta. A) Expression levels of N-cadherin (green) in EC were assessed by *en face* staining of low WSS (susceptible) or high WSS (protected) regions of the aortic arch of C57BL/6 mice. EC were identified by co-staining with anti-CD31 antibodies conjugated to FITC (green). Cell nuclei were identified using TOPRO (blue). Representative images are shown, scale bar 10 μm. EC N-cadherin junctional expression was quantified by assessing junctional overlap with CD31 staining (arrows) and data was expressed as percentage positive. B) Expression levels of VE-cadherin (red) in EC were assessed by *en face* staining of low WSS (susceptible) or high WSS (protected) regions of the aortic arch. Representative images are shown, scale bar 10 μm. VE-cadherin width was assessed by measuring junctional width (arrows) using image J of at least 5 cells/ field of view. Representative images are shown from N=4-5 independent experiments. * $p < 0.05$, ** $p < 0.01$, using a paired t-test.

The rationale was if cells at low WSS sites where GATA4, TWIST1 and SNAIL expression is enhanced were undergoing EndMT they would separate from the endothelial layer, invade and migrate into the underlying smooth muscle cell layer. Confocal microscopy coupled with Z-stack imaging revealed that Td-tomato cells were present only in the endothelial cell layer and were absent from the underlying smooth muscle cell layer (Figure 46), suggesting lack of delamination. This further supports the hypothesis that cells exposed to low WSS do not undergo a full transition into a mesenchymal state.

5.7 GATA4-TWIST1 mechanotransduction regulated EC proliferation and partial EndMT at low WSS sites in the murine aorta

Since it is known that EC dysfunction, which involves cell proliferation, is enhanced at atheroprone sites in the vasculature that are exposed to low WSS, EC proliferation was assessed by *en face* immunostaining in the murine aorta. The data revealed that ki67 staining was enhanced in cells at low WSS compared to high WSS sites, as quantified by %Ki67 positive cells (Figure 47). In addition, the number of cells was also enhanced at the low WSS sites, reflecting the increase in cell proliferation, thus confirming that EC proliferation is enhanced in EC located at low WSS sites *in vivo*. The data provides a correlation between EC proliferation and the expression of TWIST1, GATA4 and SNAIL as the expression of these genes is enhanced at these low WSS sites, indicating that the process is potentially regulated by these genes.

To assess the function of TWIST1 and GATA4 in EC at low WSS sites *in vivo*, conditional EC gene knock-out (KO) animals were generated, since the global deletion of both of these genes is embryonically lethal. TWIST1 expression was deleted from EC by crossing mice that contain loxP sites flanking the coding Twist1 exon (*Twist1^{flox/flox}*) with mice that express a Cre gene driven by the endothelial Tie2 gene (Tie2Cre) to generate *Tie2-Twist1^{KO}* animals. Similarly, GATA4 expression was deleted from EC by crossing *Gata4^{flox/flox}* mice with *SCL-Cre-ER^T* mice, followed by tamoxifen treatment to generate *SCL-Cre-ER^T; Gata4^{KO}* animals. The genotype was confirmed via PCR on ear tissue from the mice.

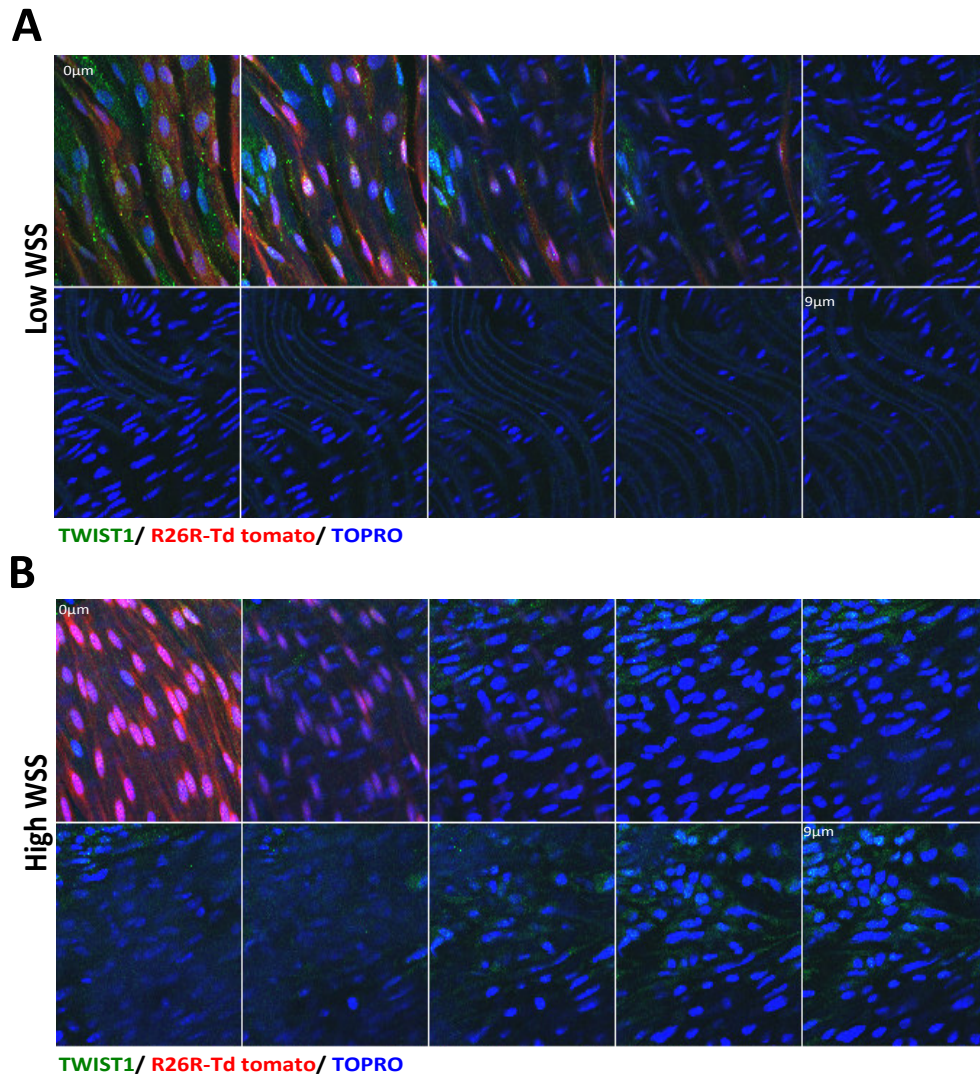


Figure 46. Intimal endothelial cells exposed to low WSS did not migrate into the media. Transgenic SCL-Cre-ERT/R26RtdTomato mice were treated with tamoxifen for 5 consecutive days to activate tdTomato (red) expression in EC. One week after the final tamoxifen treatment, flow-altering constrictive cuffs were placed on the right carotid arteries. After 14 days carotid arteries were harvested and *en face* staining was performed using anti-TWIST1 antibodies (green), and the nuclear counter stain TOPRO (blue). Confocal microscopy was used to generate z-stacks to assess whether Td-Tomato-positive EC were present in the arterial media, at regions of A) low WSS (upstream of cuff) and B) High WSS (stenosis). Representative images and quantitation of Twist1 expression (mean \pm SEM) are shown. Scale bar, 10 μ m. No evidence of EC migration was detected in either region.

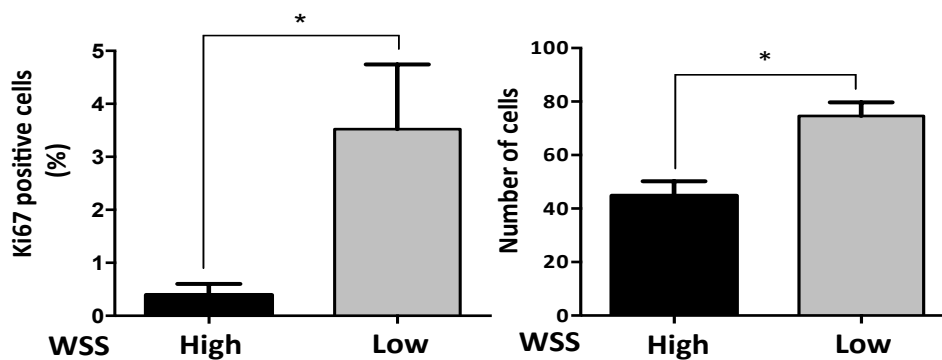
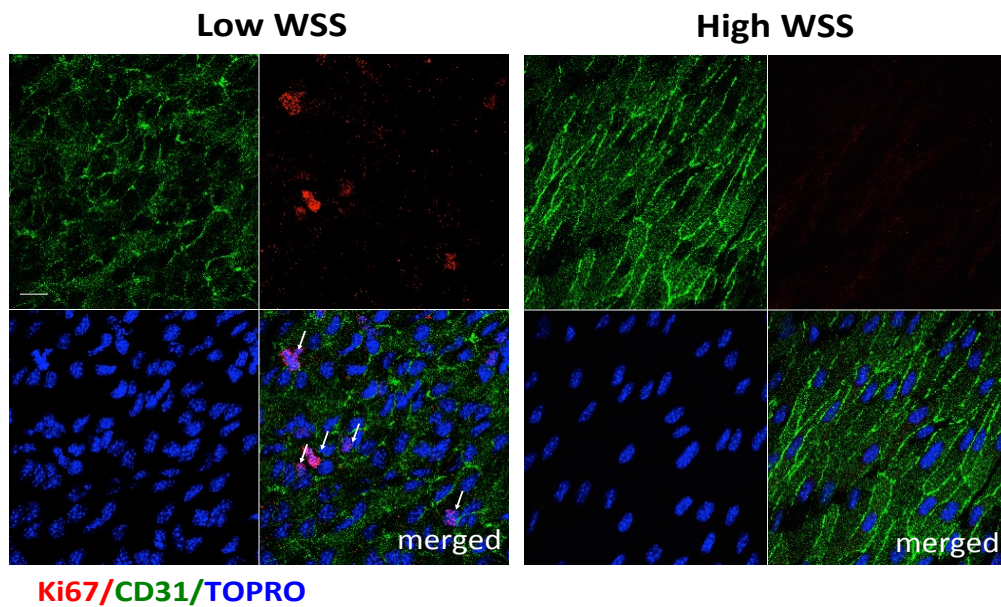


Figure 47. Low WSS promoted EC proliferation in the murine aorta. Expression levels of proliferation marker Ki67 (green) in EC were assessed by *en face* staining of low WSS (susceptible) or high WSS (protected) regions of the aortic arch of C57BL/6 mice . EC were identified by co-staining with anti-CD31 antibodies conjugated to FITC (green). Cell nuclei were identified using TOPRO (blue). Representative images are shown from five independent experiments. scale bar 10 μ m. Proliferating cells were quantified as %positive for ki67 and number of cells per field of view was quantified. * $p < 0.05$, using a paired t-test.

To further validate the deletion of TWIST1 and GATA4 from EC, *en face* immunofluorescent staining was carried out in aortic tissue from these mice. This revealed that the expression of TWIST1 and GATA4 was absent in EC in KO animals compared to floxed controls (Figure 48 A, B).

Ki67-immunostaining in EC located at low WSS sites showed that cell proliferation was significantly reduced in *SCL-Cre-ER^T; Gata4^{KO}* and *Tie2-Twist1^{KO}* animals compared to floxed controls (Figure 49). These observations reflected that TWIST1 and GATA4 control cell proliferation at low WSS sites, and thus contributing to focal EC dysfunction at atheroprone sites.

I validated the *in vitro* observation of the regulation of TWIST1 by GATA4 in EC exposed to low WSS. TWIST1 expression was assessed by *en face* immunostaining in *SCL-Cre-ER^T; Gata4^{KO}* aortic arch tissue, at regions of low (inner curvature) and high (outer curvature) WSS. TWIST1 expression in EC at low WSS sites was reduced in *SCL-Cre-ER^T; Gata4^{KO}* compared to the floxed control (Figure 50). These data suggest that TWIST1 expression in EC is mediated by GATA4 at low WSS *in vivo*.

I then assessed SNAIL and N-cadherin (markers of EndMT) expression in *Tie2-Twist1^{KO}* animals. SNAIL and junctional N-cadherin expression were both significantly reduced in *Tie2-Twist1^{KO}* animals compared to floxed controls (Figure 51), thus suggesting that TWIST1 controls partial EndMT at low WSS sites *in vivo*. Overall, these studies demonstrate that GATA4 is a positive regulator of TWIST1 and that TWIST1 induces partial EndMT associated with increased EC proliferation.

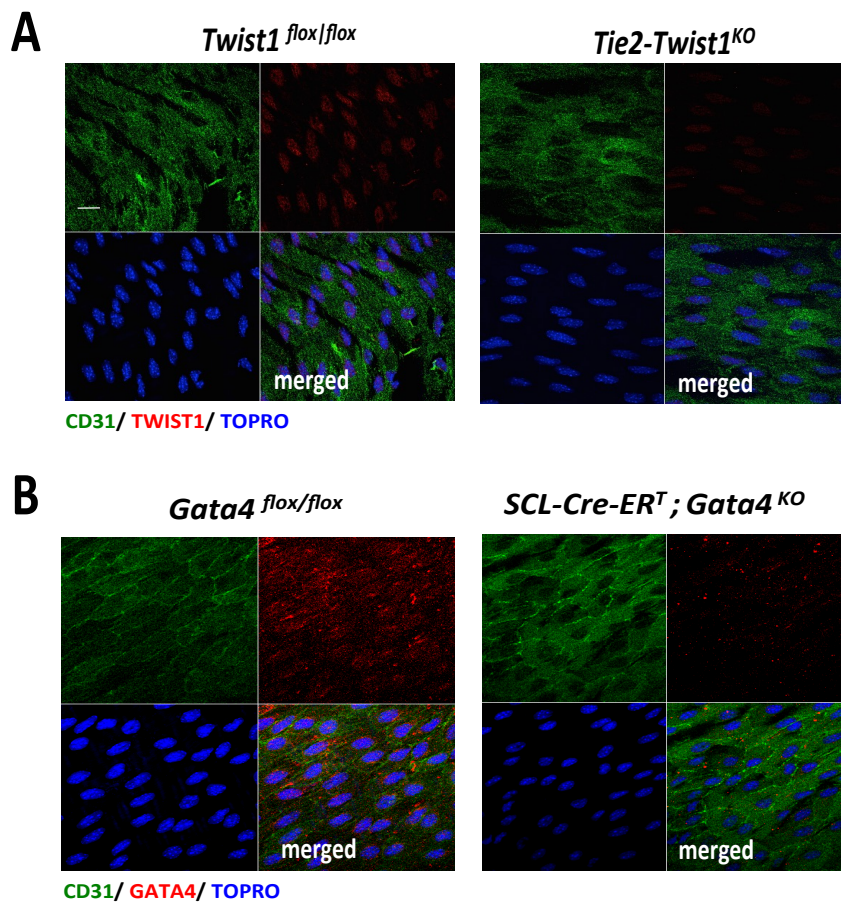


Figure 48. Validation of endothelial gene deletion of Twist1 and Gata4. **A)** Expression levels of TWIST1 (red) was assessed in either *Tie2-Twist1*^{KO} or *Twist1*^{fl/fl} mice by en face staining. EC were identified by co-staining with anti-CD31 antibodies conjugated to FITC (green). Cell nuclei were identified using TOPRO (blue). Representative images are shown from five independent experiments. **B)** Expression levels of GATA4 (red) was assessed in either *SCL-Cre-ER^T; Gata4*^{KO} or in *Gata4*^{fl/fl}. EC were identified by co-staining with anti-CD31 antibodies conjugated to FITC (green). Cell nuclei were identified using TOPRO (blue). Representative images are shown from five independent experiments. Scale bar,10um.

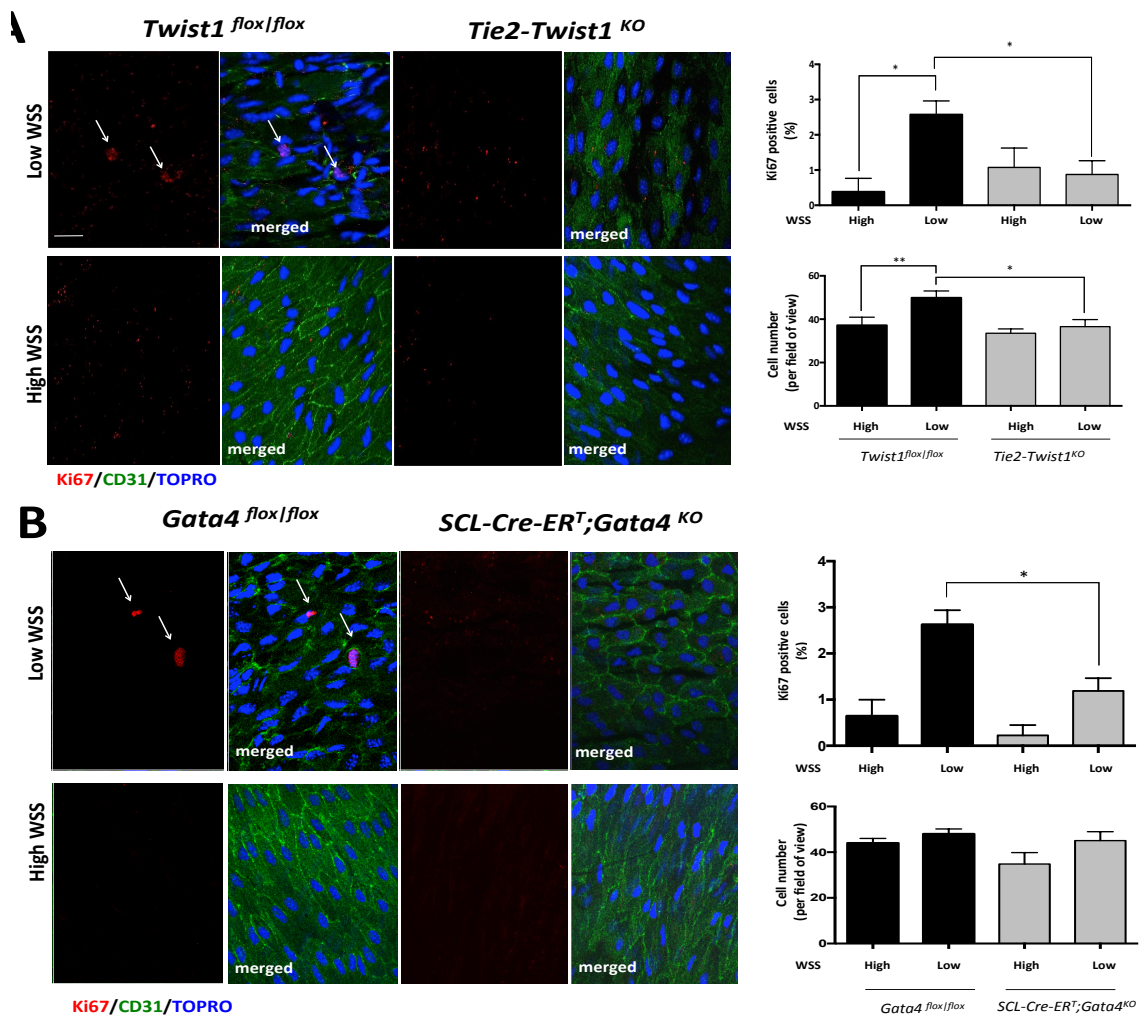


Figure 49. TWIST1 and GATA4 promoted EC proliferation at low WSS sites in the murine aorta. Expression levels of proliferation marker Ki67 (green) in EC were assessed by *en face* staining in A) *Tie2-Twist1*^{KO} or *Twist1*^{fl/fl} mice and in B) *SCL-Cre-ERT*; *Gata4*^{KO} or in *Gata4*^{fl/fl} mice. EC were identified by co-staining with anti-CD31 antibodies conjugated to FITC (green). Cell nuclei were identified using TOPRO (blue). Representative images are shown from 5 independent experiments. Scale bar 10 μ m. Proliferating cells were quantified as %positive for ki67 and number of cells per field of view was quantified. * $p < 0.05$, ** $p < 0.01$, using a two-way ANOVA.

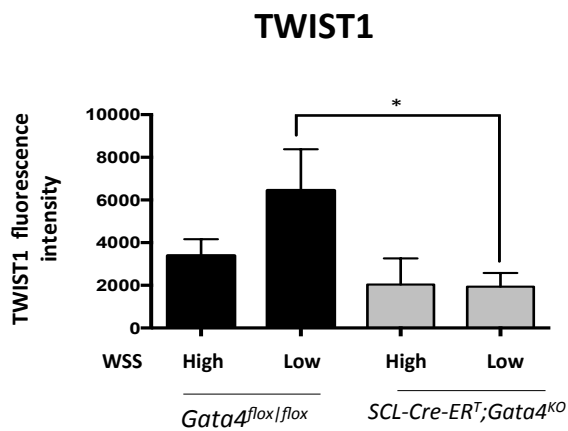
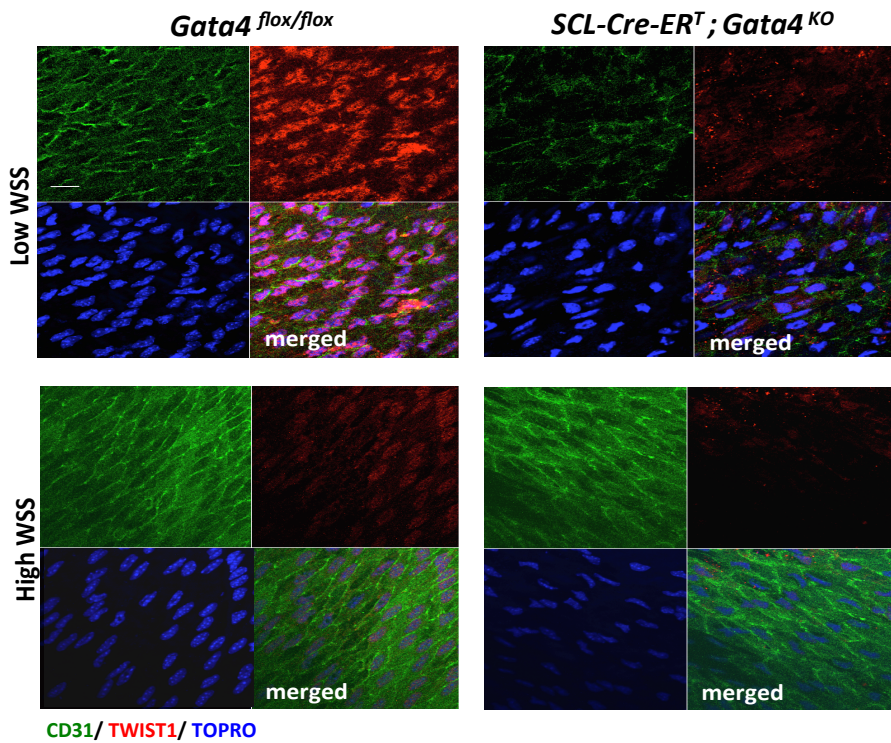


Figure 50. GATA4 regulated TWIST1 expression at low WSS sites in the murine aorta.

Expression levels of TWIST1 (red) was assessed in either *SCL-Cre-ERT; Gata4^{KO}* or in *Gata4^{flox/flox}* by *en face* staining. EC were identified by co-staining with anti-CD31 antibodies conjugated to FITC (green). Cell nuclei were identified using TOPRO (blue). Representative images are shown from 4 independent experiments. TWIST1 expression was quantified by measuring fluorescent intensity of the cells per field of view using Image J.

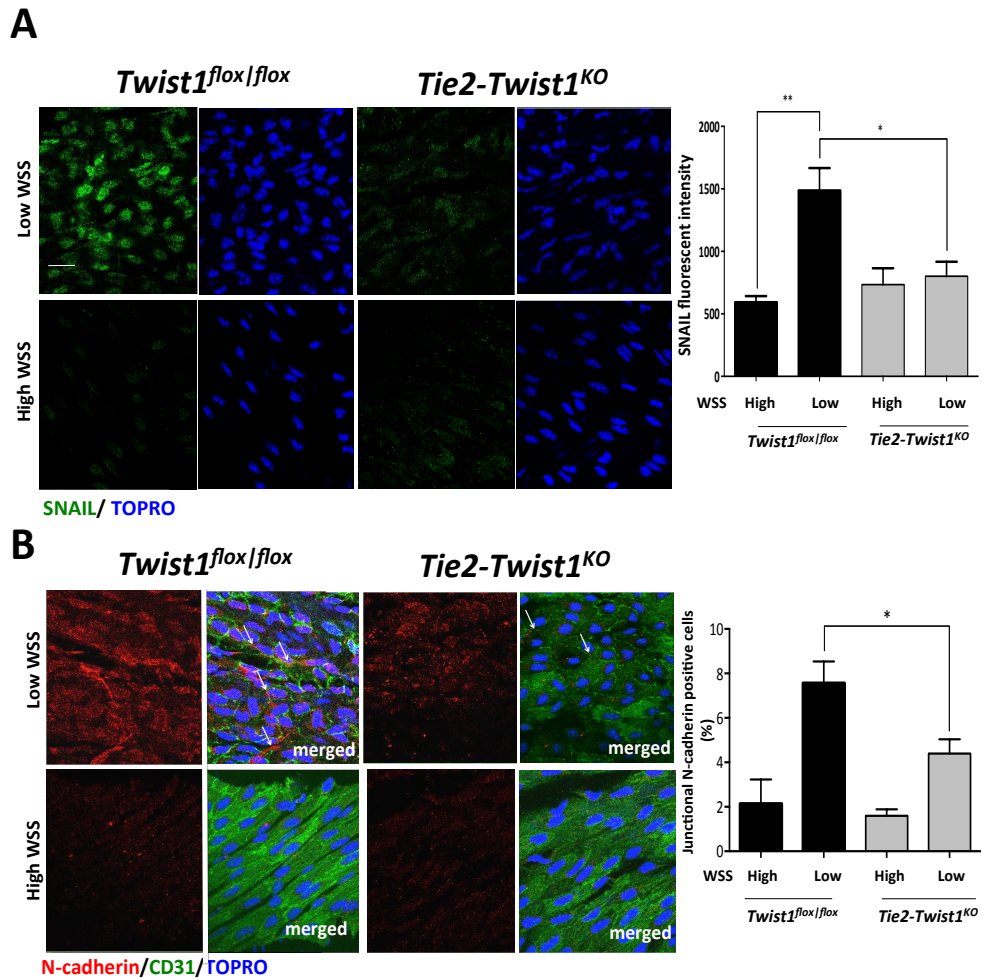


Figure 51. Twist1 promoted SNAIL and N-cadherin expression at low WSS sites in the murine aorta. Expression levels of A) SNAIL (green) or B) N-cadherin (red) was assessed in either Tie2-Twist1^{KO} or Twist1^{fl/fl} mice by en face staining. EC were identified by co-staining with anti-CD31 antibodies conjugated to FITC (green). Cell nuclei were identified using TOPRO (blue). Representative images are shown from 4-5 independent experiments. Scale bar, 10um. Data were quantified as either fluorescence intensity or %positive cells expressing junctional N cadherin as indicated by overlap with CD31 (arrows). * p<0.05, **p<0.01, using a paired t-test.

5.8 TWIST1 expression in endothelial cells is increased with atherosclerosis severity in human and murine vessels

As GATA4-mediated TWIST1 expression was enhanced by low WSS flow conditions *in vitro* and *in vivo*, this suggested that TWIST1 maybe involved in atherosclerosis development. TWIST1 expression was assessed by immunohistochemistry in human coronary artery tissue from ischemic heart disease patients (severe atherosclerotic phenotype) and from idiopathic cardiomyopathy patients (mild atherosclerotic phenotype). TWIST1 was expressed in EC overlaying plaques. Notably, there was a significant increase in TWIST1 positive luminal EC expression (identified by Von Willebrand factor (vWF) staining) in tissue from ischemic heart disease compared to cardiomyopathy patients (Figure 52). Thus, TWIST1 expression correlated with atherosclerosis severity. However, the WSS conditions that EC were exposed to in the coronary vessels were not characterised, thus it was difficult to correlate TWIST1 expression with WSS at the atherosclerotic plaques. To overcome this, atherogenic murine models were generated by treating LDLR^{-/-} transgenic animals with a high fat diet for 6 weeks to promote atherosclerosis. As a control, LDLR^{-/-} animals were given a normal chow diet. TWIST1 expression was assessed in the aortic arch at regions of low WSS (inner curvature) and high WSS (outer curvature) in atherogenic and control animals. TWIST1 expression at the low WSS site was enhanced in atherogenic animals compared to the controls, whereas there was no significant change in the high WSS site (Figure 53). This observation suggested that TWIST1 expression is enhanced in response to hyper-cholesterolemia. However the study is preliminary (contained N=2 experiments) and requires further confirmation. Future work will involve assessing GATA4 and SNAIL expression in human and murine atheroplaques.

In summary these findings reveal for the first time that TWIST1, GATA4 and SNAIL are enhanced in cells at low WSS *in vivo* and that they have functional significance. I show that GATA4-mediated TWIST1 mechanotransduction regulates low WSS-mediated SNAIL and N-cadherin expression and that transcription factors control cell proliferation in these cells, thus indicating that TWIST1 and GATA4 mediate focal EC dysfunction at atheroprone sites (Figure 54).

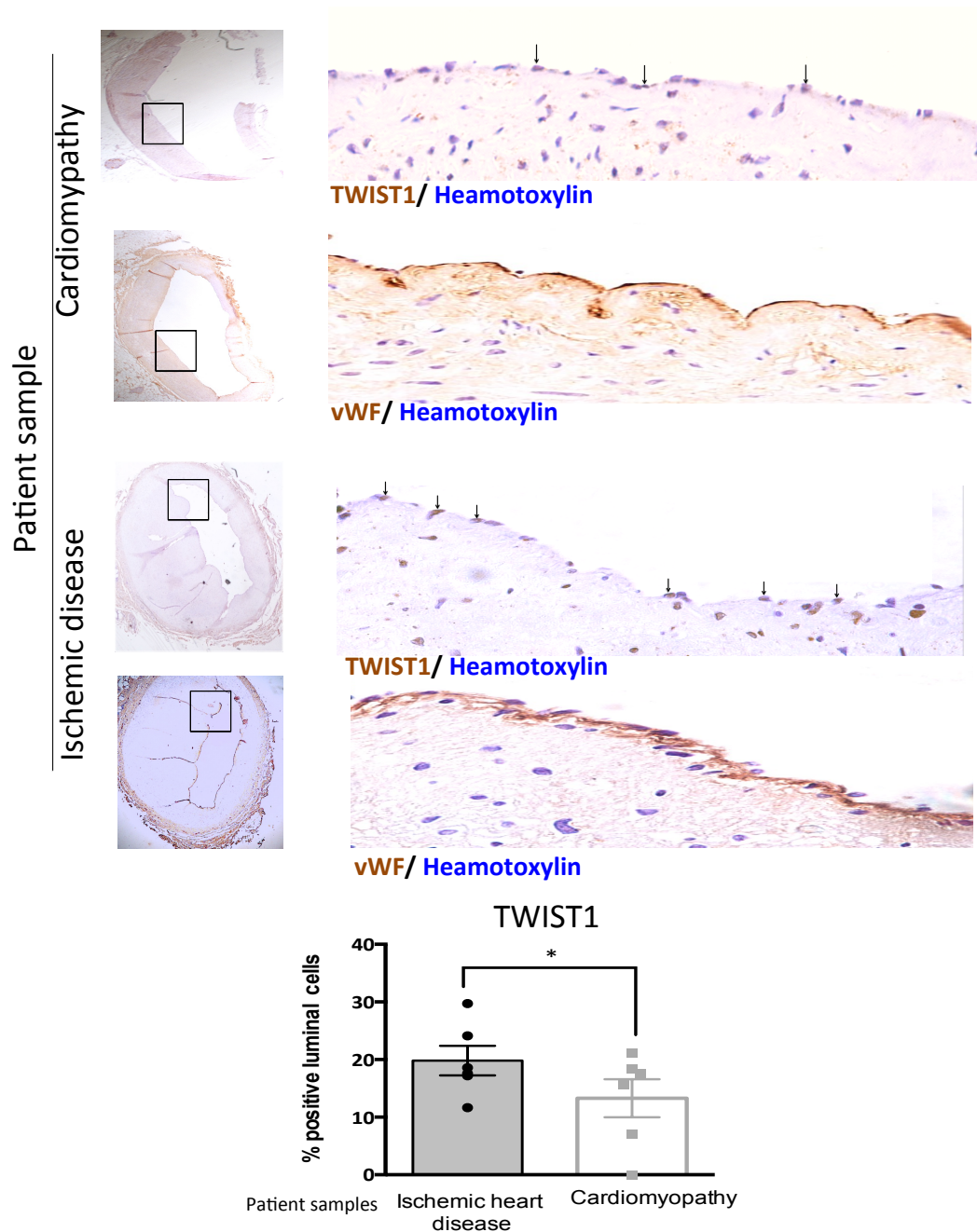


Figure 52. TWIST1 expression was increased with atheroseverity in human coronary arteries. Twist1 expression was assessed in coronary artery tissue, donated from anonymous ischemic heart disease and idiopathic cardiomyopathy patients with ethical consent. Immunohistochemistry staining was done on these tissue samples using anti-TWIST1 and vWF (to label luminal endothelial cells) specific antibodies (brown) and the nuclei were counterstained using haematoxylin (blue). Representative images are shown. The data was quantified by calculating % positive luminal Twist1 expression. Data were pooled from 6 independent experiments and mean values \pm SEM are shown. * $p < 0.05$, using a paired t-test.

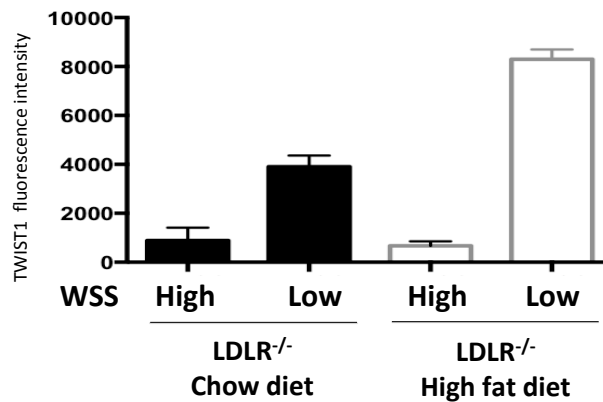
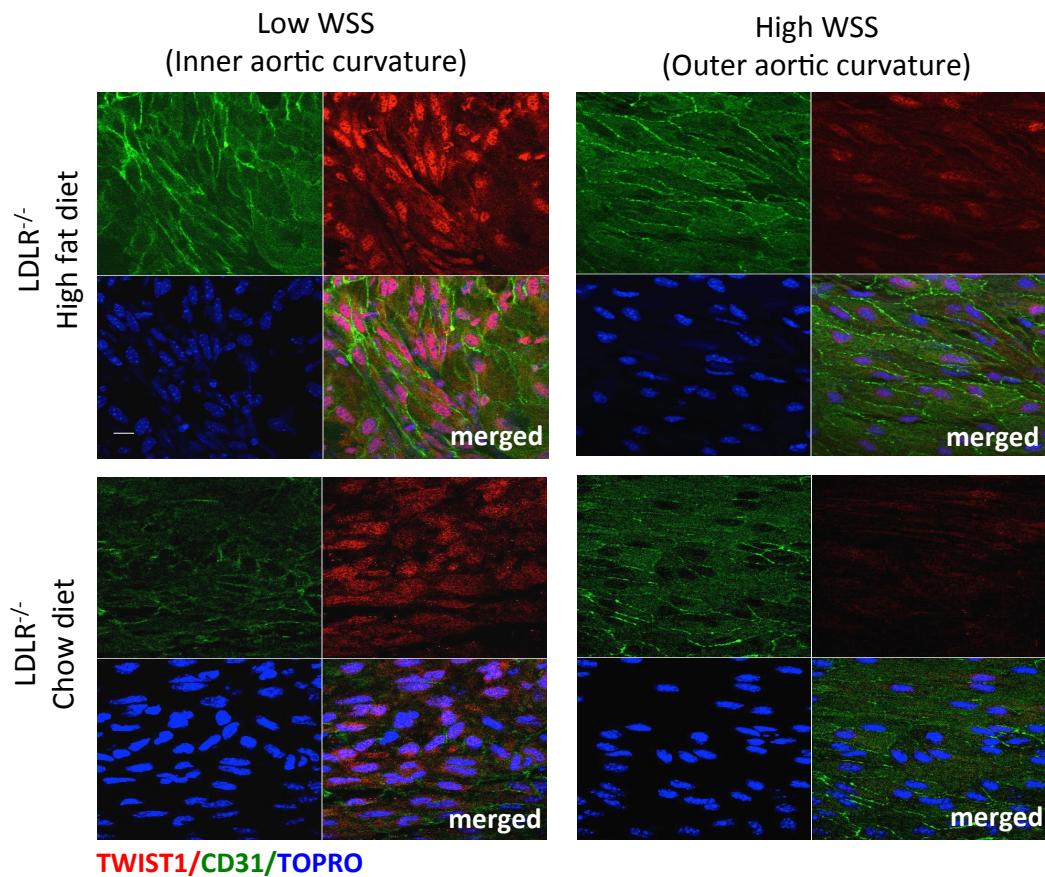


Figure 53. TWIST1 expression was increased at low WSS sites in response to hypercholesterolemia. LDLR^{-/-} animals were treated with a high fat diet or LDLR^{-/-} animals treated with a normal chow diet EC at low WSS (susceptible; inner curvature) or high WSS (protected; outer curvature) regions of the aorta in were studied by *en face* staining using an anti-TWIST1 antibody (red). EC were identified by co-staining with anti- CD31 antibodies conjugated to FITC (green). Cell nuclei were identified using TOPRO (blue). Representative images are shown. Twist1 expression was quantified by measuring fluorescent intensity of the cells per field of view using Image J. (N=2/group)

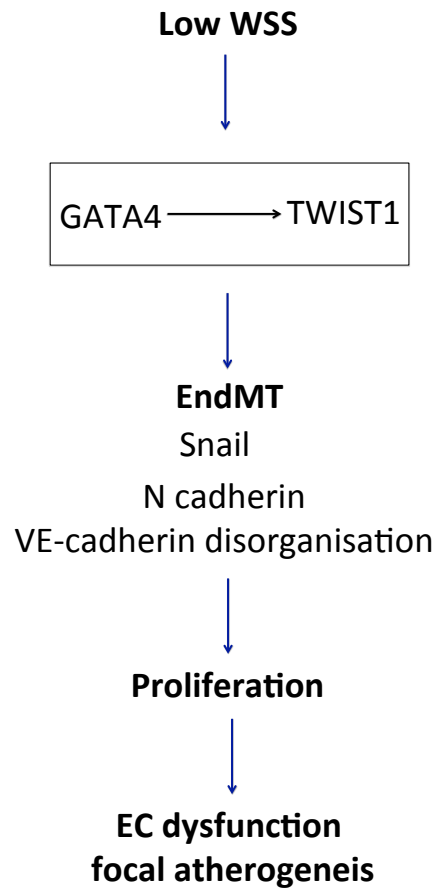


Figure 54. Model for the function of TWIST1 and GATA4 in EC at low WSS sites. Low WSS promoted Twist1 expression via GATA4. GATA4-Twist1 signalling promotes partial EndMT via the induction of SNAIL and N-cadherin at sites of low WSS. GATA4-TWIST1 signalling also promotes EC proliferation, which influences EC dysfunction and potentially affecting focal atherogenesis.

5.9 Conclusions

1. TWIST1, GATA4 and SNAIL expression was enhanced in EC at regions of low WSS compared to regions of high WSS in the murine aorta
2. Using a flow-altering cast it was demonstrated that TWIST1, GATA4 and SNAIL expression was driven by low WSS in adult EC.
3. TWIST1 controls low WSS-mediated partial EndMT at sites of low WSS in the murine aorta by regulating N-cadherin and SNAIL expression.
4. TWIST1 and GATA4 drive low WSS-mediated EC proliferation at atheroprone sites in the murine aorta, suggesting that they contribute to focal EC dysfunction.
5. TWIST1 expression correlated with athero-severity in human coronary tissue and was enhanced in response to hyper-cholesterolemia at low WSS in the murine aorta.

5.10 Discussion

Atherosclerosis is a focal disease that is driven by EC dysfunction involving enhanced EC proliferation and permeability that preferentially occurs at sites of low WSS. However the molecular mechanisms that govern focal EC behaviour and dysfunction are not fully known. In this chapter I have demonstrated that a novel mechanism for low WSS-mediated atherogenesis could be via GATA4- TWIST1 signalling, the observations made in this chapter will now be discussed.

5.10.1 The expression of TWIST1, GATA4 and SNAIL is driven by atherogenic, low WSS *in vivo*

I have shown that the expression of TWIST1, GATA4 and SNAIL was enhanced in EC at atheroprone, disturbed flow (low, oscillatory WSS) sites compared to atheroprotected non-disturbed flow (high WSS) sites, which proposed a correlation between the expression of these genes by low, oscillatory WSS *in vivo*. Moreover, I have shown that the induction of TWIST1 in cells at low, oscillatory WSS sites occurs via GATA4. Thus, GATA4 promoted Twist1 expression in EC exposed to low WSS *in vitro* and in *in vivo*.



To establish a causal link between the induction of GATA4-Twist1 and Snail by low WSS *in vivo* I directly altered flow in the murine carotid using a flow-altering cuff. This revealed that the expression of TWIST1, GATA4 and SNAIL was enhanced at the low WSS site (upstream of cuff) compared to the high WSS site (stenosis). However, whilst GATA4 and SNAIL expression was enhanced at the low, oscillatory WSS site (downstream of cuff) TWIST1 expression was reduced. Several conclusions can be made from this observations; 1) In the inner aortic arch, a region of endogenous low and oscillatory WSS (disturbed flow) where the expression of all three genes was enhanced, differs in flow magnitude and direction of flow and pulsatility to the downstream region of the cuff. Therefore, it is difficult to make accurate comparisons between the expression in the downstream from the cuff and the inner curvature as different flow patterns will activate different mechanosensors that could in turn influence TWIST1 and GATA4 expression. The data demonstrated that

flow magnitude (low WSS) is the primary mechano-stimulus that is promoting the expression of all three genes *in vivo*. 2) The activation of GATA4-TWIST1-SNAIL network that I observed in the inner aortic arch, did not translate into the expression of these genes in the cuff-inserted vessel as the expression of GATA4 and SNAIL was enhanced without TWIST1. These observations at the downstream region of the cuff, suggest that TWIST1 expression under cuff-induced low/oscillatory WSS is inhibited by unknown mechanisms, potentially one of these mechanisms could be mediated by GATA4. An increase in GATA4 expression beyond a certain threshold could promote the activation of a TWIST1 inhibitor, or it could be that the specific flow pattern in the downstream region of the cuff activates a GATA4-independent pathway that inhibits TWIST1. In addition, it is important to note that in addition to differences in WSS directionality, the WSS magnitude at the region downstream of the cuff (14 dyne/cm²) is different to that in the upstream region of the cast (10 dyne/cm²) where all three genes are activated. Taken together, this observation revealed that the interaction of all three genes is sensitive to changes in flow magnitude and directionality and suggests that a potential upstream mechanosensor(s) is responsible for the activation of GATA4- TWIST1-SNAIL axis under specific WSS conditions.

A combination of *in vitro* and *in vivo* techniques have provided a close insight into the mechanical activation of these transcription factors in EC (summarised in table 10). *In vitro* observations using the orbital plate and Ibidi™ parallel plate systems have revealed that flow magnitude- low WSS is the dominant driving force in the activation of TWIST1 and GATA4. Consistent with this, *in vivo* observations in the aortic arch (regions of low and high WSS) and the flow-constrictive cuff have also revealed that low WSS is also a more dominant factor in activating GATA4 and TWIST1. It would be interesting to investigate which flow-specific mechanosensor(s) are driving the expression of these genes in response to low WSS in order to further characterize the nature of their mechanotransduction.

Table 10 . Summary of WSS-modulation of TWIST1 and GATA4 using *in vitro* and *in vivo* systems

		<i>In vitro</i> systems					<i>In vivo</i> systems				
		Orbital plate		Ibidi™			Aortic arch		Constrictive cuff		
WSS (dyne/cm ²)		High 13	Low, oscillatory 4.8	High 13	Low 4	Low, oscillatory 4	High 15- porcine 60-250- mouse	Low, oscillatory 5-porcine 5-20- mouse	High 25	Low 10	Low, oscillatory 14
Genes	Twist1	↓	↑	↓	↑	-	↓	↑	↓	↑	-
	Gata4	↓	↑	↓	↑	-	↓	↑	↓	↑	↑

 Increased expression
 Decreased expression
 - No significant difference

Consistent with previous studies, the expression of GATA4 at atheroprone, low WSS sites has been previously reported by large-scale microarray studies (Passerini et al. 2004; Björck et al. 2012) and the expression of the snail-related EndMT regulator Slug has recently been detected at atheroprone sites in the murine aorta (Sanchez-Duffhues et al. 2015) thus supporting the activation of these genes at atheroprone, low WSS sites *in vivo*. I reveal for the first time that TWIST1 expression is enhanced at atheroprone sites. Consistent with this, TWIST1 and GATA4 expression has been shown to be prominent in EC in the heart valves and in during valve development this process is WSS-dependent and EC in the adult heart valves are mechano-sensitive (Heckel et al. 2015). Thus, suggesting that WSS has been indirectly linked with the activation of GATA4 and TWIST1 *in vivo*.

5.10.2 TWIST1 expression is detected in adult EC

It can be argued that low WSS promotes the homing of progenitor cells from the bone marrow into atheroprone sites and these cells could be expressing mesenchymal, embryonic genes including TWIST1 (Foteinos et al. 2008). Thus to test the hypothesis that TWIST1 expression at low WSS sites occurs in adult EC, I used *SCL-Cre-ER^T; R26R-Td tomato* cell tracking system to label adult EC. The cuff was inserted following Cre-activation in order to assess low WSS-mediated increase in Twist1 expression in a vessel where basal TWIST1 expression is low. Therefore inducing the labelling of the cells via an endothelial specific promoter, coupled to the creation of low WSS flow condition in the carotid artery provided a study design to clearly conclude the effects of low WSS on the expression of TWIST1 in adult EC. Of note, any progenitor cells homing into the low WSS site in modified carotid arteries would remain negative despite activation of the SCL promoter because tamoxifen administration was transient and preceded cuff placement. The results reflected that all TWIST1 positive cells regions in the cuff-mediated low WSS regions were R26R-Td

tomato positive, thus confirming that adult EC express TWIST1 at low WSS sites *in vivo*. Future work will include assessing the expression of GATA4 and SNAIL in cuff-inserted *SCL-Cre-ER^T; R26R-Td tomato* animals.

The use of the *SCL-Cre-ER^T; R26R-Td tomato* cell tracking system is established to determine EC involvement and to eliminate EPC contribution (Göthert et al., 2004, 2005). However, to provide evidence for the complete lack of EPC involvement, *en face* imaging of EPC cells in the same animals where cuff insertion and TWIST1 expression analysis was assessed should be used to determine the absence of the Td-tomato protein, to further strengthen the conclusion that TWIST1 expression at low WSS occurs in adult EC.

5.10.3 Potential mechanisms for the activation of TWIST1 and GATA4 by low WSS *in vivo*.

Signalling pathways including p38 MAPK, NF- κ B and TGF- β signalling via BMP4 have all been shown to be preferentially activated at sites of low WSS *in vivo* (Kim et al. 2012; Jo et al. 2006; Chaudhury et al., 2010; Zakkar et al. 2011). In addition, these signalling pathways are linked with EC dysfunction and atherogenesis. Twist1 and GATA4 are downstream targets of p38 MAPK, NF- κ B and TGF signalling in range of cell types, including cardiac cells, cancer cells, and valve EC (Daoud et al. 2014; Rojas et al., 2009; Gaspar-Pereira et al. 2012; Tenhunen et al. 2004; Hong et al. 2011). Thus it could be that these signalling pathways are driving TWIST1 and GATA4 expression in EC at sites of low WSS *in vivo*. Moreover mechanosensors such as cilia, which are present at low WSS and absent from high WSS sites *in vivo* (Van der Heiden et al. 2004), could also be a potential mechanism for the activation of GATA4- TWIST1 signalling in EC at low WSS sites. The primary cilium has been linked with the regulation of canonical (via β -catenin) WNT signalling (Lancaster et al. 2011). Since WNT signalling is an activator of TWIST1 and GATA4, it could be that cilia are controlling GATA4- TWIST1 activation via β -catenin (Lamouille et al. 2014; Lin & Xu 2008).

TWIST1 and GATA4 DNA binding activity is enhanced by interacting with binding partners such as FOG2, MEF2C, TBX5 for GATA4 and E47 and ID1 for TWIST1 (Reviewed in Schlesinger et al. 2011; Ghouzzi et al. 1997). Interestingly, TWIST1 and GATA4 interact with a common binding partner HAND2 (Dai et al. 2002; Firulli et al. 2005; McFadden et al. 2000). A microarray study by Bjork *et al.* identified HAND2 as a major mechano-responsive transcription factor, which showed a marked increase in expression in EC exposed to low WSS in the rat aortic arch (Björck et al. 2012). Therefore, HAND2 could be involved in stabilising and increasing GATA4 and TWIST1 activity in EC exposed to low WSS.

5.10.4 Low WSS promoted partial EndMT

I have delineated between the effect of low WSS on the activation partial or full EndMT as evidenced by the following observations; 1) Snail expression was enhanced at the low WSS sites, 2) Low WSS promoted a cadherin switch by enhancing the expression of junctional N-cadherin and promoting VE-cadherin disorganisation, 3) The expression of EC-markers VE-cadherin and CD31 was not reduced at the low WSS sites compared to the high WSS sites. 4) Low WSS does not promote cellular delamination, which EndMT cells undergo by separating from the endothelial monolayer and invading and migrating into the underlying cell layers. These observations suggest that low WSS promotes some EndMT-like processes, but does not give rise to the full transition of EC into a mesenchymal state. Consistent with this, a study by Sanchez-Duffhues *et al.* has correlated low WSS regulation of EndMT *in vivo*, demonstrating that enhanced Slug expression occurs in EC at atheroprone, low WSS sites in the murine aorta of LDLR^{-/-} animals (Sanchez-Duffhues et al. 2015). Consistent with this, a recent study by Chen *et al.* identified a significant increase in TGF- β signalling (EndMT-promoting) and reduction in FGF signalling (EndMT-inhibiting) in EC exposed to low WSS in atherogenic mice (ApoE^{-/-}, given a high fat diet), whilst not detecting a significant difference in control mice (ApoE^{-/-}, given a normal chow diet) (Chen et al. 2015). This suggests that low WSS alone did not directly induce EndMT in EC at low WSS sites. A more direct link between low WSS and EndMT *in vivo* has been recently provided using the thoracic aortic constriction method, Moonen *et al.* have shown that downstream of the constriction

where flow exerts low WSS there was an increase in the expression of EndMT-linked proteins such as α -SMA and Transgelin (Moonen et al. 2015). However these studies do not provide evidence for loss of EC-marker expression at low WSS sites *in vivo*. Thus my studies are the first to suggest that the proposed transition into EndMT was partial.

5.10.5 Potential mechanism for the induction of partial EndMT in EC exposed to low WSS

Previous studies demonstrated that TWIST1 regulated partial EMT in tubular epithelial cells during kidney fibrosis (Lovisa et al. 2015). In addition, epithelial cells isolated from TWIST1 gain of function mice, showed that Twist1 expression was sufficient to drive multiple EndMT-like changes including migration and invasion, without the loss of E-cadherin, suggesting that TWIST1 promoted partial EMT in these cells (Shamir et al. 2014). GATA4 is indirectly linked with the induction of partial EMT as suggested by the following; GATA4 is a critical regulator of myocardial infarction responses in cells of the epicardium (Heineke, Auger-messier, et al. 2007; Inagawa et al. 2012) and these cells undergo partial EMT following MI (Limana et al. 2007). Therefore, these studies provide supportive evidence for the induction of a partial mesenchymal state in cells via TWIST1 and GATA4.

Previous studies have shown that TWIST1 and GATA4 regulate EndMT in valve EC during development (Zeisberg et al. 2005; Mcfadden et al. 2005; Grande et al. 2015; Vrljicak et al. 2012). In addition, the induction of EndMT in valve EC is triggered by low WSS conditions (Mahler et al. 2014; Heckel et al. 2015). Thus previous studies correlated WSS with EndMT and TWIST1/GATA4 expression, but did not show causality. However, I show for the first time the direct involvement of GATA4-TWIST1 signalling in the induction of EndMT in EC exposed to low WSS in the murine vasculature.

There could be other mechanisms that are driving EndMT in EC exposed to low WSS, either alongside or independently of Twist1 and GATA4. TGF- β and BMP signalling through Smad 1/5/8 and Smad 2/3 and 4 proteins is well established in triggering

EndMT (Cooley et al. 2014; Maddaluno et al. 2013; Chen et al. 2015; Medici et al. 2011). In fact, both TGF- β and BMP factors have been shown to co-operatively mediate EndMT through ALK2 and ALK5 receptors (Medici et al., 2010). GATA4 regulates EndMT in valve cells via interacting with Smad 4 (Moskowitz et al., 2011), suggesting that GATA4- TWIST1 signalling could be mediating EndMT via TGF- β signalling. Moreover, GATA4 expression is driven by BMP4 during embryonic development (Daoud et al. 2014) whilst TWIST1 is required for BMP4 expression (O'Rourke et al. 2002). The expression of BMP4 is enhanced at low WSS sites *in vivo* (Kim et al. 2013; Jo et al. 2006; Sorescu et al. 2004). Therefore, GATA4- TWIST1 signalling could be interacting with BMP4 in promoting EndMT in cells exposed to low WSS. Chen et al., demonstrated that low WSS promotes EndMT by inhibiting FGF signalling, whilst increasing TGF- β signalling (Chen et al. 2015). Interestingly, TWIST1 controls the balance between FGF and TGF- β signalling during EMT regulation in gastrulation. Thus TWIST1 could be acting as a molecular switch, upstream of FGF and TGF- β signalling in EC exposed to low WSS.

Another potential mechanism could be via p38 MAPK signalling, which is preferentially activated at low WSS sites (Chaudhury et al. 2010). p38 signalling is required for TGF- β 2-mediated EndMT (Medici et al. 2011). As mentioned previously, Twist1 and GATA4 have been linked with p38 signalling, suggesting that they could be mediating EndMT via p38. Notch and WNT signalling have both been shown to regulate EndMT (Maddaluno et al. 2013; Aisagbonhi et al. 2011; Cheng et al. 2013), and both of these pathways have been shown to be WSS-sensitive (Watson et al. 2013; Rotherham & El Haj 2015). Thus WNT and Notch signalling could be involved in the regulation of low-WSS mediated EndMT.

Egorova et al., have shown that the absence of cilia triggers EndMT through the absence of KLF4. The overexpression of KLF4 in non-ciliated cells inhibited EndMT marker expression, thus suggesting that KLF4 is a negative regulator of EndMT (Egorova et al. 2011). Interestingly, KLF4 is a gene that is inhibited by low WSS and is preferentially activated in EC exposed to protective, high WSS (Fang et al. 2010; Jiang et al. 2015). It would be of interest to assess if low WSS promotes TWIST1 and

GATA4-mediated inhibition of KLF4 expression, thus enabling the EndMT process. Alternatively, whether KLF4 inhibits TWIST1 and GATA4 signalling, subsequently preventing EndMT.

5.10.6 Partial EndMT vs. Full EndMT

The notion of partial EndMT and partial EMT has recently been adopted (Grande et al. 2015; Lovisa et al. 2015; Welch-Reardon et al. 2014). It is defined by cells lacking one of the established features of EndMT/EMT, this often involves retaining cell adhesion proteins such as VE and E-cadherin. Instead of cells separating and migrating individually as seen in full EndMT, in partial EndMT the cell monolayer migrates as one sheet. (Reviewed in Welch-Reardon et al. 2014). For example, sprouting angiogenesis is a well-established example of a process that involves partial EndMT. During angiogenesis, migratory, sprouting cells express mesenchymal genes such as Snail and Slug, whilst maintaining cell-cell contacts (Reviewed in Welch-Reardon et al., 2014).

Whilst *in vitro* studies provide evidence for the loss of EC markers and the expression of mesenchymal markers in cells undergoing EndMT (Moonen et al. 2015; Egorova et al. 2011; Sanchez-Duffhues et al. 2015), *in vivo* studies fail to provide evidence for a loss or a reduction in EC or epithelial markers in EndMT or EMT. The Dejana lab provided evidence for the involvement of EndMT in cerebral cavernous malformations (CCM), as evidenced by the expression of several mesenchymal markers such as N-cadherin, Snail, Slug and α -SMA in EC from CCM lesions (Maddaluno et al. 2013). The study showed that the expression of these mesenchymal markers correlated with disorganised junctional VE-cadherin, but did not show a loss in either VE-cadherin or CD31 expression (Maddaluno et al. 2013). Similarly, studies showing the role of EndMT in renal fibrosis by Xavier *et al* or in pulmonary arterial hypertension (PAH) by Ranchoux *et al*. have shown that EC in murine and human tissue express mesenchymal markers α -SMA and vimentin, without a loss in VE-cadherin and CD31 (Xavier et al. 2015; Ranchoux et al. 2015). In addition, a recent study by Chen et al demonstrated that EndMT-promoting TGF- β

signalling was enhanced in EC at low WSS sites in atherogenic mice (ApoE^{-/-} given a high fat diet), without showing a reduction in EC marker expression. This suggests that the process identified in the described studies was partial EndMT, therefore providing similar conclusions to my observation of the induction of partial EndMT by cells exposed to low WSS.

Recently, a number of studies have shown that partial EndMT is involved in renal fibrosis. These studies clearly stated that the cells' mesenchymal transformation was partial, since these cells did not show a reduction in epithelial cell markers whilst expressing mesenchymal ones (Lovisa et al. 2015; Grande et al. 2015). One of these studies, by the Kalluri group suggests that the transition of cells into a full mesenchymal state whilst occurring during development, would rarely occur in the adult (Lovisa et al. 2015). Ubil et al reported that EndMT is reversible, via a process termed mesenchymal-endothelial transition (MEndT) in fibroblasts following cardiac injury (Ubil et al. 2014). This study provides an example of the wide spectrum of cell plasticity. The process of EC plasticity is complex and is very context dependent, thus, in my opinion; it is not accurate to restrict EC plasticity under one definition. Rather than EC strictly either undergoing EndMT or not, partial EndMT could be one example of cell plasticity across a wide spectrum, which is controlled by the context to which EC are exposed to.

The switch between the transition into full or partial EndMT could heavily depend on the presence of a specific activating stimulus. Such stimulus could therefore control the magnitude of EndMT-promoting pathways, thus controlling the magnitude of EndMT. It seems that the activation of EndMT in adult EC, in the disease context may be via a common stimulus. Fibrotic diseases, including atherosclerosis and cancer all have a common link of EC stress and injury (Civelek et al. 2009; Lovisa et al. 2015; Klaunig et al. 2010). Thus, it could be that partial EndMT is activated to provide an adaptive role in response to an injury stimulus. Evolutionarily, it is more efficient to re-activate ancient pathways in a situation that requires extensive changes in cellular behavior (proliferation and migration) such as in the response to injury. Thus, it can be argued partial EndMT in the adult has evolved to facilitate such changes

efficiently. The potential adaptive significance of TWIST1 and GATA4-mediated regulation of partial EndMT in response to low WSS will be discussed in detail in the next chapter

5.10.7 Regulation of EC proliferation by GATA4 and TWIST1, is it detrimental or protective?

Low-WSS-mediated increases in EC proliferation is a key process in vascular dysfunction and atherosusceptibility (Obikane et al. 2007; Amini et al. 2014; Chaudhury et al. 2010; Warboys et al. 2014). I have shown that TWIST1 and GATA4 drive EC proliferation at sites of low WSS. This suggested that TWIST1 and GATA4 potentially regulate EC dysfunction at these sites. This conclusion was further strengthened by the following observations; 1) VE-cadherin junctional widths were increased at the low WSS sites, suggesting an enhancement of cell permeability, 2) TWIST1 and GATA4 induction by low WSS *in vitro* promoted cell permeability. Since cell permeability is another feature of EC dysfunction, this further supports the conclusion that TWIST1 and GATA4 promote EC dysfunction at sites of low WSS through the induction of proliferation.

However, cell proliferation at low WSS may be atheroprotective. It was proposed by Schober *et al.*, that proliferation at low WSS provides a protective function by serving as a repair mechanism in response to injury (Schober et al. 2014). It has been shown that both Twist1 and GATA4 play a significant role in wound healing and fibrosis following injury (Gupta et al. 2013; Heineke, Auger-messier, et al. 2007; Mammoto et al. 2013; Lovisa et al. 2015). Similarly, EndMT is known to be activated following an injury stimulus, such as in ischaemic/reperfusion injury (Curci et al., 2014). It has been shown by Lovisa *et al.*, that in response to renal injury, Twist1 and Snail are involved in the regulation of cell proliferation as a consequence of partial EMT leading to kidney fibrosis (Lovisa et al. 2015). Therefore, the activation GATA4-TWIST1-SNAIL signalling in EC at low WSS sites and subsequent proliferation could be a repair response to low WSS, potentially at the consequence of EC dysfunction and atherogenesis.

To fully determine the significance of the role of TWIST1 and GATA4 in promoting cell proliferation at sites of low WSS, conditional-EC knock out animals should be crossed with atherogenic mice followed by the assessment of lesion formation and composition in future studies.

5.10.8 Mechanism for the role of TWIST1 and GATA4 in EC proliferation at sites of low WSS.

One mechanism for the regulation of EC proliferation at low WSS sites could be via SNAIL-mediated EndMT, since GATA4-TWIST1 regulated SNAIL expression *in vivo* and that SNAIL promoted proliferation *in vitro*. However, it could be that Twist1 and GATA4 promote cell proliferation at low WSS *in vivo* via an EndMT-independent mechanism involving activation of target genes. Platelet-derived growth factors (PDGFs) and their receptors have been previously linked with the promotion of cell turnover at low WSS sites *in vivo* and have been detected in atherosclerotic plaques (Wilcox et al. 1988; Son et al. 2013; Son et al. 2012; He et al. 2015). Interestingly Pdgfr- α is a TWIST1 target gene (Eckert et al. 2011), thus this could be a potential candidate for elucidating the mechanism for TWIST1-mediated EC proliferation at low WSS sites. GATA4 has been shown to regulate Smad signalling (Moskowitz et al. 2011), which in turn has been shown to promote proliferation at low WSS sites *in vivo* (Zhou et al. 2013). Also, both TWIST1 and GATA4 can act upstream and downstream of p38-mediated MAPK signalling (Ryasa et al. 2010; Monzen et al. 2001; Hong et al., 2011, which is also induced by atheroprone low WSS and involved in the regulation of proliferation (Zakkar et al. 2008; Zhang & Liu 2002).

Interestingly, p38, Smad5 and PDGFR- α are also signalling components that have been linked with EndMT regulation (van Meeteren & ten Dijke 2012; Gasperini et al. 2012; Smith et al. 2011) this provides a link between the regulation of GATA4-TWIST1 of EndMT and potentially consequent cell proliferation. Nevertheless, it remains to be determined whether the effect of TWIST1 and GATA4 on cell

proliferation occurs via EndMT or via an independent mechanism or through a combination of both.

5.10.9 Do TWIST1 and GATA4 regulate atherogenesis?

I have shown that TWIST1 luminal EC expression was enhanced in tissue from ischemic heart disease compared to cardiomyopathy patients, reflecting that TWIST1 expression correlated with athero-severity. At low WSS sites in LDLR^{-/-} mice, I have shown that TWIST1 expression is enhanced in response to hyper-cholesterolemia. Thus these observations provide a correlation between TWIST1 activation in EC and atherogenesis. Interestingly, Cheng *et al* reported enhanced atherosclerotic plaque size and expression of inflammatory VCAM-1 expression in areas subjected to low WSS upstream of a flow-altering cuff compared to the constriction and downstream sites (Cheng et al. 2006). The upstream area of the cuff showed high expression of TWIST1 and GATA4 in my studies, therefore this provides a correlation between the expression of TWIST1 and GATA4 with atherosclerosis severity and inflammation. As discussed previously, I propose that GATA4-TWIST1 signalling promotes EC dysfunction at low WSS sites via proliferation and permeability. Whilst this hypothesis will be tested in future studies, it is interesting to speculate whether TWIST1 and GATA4 activation at low WSS sites promotes atherogenesis.

There is some indirect evidence to support the role of TWIST1 and GATA4 in promoting focal atherogenesis. Genome wide association studies, which identify associations in genetic polymorphisms (single nucleotide polymorphisms; SNPs) with disease aetiology, have shown that SNPs in the TWIST1 locus are involved in ischemic stroke and in coronary artery disease (Samani et al. 2007; Matarín et al. 2007), suggesting that it plays a role in atherogenesis. SNPs in the GATA4 locus have been associated with plasma triglyceride levels in humans. Since an increase in triglyceride levels is a known risk factor for atherogenesis, this GWAS study provides a link between GATA4 and atherogenesis (Lamina et al. 2011).

TWIST1 and GATA4 are regulated by and act upstream to activate pro-inflammatory p38 and NF- κ B signalling (Ryśa et al. 2010; Hong et al. 2011; Tenhunen et al. 2004; Li et al. 2012; Gaspar-Pereria et al. 2012), which is suggestive for an involvement of TWIST1 and GATA4 in pro-inflammatory signalling and subsequently atherogenesis. TWIST1 induction of partial EMT in tubular cells promotes inflammatory cell infiltration, leading to renal fibrosis (Lovisa et al. 2015), thus providing a link between TWIST1 and the induction of inflammation. In addition, GATA4 protein expression was detected in inflammatory bowel disease tissue (Haveri et al. 2009), which indicates the potential involvement of GATA4 in inflammation. In addition, GATA4 was shown to promote inflammation via NF- κ B and the release of interleukin 6 (IL-6) which subsequently promoted cellular senescence in fibroblasts, in response to DNA damage (Kang et al. 2015). Senescence is activated by low WSS in EC (Warboys et al. 2014), therefore GATA4-mediated senescence in EC exposed to low WSS could be a mechanism by which it promotes EC dysfunction and atherogenesis.

TWIST1 and GATA4 could be regulating inflammation and atherosclerosis through EndMT. Chen et al. proposed that a reduction in FGF signaling triggers an increase in TGF- β , which in turn triggers EndMT, including an increase in proatherogenic fibronectin expression. Additionally Chen *et al.* have shown that EndMT potentiates atherosclerosis development, as evidenced by an increase in lesion size in atherogenic mice with an EC-specific deletion of FGF receptor adaptor protein FRS2 α (FRS2 α ^{ECKO} Apoe^{-/-}). TWIST1 and GATA4 interact with FGF and TGF- β signalling during embryonic development (Connerney et al. 2008; Loebel et al. 2002; Moskowitz et al. 2011; Chen et al. 2014; O'Rourke et al. 2002). Specifically, TWIST1 is activated by FGF signaling (in combination with SHH) and regulates the balance between FGF and TGF- β signaling during gastrulation. Thus GATA4- TWIST1 activation in EC exposed to low WSS could promote atherogenesis through reducing FGF signaling and increasing TGF- β signaling (Bialek et al. 2004; Connerney et al. 2008; Loebel et al. 2002; Rice et al. 2010). Future studies should include testing the effect of Twist1 and GATA4 on EC inflammation at low WSS sites and by assessing

lesion formation and plaque composition in EC-specific TWIST1 and/or GATA4 atherogenic mice.

5.10.10 Potential therapeutic strategies to inhibit TWIST1 and GATA4 induction of EC dysfunction.

TWIST1 and GATA4 are both prominent oncogenes, which drive cancer cell survival and metastasis (Chia et al. 2015; Yang et al. 2004; Tagaki et al. 2014). Thus, both of these transcription factors are key anti-cancer drug targets. There are several potential inhibitory drugs that have been tested for the targeting of TWIST1 and GATA4 in cancer cells (summarised in table 11). These drugs include widely used EndMT inhibiting drugs LY364947 and SB431542, which inhibit Twist1 activation and subsequent TGF β 2 signalling (Xue et al. 2012). These drugs may be useful in potentially reducing or preventing atherosclerosis in human patients. However, although Twist1 and GATA4 inhibitory drugs have been shown to be successful in reducing EndMT-mediated fibrotic conditions and by limiting cancer cell survival, they are not Twist1 and GATA4 specific, since they inhibit either upstream or downstream signalling events. Therefore, these drugs may have off-target detrimental effects. However, GATA4 and Twist1- specific small molecule inhibitors are under development (El-Hachem & Nemer 2011; Burns et al. 2013) using such drugs could a potential intervention for inhibiting GATA4-Twist1-mediated EC dysfunction and potential atherogenesis.

Another caveat in inhibiting GATA4-Twist1 signalling is that the activation of this pathway preferentially occurred in EC at sites of low WSS, thus the therapeutic intervention should be targeted to EC at low WSS sites. Recently, a study by the Jo group has demonstrated that therapeutics can be targeted to EC at low WSS sites via utilising the increased VCAM-1 expression on EC surface at low WSS sites, the Jo group developed anti-cationic lipoparticles (CCLs) containing anti-miR-712 and coated with a VCAM-1 targeting peptide (VHPK). The CCLs efficiently delivered anti-miR-712 and resulted in a marked reduction in low WSS-mediated atherogenesis (Kheirloom et al. 2015). The use of CCLs to deliver specific Twist1 and/or GATA4 specific inhibitors could be a novel, promising therapeutic strategy to either limit or prevent focal atherosclerosis.

Table 11. Summary of TWIST1 and GATA4 inhibitory drugs

Drug	Target/mechanism	Reference
LY-364947/ SB-431542	Inhibition of TWIST1-mediated activation of TGF β -2 and EndMT	Xue et al., 2012 Maddaluno et al., 2013
Paclitaxel	<ul style="list-style-type: none">• Inhibition of TWIST1 protein and mRNA• Inhibits cancer cell proliferation• Mechanism of action is unknown	Yu et al., 2009
Curcumin (Component of Turmeric)	Inhibition of TWIST1 protein expression through inhibiting NF- κ B-Snail axis	Tao Huang et al., 2012
Metformin	Inhibition of KLF5/GATA4/GATA6 target genes and cancer proliferation	Chia et al., 2015

5.12 Future work

1. To assess GATA4 and SNAIL expression in human coronary tissue sections and in low WSS sites of LDLR^{-/-} animals vs. controls.
2. To determine the mechanism by which TWIST1 and GATA4 promote EC proliferation, target gene expression in the murine aorta at regions of low and high WSS will be carried out, followed by the generation of gene-specific knock outs and the assessment of subsequent cell proliferation.
3. To dissect whether the effect of Twist1 and GATA4 on cell proliferation is via SNAIL-mediated EndMT, Twist1 and Gata4 KO mice can be treated with Snail siRNA or cDNA to assess the involvement of Snail signalling on the effects on cell proliferation and on EndMT at sites of low WSS in the murine aorta.
4. To assess whether TWIST1 and GATA4 control cell permeability at sites of low WSS.
5. To determine whether the effects of TWIST1 and GATA4 on cell proliferation is promoting EC dysfunction and atherogenesis, *SCL-Cre-ER^T*; *GATA4^{KO}* and *Tie2-Twist1^{KO}* animals would be crossed with atherogenic LDLR^{-/-} animals and given a high fat diet. Lesion formation and plaque composition in the KO animals compared to the controls will be used as a measuring of assessing atherogenesis.

Chapter 6: General discussion

6.1 Mechanical TWIST1 activation has divergent effects during development and disease

TWIST1 and GATA4 mechanotransduction is central to cell function in multiple contexts (Figure 55); it is involved in gastrulation and organ development in the embryo. During morphogenesis in the *Drosophila* embryo, tissue deformations activate TWIST1 via a mechanism involving Src42A-dependent nuclear translocation of β -catenin (Desprat et al. 2008). TWIST1 then subsequently promotes tissue differentiation. Additionally, TWIST1 and SNAIL control *Drosophila* gastrulation by first promoting apical membrane tension, which is important for the induction of mesoderm invagination (Seher et al. 2007; Pouille et al. 2009).

Vascular development involves the induction of angiogenic sprouting and the cellular processes migration and proliferation are key to this step (Ellertsdóttir et al. 2010). Since vascular development occurs prior to the onset of cardiac contraction, the process of angiogenic sprouting occurs in the absence of flow. The subsequent onset of flow influences vascular maturation by altering EC physiology. For example, it has been shown that during chick embryogenesis, the enhancement of WSS inhibited sprouting angiogenesis, whereas the reduction of WSS enhanced this process (Chouinard-Pelletier et al. 2013). Work from our group has shown that in the developing zebrafish embryo *twist1* mechano-regulation is important in vascular development. Zebrafish possess three orthologues of mammalian *twist* genes; *twist1b*, *twist1a* and *twist2*. *In situ* hybridisation revealed that each of them was expressed in the trunk vasculature before cardiac contraction (Figures 56 A-56 C; 24 hpf). *twist* expression was reduced following the onset of flow in control embryos but was maintained in troponin T type 2 (*tnnt2*) morphants that lack flow (Fig. 56 A-56 C; 52hpf). The function of *twist* was studied by enhancing its expression in vessels exposed to flow via injection of mRNA (gain-of-function). This revealed an increase in EndMT marker Snail and N-cadherin expression (Figures 56 D and 56 E), suggesting that *twist* regulates EndMT in the absence of flow.

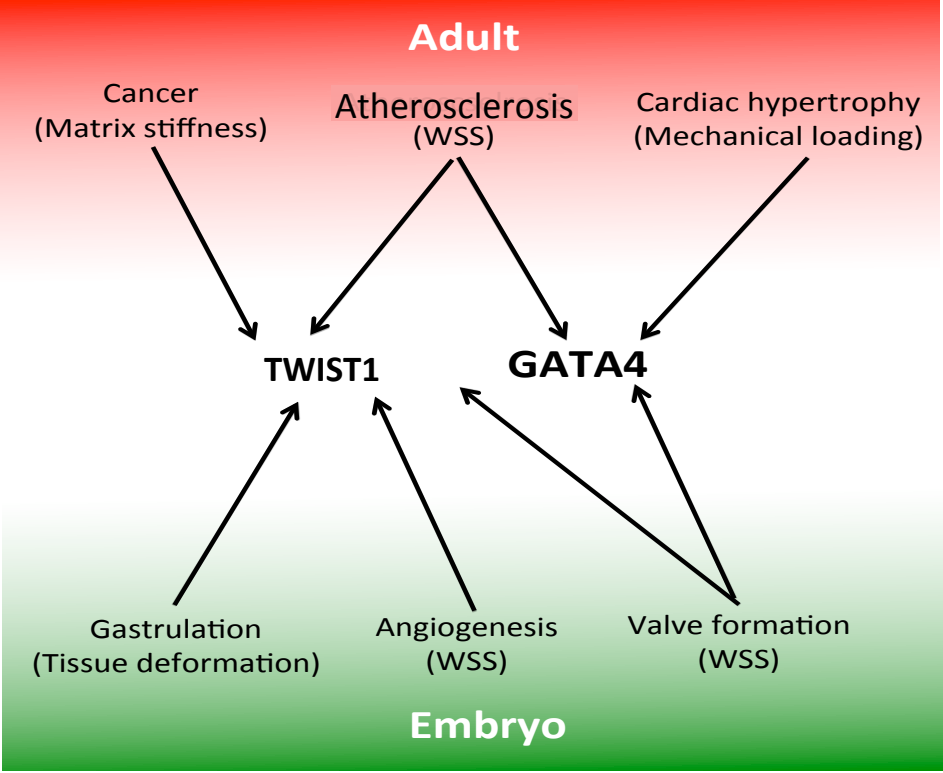


Figure 55. Schematic summary of TWIST1 and GATA4 mechanical activation in embryonic and adult systems.

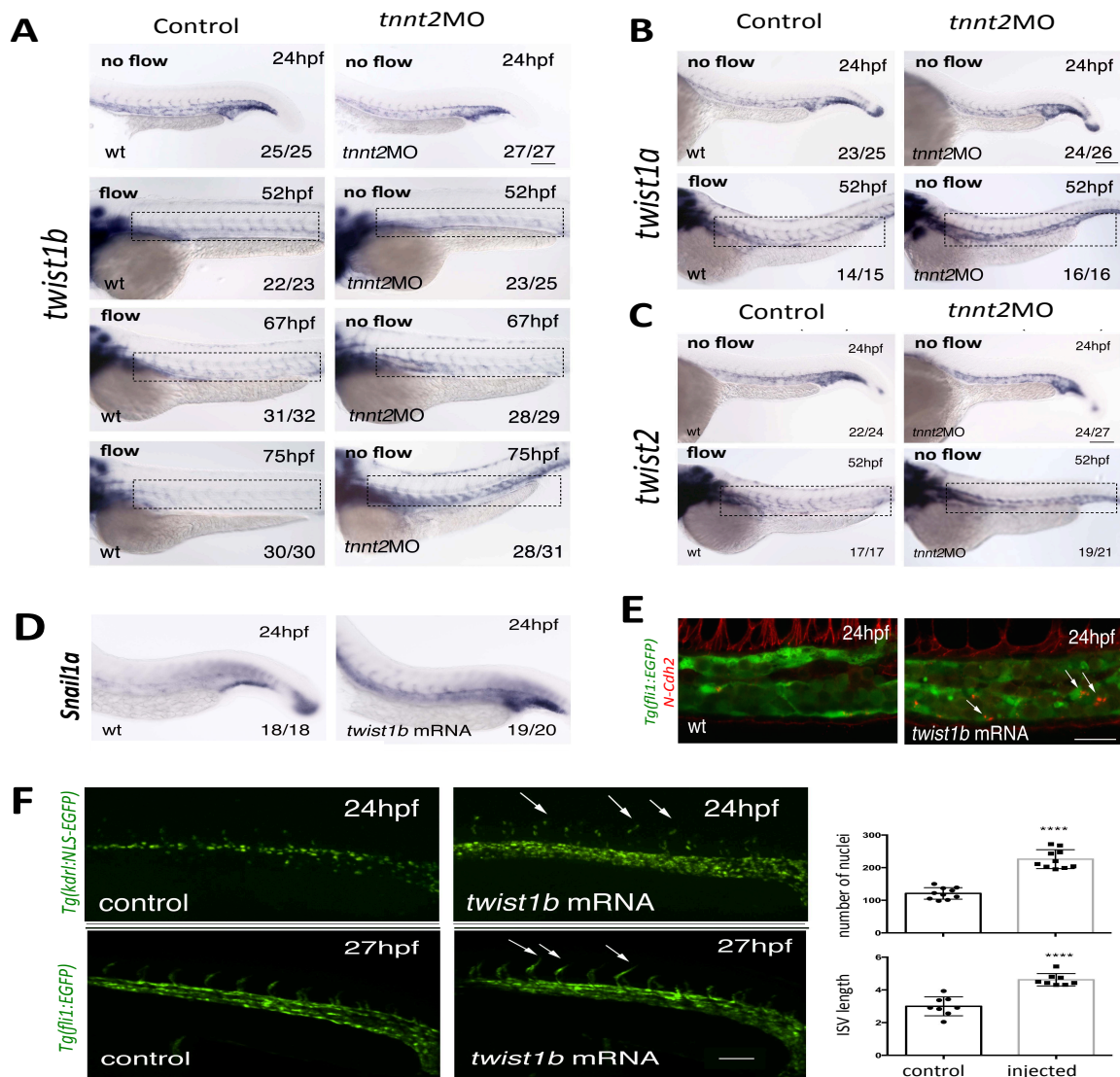


Figure 56. *twist* expression was downregulated by flow in zebrafish embryonic vasculature. The influence of flow on *twist* expression was studied using zebrafish embryos that were treated with *tnnt2* MOs to suppress cardiac contraction or remained untreated as a control. (A) The boxed area identifies the region studied (Dorsal aorta and posterior caudal vein). *In situ* hybridisation analysis of *twist1b* (A), *twist1a* (B) or *twist2* (C) in embryos at 24 – 75 hpf. Note that flow was initiated in the trunk at 26 hpf in wild-type fish. Scale bar, 100 μm. (D-E) Zebrafish embryos (wild-type with/without *Tg(fli1:EGFP)* or *Tg(kdrl:NLS-EGFP)*) were treated with *twist1b* mRNA (to enforce expression) or treated with mCherry mRNA as a control (D) *In situ* hybridisation analysis of *snail1a* (E) Fluorescent immunostaining of N-cadherin in transgenic *Tg(fli1:EGFP)* fish (EGFP-positive endothelium). F) Confocal microscopy was used to visualise EC nuclei (*Tg(kdrl:NLS-EGFP)*; upper panel) or angiogenic sprouts (*Tg(fli1:EGFP)*; lower panels; arrows). Representative images are shown. Cell numbers were quantified in multiple embryos and mean values +/- SEM are shown (upper right panel). The length of ISVs (3rd-5th vessels in the field view) was quantified using image J software. Data were collected from multiple embryos and mean values +/- SEM are shown (lower right panel). **** p<0.0001 using an unpaired t-test. Scale bar, 100 μm. (A-E) Data are representative of the majority of embryos analysed (proportion indicated lower right of each panel) and were closely similar in at least three independent experiments. These data were generated by Dr. Rosemary Kim in Evan's laboratory.

In addition, *twist* injection increased proliferation and sprouting (Figure 53 F). These results revealed that *twist* controls vascular sprouting and EndMT in the absence of flow. Therefore modulation of the Twist1-Snail activation by WSS plays an important role in regulating angiogenic sprouting in the developing zebrafish.

In the adult, TWIST1 mechanotransduction is involved in promoting cancer metastasis (Yang et al. 2004). GATA4 is important in regulating mechanically controlled tissue homeostasis, as it is central to the transcriptional induction of cardiac hypertrophy following mechanical load of the heart ventricles (Tenhunen et al. 2004). My studies have shown that in adult EC, low WSS activates the GATA4-TWIST1-SNAIL axis and that GATA4-TWIST1 promoted EC proliferation and permeability. Since high WSS inhibited GATA4-TWIST1 activation in the developing zebrafish and in adult EC, this indicates that there are parallels in TWIST1 mechanotransduction in response to WSS in both embryonic development and in focal EC dysfunction in the adult. It could be argued that EC responses at low WSS sites are a reflection of an early embryonic stage before the onset of flow (Figure 57).

The mechanism that drives conserved TWIST1 activation in embryo and adult vessels should be considered. It is plausible that In the adult, EC retain “memory” of the WSS-mediated cues that they have received during development. This results in EC at low WSS displaying enhanced EC proliferation and migration, leading to permeability, EC dysfunction and atherogenesis. Whereas, this process is inhibited in EC exposed to high WSS sites. Therefore, it can be proposed that EC responses to flow under low WSS are default, whereas responses to high WSS result in a change in EC transcriptional activity and function.

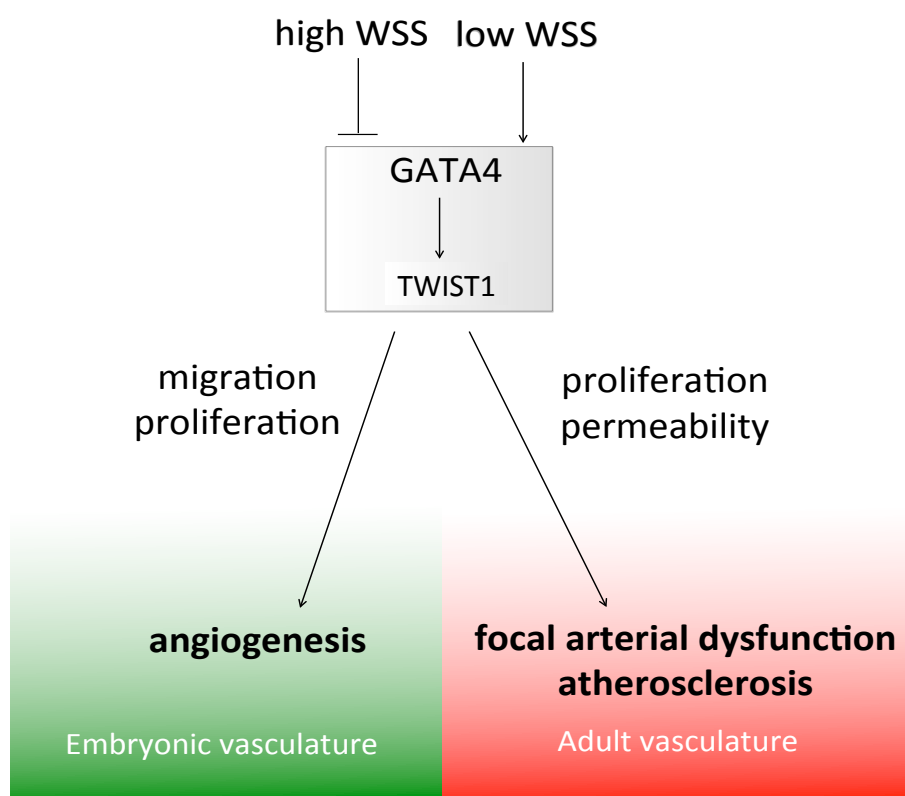


Figure 57. Model for activation of GATA4-TWIST1 by WSS in developmental angiogenesis and EC dysfunction in the adult. Low wall shear stress (WSS) induces Twist1 via GATA4. This process promotes EC proliferation and migration to drive angiogenesis (left). The development of a patent vessel allows blood flow which exerts high WSS on the vessel wall. This mechanical stimulus suppresses further angiogenic sprouting by inhibiting Twist expression. In adult arteries, low WSS at branches and bends triggers GATA4-Twist1 induction which drives proliferation and enhanced permeability leading to atherosclerosis.

The antagonistic pleiotropy hypothesis coined by George C. Williams in 1957 to explain the evolutionary significance of the occurrence of cellular senescence, is a description that is given to a gene or pathway that controls multiple traits in an organism, where one of these traits is beneficial to the organism's fitness during development and one trait is detrimental after child-bearing years (Williams 1957). Although it is understood how low WSS promotes EC dysfunction, it is not understood "why" low WSS triggers EC dysfunction and subsequently atherosclerosis. I propose that there is an evolutionary explanation to EC responses to low WSS, where GATA4- TWIST1 mechanotransduction in EC is an example of antagonistic pleiotropy. Whilst Twist1 mechanotransduction promotes vascular development in the embryo, it also contributes to focal EC dysfunction and potentially atherogenesis in the adult, following childbearing years. TWIST1 mechanoactivation in tumour metastasis and cancer cell survival could be other examples of Twist1 antagonistic pleiotropy.

6.1.1 Does GATA4-TWIST1 re-activation in adult EC promote repair in response to low WSS-mediated injury?

A second mechanism for the activation of GATA4- TWIST1 signalling at EC located at low WSS sites in the adult vasculature could be to promote repair in response to injury. It was proposed by Fry et al., in 1969 that cell injury as a result of blood flow is a causal factor for the spatial distribution of EC dysfunction and atherosclerosis (Fry 1969). It was later revealed that EC at low WSS are dysfunctional as a consequence of the induction of an injury/ stress response (Civelek et al. 2009; Davies 2009). Furthermore, Davies et al. proposed that responses to low WSS-mediated stress triggers "a chronic low-level inflammatory state, an adaptive response to ensure continued function at the expense of increased susceptibility to atherogenesis" (Davies et al. 2009).

TWIST1 and GATA4 signaling and subsequent changes in cell function such as EndMT have all been linked with responses to cell injury and cell plasticity (Curci et al. 2014; Gupta et al. 2013; Heineke et al. 2007; Mammoto et al. 2013; Lovisa et al. 2015). Interestingly, GATA4 and TWIST1 activation in response to injury in renal or cardiac cells promoted repair via proliferation (Heineke et al. 2007; Lovisa et al. 2015). This subsequently promoted cell proliferation and inflammation. It could be proposed that EC at low WSS sites are responding to low WSS-mediated injury by “switching” to a more plastic transcriptional network, that is controlled by GATA4- TWIST1 signalling, which could be controlling EC repair via proliferation.

One potential mechanism for the proliferative, repair process could partly involve the induction of an angiogenic response. This notion is supported by studies that demonstrated that angiogenic activation, involving the induction of proliferation occurs following an injury stimulus (Reviewed in Khurana et al. 2005; Heinke et al. 2007). Studies by the Jones lab provide evidence for the role of low WSS is promoting angiogenesis in the developing chick (Chouinard-Pelletier et al. 2013). Consistent with this, studies in the developing zebrafish by our laboratory showed that TWIST1 controlled angiogenesis and EndMT and that this process was inhibited by high WSS. Therefore there seems to be supportive evidence for the activation of angiogenesis by low WSS. TWIST1 and GATA4 control angiogenesis and are both upstream activators of pro-angiogenic VEGFR2 (Li et al. 2014; Kamei et al. 2011). My studies have shown that TWIST1 and GATA4 control tube formation under low WSS and that they are activators of partial EndMT, a process that is known to occur during angiogenesis (Reviewed in Welch-Reardon. 2014). Taken together, the activation of GATA4-TWIST1 signalling under low WSS could be promoting repair in response to low WSS-mediated injury, this process may involve some aspects of cell behavior such as proliferation that are linked to angiogenesis.

The induction of partial EndMT by GATA4 and TWIST1 could also be promoting EC repair via inflammation, which is known to be activated in response to injury (Reviewed in Libby 2002; Davies et al. 2009). It was recently shown that atherosclerosis-mediators- low WSS and inflammatory cytokines have an additive effect on promoting EndMT, once active, EndMT potentiates atherosclerosis development (Chen et al. 2015). Furthermore, Lovisa et al. showed that TWIST1-mediated partial EMT controlled inflammatory activation and renal fibrosis. These studies provide evidence for the role of EndMT in promoting inflammation and atherosclerosis. Therefore partial EndMT induction by GATA4- TWIST1 could trigger EC dysfunction via EC proliferation and permeability, which in turn gives rise to an “unwanted” consequence of inflammation and atherosclerosis.

6.2 TWIST1 and GATA4 may regulate EC mechanosensing in response to low WSS

VE-cadherin is part of a cell surface complex in EC with CD31 and VEGFR2, which together mediate EC mechanosensing in response to WSS (Tzima et al., 2005, Conway et al., 2013). This mechanosensory complex relays mechanical cues to integrins, which subsequently activate signalling pathways depending on the context (Tzima et al. 2005; Orr et al. 2006). I have shown that GATA4- TWIST1 activation promoted an increase in N-cadherin junctional expression and increased VE-cadherin junctional width, which is indicative of VE-cadherin endocytosis and disorganisation (Huveneers et al. 2012; Orsenigo et al. 2012; Miao et al. 2005). Therefore, the modulation of cadherin expression could be influencing EC mechanosensing. Recently, the Schwartz lab studied the relative contribution of VE and N-cadherin to EC mechanosensing by studying EC alignment in response to WSS in VE-cadherin^{-/-} null cells, transfected with a lentivirus for N-cadherin or VE-cadherin (Coon et al. 2015). They showed that whilst VE-cadherin expressing cells showed an alignment in the direction of WSS, N-cadherin expression completely abrogated cell alignment. Furthermore, they showed that OSS-mediated activation of VCAM-1 expression was mediated by VE-cadherin-VEGFR2/3 mechanosensing, whereas N-cadherin inhibited VCAM-1 expression (Coon et al. 2015). Thus, it seems as though N-cadherin inhibits

EC mechanoresponses, via a possible mechanism involving integrins. Therefore, increased N-cadherin expression via GATA4- TWIST1 in EC exposed to low WSS, could be modulating EC mechanosensing via promoting a “no-flow” EC response. This could be involved in driving EC dysfunction and potentially atherogenesis.

VE- and N-cadherin balance is involved in the control of angiogenesis. N-cadherin promotes angiogenic processes including proliferation and migration, whereas VE-cadherin inhibits these events (Giampietro et al. 2012; Bentley et al. 2014). This could therefore be a mechanism by which GATA4- TWIST1 signalling is promoting angiogenic sprouting in the developing zebrafish embryo and EC dysfunction in adult EC. More work is required to dissect the downstream mechano-signalling and changes in EC function that occurs following the stimulation of N-cadherin expressing cells with low or high WSS, along with the significance to atherosclerosis.

Chapter 7: Appendix

Appendix 1. Growth media constituents

Media name	Serum content	Antibiotics	Supplements
Complete M199 growth medium	20% FBS (Unless specified otherwise)	100U/ml Pen-strep 10 µg/ml Amphotericin B	5 mM L-Glutamine. 25µg/ml ECGF 90µg/ml heparin
Transfection media complete M199 growth medium	10%FBS	-	5 mM L-Glutamine. 25µg/ml ECGF 90µg/ml heparin
Complete DMEM (With 1g/L glucose) growth medium 1	10% FBS	100U/ml Pen-strep. 10 µg/ml Amphotericin B. 100µg/ml Gentamycin	5 mM L-Glutamine. 25µg/ml ECGF 90µg/ml heparin
Complete DMEM (With 1g/L glucose) growth medium 2	20% FBS	100U/ml Pen-strep. 10 µg/ml Amphotericin B	5 mM L-Glutamine. 25µg/ml ECGF 90µg/ml heparin
(Transport media) PBS	-	100U/ml Pen-strep. 10 µg/ml Amphotericin B 100µg/ml Gentamycin	-

Appendix 2. PCR genotyping information

Primer name	Forward primer	Reverse primer	Expected product sizes	Genotyping information
GATA4 Flox	CCC AGT AAA GAA GTC AGC ACA AGG AAA C	AGA CTA TTG ATC CCG GAG TGA ACA TT	GATA4 flox positive = 455 bp Wild type = 355 bp	https://www2.jax.org/protocolsdb/f?p=116:2:0::NO:2:P2_MASTER_PROTOCOL_ID,P2_JRS_CODE:7608,008194
Tal tg SCL-Cre	TGCATGATCTCCGGTATTGA	CGTACTGACGGTGGGAGAAT	Cre positive= 300bp	Gother et al., 2007
Rosa td flox	CTG TTC CTG TAC GGC ATG G	GGC ATT AAA GCA GCG TAT CC	Mutant = 196 bp	http://jaxmice.jax.org/protocolsdb/f?p=116:2:0::NO:2:P2_MASTER_PROTOCOL_ID,P2_JRS_CODE:6753,007914
Rosa td flox WT	AAG GGA GCT GCA GTG GAG TA	CCG AAA ATC TGT GGG AAG TC	Wild type = 297 bp	
Tie2 Cre	GCG GTC TGG CAG TAA AAA CTA TC	GTG AAA CAG CAT TGC TGT CAC TT	Cre positive= 100 bp	https://www2.jax.org/protocolssdb/f?p=116:2:::NO:2:P2_MASTER_PROTOCOL_ID,P2_JRS_CODE:288,004128
Internal positive control	CTA GGC CAC AGA ATT GAA AGA TCT	GTA GGT GGA AAT TCT AGC ATC ATC C	Internal positive control= 324bp	

Chapter 8: Abbreviations

ABC- Avidin-biotin complex
ApoE- Apolipoprotein E
bHLH-beta-Helix-Loop-Helix
BMP- Bone morphogenic protein
CD31- Cluster of differentiation 31
CDC42- Cell division control protein 42 homolog
Cdk4- Cyclin-dependent kinase 4
ChIP- Chromatin immunoprecipitation
COUP-TFII- COUP transcription factor 2
Tal- T-Cell Acute Lymphocytic Leukemia 1
CREB- *cAMP response element-binding* protein
DAB-3,3'-Diaminobenzidine
DAPI-4',6-diamidino-2-phenylindole
Dnmt- DNA methyltransferase
EC- Endothelial cells
ECM-Extracellular matrix protein
PDGFR α -Platelet derived growth factor- α
EFnb2- Ephrin-B2
EMT- Epithelial mesenchymal transition
EndMT- Endothelial mesenchymal transition
eNOS- endothelial Nitric oxide synthase
Ephb4- EPH Receptor B4
ERBB3- Epidermal growth factor receptor tyrosine kinase 3
ERK- extracellular-signal-regulated kinases
FGF- Fibroblast growth factor
FOG- Friend of GATA
Fzd- Frizzled
Gadd45a-growth arrest and DNA-damage-Inducible, 45 α
GATA2-GATA-binding protein
HAT-Histone acetyltransferase

HDAC- Histone deacetylase
HIF-1 α -Hypoxia inducible factor- α
FOG 2- Hepatocyte nuclear factor
HOX -Homeobox binding protein
HUVEC- Human umbilical vein EC
ICAM1- intercellular Adhesion Molecule
ID1- inhibitor of DNA binding-1
IL-1- Interleukin-1
JAK/STAT- Janus kinase/ Signal Transducer and Activator of Transcription
JNK- c-Jun N-terminal kinases
KLF- Kruppel-like factor
LDL- Low density lipoproteins
LDLR- lipoprotein receptor
MAPK- Mitogen-activated protein kinases
MCP-1- Monocyte chemoattractant protein-1
Mef2c- myocyte enhancer factor 2C
MEK-MAPK/ERK kinase
MEndT-Mesenchymal-endothelial transition
miR-micro RNA
MMP- Matrix metalloproteinase
MO- Morpholino
MYB- Myeloblastosis transcription factor
N-cadherin- neuronal cadherin
NF- κ B - Nuclear factor kappa-light-chain-enhancer of activated B cells
NFAT- nuclear factor of activated T-cells
Nkx2.5-NK2 homeobox 5
NLS- nuclear localisation signal
NO- nitric oxide
Nrf2- nuclear factor (erythroid-derived 2)-like 2
nSLCC-Non-small lung cell carcinoma
OB-cadherin- Osteoblast cadherin
Ox-LDL- Oxidised LDL

PAEC-Porcine aortic EC
PCAF- P300/CBP-associated factor
PCR-Polymerase chain factor
PI3K- Phosphatidylinositol-4,5-bisphosphate 3-kinase
qRT-PCR- quantitative real time PCR
Rb- Retinoblastoma
Re- Reynolds
ROS- Reactive oxygen species
SCL- Stem cell leukemia
SHH- Sonic hedgehog
SMA- Smooth muscle cell actin
SNP- Single nucleotide polymorphism
Srf- Serum response factor
SRPX -Sushi-repeat containing protein, X-linked
Tbx-T-Box protein
TGF- β - Transforming growth factor β
TNF-a- Tumour necrosis factor a
Tnnt2- troponin type 2
VCAM1- Vascular cell adhesion protein -1
VE-cadherin- Vascular endothelial cadherin
VEGFR2- Vascular endothelial growth factor receptor 2
VHPK -VCAM-1 targeting peptide
VIC- Valve interstitial cells
vWF-von Willibrand factor
WSS- Wall shear stress
ZFN- Zinc finger domain

9. References

- Agnihotri, S. et al., 2011. A GATA4-regulated tumor suppressor network represses formation of malignant human astrocytomas. *The Journal of Experimental Medicine*, 208 (4), pp.689–702.
- Aisagbonhi, O. et al., 2011. Experimental myocardial infarction triggers canonical WNT signaling and endothelial-to-mesenchymal transition. *Disease models & mechanisms*, 4(4), pp.469–83.
- Alexander, C.M. et al. 2000. Syndecan-1 is required for wnt-1 induced mammary tumorigenesis in mice. *Nature Genetics*, 25 (3), pp. 329-332.
- Alexander, N.R. et al., 2006. N-cadherin gene expression in prostate carcinoma is modulated by integrin-dependent nuclear translocation of Twist1. *Cancer research*, 66(7), pp.3365–9.
- Alvarado, D.M. et al., 2011. Downstream Targets of GATA3 in the Vestibular Sensory Organs of the Inner Ear. *developmental dynamics*, 238(12), pp.3093–3102.
- Amini, N. et al., 2014. Requirement of JNK1 for endothelial cell injury in atherogenesis. *Atherosclerosis*, 235(2), pp.613–618.
- Andreassi, M., 2008. DNA damage, vascular senescence and atherosclerosis. *Journal of Molecular Medicine*, 86(9), pp.1033–1043.
- Aristotle, Platt, A., 1910. De Generatione Animalium. In Oxford: Clarendon Press, p. 240.
- Azhar, M. et al., 2009. Ligand-Specific Function of Transforming Growth Factor Beta in Epithelial-Mesenchymal Transition in Heart Development. *Developmental dynamics : an official publication of the American Association of Anatomists*, 238(2), pp.431–442.
- Bailey, E.L. et al., 2015. Mass Transport Properties of the Rabbit Aortic Wall S. Subbian, ed. *PLoS ONE*, 10(3), p.e0120363.
- Bartman, T. et al., 2004. Early Myocardial Function Affects Endocardial Cushion Development in Zebrafish. *PLoS Biology*, 2(5), p.e129.
- Belaguli, N.S. et al., 2007. Cooperation between GATA4 and TGF- β signaling regulates intestinal epithelial gene expression. *American Journal of Physiology - Gastrointestinal and Liver Physiology*, 292(6), pp.G1520–G1533.
- Bentley, K. et al., 2014. The role of differential VE-cadherin dynamics in cell rearrangement during angiogenesis. *Nat Cell Biol*, 16(4), pp.309–321.

- Berbée, J.F.P. et al., 2013. Resveratrol protects against atherosclerosis, but does not add to the antiatherogenic effect of atorvastatin, in APOE*3-Leiden.CETP mice. *Journal of Nutritional Biochemistry*, 24(8), pp.1423–1430.
- van Berlo, J.H. et al., 2011. Serine 105 phosphorylation of transcription factor GATA4 is necessary for stress-induced cardiac hypertrophy in vivo. *Proceedings of the National Academy of Sciences of the United States of America*, 108(30), pp.12331–12336.
- Bernanke, D.H. & Markwald, R.R., 1982. Migratory behavior of cardiac cushion tissue cells in a collagen-lattice culture system. *Developmental Biology*, 91(2), pp.235–245.
- Bialek, P. et al., 2004. A Twist Code Determines the Onset of Osteoblast Differentiation. *Developmental Cell*, 6(3), pp.423–435.
- Birukova, A.A. et al., 2004. Role of Rho GTPases in thrombin-induced lung vascular endothelial cells barrier dysfunction. *Microvascular Research*, 67(1), pp.64–77.
- Biswas, P. et al., 2003. PECAM-1 promotes β -catenin accumulation and stimulates endothelial cell proliferation. *Biochemical and Biophysical Research Communications*, 303(1), pp.212–218.
- Björck, H.M. et al., 2012. Characterization of shear-sensitive genes in the normal rat aorta identifies Hand2 as a major flow-responsive transcription factor. *PLoS one*, 7(12), p.e52227.
- Bourgeois, P. et al., 1998. The Variable Expressivity and Incomplete Penetrance of the twist-Null Heterozygous Mouse Phenotype Resemble Those of Human Saethre-Chotzen Syndrome. *Human Molecular Genetics*, 7 (6), pp.945–957.
- Brooks, A.R. et al., 2012. Gene expression profiling of human aortic endothelial cells exposed to disturbed flow and steady laminar flow Gene expression profiling of human aortic endothelial cells exposed to disturbed flow and steady laminar flow. *physiological genomics*, 9, pp.27–41.
- Buchanan, J.R. et al., 1999. Relation between non-uniform hemodynamics and sites of altered permeability and lesion growth at the rabbit aorto-celiac junction. *Atherosclerosis*, 143(1), pp.27–40.
- Burns, T.F. et al., 2013. Inhibition of TWIST1 Leads to Activation of Oncogene-Induced Senescence in Oncogene Driven Non-Small Cell Lung Cancer. *Molecular cancer research : MCR*, 11(4), pp.329–338.
- Cai, X. et al., 2013. Tbx20 acts upstream of WNT signaling to regulate endocardial cushion formation and valve remodeling during mouse cardiogenesis.

- Development (Cambridge, England)*, 140(15), pp.3176–3187.
- Callis, T.E. et al., 2009. MicroRNA-208a is a regulator of cardiac hypertrophy and conduction in mice. *The Journal of Clinical Investigation*, 119(9), pp.2772–2786.
- Cancel, L.M. & Tarbell, J.M., 2010. The role of apoptosis in LDL transport through cultured endothelial cell monolayers. *Atherosclerosis*, 208(2), p.335.
- Cancel, L.M. & Tarbell, J.M., 2011. The role of mitosis in LDL transport through cultured endothelial cell monolayers. *American Journal of Physiology - Heart and Circulatory Physiology*, 300(3), pp.H769–H776.
- Caro, C.G., 1966. Dispersion of indicator flowing through simplified models of the circulation and. *Journal of Physiology*, 185, pp.501–519.
- Caro, C.G., Fitz-Gerald, J.M. & Schroter, R.C., 1971. Atheroma and Arterial Wall Shear Observation, Correlation and Proposal of a Shear Dependent Mass Transfer Mechanism for Atherogenesis. *Proceedings of the Royal Society B: Biological Sciences*, 177(1046), pp.109–133.
- Carrasco, M. et al., 2012. GATA4 and GATA6 control mouse pancreas organogenesis. *The Journal of Clinical Investigation*, 122(10), pp.3504–3515.
- Castanon, I. & Baylies, M.K., 2002. A Twist in fate: evolutionary comparison of Twist structure and function. *Gene*, 287(1–2), pp.11–22.
- Celermajer DS, Sorensen KE, B.C., 1994. Endothelium-dependent dilation in the systemic arteries of asymptomatic subjects relates to coronary risk factors and their interactions. *Journal of the American College of Cardiology*, 24, pp.1468–1474.
- Chakraborty, S. et al., 2010. Twist1 promotes heart valve cell proliferation and extracellular matrix gene expression during development in vivo and is expressed in human diseased aortic valves. *Developmental biology*, 347(1), pp.167–179.
- Chang, A.C.Y. et al., 2011. Notch Initiates the Endothelial-to-Mesenchymal Transition in the Atrioventricular Canal through Autocrine Activation of Soluble Guanylyl Cyclase. *Developmental Cell*, 21(2), pp.288–300.
- Charron, F. et al., 1999. Cooperative Interaction between GATA-4 and GATA-6 Regulates Myocardial Gene Expression. *Molecular and Cellular Biology*, 19(6), pp.4355–4365.
- Chaudhury, H. et al., 2010. c-Jun N-terminal kinase primes endothelial cells at atheroprone sites for apoptosis. *Arteriosclerosis, thrombosis, and vascular biology*, 30(3), pp.546–53.

- Chen, G. et al., 2011. The effect of NF- κ B pathway on proliferation and apoptosis of human umbilical vein endothelial cells induced by intermittent high glucose. *Molecular and Cellular Biochemistry*, 347(1-2), pp.127–133.
- Chen, H.-F. et al., 2014. Twist1 induces endothelial differentiation of tumour cells through the Jagged1-KLF4 axis. *Nat Commun*, 5.
- Chen, P. et al., 2015. Endothelial-to-mesenchymal transition drives atherosclerosis progression. *The Journal of Clinical Investigation*, 125, pp.1–15.
- Chen, Z.F. & Behringer, R.R., 1995. twist is required in head mesenchyme for cranial neural tube morphogenesis. *Genes & Development*, 9 (6), pp.686–699.
- Cheng, C. et al., 2006. Atherosclerotic lesion size and vulnerability are determined by patterns of fluid shear stress. *Circulation*, 113(23), pp.2744–53.
- Cheng, G.Z. et al., 2008. Twist Is Transcriptionally Induced by Activation of STAT3 and Mediates STAT3 Oncogenic Function. *Journal of Biological Chemistry*, 283 (21), pp.14665–14673.
- Cheng, S. et al., 2013. Regulate the Endothelial – Mesenchymal Transition in Aortic Endothelial Cells. , pp.1679–1689.
- Cheung, C. et al., 2014. Directed differentiation of embryonic origin–specific vascular smooth muscle subtypes from human pluripotent stem cells. *Nat. Protocols*, 9(4), pp.929–938.
- Chia, N.-Y. et al., 2015. Regulatory crosstalk between lineage-survival oncogenes KLF5, GATA4 and GATA6 cooperatively promotes gastric cancer development. *Gut*, 64 (5), pp.707–719.
- Chien, S., 2008. Effects of disturbed flow on endothelial cells. *Annals of biomedical engineering*, 36(4), pp.554–62.
- Chiu, J.-J. & Chien, S., 2011. Effects of Disturbed Flow on Vascular Endothelium : Pathophysiological Basis and Clinical Perspectives. *Physiological review*, 91, pp.327–387.
- Choi, B.-J. et al., 2014. Coronary Endothelial Dysfunction Is Associated With Inflammation and Vasa Vasorum Proliferation in Patients With Early Atherosclerosis. *Arteriosclerosis, Thrombosis, and Vascular Biology*, 34 (11), pp.2473–2477.
- Chouinard-Pelletier, G., Jahnsen, E. & Jones, E.V., 2013. Increased shear stress inhibits angiogenesis in veins and not arteries during vascular development. *Angiogenesis*, 16(1), pp.71–83.

- Civelek, M. et al., 2009. Chronic Endoplasmic Reticulum Stress Activates Unfolded Protein Response in Arterial Endothelium in Regions of Susceptibility to Atherosclerosis. *Circulation Research* , 105 (5), pp.453–461.
- Clarke, L.A., Mohri, Z. & Weinberg, P.D., 2012. High throughput en face mapping of arterial permeability using tile scanning confocal microscopy. *Atherosclerosis*, 224(2), pp.417–425.
- Clement, C.A. et al., 2013. TGF- β Signaling Is Associated with Endocytosis at the Pocket Region of the Primary Cilium. *Cell Reports*, 3(6), pp.1806–1814.
- Conklin, B.S. et al., 2002. Shear Stress Regulates Occludin and VEGF Expression in Porcine Arterial Endothelial Cells. *Journal of Surgical Research*, 102(1), pp.13–21.
- Connerney, J. et al., 2006. Twist1 dimer selection regulates cranial suture patterning and fusion. *Developmental Dynamics*, 235(5), pp.1334–1346.
- Connerney, J. et al., 2008. Twist1 homodimers enhance FGF responsiveness of the cranial sutures and promote suture closure. *Developmental biology*, 318(2), pp.323–334.
- Conway, D.E. et al., 2013. Fluid Shear Stress on Endothelial Cells Modulates Mechanical Tension across VE-Cadherin and PECAM-1. *Current Biology*, 23(11), pp.1024–1030.
- Cooley, B.C. et al., 2014. TGF- β signaling mediates endothelial to mesenchymal transition (EndMT) during vein graft remodeling. *Science translational medicine*, 6(227), pp.227ra34–227ra34.
- Coon, B.G. et al., 2015. Intramembrane binding of VE-cadherin to VEGFR2 and VEGFR3 assembles the endothelial mechanosensory complex. *The Journal of Cell Biology* , 208 (7), pp.975–986.
- Corada, M., Morini, M.F. & Dejana, E., 2014. Signaling Pathways in the Specification of Arteries and Veins. *Arteriosclerosis, Thrombosis, and Vascular Biology* .
- Cornhill, F.J. & Roach, M.R., 1976. A quantitative study of the localization of atherosclerotic lesions in the rabbit aorta. *Atherosclerosis*, 23, pp.489–501.
- Coultas, L., Chawengsaksohak, K. & Rossant, J., 2005. Endothelial cells and VEGF in vascular development. *Nature*, 438(7070), pp.937–945.
- Cuhlmann, S. et al., 2011. Disturbed blood flow induces RelA expression via c-Jun N-terminal kinase 1: a novel mode of NF- κ B regulation that promotes arterial inflammation. *Circulation research*, 108(8), pp.950–9.

- Curci, C. et al., 2014. Endothelial-to-mesenchymal transition and renal fibrosis in ischaemia/reperfusion injury are mediated by complement anaphylatoxins and Akt pathway. *Nephrology Dialysis Transplantation* , 29 (4), pp.799–808.
- Dai, Y.-S. et al., 2002a. The Transcription Factors GATA4 and dHAND Physically Interact to Synergistically Activate Cardiac Gene Expression through a p300-dependent Mechanism. *Journal of Biological Chemistry* , 277 (27), pp.24390–24398.
- Dai, Y.-S. et al., 2002b. The transcription factors GATA4 and dHAND physically interact to synergistically activate cardiac gene expression through a p300-dependent mechanism. *The Journal of biological chemistry*, 277(27), pp.24390–8.
- Daoud, G. et al., 2014. BMP-mediated induction of GATA4/5/6 blocks somitic responsiveness to SHH. *Development (Cambridge, England)*, 141(20), pp.3978–3987.
- Dardik, A. et al., 2005. Differential effects of orbital and laminar shear stress on endothelial cells. *Journal of vascular surgery*, 41(5), pp.869–80.
- Das, A. & Crump, J.G., 2012. Bmps and Id2a Act Upstream of Twist1 To Restrict Ectomesenchyme Potential of the Cranial Neural Crest. *PLoS Genet*, 8(5), p.e1002710.
- Davies, P.F., 2009. Hemodynamic shear stress and the endothelium in cardiovascular pathophysiology. *Nature clinical practice. Cardiovascular medicine*, 6(1), pp.16–26.
- Davies, P.F. et al., 2013. The atherosusceptible endothelium: Endothelial phenotypes in complex hemodynamic shear stress regions in vivo. *Cardiovascular research*, ahead of p.
- Davies, P.F. et al., 1986. Turbulent fluid shear stress induces endothelial cell turnover in vitro. *Proceedings of the National Academy of Sciences*, 83, pp.2114–2117.
- Davies, P.F. et al., 1986. Turbulent fluid shear stress induces vascular endothelial cell turnover in vitro. *Proceedings of the National Academy of Sciences of the United States of America*, 83(7), pp.2114–2117.
- Davignon, J. & Ganz, P., 2004. Role of Endothelial Dysfunction in Atherosclerosis. *Circulation* , 109 (23 suppl 1), pp.III–27–III–32.
- Davis, S. et al., 1996. Isolation of Angiopoietin-1, a Ligand for the TIE2 Receptor, by Secretion-Trap Expression Cloning. *Cell*, 87(7), pp.1161–1169.
- Deissler, H. et al., 2006. TGF β induces transdifferentiation of iBREC to α SMA-

- expressing cells. *International Journal of Molecular Medicine*, 18.4, pp.577–582.
- Desprat, N. et al., 2008. Tissue Deformation Modulates Twist Expression to Determine Anterior Midgut Differentiation in *Drosophila* Embryos. *Developmental Cell*, 15(3), pp.470–477.
- Dolan, J.M. et al., 2012. Endothelial cells express a unique transcriptional profile under very high wall shear stress known to induce expansive arterial remodeling. *American Journal of Physiology - Cell Physiology*, 302(8), pp.C1109–C1118.
- Dolmetsch, R.E. et al., 1997. Differential activation of transcription factors induced by Ca²⁺ response amplitude and duration. *Nature*, 386(6627), pp.855–858.
- Dong, F. et al., 2005. Endothelin-1 enhances oxidative stress, cell proliferation and reduces apoptosis in human umbilical vein endothelial cells: role of ET(B) receptor, NADPH oxidase and caveolin-1. *British Journal of Pharmacology*, 145(3), pp.323–333.
- Dunn, J. et al., 2014. Flow-dependent epigenetic DNA methylation regulates endothelial gene expression and atherosclerosis. *The Journal of Clinical Investigation*, 124(7), pp.3187–3199.
- Echeverría, C. et al., 2014. Endotoxin Induces Fibrosis in Vascular Endothelial Cells through a Mechanism Dependent on Transient Receptor Protein Melastatin 7 Activity. *PLoS ONE*, 9(4), p.e94146.
- Eckert, M.A. et al., 2011. Twist1-induced invadopodia formation promotes tumor metastasis. *Cancer cell*, 19(3), pp.372–386.
- Egorova, A.D. et al., 2011. Lack of primary cilia primes shear-induced Endothelial-to-Mesenchymal Transition. *Circulation research*, 108(9), pp.1093–1101.
- El-Hachem, N. & Nemer, G., 2011. Identification of new GATA4-small molecule inhibitors by structure-based virtual screening. *Bioorganic & Medicinal Chemistry*, 19(5), pp.1734–1742.
- Ellertsdóttir, E. et al., 2010. Vascular morphogenesis in the zebrafish embryo. *Developmental Biology*, 341(1), pp.56–65.
- Evans, P.C., 2011. The influence of sulforaphane on vascular health and its relevance to nutritional approaches to prevent cardiovascular disease. *The EPMA Journal*, 2(1), pp.9–14.
- Fang, Y. et al., 2010. MicroRNA-10a regulation of proinflammatory phenotype in athero-susceptible endothelium in vivo and in vitro. *Proceedings of the National Academy of Sciences of the United States of America*, 107(30), pp.13450–5.

- Feng, M.-Y. et al., 2009. Gene Expression Profiling in TWIST-Depleted Gastric Cancer Cells. *The Anatomical Record: Advances in Integrative Anatomy and Evolutionary Biology*, 292(2), pp.262–270.
- Figeac, N. et al., 2007. Muscle stem cells and model systems for their investigation. *Developmental Dynamics*, 236(12), pp.3332–3342.
- Firulli, B.A. et al., 2005. Altered Twist1 and Hand2 dimerization is associated with Saethre-Chotzen syndrome and limb abnormalities. *Nature genetics*, 37(4), pp.373–381.
- Flamme, I., Frölich, T. & Risau, W., 1997. Molecular mechanisms of vasculogenesis and embryonic angiogenesis. *Journal of Cellular Physiology*, 173(2), pp.206–210.
- Fledderus, J.O. et al., 2007. Prolonged shear stress and KLF2 suppress constitutive proinflammatory transcription through inhibition of ATF2. *Blood*, 109(10), pp.4249–57.
- Florian, J.A. et al., 2003. Heparan Sulfate Proteoglycan Is a Mechanosensor on Endothelial Cells. *Circulation Research*, 93 (10), pp.e136–e142.
- Foteinos, G. et al., 2008. Rapid Endothelial Turnover in Atherosclerosis-Prone Areas Coincides With Stem Cell Repair in Apolipoprotein E-Deficient Mice. *Circulation*, 117 (14), pp.1856–1863.
- Froese, N. et al., 2011. GATA6 Promotes Angiogenic Function and Survival in Endothelial Cells by Suppression of Autocrine Transforming Growth Factor β /Activin Receptor-like Kinase 5 Signaling. *The Journal of Biological Chemistry*, 286(7), pp.5680–5690.
- Fry, D.L., 1969. Certain Histological and Chemical Responses of the Vascular Interface to Acutely Induced Mechanical Stress in the Aorta of the Dog. *Circulation Research*, 24(1), pp.93–108.
- Gajula, R.P., 2013. The Twist1 Box Domain Is Required for Twist1-induced Prostate Cancer Metastasis. *Molecular Cancer Research*, 11 pp. 1387
- Gambillara, V. et al., 2006. Plaque-prone hemodynamics impair endothelial function in pig carotid arteries. *American journal of physiology. Heart and circulatory physiology*, 290(6), pp.H2320–8.
- Gareus, R. et al., 2008. Endothelial cell-specific NF-kappaB inhibition protects mice from atherosclerosis. *Cell metabolism*, 8(5), pp.372–83.
- Garg, V. et al., 2003. GATA4 mutations cause human congenital heart defects and reveal an interaction with TBX5. *Nature*, 424(6947), pp.443–447.

- Gaspar-Pereira, S. et al., 2012. The NF- κ B Subunit c-Rel Stimulates Cardiac Hypertrophy and Fibrosis. *The American Journal of Pathology*, 180(3), pp.929–939.
- Gasperini, P. et al., 2012. Kaposi Sarcoma Herpesvirus Promotes Endothelial-to-Mesenchymal Transition through Notch-Dependent Signaling. *Cancer research*, 72(5), pp.1157–1169.
- Gavard, J. & Gutkind, J.S., 2006. VEGF controls endothelial-cell permeability by promoting the [beta]-arrestin-dependent endocytosis of VE-cadherin. *Nat Cell Biol*, 8(11), pp.1223–1234.
- George, R.M. et al., 2015. Notch signaling represses GATA4-induced expression of genes involved in steroid biosynthesis. *Reproduction*, 150 (4), pp.383–394.
- Ghouzzi, V. El et al., 1997. Mutations of the TWIST gene in the Saethre-Chotzene syndrome. *Nat Genet*, 15(1), pp.42–46.
- Giampietro, C. et al., 2012. Overlapping and divergent signaling pathways of N-cadherin and VE-cadherin in endothelial cells. *Blood*, 119(9), pp.2159–70.
- von Gise, A. & Pu, W.T., 2012. Endocardial and epicardial epithelial to mesenchymal transitions in heart development and disease. *Circulation research*, 110(12), pp.1628–1645.
- Glagov S, Vito R, Giddens DP, Z.C., 1992. Micro-architecture and composition of artery walls: relationship to location, diameter and the distribution of mechanical stress. *Journal of Hypertension*, 6, pp.S101–104.
- Göthert, J.R. et al., 2004. Genetically tagging endothelial cells in vivo: bone marrow-derived cells do not contribute to tumor endothelium. *Blood*, 104(6), pp.1769–1777.
- Gould, K.L. et al., 1994. Short-term cholesterol lowering decreases size and severity of perfusion abnormalities by positron emission tomography after dipyridamole in patients with coronary artery disease. A potential noninvasive marker of healing coronary endothelium. *Circulation*, 89 (4), pp.1530–1538.
- Grande, M.T. et al., 2015. Snail1-induced partial epithelial-to-mesenchymal transition drives renal fibrosis in mice and can be targeted to reverse established disease. *Nat Med*, 21(9), pp.989–997.
- Grépin, C. et al., 1995. Inhibition of transcription factor GATA-4 expression blocks in vitro cardiac muscle differentiation. *Molecular and Cellular Biology*, 15(8), pp.4095–4102.
- Guevara, N. V et al., 1999. The absence of p53 accelerates atherosclerosis by

- increasing cell proliferation in vivo. *Nat Med*, 5(3), pp.335–339.
- Gupta, V. et al., 2013. An Injury-Responsive Gata4 Program Shapes the Zebrafish Cardiac Ventricle. *Current biology : CB*, 23(13), pp.1221–1227.
- Hahn, C. et al., 2011. JNK2 Promotes Endothelial Cell Alignment under Flow L. Zhang, ed. *PLoS ONE*, 6(8), p.e24338.
- Hajra, L. et al., 2000. The NF- κ B signal transduction pathway in aortic endothelial cells is primed for activation in regions predisposed to atherosclerotic lesion formation. *Proceedings of the National Academy of Sciences of the United States of America*, 97(16), pp.9052–9057.
- Halcox JPJ, Schenk WH, Z.G., 2002. Prognostic value of coronary vascular endothelial function. *Circulation*, 106, pp.653–658.
- Hamamori, Y. et al., 1999. Regulation of Histone Acetyltransferases p300 and PCAF by the bHLH Protein Twist and Adenoviral Oncoprotein E1A. *Cell*, 96(3), pp.405–413.
- Han, M. et al., 2012. GATA4 expression is primarily regulated via a miR-26b-dependent post-transcriptional mechanism during cardiac hypertrophy. *Cardiovascular Research*, 93(4), pp.645–654.
- Han, Y, Moon, J You, R, Kim, S. Z., Kim, S. H., Park, W.H., 2009. JNK and p38 inhibitors increase and decrease apoptosis, respectively, in pyrogallol-treated calf pulmonary arterial endothelial cells. *International Journal of Molecular Medicine*, 24.5, pp.717–722.
- Hansson, G.K. et al., 1985. Aortic endothelial cell death and replication in normal and lipopolysaccharide-treated rats. *The American Journal of Pathology*, 121(1), pp.123–127.
- Harvey, W., 1928. *Exercitatio anatomica de motu cordis et sanguinis in animalibus (English translation)* Tercentenn., Illinois: Charles C Thomas.
- Haveri, H. et al., 2009. Enhanced expression of transcription factor GATA-4 in inflammatory bowel disease and its possible regulation by TGF-beta1. *Journal of clinical immunology*, 29(4), pp.444–53.
- He, C. et al., 2015. PDGFR[beta] signalling regulates local inflammation and synergizes with hypercholesterolaemia to promote atherosclerosis. *Nat Commun*, 6.
- Heckel, E. et al., 2015. Oscillatory Flow Modulates Mechanosensitive klf2a Expression through trpv4 and trpp2 during Heart Valve Development. *Current Biology*, 25(10), pp.1354–1361.

- Heerboth, S. et al., 2015. EMT and tumor metastasis. *Clinical and Translational Medicine*, 4, pp.0015–0048.
- Van der Heiden, K. et al., 2007. Endothelial primary cilia in areas of disturbed flow are at the base of atherosclerosis. *Atherosclerosis*, 196(2), pp.542–550.
- Heineke, J., Auger-messier, M., et al., 2007. Cardiomyocyte GATA4 functions as a stress- responsive regulator of angiogenesis in the murine heart. *The Journal of Clinical investigation*, 117(11), pp.3198– 3210.
- Heineke, J., Auger-Messier, M., et al., 2007. Cardiomyocyte GATA4 functions as a stress-responsive regulator of angiogenesis in the murine heart. *The Journal of Clinical Investigation*, 117(11), pp.3198–3210.
- Hirasawa, M. et al., 2011. Transcriptional factors associated with epithelial-mesenchymal transition in choroidal neovascularization. *Molecular Vision*, 17, pp.1222–1230.
- His, W., 1865. *Die Häute und Höhlen des Körpersle*, Basel: Schwighauser.
- Hoefler, I.E., Den Adel, B. & Daemen, M.J. a P., 2013. Biomechanical factors as triggers of vascular growth. *Cardiovascular Research*, 99, pp.276–283.
- Hong, J. et al., 2011a. Phosphorylation of Serine 68 of Twist1 by MAPKs Stabilizes Twist1 Protein and Promotes Breast Cancer Cell Invasiveness. *Cancer research*, 71(11), pp.3980–3990.
- Hong, J. et al., 2011b. Phosphorylation of serine 68 of Twist1 by MAPKs stabilizes Twist1 protein and promotes breast cancer cell invasiveness. *Cancer research*, 71(11), pp.3980–90.
- Hornik, C. et al., 2004. Twist is an integrator of SHH, FGF, and BMP signaling. *Anatomy and Embryology*, 209(1), pp.31–39.
- Hove, J.R. et al., 2003. Intracardiac fluid forces are an essential epigenetic factor for embryonic cardiogenesis. *Nature*, 421(6919), pp.172–177.
- Howard, T.D. et al., 1997. Mutations in TWIST, a basic helix-loop-helix transcription factor, in Saethre-Chatzen syndrome. *Nat Genet*, 15(1), pp.36–41.
- Hu, Y.-C., Okumura, L.M. & Page, D.C., 2013. *Gata4* Is Required for Formation of the Genital Ridge in Mice. *PLoS Genet*, 9(7), p.e1003629.
- Huveneers, S. et al., 2012. Vinculin associates with endothelial VE-cadherin junctions to control force-dependent remodeling. *The Journal of Cell Biology* , 196 (5), pp.641–652.

- Huynh, J. et al., 2011. Age-Related Intimal Stiffening Enhances Endothelial Permeability and Leukocyte Transmigration. *Science Translational Medicine*, 3(112), pp.112ra122–112ra122.
- Hwang, J. et al., 2003. Pulsatile versus oscillatory shear stress regulates NADPH oxidase subunit expression: implication for native LDL oxidation. *Circulation research*, 93(12), pp.1225–32.
- Ieda, M. et al., 2010. Direct Reprogramming of Fibroblasts into Functional Cardiomyocytes by Defined Factors. *Cell*, 142(3), pp.375–386.
- Ikeda, S. et al., 2009. MicroRNA-1 Negatively Regulates Expression of the Hypertrophy-Associated Calmodulin and Mef2a Genes. *Molecular and Cellular Biology*, 29(8), pp.2193–2204.
- Inagawa, K. et al., 2012. Induction of Cardiomyocyte-Like Cells in Infarct Hearts by Gene Transfer of Gata4, Mef2c, and Tbx5. *Circulation Research*, 111(9), pp.1147–1156.
- Ingber, D., 1998. In search of cellular control: Signal transduction in context. *Journal of Cellular Biochemistry*, 72(S30–31), pp.232–237.
- Ingber, D., 1991. Integrins as mechanochemical transducers. *Current Opinion in Cell Biology*, 3(5), pp.841–848.
- Ishii, H. & Saito, T., 2008. Cancer Metastasis as Disrupted Developmental Phenotype. *Current Genomics*, 9(1), pp.25–28.
- Jay, P.Y. et al., 2007. Impaired mesenchymal cell function in Gata4 mutant mice leads to diaphragmatic hernias and primary lung defects. *Developmental biology*, 301(2), pp.602–614.
- Jiang, Y., Drysdale, T.A. & Evans, T., 1999. A Role for GATA-4/5/6 in the Regulation of Nkx2.5 Expression with Implications for Patterning of the Precardiac Field. *Developmental Biology*, 216(1), pp.57–71.
- Jiang, Y.-Z. et al., 2015. Arterial endothelial methylome: differential DNA methylation in athero-susceptible disturbed flow regions in vivo. *BMC Genomics*, 16(1), p.506.
- Jo, H., Song, H. & Mowbray, A., 2006. Role of NADPH Oxidases in Disturbed Flow- and BMP4- Induced Inflammation and Atherosclerosis. *Antioxidants & Redox Signaling*, 8, pp.1609–1619.
- Jones, L.R. et al., 1998. Regulation of Ca²⁺ signaling in transgenic mouse cardiac myocytes overexpressing calsequestrin. *Journal of Clinical Investigation*, 101(7), pp.1385–1393.

- Kamei, C.N. et al., 2011. Promotion of Avian Endothelial Cell Differentiation by GATA Transcription Factors. *Developmental biology* 353 (1), pp. 29–37.
- Kang, C. et al., 2015. The DNA damage response induces inflammation and senescence by inhibiting autophagy of GATA4. *Science* , 349 (6255).
- Keele & KD., 1952. Leonardo da Vinci's Anatomia Naturale. *The Yale Journal of Biology and Medicine.*, 52, pp.369–409.
- Kempe, S. et al., 2005. NF- κ B controls the global pro-inflammatory response in endothelial cells: evidence for the regulation of a pro-atherogenic program. *Nucleic Acids Research*, 33(16), pp.5308–5319.
- Kheirloom, A. et al., 2015. Multifunctional Nanoparticles Facilitate Molecular Targeting and miRNA Delivery to Inhibit Atherosclerosis in ApoE^{-/-} Mice. *ACS Nano*, 9(9), pp.8885–8897.
- Khurana, R. et al. 2005. Role of angiogenesis in Cardiovascular Disease: A Critical Appraisal. *Circulation*. 112 pp. 1813-1824
- Kim, C.W. et al., 2013. Anti-inflammatory and anti-atherogenic role of BMP Receptor II in endothelial cells. *Arteriosclerosis, thrombosis, and vascular biology*, 33(6), pp.1350–1359.
- Kinlay, S. & Ganz, P., 2000. Relation between endothelial dysfunction and the acute coronary syndrome: implications for therapy. *American Journal of Cardiology*, 86(8), pp.10–13.
- Kisanuki, Y.Y. et al., 2001. Tie2-Cre Transgenic Mice: A New Model for Endothelial Cell-Lineage Analysis in Vivo. *Developmental Biology*, 230(2), pp.230–242.
- Klaunig, J.E., Kamendulis, L.M. & Hocevar, B.A., 2010. Oxidative Stress and Oxidative Damage in Carcinogenesis. *Toxicologic Pathology* , 38 (1), pp.96–109.
- Kokudo, T. et al., 2008. Snail is required for TGF β -induced endothelial-mesenchymal transition of embryonic stem cell-derived endothelial cells. *Journal of Cell Science*, 121(20), pp.3317–3324.
- Kuo, C.T. et al., 1997. GATA4 transcription factor is required for ventral morphogenesis and heart tube formation. *Genes & development*, 11(8), pp.1048–60.
- Kyriakis, J.M. & Avruch, J., 2001. Mammalian mitogen-activated protein kinase signal transduction pathways activated by stress and inflammation. *Physiological*

- reviews*, 81(2), pp.807–69.
- Kyrölahti, A. et al., 2008. GATA-4 regulates Bcl-2 expression in ovarian granulosa cell tumors. *Endocrinology*, 149(11), pp.5635–42.
- Kyrölahti, A. et al., 2010. GATA4 protects granulosa cell tumors from TRAIL-induced apoptosis. *Endocrine-Related Cancer*, 17 (3), pp.709–717.
- Lamina, C. et al., 2011. Look beyond one's own nose: Combination of information from publicly available sources reveals an association of GATA4 polymorphisms with plasma triglycerides. *Atherosclerosis*, 219(2), pp.698–703.
- Lamouille, S., Xu, J. & Derynck, R., 2014. Molecular mechanisms of epithelial–mesenchymal transition. *Nature reviews. Molecular cell biology*, 15(3), pp.178–196.
- Lancaster, M.A., Schroth, J. & Gleeson, J.G., 2011. Subcellular Spatial Regulation of Canonical WNT Signaling at the Primary Cilium. *Nature cell biology*, 13(6), pp.700–707.
- Laufs, U. et al., 1998. Upregulation of Endothelial Nitric Oxide Synthase by HMG CoA Reductase Inhibitors. *Circulation*, 97 (12), pp.1129–1135.
- Lee, D.-Y. et al., 2012. Role of histone deacetylases in transcription factor regulation and cell cycle modulation in endothelial cells in response to disturbed flow. *Proceedings of the National Academy of Sciences*, 109 (6), pp.1967–1972.
- Lee, J.G. & Kay, E.P., 2006. FGF-2-mediated signal transduction during endothelial mesenchymal transformation in corneal endothelial cells. *Experimental Eye Research*, 83(6), pp.1309–1316.
- Lee, J.S. et al., 2006. Klf2 is an essential regulator of vascular hemodynamic forces in vivo. *Developmental cell*, 11(6), pp.845–57.
- Lee, M.P. & Yutzey, K.E., 2011. Twist1 directly regulates genes that promote cell proliferation and migration in developing heart valves. *PLoS one*, 6(12), p.e29758.
- Lee, Y. et al., 1998. The Cardiac Tissue-Restricted Homeobox Protein Csx/Nkx2.5 Physically Associates with the Zinc Finger Protein GATA4 and Cooperatively Activates Atrial Natriuretic Factor Gene Expression. *Molecular and Cellular Biology*, 18(6), pp.3120–3129.
- Leopold, J.A., 2012. Cellular Mechanisms of Aortic Valve Calcification. *Circulation: Cardiovascular Interventions*, 5 (4), pp.605–614.
- Leroy, P. & Mostov, K.E., 2007. Slug Is Required for Cell Survival during Partial

- Epithelial-Mesenchymal Transition of HGF-induced Tubulogenesis B. Margolis, ed. *Molecular Biology of the Cell*, 18(5), pp.1943–1952.
- Li, J. et al., 2014. Endothelial TWIST1 Promotes Pathological Ocular Angiogenesis. *Investigative Ophthalmology & Visual Science*, 55(12), pp.8267–8277.
- Li, R. et al., 2014. Shear Stress-Activated WNT-Angiopoietin-2 Signaling Recapitulated Vascular Repair in Zebrafish Embryos. *Arteriosclerosis, thrombosis, and vascular biology*, 34(10), pp.2268–2275.
- Libby, P., 2002. Inflammation and Atherosclerosis. *Circulation*, 105(9), pp.1135–1143.
- Liebner, S. et al., 2004. β -Catenin is required for endothelial-mesenchymal transformation during heart cushion development in the mouse. *The Journal of Cell Biology*, 166(3), pp.359–367.
- Lim, J. & Thiery, J.P., 2012a. Epithelial-mesenchymal transitions: insights from development. *Development*, 139(19), pp.3471–3486.
- Limana, F. et al., 2007. Identification of Myocardial and Vascular Precursor Cells in Human and Mouse Epicardium. *Circulation Research*, 101(12), pp.1255–1265.
- Lin, F., Wang, N. & Zhang, T.-C., 2012. The role of endothelial–mesenchymal transition in development and pathological process. *IUBMB Life*, 64(9), pp.717–723.
- Lin, K. et al., 2000. Molecular mechanism of endothelial growth arrest by laminar shear stress. *Proceedings of the National Academy of Sciences of the United States of America*, 97(17), pp.9385–9.
- Lin, X. & Xu, X., 2008. Distinct functions of WNT/ β -catenin signaling in KV development and cardiac asymmetry. *Development*, 136(2), pp.207–217.
- Liu, J. et al., 2009. Integrins are required for the differentiation of visceral endoderm. *Journal of Cell Science*, 122(2), pp.233–242.
- Liu, Y. et al., 2015. Loss of BRMS1 Promotes a Mesenchymal Phenotype through NF- κ B-Dependent Regulation of Twist1. *Molecular and Cellular Biology*, 35(1), pp.303–317.
- Liu, Y. et al., 2004. Rho Kinase–Induced Nuclear Translocation of ERK1/ERK2 in Smooth Muscle Cell Mitogenesis Caused by Serotonin. *Circulation Research*, 95(6), pp.579–586.
- Loebel, D.A.F. et al., 2002. Isolation of differentially expressed genes from wild-type and Twist mutant mouse limb buds. *genesis*, 33(3), pp.103–113.

- Lopez, D. et al., 2009. Tumor-induced upregulation of Twist, Snail, and Slug represses the activity of the human VE-cadherin promoter. *Archives of Biochemistry and Biophysics*, 482(1–2), pp.77–82.
- Lourenço, D. et al., 2011. Loss-of-function mutation in GATA4 causes anomalies of human testicular development. *Proceedings of the National Academy of Sciences of the United States of America*, 108(4), pp.1597–1602.
- Lovisa, S. et al., 2015. Epithelial-to-mesenchymal transition induces cell cycle arrest and parenchymal damage in renal fibrosis. *Nature Medicine*, 21(9), pp.998–1009.
- Luna-Zurita, L. et al., 2010. Integration of a Notch-dependent mesenchymal gene program and Bmp2-driven cell invasiveness regulates murine cardiac valve formation. *The Journal of Clinical Investigation*, 120(10), pp.3493–3507.
- Luo, Y. & Radice, G.L., 2005. N-cadherin acts upstream of VE-cadherin in controlling vascular morphogenesis. *The Journal of Cell Biology*, 169(1), pp.29–34.
- Ma, L. et al., 2005. Bmp2 is essential for cardiac cushion epithelial-mesenchymal transition and myocardial patterning. *Development*, 132(24), pp.5601–5611.
- Mabile, L. et al., 1997. Mitochondrial Function Is Involved in LDL Oxidation Mediated by Human Cultured Endothelial Cells. *American heart association*, 17, pp.1575–1582.
- Maddaluno, L. et al., 2013. EndMT contributes to the onset and progression of cerebral cavernous malformations. *Nature*, 498(7455), pp.492–6.
- Maestro, R. et al., 1999. twist is a potential oncogene that inhibits apoptosis. *Genes & Development*, 13(17), pp.2207–2217.
- Mahler, G.J. et al., 2014. Effects of shear stress pattern and magnitude on mesenchymal transformation and invasion of aortic valve endothelial cells. *Biotechnology and bioengineering*, 111(11), pp.2326–2337.
- Malpighi, M., 1685. *De Externo Tactus Organo Anatomica Observatio*, Naples, Italy: Aegidium Longum.
- Mammoto, A. et al., 2009. A mechanosensitive transcriptional mechanism that controls angiogenesis. *Nature*, 457(7233), pp.1103–1108.
- Mammoto, T. et al., 2013. Twist1 Controls Lung Vascular Permeability and Endotoxin-Induced Pulmonary Edema by Altering Tie2 Expression. *PLoS ONE*, 8(9), p.e73407.
- Markwald, R.R., Fitzharris, T.P. & Smith, W.N.A., 1975. Structural analysis of

- endocardial cytodifferentiation. *Developmental Biology*, 42(1), pp.160–180.
- Masckauchán, T.N. et al., 2005. WNT/ β -Catenin Signaling Induces Proliferation, Survival and Interleukin-8 in Human Endothelial Cells. *Angiogenesis*, 8(1), pp.43–51.
- Matarín, M. et al., 2007. A genome-wide genotyping study in patients with ischaemic stroke: initial analysis and data release. *Lancet neurology*, 6(5), pp.414–420.
- McCulley, D.J. et al., 2008. BMP4 is required in the anterior heart field and its derivatives for endocardial cushion remodeling, outflow tract septation, and semilunar valve development. *Developmental dynamics : an official publication of the American Association of Anatomists*, 237(11), pp.3200–3209.
- McFadden, D.G. et al., 2000. A GATA-dependent right ventricular enhancer controls dHAND transcription in the developing heart. *Development (Cambridge, England)*, 127(24), pp.5331–41.
- Mcfadden, D.G. et al., 2002. Misexpression of dHAND induces ectopic digits in the developing limb bud in the absence of direct DNA binding. *Development*, 3088, pp.3077–3088.
- Medici, D. et al., 2010. Conversion of vascular endothelial cells into multipotent stem-like cells. *Nat Med*, 16(12), pp.1400–1406.
- Medici, D. & Kalluri, R., 2012. Endothelial-mesenchymal transition and its contribution to the emergence of stem cell phenotype. *Seminars in cancer biology*, 22(5-6), pp.379–84.
- Medici, D., Potenta, S. & Kalluri, R., 2011. Transforming Growth Factor- β 2 promotes Snail-mediated endothelial-mesenchymal transition through convergence of Smad-dependent and Smad-independent signaling. *The Biochemical journal*, 437(3), pp.515–520.
- van Meeteren, L. a & ten Dijke, P., 2012. Regulation of endothelial cell plasticity by TGF- β . *Cell and tissue research*, 347(1), pp.177–86.
- Meng, H. et al., 2007. Complex Hemodynamics at the Apex of an Arterial Bifurcation Induces Vascular Remodeling Resembling Cerebral Aneurysm Initiation. *Stroke; a journal of cerebral circulation*, 38(6), pp.1924–1931.
- Merindol, N. et al., 2014. The emerging role of Twist proteins in hematopoietic cells and hematological malignancies. *Blood Cancer Journal*, 4, p.e206.
- Miao, H. et al., 2005. Effects of Flow Patterns on the Localization and Expression of VE-Cadherin at Vascular Endothelial Cell Junctions: In vivo and in vitro Investigations. *Journal of Vascular Research*, 42(1), pp.77–89.

- Michiels, C., 2003. Endothelial cell functions. *Journal of Cellular Physiology*, 196(3), pp.430–443.
- Minoux, M. & Rijli, F.M., 2010. Molecular mechanisms of cranial neural crest cell migration and patterning in craniofacial development. *Development*, 137(16), pp.2605–2621.
- Miyazaki, T. et al., 2011. m-Calpain Induction in Vascular Endothelial Cells on Human and Mouse Atheromas and Its Roles in VE-Cadherin Disorganization and Atherosclerosis. *Circulation*, 124 (23), pp.2522–2532.
- Mohri, Z. & Weinberg, P.D., 2012. Patterns of permeability in the mouse aortic arch are determined by pecam-1. *Atherosclerosis*, 225(2), p.e1.
- Moonen, J.-R. a J. et al., 2015. Endothelial-to-mesenchymal transition contributes to fibro-proliferative vascular disease and is modulated by fluid shear stress. *Cardiovascular research*, pp.1–10.
- Morad, M. & Suzuki, Y., 2000. edox regulation of cardiac muscle calcium signaling. *Antioxidant Redox Signalling*, 2, pp.65–71.
- Moskowitz, I.P. et al., 2011. Transcription factor genes Smad4 and Gata4 cooperatively regulate cardiac valve development. *Proceedings of the National Academy of Sciences of the United States of America*, 108(10), pp.4006–4011.
- Murre, C., McCaw, P.S. & Baltimore, D., 1989. A new DNA binding and dimerization motif in immunoglobulin enhancer binding, daughterless, MyoD, and myc proteins. *Cell*, 56(5), pp.777–783.
- Nairismägi, M. et al., 2013. The Proto-Oncogene TWIST1 Is Regulated by MicroRNAs. *PLoS ONE*, 5, p.e66070.
- Nauli, S.M. et al., 2008. Endothelial Cilia Are Fluid Shear Sensors That Regulate Calcium Signaling and Nitric Oxide Production Through Polycystin-1. *Circulation*, 117 (9), pp.1161–1171.
- Navarro, P., Ruco, L. & Dejana, E., 1998. Differential localization of VE- and N-cadherins in human endothelial cells: VE-cadherin competes with N-cadherin for junctional localization. *The Journal of cell biology*, 140(6), pp.1475–84.
- Niu, R. et al., 2007. Up-regulation of Twist induces angiogenesis and correlates with metastasis in hepatocellular carcinoma. *Cancer Research*, 67 (9 Supplement), p.5364.
- Nusslein-Volhard, C., Frohnhof, H.G. & Lehmann, R., 1987. Determination of

- anteroposterior polarity in *Drosophila*. *Science*, 238 (4834), pp.1675–1681.
- O'Rourke, M.P. et al., 2002. Twist Plays an Essential Role in FGF and SHH Signal Transduction during Mouse Limb Development. *Developmental Biology*, 248(1), pp.143–156.
- Obikane, H. et al., 2007. Effect of endothelial cell proliferation on atherogenesis: A role of p21Sdi/Cip/Waf1 in monocyte adhesion to endothelial cells. *Atherosclerosis*, 212(1), pp.116–122.
- Oda, M. et al., 2013. DNA Methylation Restricts Lineage-specific Functions of Transcription Factor Gata4 during Embryonic Stem Cell Differentiation J. M. Greally, ed. *PLoS Genetics*, 9(6), p.e1003574.
- Oka, T. et al., 2006. Cardiac-Specific Deletion of Gata4 Reveals Its Requirement for Hypertrophy, Compensation, and Myocyte Viability. *Circulation Research*, 98 (6), pp.837–845.
- Orr, A.W. et al., 2005. The subendothelial extracellular matrix modulates NF- κ B activation by flow: a potential role in atherosclerosis. *The Journal of Cell Biology*, 169(1), pp.191–202.
- Orsenigo, F. et al., 2012. Phosphorylation of VE-cadherin is modulated by haemodynamic forces and contributes to the regulation of vascular permeability in vivo. *Nature Communications*, 3, p.1208.
- Ostrowski, M.A. et al., 2014. Microvascular Endothelial Cells Migrate Upstream and Align Against the Shear Stress Field Created by Impinging Flow. *Biophysical Journal*, 106(2), pp.366–374.
- Park, A.-M. et al., 2010. PULMONARY HYPERTENSION-INDUCED GATA4 ACTIVATION IN THE RIGHT VENTRICLE. *Hypertension*, 56(6), pp.1145–1151.
- Passerini, A.G. et al., 2004. Coexisting proinflammatory and antioxidative endothelial transcription profiles in a disturbed flow region of the adult porcine aorta. *Proceedings of the National Academy of Sciences of the United States of America*, 101(8), pp.2482–7.
- Patan, S., 2004. Vasculogenesis and angiogenesis. *Cancer Treatment Research*, 117, pp.3–32.
- Piccinin, S. et al., 2012. A “Twist box” Code of p53 Inactivation: Twist box:p53 Interaction Promotes p53 Degradation. *Cancer Cell*, 22(3), pp.404–415.
- Platt, J., 1894. Ontogenetische differenzierung des ektoderms in necturus. *Archiv für*

- Mikroskopische Anatomie*, 43, pp.911–966.
- Pouille, P.-A. et al., 2009. Mechanical Signals Trigger Myosin II Redistribution and Mesoderm Invagination in Drosophila Embryos. *Science Signaling*, 2(66), pp.ra16–ra16.
- Qin, Q. et al., 2012. Normal and disease-related biological functions of Twist1 and underlying molecular mechanisms. *Cell Research*, 22(1), pp.90–106.
- Rader, D.J. & Daugherty, A., 2008. Translating molecular discoveries into new therapies for atherosclerosis. *Nature*, 451(7181), pp.904–13.
- Rajagopal, S.K. et al., 2007. Spectrum of Heart Disease Associated with Murine and Human GATA4 Mutation. *Journal of molecular and cellular cardiology*, 43(6), pp.677–685.
- Ranchoux, B. et al., 2015. Endothelial-to-Mesenchymal Transition in Pulmonary Hypertension. *Circulation*, 131(11), pp.1006–1018.
- Rehm, M. et al., 2007. Shedding of Endothelial Glycocalyx In Patients Undergoing Major Vascular Surgery With Global And Regional Ischemia. *Circulation*, 116, pp. 1896-1906.
- Reinhold, M.I. et al., 2006. The WNT-inducible transcription factor Twist1 inhibits chondrogenesis. *The Journal of biological chemistry*, 281(3), pp.1381–8.
- Ribatti, D., 2009. William Harvey and the discovery of the circulation of the blood. *Journal of Angiogenesis Research*, 1, p.3.
- Rice, D.P.C. et al., 2010. Gli3(Xt–J/Xt–J) mice exhibit lambdoid suture craniosynostosis which results from altered osteoprogenitor proliferation and differentiation. *Human Molecular Genetics*, 19(17), pp.3457–3467.
- Rivera-Feliciano, J. et al., 2006. Development of heart valves requires Gata4 expression in endothelial-derived cells. *Development (Cambridge, England)*, 133(18), pp.3607–3618.
- Rojas, A. et al., 2005. Gata4 expression in lateral mesoderm is downstream of BMP4 and is activated directly by Forkhead and GATA transcription factors through a distal enhancer element. *Development*, 132(15), pp.3405–3417.
- Rojas, A. et al., 2008. GATA4 Is a Direct Transcriptional Activator of Cyclin D2 and Cdk4 and Is Required for Cardiomyocyte Proliferation in Anterior Heart Field-Derived Myocardium. *Molecular and Cellular Biology*, 28(17), pp.5420–5431.
- Rokitansky, C., 1855. *A manual of pathological anatomy*, Philadelphia: Blanchard and Lea.

- Rotherham, M. & El Haj, A.J., 2015. Remote Activation of the WNT/ β -Catenin Signalling Pathway Using Functionalised Magnetic Particles S.-J. Tang, ed. *PLoS ONE*, 10(3), p.e0121761.
- Runyan, R.B. & Markwald, R.R., 1983. Invasion of mesenchyme into three-dimensional collagen gels: A regional and temporal analysis of interaction in embryonic heart tissue. *Developmental Biology*, 95(1), pp.108–114.
- Rysä, J. et al., 2010. GATA-4 is an angiogenic survival factor of the infarcted heart. *Circulation. Heart failure*, 3(3), pp.440–50.
- Samani, N.J. et al., 2007. Genomewide Association Analysis of Coronary Artery Disease. *The New England journal of medicine*, 357(5), pp.443–453.
- Sánchez-Duffhues, G. et al., 2015. SLUG Is Expressed in Endothelial Cells Lacking Primary Cilia to Promote Cellular Calcification. *Arteriosclerosis, Thrombosis, and Vascular Biology*, 35 (3), pp.616–627.
- Schaar, J. a et al., 2004. Terminology for high-risk and vulnerable coronary artery plaques. Report of a meeting on the vulnerable plaque, June 17 and 18, 2003, Santorini, Greece. *European heart journal*, 25(12), pp.1077–82.
- Schächinger V, Britten MB, Z.A., 2000. Prognostic impact of coronary vasodilator dysfunction and adverse long-term outcome of coronary heart disease. *Circulation*, 101, pp.1899–1906.
- Schaefer, C.A. et al., 2006. Statins inhibit hypoxia-induced endothelial proliferation by preventing calcium-induced ROS formation. *Atherosclerosis*, 185(2), pp.290–296.
- Schlesinger, J. et al., 2011. The Cardiac Transcription Network Modulated by Gata4, Mef2a, Nkx2.5, Srf, Histone Modifications, and MicroRNAs. *PLoS Genet*, 7(2), p.e1001313.
- Schmittgen, T.D. & Livak, K.J., 2008. Analyzing real-time PCR data by the comparative CT method. *Nature Protocols*, 3(6), pp.1101–1108.
- Schober, A. et al., 2014. MicroRNA-126-5p promotes endothelial proliferation and limits atherosclerosis by suppressing Dlk1. *Nature medicine*, (November 2013).
- Seher, T.C. et al., 2007. Analysis and reconstitution of the genetic cascade controlling early mesoderm morphogenesis in the Drosophila embryo. *Mechanisms of Development*, 124(3), pp.167–179.
- SenBanerjee, S., Lin, Z., Atkins, G.B., Greif, D.M., Rao, R.M., Kumar, A., Feinberg,

- M.W., Chen, Z., Simon, D.I., Lusinskas, F.W., Michel, T.M., Gimbrone, M.A., et al., 2004. KLF2 Is a Novel Transcriptional Regulator of Endothelial Proinflammatory Activation. *The Journal of Experimental Medicine* , 199 (10), pp.1305–1315.
- Shamir, E.R. et al., 2014. Twist1-induced dissemination preserves epithelial identity and requires E-cadherin. *The Journal of Cell Biology* , 204 (5), pp.839–856.
- Shelton, E.L. & Yutzey, K.E., 2008. Twist1 function in endocardial cushion cell proliferation, migration, and differentiation during heart valve development. *Developmental biology*, 317(1), pp.282–295.
- Shih, W. & Yamada, S., 2012. N-cadherin as a key regulator of collective cell migration in a 3D environment. *Cell Adhesion & Migration*, 6(6), pp.513–517.
- Shyy, J.Y.-J. & Chien, S., 2002. Role of Integrins in Endothelial Mechanosensing of Shear Stress. *Circulation Research* , 91 (9), pp.769–775.
- Sill, H.W. et al., 1995. Shear stress increases hydraulic conductivity of cultured endothelial monolayers. *American Journal of Physiology - Heart and Circulatory Physiology*, 268(2), pp.H535–H543.
- Simpson, P., 1983. Maternal-Zygotic Gene Interactions during Formation of the Dorsoventral Pattern in *Drosophila* Embryos. *Genetics*, 105(3), pp.615–632.
- Smit, M.A. et al., 2009. A Twist-Snail Axis Critical for TrkB-Induced Epithelial-Mesenchymal Transition-Like Transformation, Anoikis Resistance, and Metastasis . *Molecular and Cellular Biology*, 29(13), pp.3722–3737.
- Smith, C.L. et al., 2011. Epicardial derived cell epithelial to mesenchymal transition and fate specification require PDGF receptor signaling. *Circulation research*, 108(12), pp.e15–e26.
- Son, D.J. et al., 2012. Piperlongumine inhibits atherosclerotic plaque formation and vascular smooth muscle cell proliferation by suppressing PDGF receptor signaling. *Biochemical and biophysical research communications*, 427(2), pp.349–354.
- Son, D.J. et al., 2013. The atypical mechanosensitive microRNA-712 derived from pre-ribosomal RNA induces endothelial inflammation and atherosclerosis. *Nature communications*, 4, p.3000.

- Song, H. et al., 2009. Critical Role for GATA3 in Mediating Tie2 Expression and Function in Large Vessel Endothelial Cells. *The Journal of Biological Chemistry*, 284(42), pp.29109–29124.
- Song, M.-R. et al., 2006. T-Box transcription factor Tbx20 regulates a genetic program for cranial motor neuron cell body migration. *Development*, 133(24), pp.4945–4955.
- Soo, K. et al., 2002. Twist Function Is Required for the Morphogenesis of the Cephalic Neural Tube and the Differentiation of the Cranial Neural Crest Cells in the Mouse Embryo. *Developmental Biology*, 247(2), pp.251–270.
- Sorescu, G.P. et al., 2004. Bone morphogenic protein 4 produced in endothelial cells by oscillatory shear stress induces monocyte adhesion by stimulating reactive oxygen species production from a nox1-based NADPH oxidase. *Circulation research*, 95(8), pp.773–9.
- Šošić, D. et al., 2003. Twist regulates cytokine gene expression through a negative feedback loop that represses NF-kappaB activity. *Cell*, 112(2), pp.169–80.
- Staughton, T.J., Lever, M.J. & Weinberg, P.D., 2001. Effect of altered flow on the pattern of permeability around rabbit aortic branches. *American Journal of Physiology - Heart and Circulatory Physiology*, 281(1), pp.H53–H59.
- Stefanovic, S. et al., 2014. GATA-dependent regulatory switches establish atrioventricular canal specificity during heart development. *Nat Commun*, 5.
- Steinman, D. a., 2002. Image-Based Computational Fluid Dynamics Modeling in Realistic Arterial Geometries. *Annals of Biomedical Engineering*, 30(4), pp.483–497.
- Stone, P.H. et al., 2003. Effect of endothelial shear stress on the progression of coronary artery disease, vascular remodeling, and in-stent restenosis in humans: in vivo 6-month follow-up study. *Circulation*, 108(4), pp.438–44.
- Stoneman, V.E. a & Bennett, M.R., 2004. Role of apoptosis in atherosclerosis and its therapeutic implications. *Clinical science (London, England : 1979)*, 107(4), pp.343–54.
- Sun, S. et al., 2009. Hypoxia-inducible factor-1[alpha] induces Twist expression in tubular epithelial cells subjected to hypoxia, leading to epithelial-to-mesenchymal transition. *Kidney Int*, 75(12), pp.1278–1287.
- Sun, Y. et al., 2010. Mammalian target of rapamycin regulates miRNA-1 and follistatin in skeletal myogenesis. *The Journal of Cell Biology*, 189(7), pp.1157–1169.

- Suo, J. et al., 2007. Hemodynamic shear stresses in mouse aortas: implications for atherogenesis. *Arteriosclerosis, thrombosis, and vascular biology*, 27(2), pp.346–51.
- Sussman, M.A. et al., 1998. Prevention of cardiac hypertrophy in mice by calcineurin inhibition. *Science*, 11, pp.1690–1693.
- Szymanski, M.P. et al., 2008. Endothelial Cell Layer Subjected to Impinging Flow Mimicking the Apex of an Arterial Bifurcation. *Annals of biomedical engineering*, 36(10), pp.1681–1689.
- Takagi, K. et al., 2014. GATA4 immunolocalization in breast carcinoma as a potent prognostic predictor. *Cancer Science*, 105(5), pp.600–607.
- Takeuchi, J.K. & Bruneau, B.G., 2009. Directed transdifferentiation of mouse mesoderm to heart tissue by defined factors. *Nature*, 459(7247), pp.708–711.
- Tarbell, J.M., 2003. Mass Transport in Arteries and the Localization of Atherosclerosis. *Annual Review of Biomedical Engineering*, 5(1), pp.79–118.
- Tenhunen, O. et al., 2004. Mitogen-activated protein kinases p38 and ERK 1/2 mediate the wall stress-induced activation of GATA-4 binding in adult heart. *The Journal of biological chemistry*, 279(23), pp.24852–60.
- Tevosian, S.G. et al., 2002. Gonadal differentiation, sex determination and normal Sry expression in mice require direct interaction between transcription partners GATA4 and FOG2. *Development*, 129(19), pp.4627–4634.
- Theveneau, E. & Mayor, R., 2011. Collective cell migration of the cephalic neural crest: The art of integrating information. *genesis*, 49(4), pp.164–176.
- Thiery, J.P. et al., 2009. Epithelial-Mesenchymal Transitions in Development and Disease. *Cell*, 139(5), pp.871–890.
- Thisse, B. et al., 1988. Sequence of the twist gene and nuclear localization of its protein in endomesodermal cells of early Drosophila embryos. *The EMBO Journal*, 7(7), pp.2175–2183.
- Timmerman, L.A. et al., 2004. Notch promotes epithelial-mesenchymal transition during cardiac development and oncogenic transformation. *Genes & Development*, 18(1), pp.99–115.
- Tressel, S.L. et al., 2007. Laminar Shear Inhibits Tubule Formation and Migration of Endothelial Cells by an Angiopoietin-2–Dependent Mechanism. *Arteriosclerosis, thrombosis, and vascular biology*, 27(10), pp.2150–2156.
- Trigueros-Motos, L. et al., 2013. Embryological-Origin–Dependent Differences in

- Homeobox Expression in Adult Aorta: Role in Regional Phenotypic Variability and Regulation of NF- κ B Activity . *Arteriosclerosis, Thrombosis, and Vascular Biology* , 33 (6), pp.1248–1256.
- Tsai, S.-F. et al., 1989. Cloning of cDNA for the major DNA-binding protein of the erythroid lineage through expression in mammalian cells. *Nature*, 339(6224), pp.446–451.
- Tzima, E. et al., 2005. A mechanosensory complex that mediates the endothelial cell response to fluid shear stress. *Nature*, 437(7057), pp.426–31.
- Tzima, E., 2006. Role of Small GTPases in Endothelial Cytoskeletal Dynamics and the Shear Stress Response. *Circulation Research* , 98 (2), pp.176–185.
- Ubil, E. et al., 2014. Mesenchymal-endothelial transition contributes to cardiac neovascularization. *Nature*, 514(7524), pp.585–590.
- De Val, S., 2011. Key Transcriptional Regulators of Early Vascular Development. *Arteriosclerosis, Thrombosis, and Vascular Biology* , 31 (7), pp.1469–1475.
- De Val, S. & Black, B.L., 2009. Transcriptional Control of Endothelial Cell Development. *Developmental cell*, 16(2), pp.180–195.
- Valesco, V., 2015. An Orbital Shear Platform For Real-Time, In Vitro Endothelium Characterization. *Biotechnology and Bioengineering*, pp.1097-0290.
- Vion, A.-C. et al., 2013. Shear Stress Regulates Endothelial Microparticle Release. *Circulation Research* , 112 (10), pp.1323–1333.
- Virchow, R., 1971. *Cellular pathology as based upon physiological and pathological histology* (English t., Philadelphia: JB, Lippincott.
- Vrljicak, P. et al., 2012. Twist1 Transcriptional Targets in the Developing Atrio-Ventricular Canal of the Mouse. *PLoS ONE*, 7(7), p.e40815.
- Wang, E. et al., 2013. Identification of Functional Mutations in GATA4 in Patients with Congenital Heart Disease M. Toft, ed. *PLoS ONE*, 8(4), p.e62138.
- Wang, S.M. et al., 1997. Cloning of the human twist gene: Its expression is retained in adult mesodermally-derived tissues. *Gene*, 187(1), pp.83–92.
- Wang, X. et al., 2003. Identification of a novel function of TWIST, a bHLH protein, in the development of acquired taxol resistance in human cancer cells. *Oncogene*, 23(2), pp.474–482.
- Warboys, C.M. et al., 2010. Acute and chronic exposure to shear stress have opposite effects on endothelial permeability to macromolecules. *American*

- journal of physiology. Heart and circulatory physiology*, 298(6), pp.H1850–6.
- Warboys, C.M. et al., 2014. Disturbed Flow Promotes Endothelial Senescence via a p53-Dependent Pathway. *Arteriosclerosis, Thrombosis, and Vascular Biology*, 34 (5), pp.985–995.
- Watson, O. et al., 2013. Blood flow suppresses vascular Notch signalling via dll4 and is required for angiogenesis in response to hypoxic signalling. *Cardiovascular Research*, 100(2), pp.252–261.
- Wei, S.C. et al., 2015. Matrix stiffness drives epithelial-mesenchymal transition and tumour metastasis through a TWIST1-G3BP2 mechanotransduction pathway. *Nat Cell Biol*, 17(5), pp.678–688.
- Welch-Reardon, K.M. et al., 2014. Angiogenic sprouting is regulated by endothelial cell expression of Slug. *Journal of Cell Science*, 127(9), pp.2017–2028.
- Wentzel, J.J. et al., 2005. Does shear stress modulate both plaque progression and regression in the thoracic aorta? Human study using serial magnetic resonance imaging. *Journal of the American College of Cardiology*, 45(6), pp.846–54.
- Wentzel, J.J. et al., 2012. Endothelial shear stress in the evolution of coronary atherosclerotic plaque and vascular remodelling: current understanding and remaining questions. *Cardiovascular research*, 7044044, pp.10–13.
- Wilcox, J.N. et al., 1988. Platelet-derived growth factor mRNA detection in human atherosclerotic plaques by in situ hybridization. *Journal of Clinical Investigation*, 82(3), pp.1134–1143.
- Willett, N.J. et al., 2011. Redox Signaling in an In Vivo Murine Model of Low Magnitude Oscillatory Wall Shear Stress. *Antioxidants & Redox Signaling*, 15(5), pp.1369–1378.
- Williams, G.C., 1957. Pleiotropy, Natural Selection, and the Evolution of Senescence. *Evolution*, 11(4), pp.398–411.
- Wirrig, E.E. & Yutzey, K.E., 2014. Conserved transcriptional regulatory mechanisms in aortic valve development and disease. *Arteriosclerosis, thrombosis, and vascular biology*, 34(4), pp.737–741.
- Witztum, J.L., 1994. The oxidation hypothesis of atherosclerosis. *Lancet*, 344(8925), pp.793–5.
- Wojciak-Stothard, B. & Ridley, A.J., 2003. Shear stress–induced endothelial cell polarization is mediated by Rho and Rac but not Cdc42 or PI 3-kinases. *The Journal of Cell Biology*, 161(2), pp.429–439.

- Wolfrum, S. et al., 2007. The protective effect of A20 on atherosclerosis in apolipoprotein E-deficient mice is associated with reduced expression of NF- κ B target genes. *Proceedings of the National Academy of Sciences of the United States of America*, 104(47), pp.18601–18606.
- Xavier, S. et al., 2015. Curtailing Endothelial TGF- β Signaling Is Sufficient to Reduce Endothelial-Mesenchymal Transition and Fibrosis in CKD. *Journal of the American Society of Nephrology*, 26 (4), pp.817–829.
- Xue, G., Restuccia, D.F., et al., 2012. Akt/PKB-mediated phosphorylation of Twist1 promotes tumor metastasis via mediating cross-talk between PI3K/Akt and TGF- β signaling axes. *Cancer Discovery*, 2(3), pp.248–259.
- Xue, G., Restuccia, D., et al., 2012. Akt/PKB-Mediated Phosphorylation of Twist1 Promotes Tumor Metastasis via Mediating Cross-Talk between PI3K/Akt and TGF- β Signaling Axes. *Cancer Discovery*, 2(3), pp.248–259.
- Yanazume, T. et al., 2002. Rho/ROCK Pathway Contributes to the Activation of Extracellular Signal-regulated Kinase/GATA-4 during Myocardial Cell Hypertrophy. *Journal of Biological Chemistry*, 277 (10), pp.8618–8625.
- Yang, J. et al., 2004. Twist, a Master Regulator of Morphogenesis, Plays an Essential Role in Tumor Metastasis. *Cell*, 117(7), pp.927–939.
- Yang, M.-H. et al., 2008. Direct regulation of TWIST by HIF-1[α] promotes metastasis. *Nat Cell Biol*, 10(3), pp.295–305.
- Yang, W.-H. et al., 2012. RAC1 activation mediates Twist1-induced cancer cell migration. *Nat Cell Biol*, 14(4), pp.366–374.
- Yao, Y., Rabodzey, A. & Dewey, C.F., 2007. Glycocalyx modulates the motility and proliferative response of vascular endothelium to fluid shear stress. *American Journal of Physiology - Heart and Circulatory Physiology*, 293(2), pp.H1023–H1030.
- Yin, G. et al., 2010. TWISTing Stemness, Inflammation, and Proliferation of Epithelial Ovarian Cancer Cells through MIR199A2/214. *Oncogene*, 29(24), pp.3545–3553.
- Zakkar, M. et al., 2009. Activation of Nrf2 in endothelial cells protects arteries from exhibiting a proinflammatory state. *Arteriosclerosis, thrombosis, and vascular biology*, 29(11), pp.1851–7.
- Zakkar, M. et al., 2008. Increased endothelial mitogen-activated protein kinase phosphatase-1 expression suppresses proinflammatory activation at sites that are resistant to atherosclerosis. *Circulation research*, 103(7), pp.726–32.
- Zeisberg, E. et al., 2007. Discovery of Endothelial to Mesenchymal Transition as a

- Source for Carcinoma-Associated Fibroblasts. *Cancer Research*, 67, pp.10123–8.
- Zeisberg, E.M. et al., 2007. Endothelial-to-mesenchymal transition contributes to cardiac fibrosis. *Nat Med*, 13(8), pp.952–961.
- Zeisberg, E.M. et al., 2008. Fibroblasts in Kidney Fibrosis Emerge via Endothelial-to-Mesenchymal Transition. *Journal of the American Society of Nephrology : JASN*, 19(12), pp.2282–2287.
- Zeisberg, E.M. et al., 2005. Morphogenesis of the right ventricle requires myocardial expression of Gata4. *Journal of Clinical Investigation*, 115(6), pp.1522–1531.
- Zhang, J. et al., 2013. AKT activation by N-cadherin regulates beta-catenin signaling and neuronal differentiation during cortical development. *Neural Development*, 8(1), pp.1–16.
- Zhang, W. & Liu, H.T., 2002. MAPK signal pathways in the regulation of cell proliferation in mammalian cells. *Cell Res*, 12(1), pp.9–18.
- Zhao, P. & Hoffman, E.P., 2004. Embryonic myogenesis pathways in muscle regeneration. *Developmental Dynamics*, 229(2), pp.380–392.
- Zhao, Y. et al., 2007. Morphological Observation and In Vitro Angiogenesis Assay of Endothelial Cells Isolated From Human Cerebral Cavernous Malformations. *Stroke*, 38 (4), pp.1313–1319.
- Zheng, R. & Blobel, G.A., 2010. GATA Transcription Factors and Cancer I. H. Gelman & M. Sudol, eds. *Genes & Cancer*, 1(12), pp.1178–1188.
- Zhou, B. et al., 2009. Fog2 is critical for cardiac function and maintenance of coronary vasculature in the adult mouse heart. *The Journal of Clinical Investigation*, 119(6), pp.1462–1476.
- Zhou, J. et al., 2013. BMP receptor-integrin interaction mediates responses of vascular endothelial Smad1/5 and proliferation to disturbed flow. *Journal of Thrombosis and Haemostasis*, 11(4), pp.741–755.
- Zhou, J. et al., 2012. Force-specific activation of Smad1/5 regulates vascular endothelial cell cycle progression in response to disturbed flow. *Proceedings of the National Academy of Sciences*, 109 (20), pp.7770–7775.
- Zhou, P., He, A. & Pu, W.T., 2012. Chapter five - Regulation of GATA4 Transcriptional Activity in Cardiovascular Development and Disease. In B. G. B. B. T.-C. T. in D. Biology, ed. *Heart Development*. Academic Press, pp. 143–169.

Zoja, C. et al., 2002. Shiga toxin-2 triggers endothelial leukocyte adhesion and transmigration via NF- κ B dependent up-regulation of IL-8 and MCP-11. *Kidney Int*, 62(3), pp.846–856.